

STORMWATER HYDROLOGY AND DRAINAGE

D. STEPHENSON

*Professor of Hydraulic Engineering, University of the Witwatersrand,
Johannesburg, South Africa*



ELSEVIER SCIENTIFIC PUBLISHING COMPANY
Amsterdam—Oxford—New York

1981

ELSEVIER SCIENTIFIC PUBLISHING COMPANY
Molenwerf 1, 1014 AG Amsterdam,
P.O. Box 211, 1000 AE Amsterdam, The Netherlands

Distributors for the United States and Canada:

ELSEVIER/NORTH-HOLLAND INC.
52, Vanderbilt Avenue
New York, N.Y. 10017

With 131 figures and 30 tables.

Library of Congress Cataloging in Publication Data

Stephenson, David, 1943-
Stormwater hydrology and drainage.

(Developments in water science ; v. 14)

Bibliography: p.

Includes indexes.

1. Urban hydrology. 2. Urban runoff. 3. Storm
sewers. I. Title. II. Series.

TD657.S73 628'.212 81-7864

ISBN 0-444-41998-5 AACR2

ISBN 0-444-41998-5 (Vol. 14)

ISBN 0-444-41669-2 (Series)

© Elsevier Scientific Publishing Company, 1981

All rights reserved. No part of this publication may be reproduced, stored in a retrieval system or transmitted in any form or by any means, electronic, mechanical, photocopying, recording or otherwise, without the prior written permission of the publisher, Elsevier Scientific Publishing Company, P.O. Box 330, 1000 AH Amsterdam, The Netherlands

Printed in The Netherlands

PREFACE

Considerable research in urban drainage is being conducted at Universities and research establishments throughout the world. The subject matter varies from rainfall analysis to design of stormwater inlet gratings. A lot of the results of the research have been published, but not necessarily in a form suitable for the design engineer. The book attempts to condense some of the data and conclusions, to present it in a unified form suitable for an overall appreciation by engineers and students, and to guide the engineer in methods of computation. Thus while there are many design aids, there is also a sound hydraulic background sufficient for a postgraduate student course as well as enough ideas for research and development.

The approach is that of the designer as opposed to the analyst. This may be a result of the author's background, which was in practice with a water authority and subsequently as a consulting engineer. Methods of hydrological analysis and computer modelling are essential tools of the designer, but the description of these methods is restrained as they are probably more academic. In fact there are a number of excellent books on the simulation approach.

The layout of the book is essentially in the order in which a drainage engineer would perform his calculations. Thus the sections on hydrology precede those on hydraulic design. Whereas a number of common design methods eg. the rational method, are summarized in an early chapter, the author has paid a disproportionate attention to the kinematic method. This method illustrates some of the shortcomings in isochronal methods, but chapter 5 in particular may be skipped if desired.

Runoff is followed through the chapters on roof drainage, road drainage, design of drain pipes and channels and culverts and bridges. Many basic principles of hydraulics are revisited in order to provide a complete reference, but there are also many design aids which it is hoped will be of use to the engineer. Generalized graphs and equations supplement the description wherever possible.

Urban pollution and runoff quality are becoming increasingly important. Quality of surface runoff is discussed briefly but no attempt is made to consider wastewater sewerage or the treatment of polluted water.

CHAPTER 1

DESIGN ALTERNATIVES

THE ROLE OF THE DRAINAGE ENGINEER

Urban development is spreading over more and more of the earth's surface. The problems associated with urbanization are compounded as the density and extent of development proceeds (Schneider, 1975). The effect of particular concern is the elimination of most natural processes and their replacement by man-made streamlined procedures. One such system is the water cycle. Excess rain is no longer free to flow overland and meander along unlined channels. Instead, precipitation is on roofs or concrete or bitumen pavements, and it washes off conveying pollution created by mankind. Stormwater drains replace streams. They intensify runoff and destroy nature's balance. Channels flow more strongly in times of flood. Erosion and deposition occur. Natural self-purification processes such as reoxygenation may be destroyed as the ecology is affected. Ground water is starved due to increased surface runoff. Vegetation, dust problems and the habitat may be affected. These factors demand a thorough environmental study in parallel with town planning and design of the infrastructure.

Civilization has focussed attention on the urban system. The convenience of central facilities, mass transport systems and easy trade, have encouraged a concentration at nodes we call towns or cities. The resulting disadvantages, such as pollution and elimination of natural fields and streams, follow because man's ambition exceeds his desire for a balanced life. Many of the problems are unavoidable except at extreme expense. It is no use blaming the engineer for problems which manifest. The engineer is able to solve problems at a minimum of cost, but must work within a budget. The municipal councillor or national politician is also limited in his abilities and budget. He must balance the ballot against the fulfillment of ideals.

This book is aimed at the drainage engineer. It provides ideas and technology to compromise between limited budgets and best solutions. It presents design methodology for evaluating a best design to be achieved for stormwater drainage. Stormwater design objectives have changed over the years. The engineer used to attempt to remove stormwater as rapidly

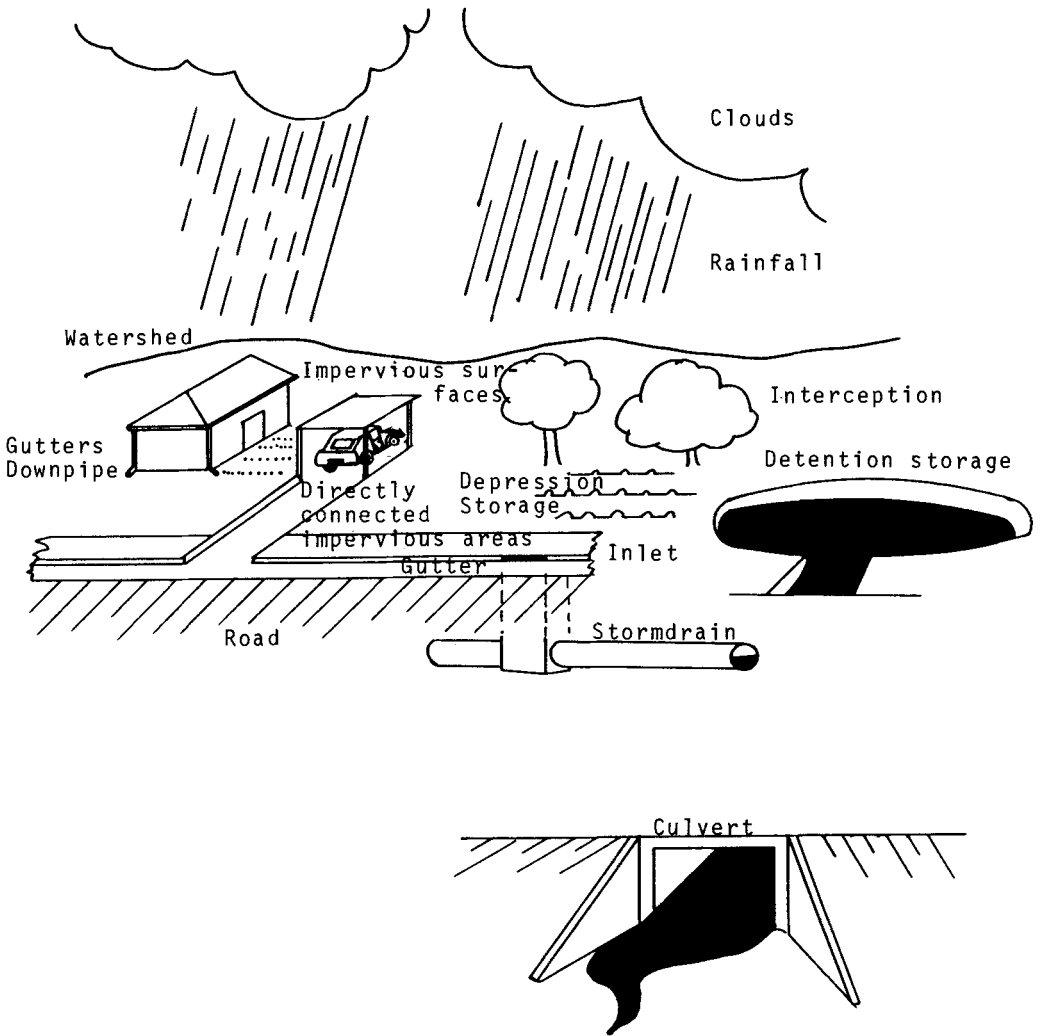


Fig. 1.1 Urban drainage processes

as possible. Nowadays the consequences of downstream flooding and alteration of the water cycle's regime are recognised.

The science of urban drainage has received considerable attention in recent years, especially in the United States. Legislation has forced engineers to think carefully about the drainage process. As a result there have developed numerous research groups and mathematical models for simulating the runoff process.

The components of stormwater systems (Fig. 1.1.) can be split into two groups: (Yen, 1978). One, the surfaces, basins, groundcover, gutters and inlets which are evident to all. The other is the major component from the engineer's point of view; namely the drains, controls, underpasses, treatment or holding works, and final discharge rates and effluent quality.

STORMWATER MANAGEMENT PRACTICES

The construction of a stormwater drainage system is not the only way to avoid flooding or pollution. The day-to-day operation or management of the catchment will have an important bearing on runoff quantity and quality. On-site detention, retention and regular cleaning could relieve the drains of a considerable load. A reasonable management policy will be assumed at the time of design. Failure to maintain this programme could result in exceedance of the capacity of the system. On the other hand improved management could alleviate the load on an underdesigned system, or enable more intensive development to take place in the catchment. Control measures may be structural (e.g. diversion, storage or channel improvements) or policy (e.g. insurance, flood warning systems or building control regulations for flood zones). Trotta et al (1977) described an automatically controlled drainage system.

Pollution control is the most obvious result of catchment management. Street sweeping, efficient refuse disposal, discharge monitoring and treatment of runoff are some of the possibilities.

Runoff control is a more difficult and more recent practice. Stormwater retention, groundwater recharge, provision of rough surfaces to retard flow and disconnection of impervious areas, are all logical practices but not explicitly required until recently in the United States and Europe. The methods are still not practiced in many countries.

The accompanying Table (1.1) summarizes some practices and their accomplishment. The efficiencies and costs are discussed by Wanielista (1979).

TABLE 1.1
Stormwater Management Practices

<i>Purpose</i>	<i>Method</i>	<i>Reason</i>
Peak flow rate attenuation	Storm monitoring	Flood prediction
	Detention storage	Flood routing
	Channel storage	Flood routing
	Gravel surfaces	Retardation
	Rooftop storage	Routing and lag
	Parking lot storage	Routing and lag
Runoff volume reduction	Disconnected impervious areas	Infiltration, attenuation
	Retention storage	Removal of flow
	Diversion	Subtraction of flow
	Soakaways	Infiltration
	Basin recharge	Increase groundwater
	Infiltration	Flow reduction
	French drains	Seepage
	Swales	Retard flow, infiltration
Provision for flooding	Porous pavements	Infiltration
	Contour ploughing	Infiltration
	Insurance	Compensation
Catastrophy aversion	Building control regulation in flood zone	Limit damage
	Flood warning	Evacuation or diversion
	Evacuation	Structural failure
Erosion Control	Sandbagging	High water levels
	Emergency overflows	Water flow control
	Weir strengthening	Dangerous flood levels
	Water tanks	Polluted water supplies
	Berms	Settling
Pollution control	Vegetation	Stabilization, retardation
	Rockfill	Flow control
	Mulching	Runoff Control
	Fertilizing	Encourages vegetation
	Settling basins	Catching sediment
	Sediment removal	Basin renewal
	Screen	Detritus
	Centrifuge	Separation
	Contour ploughing	Surface Storage
	Street sweeping	Catching solids
	Street vacuuming	Catching fines
	Street flushing	Total removal
	Street deicing	Ice removal
	Catching first flush	Most concentrated
Refuse removal	Avoidance of pollution	
Storage	Settling	
Aeration	Biochemical oxidation	
Chemicals	Neutralization, pre- cipitation	
Pollution control	Comminuters	Grinding large solids
	Flotation	Scum, emulsion, oil
	Legislation	Enforcement of standards
	Summons or fines	Discouragement
	Waste dump isolation	Runoff detention
	Grassing street verges	Catching fines, scums

Fertilization methods
Land disposal

Minimization of washoff
Removal of recoveries

Many of the systems for flow reduction must be incorporated at design stage. These include means of retarding the concentration time (increased surface roughness and detention basins), methods of catching part of the volume of runoff (diversion systems and retention basins), and means of reducing excess runoff (percolation basins, catchment cultivation and restricted capacity drains) (Carcich, et al 1974) combined with surface channels.

The system or combination of systems to adopt for any particular catchment will depend on the catchment characteristics, such as topography, soil type and cover, climate (rainfall and evaporation pattern) desired risk and the consequences of flooding. It should be recalled that interference with the runoff process complicates the relationship between storm recurrence interval and the recurrence interval of a failure of the stormwater system to do its duty. This aspect was studied by Kamedulski and McCuen (1978).

In order to at least reduce the flood flows from developed areas to the figures before man-made development proceeded, it is useful to understand the runoff process and its assessment. Urbanization reduces the average permeability of the ground by the construction of pavements and buildings. The concentration time is reduced due to the increased runoff intensity, smoother surfaces and man-made channels. The design storm is therefore a shorter, more intense storm than that resulting in maximum development. Natural basins or depressions may be levelled, thereby increasing excess runoff even further.

SAFETY FACTORS

Any design or structure will normally be constructed with certain safety margins. This is not the same as the risk of overtopping or exceeding the capacity of the system. A storm of a certain recurrence interval will be selected from economic considerations using probability theory as outlined in a later chapter. (Walesh and Videkovich, 1978). The present consideration is the margin of safety on top of the estimated design figure.

In the case of structures such as pipes, manholes, kerbs or weirs the factor of safety with respect to strength is established routinely by designing according to a structural code of practice. Thus design stresses may be 50 percent of yield stress of steel or 30 percent of the crushing strength of concrete. Hydraulic designs usually have little

such margin. Thus freeboards may be calculated from wave height formula and not an arbitrary additional depth. In stability calculations for dams or weirs a reasonably severe loading condition with extreme uplift and minimal resistance factors, should be allowed. In view of the dire consequences of failing of such a structure by overturning, the hydraulic engineer should consider applying safety factors in addition to designing for a high recurrence interval hydrological event.

The acceptance of mathematical models for hydrological and hydraulic analysis of a drainage system may lull the design engineer into a false sense of security. Impressive sensitivity studies and verification runs by computer may indicate reasonable margins of safety, but they may remain unknowns in the input data, the programming assumptions or in the interpretation of output. The engineer who is responsible for the design drawings should therefore continue to apply normal safety factors based on judgement and the consequences of a failure.

Increasing legal action against drainage engineers in the United States of America has highlighted the need for precautions in design. Hopefully this will not result in excessive conservatism and increase in costs. The balance between economy of design and consequences of failure must not be imposed on the designer or constructor but on the responsible authority or its insurers. It is good practice to inform the affected public of design risks, flood levels and about insurance.

Where design alternatives exist which have similar costs it is sensible to select the least-risk system. Thus an open channel has usually a higher margin of safety against flooding than a closed conduit. This is because the capacity increases rapidly with increased depth in a channel.

Adjacent low-lying parking lots and parks, even if not designed detention ponds, could in an emergency serve as such. Thus the drainage system should be integrated with the town planning.

DETENTION AND RETENTION PONDS

To compensate for runoff intensification due to urbanization, storm-water could be stored in man-made basins within the catchment. The ponds can be sited in non-essential areas, e.g. parks, recreational grounds or parking lots, (Miles, 1979). In parks, the storage may be provided in depressions, which can subsequently be drained (or water permitted to percolate or evaporate in isolated situations, termed dry basins). Alternatively, the storage may be in channel freeboard on ornamental ponds or recreational lakes (referred to as wet ponds).

Drains could be led directly into the basins, in which case all initial flow would be caught before the drain overflowed and water filled the downstream drains. In this situation the end-weir arrangement may induce a routing effect by the basin. Thus in addition to retention, the upper levels of the pond would act as a detention system. Detention is the temporary storage of runoff such as in freeboards while retention involves the permanent diversion into evaporation or seepage ponds i.e. flow is not returned to the drainage system. A comparison of different methods was made by Poertner (1978). Detention ponds are often referred to as onstream, or outlet controlled, but they are not necessarily so. Offstream ponds are usually inlet controlled.

The pond could be off-channel and water could be diverted from the drainage system. Here an unrestricted inlet such as a channel with a drop into the pond, could be constructed in which case the pond would fill during the initial stage of the storm. In such a situation the pond may not affect the peak flow much in case of extreme event storms. Alternatively, the inlet could be designed to divert flow only above a certain minimum to an off-channel pond. Such a device could be a side channel weir. The rate of diversion would increase with increasing discharge in the drain. Various control devices for influencing the stage-discharge characteristics of pond outlets were described by Hall and Hockin (1980).

Retention can be at the outfall of the catchment, in which case a large-scale pond is often required such as a lake or in a park. The retention may be provided along the drains, or it may be at the head of the drains (on site). The latter may not require any single large volume; it may be sufficient to plant dense vegetation, till the land, or construct terracing.

The difference between retention and detention storage is illustrated in Figs. 1.2 to 1.4. (The reason for the difference in time to peak for high and low return periods will become clear when the section on kinematic hydrology has been studied).

The method of design of retention basins is to select a design risk and plot the corresponding design hydrograph. Select a design discharge rate and indicate this on the hydrograph. The area under the hydrograph above the design discharge is the volume of storage required. It should be borne in mind that the critical storm duration is not that associated with the most intense storm. It will be considerably longer for the maximum volume of runoff. The critical storm duration depends on the pond design and must be determined by trial. For instream detention storage, the volume required may be estimated by drawing a straight line

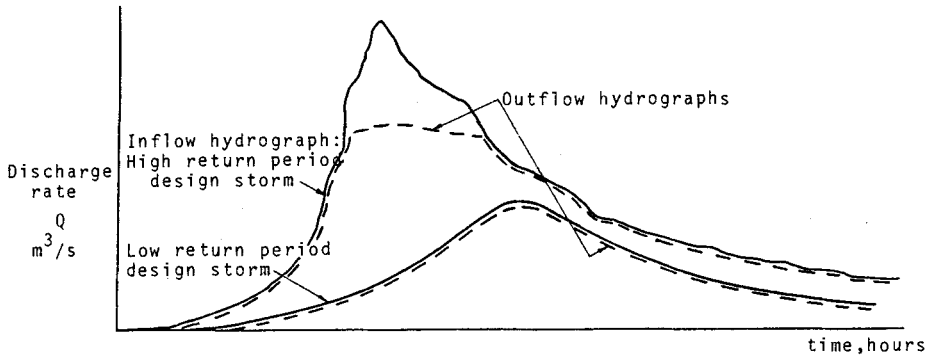


Fig. 1.2 Effect of off-channel retention storage on runoff, assuming an inlet weir to pond off drain

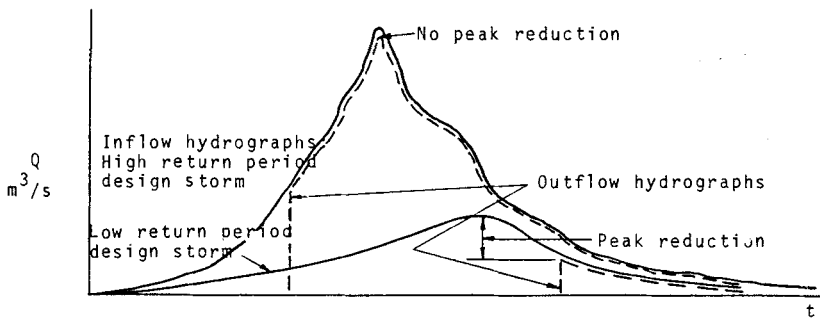


Fig. 1.3 Effect of in-line retention storage on runoff

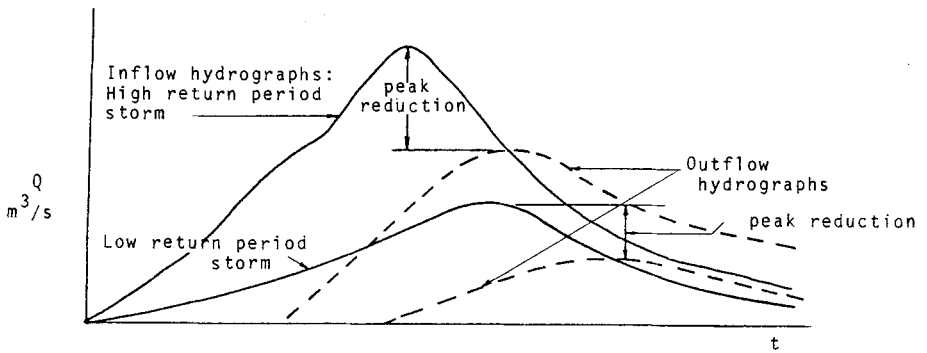


Fig. 1.4 Effect of detention storage on runoff

from the start of the inflow hydrograph to a point on the recession limb equal to the desired peak outflow rate. The area above the line below the hydrograph is an indication of the pond volume. Flood routing using numerical or graphical methods (e.g. Wilson, 1974) must be performed for the ultimate design. Approximate mathematical methods have also been proposed (Sarginson, 1973). It may be necessary to correct for the storage - discharge characteristics of the inlet to the pond, which means the cut-off line is not horizontal. In the case of in-line retention storage, the volume under the design hydrograph is stored. For detention storage, alternative storage - discharge characteristics will have to be tried until a satisfactory compromise for a range of design hydrographs is achieved. A reduction will be achieved on all recurrence interval design storms.

To determine the critical inflow duration for an instream detention pond with controlled discharge, Wright-McLaughlin (1969) proposed a graphical method. The ordinates of the intensity-duration curve are multiplied by the storm duration and runoff coefficient, C. The resulting ordinates are plotted in a mass-flow curve of volume versus time. Now for any discharge (outflow) rate which plots as a straight line on the same plot the storage required is the maximum difference between the massed inflow and outflow curves.

For an intensity-duration relationship such as

$$i = \frac{a}{(b+t)^c} \quad (1.1)$$

an analytical solution for maximum storage is possible. Here i is storm intensity, t is storm duration, and a , b and c are constants for any locality and storm recurrence interval T . Now storage required is

$$S = \frac{CAat}{(b+t)^c} - Qt \quad (1.2)$$

$$\text{For maximum } S, \quad dS/dt=0, \quad (1.3)$$

$$\text{Hence } Q/CA = a\{b+t-ct\}/(b+t)^{c+1} \quad (1.4)$$

Thus one can plot S/CA versus Q/CA with t as a parameter. Fig. 1.5 is such a plot prepared by Watson (1981) for $a=1200T^{0.3}$ (mm/h), $b=14.4$ min and $C=0.883$. From this chart one is able to calculate the critical storm duration and storage S for any desired outflow rate Q , provided CA and T are known.

PERCOLATION BASINS

In theory, the ground can provide storage capacity equal to any storm which could be anticipated. The volume of storage per unit area is Dn where D is the depth to the water table and n is the soil porosity.

n is the ratio of volume of voids between soil particles to total volume, and is usually between 0.3 and 0.4, irrespective of soil particle size. Thus 1 m of soil could contain at least 300 mm of rainfall provided it could be absorbed sufficiently rapidly. Unfortunately the permeability of the soil usually limits the rate of infiltration. The rate of seepage per unit area is $\bar{v}=ki$ (1.5)

where \bar{v} is the apparent seepage velocity (flow rate per unit area). k is the permeability, which may be as low as 10^{-9} m/s for impermeable clays. For granular soils it may be approximated by the equation $k=gd^2n/800v$ (1.6)

where d is particle size, and v is the kinematic viscosity of water. Thus for 1 mm particle, $k = 9.8 \times 10^{-6} \times 0.3 / 800 \times 10^{-6} = 0.004$ m/s. This is greater than any rainfall rate. The hydraulic gradient i can reach a maximum value of unity. The actual rate of penetration of water is $v = k/n$ (1.7)

Thus the depth required to store p mm of rain is p/n and the time to infiltrate it is p/k .

Factors affecting the theoretical percolation will include the initial moisture content, which is water suspended on soil particles by surface tension, and this may be anything up to the full porosity for fine clays, although it is lower for coarse granular soils.

Air will also have to be released from the aquifer as water permeates down. The upflowing air will tend to suspend the water permeating downwards and may cause airlocks or impermeable barriers. Perched water tables may also form on the slightest lense of impermeable material. Attention should be paid to the drainage of the aquifer subsequent to saturation. The drainage rate will increase as the water table is raised and this may result in unexpected springs, marshes, soil erosion or even embankment instability.

Effect of holding on water quality

The retardation of escaping water by basins or seepage pits will reduce the rate of reoxygenation. In the case of wastewaters, or polluted runoff, this may result in obnoxious smells, or affect the ecosystem. If the water turns anaerobic this problem is severe.

Oxygenation plays an important part in natural purification processes, by reducing bio-degradable material, emulsifying solutions or oxidizing pollutants. The rate of oxygen absorption depends not only on the water surface area exposed, but also on the water depth and more particularly on the energy input. Turbulence in flowing water is a natural mixing

device and considerably improves aeration. Stagnant water will lack this

On the other hand, if treatment is required before the water can be discharged into natural water bodies, the storage pond may be the place for it. (Wipple, 1979). Aerators, skimmers or sediment removal facilities may be constructed in ponds.

It must be realized that a pond will act as a natural silt trap and the ground may become unusable after a storm. The same adverse effect applies to floating pollution, such as oils, or to debris such as broken glass, tin cans, etc. The use of recreation fields for storage is therefore open to question.

On-Site Detention

Where practicable, property developers and owners should be encouraged to minimize direct runoff by directing gutters and downpipes to pervious or planted areas. The detention is thus spread over a large area and the depth of water are not at all inconvenient. Where the entire property is paved or covered, holding basins, porous layers or restricted capacity stormwater discharge pipes should be considered. In many countries legislation is sufficiently advanced to force owners to discharge at a rate not greater than the virgin land would. Economic incentive to provide even greater control may be difficult though.

Such flow attenuation also minimizes soil erosion and may reduce the concentration of pollutants such as may settle or float or even have time to react. The concept of gutterless roofs used in some countries, actually retards runoff if runoff from the roof is direct onto the garden. Although gutters detain runoff, they concentrate it with a resulting net increase in peak flow.

Parking-Lot Storage

Parking lots offer one of the most convenient areas for ponding of water in densely built, commercial or industrial areas. By careful grading or dishing of the area, the ponds can be confined to isolated areas which are rarely used except at peak shopping hours.

Porous verges (Fig. 1.6) may be constructed adjacent to the parked area to absorb or convey the surplus runoff. They will also arrest sheet flow and retard flow into drains.

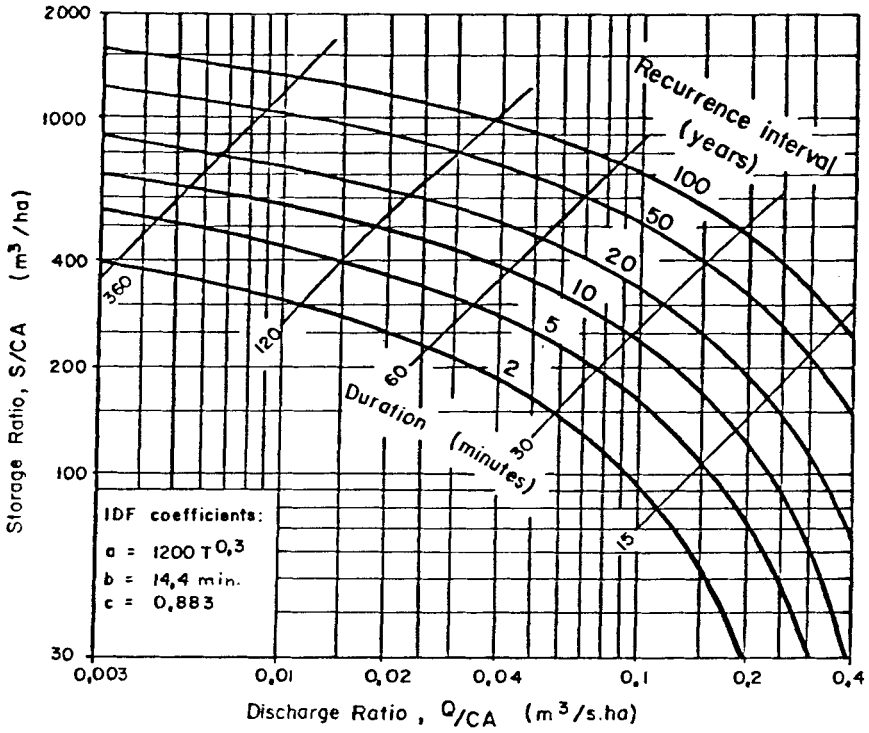


Fig. 1.5 Example curves for the preliminary design of storage ponds

Rooftop Detention

Flat roofs may be constructed with parapets to contain precipitation. Although the idea offers an otherwise unused area, it may increase the cost of construction considerably. Special attention will have to be paid to waterproofing. Additional loading must be allowed for in the structural design. Well designed control inlets to downpipes are

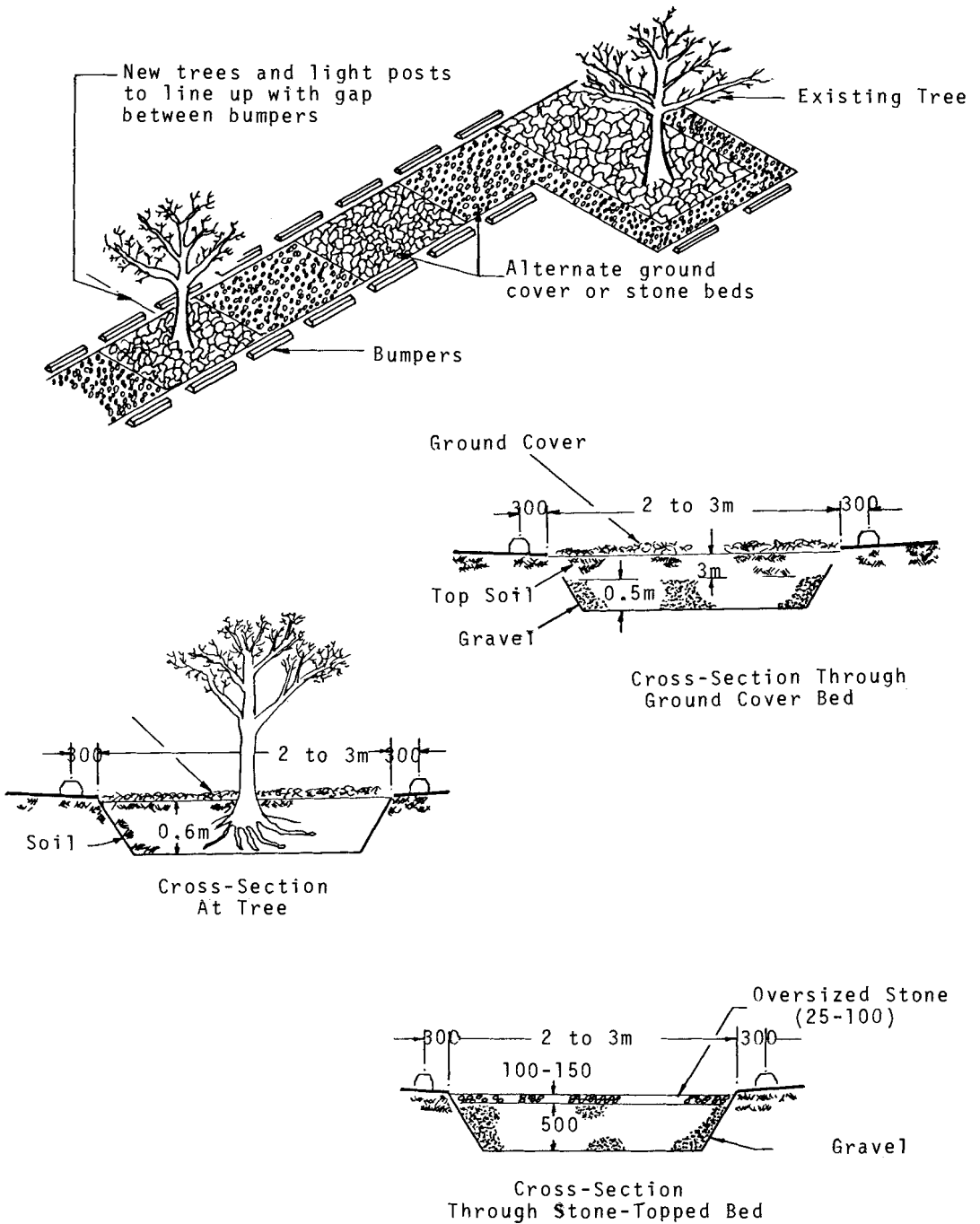


Fig. 1.6 Details of median strip for parking lot drainage

required. These must also be covered by grates to minimize blockage by debris.

OVERLAND AND CHANNEL RETARDATION

Although detention storage has been proposed as one solution to the attenuation of floods, this is in fact an artificial way, and suffers a number of disadvantages. Not least is the fact that valuable space is required to store floods. The factor of risk becomes increasingly difficult to assess. Whereas storage may be provided for a flood of a certain recurrence interval (the so-called design flood), what about greater floods? The attenuation effect is certainly not proportional to the flow rate, and in fact the reduction in the peak may be negligible in the case of larger floods than the design flood. There is also the question of storm duration to consider. The design storm duration for detention storage is invariably greater than for the channel design storm. The relationship between storage capacity and risk is therefore complex.

A better solution in many cases is to provide channel storage. This is a form of detention storage. Channel storage is effected by decreasing the flow velocity. This again has two effects. It increases the concentration time of the catchment thereby reducing the design inflow since storm intensity is known to reduce with duration for any particular recurrence interval. The channel storage also provides a way of holding back water and so reducing the peak discharge rate lower down.

One way to reduce flow velocity is to roughen the channel perimeter. The cross sectional area required for any discharge is therefore increased, but certainly not in inverse proportion to the flow velocity. This is because the discharge rates actually reduce through the collecting system if the channel system is so designed to retard flow.

The flow at any section for any storm intensity could be obtained by routing excess rain down the system, but a simpler approach would be to estimate the concentration time, or time to reach equilibrium for any storm and design the channel to convey the excess runoff corresponding to that storm. The kinematic approach could be used to estimate concentration time at any section. Flow retardation can be carefully controlled and easily designed if rockfill is used as a channel lining. The design of rockfill linings is considered in the chapter on open channels.

REFERENCES

- Carcich, I.G. Hetling, L.J., and Farrell, R.P., February 1974. Pressure sewer demonstration. Proc. ASCE, 100 (EE1), 10315, p25-40.
- Hall, M.J., and Hockin, D.L., 1980. Guide to the Design of Storage Ponds for Flood Control in Partly Urbanized Catchment Areas. CIRIA, Tech. Note 100. London.
- Kamedulski, G.E., and McCuen, R.H., 1978. Comparison of stormwater detention policies. Proc. ASCE Conf. Verification of Mathematical and Physical Models in Hydraulic Engineering, Maryland.
- Miles, L.C., 1979. Stormwater drainage in urban area. Municipal Engineer, Johannesburg. 10(2) March-April, p27-35.
- Poertner, H.G., 1978. Stormwater detention and flow attenuation. In Storm Sewer System Design by Yen, B.C., (Editor), University of Illinois.
- Sarginson, E.J. 1973. Flood control in reservoirs and storage ponds, J. Hydrol. 19, p351-359. Also discussion by West, M.J.H. 1974. 23, p67-71.
- Schneider, W.J., 1975. Aspects of hydrological effects of urbanization. Proc. ASCE 101(HY5), 11301, 449-468.
- Transport and Roads Research Laboratory, 1976. A Guide for Engineers to the Design of Storm Sewer Systems, Road Note 35, HMSO, London.
- Trotta, P.D., Labadie, J.W., and Grigg, N.S., December 1977. Automatic control for urban stormwater. Proc. ASCE. 103 (HY12), 13396, 1443-1459.
- Walesh, S.G. and Videkovich, R.M., February 1978. Urbanization: damage effects. Proc. ASCE, 104 (HY2), 141-155.
- Wanielista, M.P., 1979. Stormwater Management, Quantity and Quality. Ann Arbor Science, Ann Arbor, Michigan, 383 pp.
- Watson, M.D. 1981. Sizing of urban flood control ponds. Hydrological Research Unit, University of the Witwatersrand, Johannesburg.
- Wilson, E.M., 1974. Engineering Hydrology, 2nd Edn. Macmillan, London.
- Wipple, W., 1979. Dual-purpose detention basins. Proc. ASCE, 105 (WR2), p403-412.
- Wright- McLaughlin, Engineers, 1969. Urban Storm Drainage Criteria Manual, Denver.
- Yen, B.C., 1978. Storm Sewer System Design, Dept. Civil Engineering, University of Illinois, 282pp.

RAINFALL AND RUNOFF

THE HYDROLOGICAL CYCLE

Precipitation, abstraction, runoff and evaporation comprise basic components of the hydrological cycle. In order to understand the runoff process it is necessary to appreciate the factors affecting it. Precipitation, in the form of rain, snow, hail, or surface condensation does not all find its way into stormwater drains. Much of it either evaporates, is absorbed or is retained on the surface on which it falls. Even then, the rate at which runoff occurs depends not only on the rate of precipitation, but also on the surface configuration, and the depth-discharge relationship.

Rainfall is not as a rule uniform in time. The rate of precipitation varies in time and over a catchment. Wind plays an important effect in bringing in the moisture which has evaporated from exposed waters or transpired from surfaces. Wind causes clouds to travel across the catchment. Precipitation will result if the temperature of the clouds of water vapour drops below dew point. Condensation is followed by precipitation. The cooling action may be caused by rising air; against mountains (orographic precipitation) due to cold fronts (frontal or cyclonic precipitation) or due to thermal currents (convictional precipitation). The latter gives rise to thunderstorms, an intense form of precipitation but often of relatively short duration, i.e. over a few minutes or hours.

Snow, sleet and hail will also give rise to runoff. The necessary surface holding and drainage systems are important, but beyond the scope of this work.

The cycle of evaporation, cloud movement, precipitation and runoff are illustrated in Fig. 2.1.

There are so many variables influencing solar radiation and atmospheric movements that the process can be regarded as somewhat random from the point of view of the engineer. In fact the engineer will never know at design stage what the maximum flow through his storm drains will be. He can only estimate likely flows from an analysis of past data. He does however have an influence on the runoff process, by

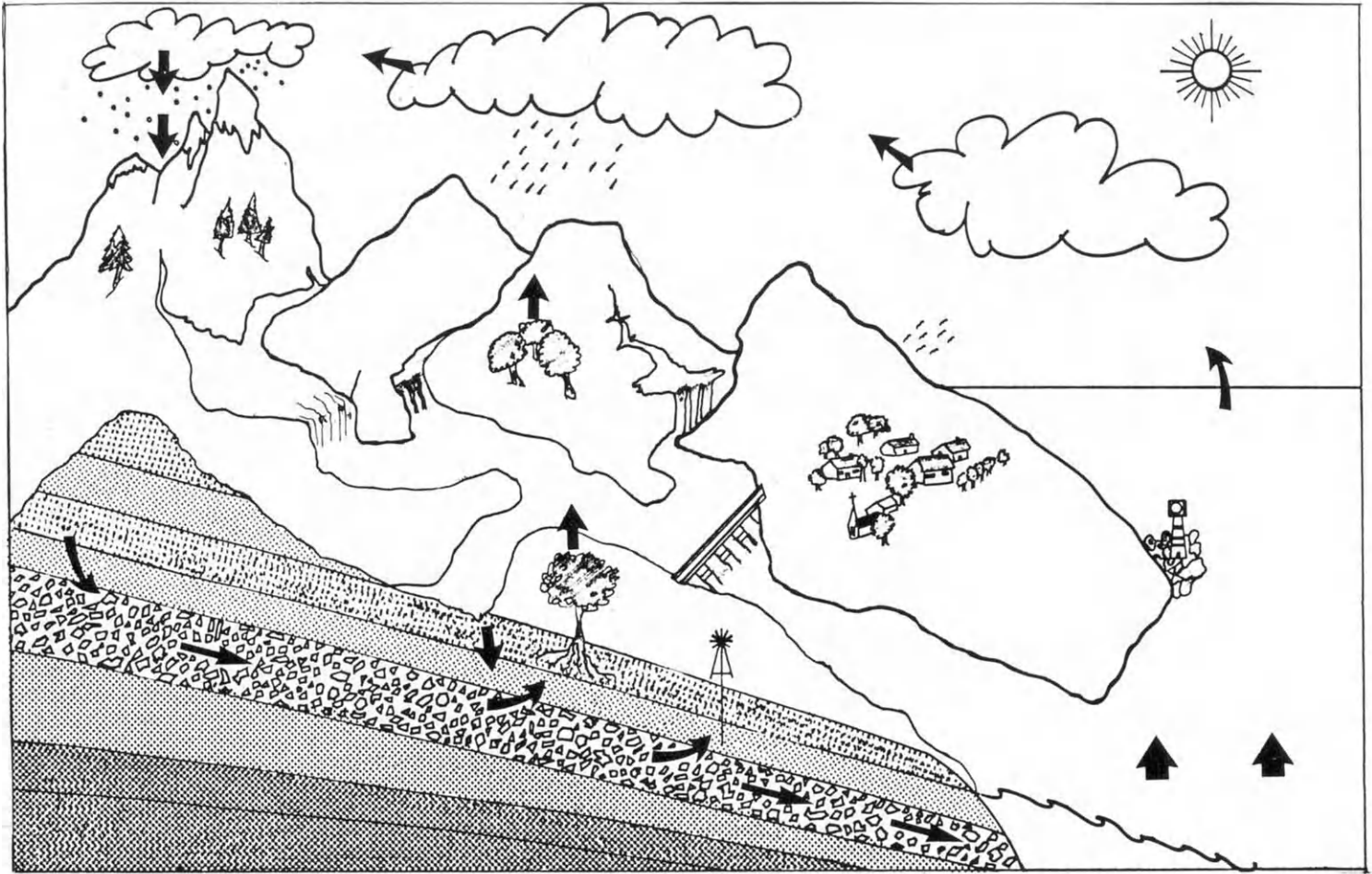


Fig. 2.1 The Hydrological Cycle

channelling the water, by storing it or by diverting it.

If we bear in mind that 71 percent of the earth's surface is covered by water, we realize how easily moisture can be brought inland to result in precipitation. Yet there are forces of nature controlling the system, such as the earth's surface drag on winds and limits to the moisture content in the atmosphere. There is therefore some physical limit to the maximum rainfall intensity one can expect.

Much of the precipitation on the earth's surface infiltrates into the ground. In fact 98% of all the earth's fresh water (excluding ice caps) occurs as groundwater. This water moves slowly through aquifers towards lower lying rivers, lakes or seas, gradually receding in times of drought. It rises again as the aquifer is replenished by rain. Some ground water is abstracted by plants. Most of this is lost by transpiration.

RAINFALL INTENSITY AND DURATION

Historic records of rainfall are seldom as detailed as would be desired by the engineer. He can only use samples to estimate a true rainfall pattern. From the data he must estimate intensity, duration and frequency of storms. Very few countries maintain continuous storm records for the purpose of determining time variation of precipitation during storms. It is frequently assumed that the rate of precipitation is uniform i.e. the hyetograph (graph of rainfall rate versus time) is square-topped. In fact storms may vary in time increasing in intensity starting from a drizzle, and subsequently recede. In such cases it is difficult to define the 'storm' duration or intensity. Storm intensity is given in m/s in S.I. units or more realistically in mm/h. Thus the starting point and end of a storm are subjective as well as the 'intensity'. Thus tabulated data with average rainfall intensities should be used with circumspection.

Theory indicates that rainfall patterns could be affected by urbanization. Radiation from the ground, air pollution and wind speeds are different from rural circumstances. Verification of the effects is hampered by the very causes of the effects, especially in the assessment of radar measurements.

Analysis of storms on a worldwide basis by Bell (1969) has revealed similarities in relationships between total precipitation, storm duration and frequency. He preferred to plot total precipitation over different storm durations rather than storm intensity, as mean intensity is misleading. It varies considerably during a storm. He also selected

the partial series rather than annual series in evaluating frequency. That is, some years may contain more than one high storm used in the analysis while other years may have none.

Storm data from the United States, Australia, South Africa and other countries were plotted by Bell. The data covered storm duration between five minutes and two hours, and recurrence intervals from 2 to 100 years. He found the following equation predicted precipitation depth in each case with remarkable accuracy:

$$P_T^t = (0.21 \ln T + 0.52) (0.54t^{0.25} - 0.50) P_{10}^{60} \quad (2.1)$$

where P_T^t is the rainfall depth over t minutes which is exceeded with a T -year recurrence interval. P_{10}^{60} is the one-hour precipitation for a 10 year recurrence interval. The units of P can be inches or millimetres as long as they are consistent. Thus provided the precipitation over any one duration and recurrence interval are known others can be established. In fact Bell indicated P_{10}^{60} could be evaluated from empirical relationships as follows:

$$P_{10}^{60} = 0.27MN^{0.33} \quad (0 < M < 50) \quad \text{and} \quad (2.2a)$$

$$P_{10}^{60} = 0.97M^{0.67}N^{0.33} \quad (50 < M < 115) \quad (2.2b)$$

where P is the 1-hour, 10-year rainfall in millimetres, M is the mean of the maximum annual observational-day precipitation in millimetres, and N is the mean annual number of rainfall days, ($1 < N < 80$).

In general precipitation is more intense the shorter the duration of a storm. Thus short storm rainfall rates as high as 30 mm per minute have been recorded in India, whereas continuous rainfall rates of 30 mm per hour are more typical of European conditions.

Relationships between rainfall intensity and duration are of prime interest to the engineer, who must select a design storm duration if it affects the intensity. The relationship between intensity and duration is usually plotted in the form of Fig. 2.2 on a regional basis for different recurrence intervals. This form may be misleading as intensity implies uniform intensity which may not be the case. Total depth of precipitation (Fig. 2.3) may be a better ordinate.

Frequency analysis is done separately as outlined later, in order to yield intensities for selected frequencies. Yarnall (1935) and others have plotted rainfall intensity maps for a country. Such data can readily be employed to prepare co-axial plots.

The frequency with which precipitation exceeds any particular rate is of concern to the engineer. He will design his drainage system against a certain risk of failure. Rainfall data may be ranked and

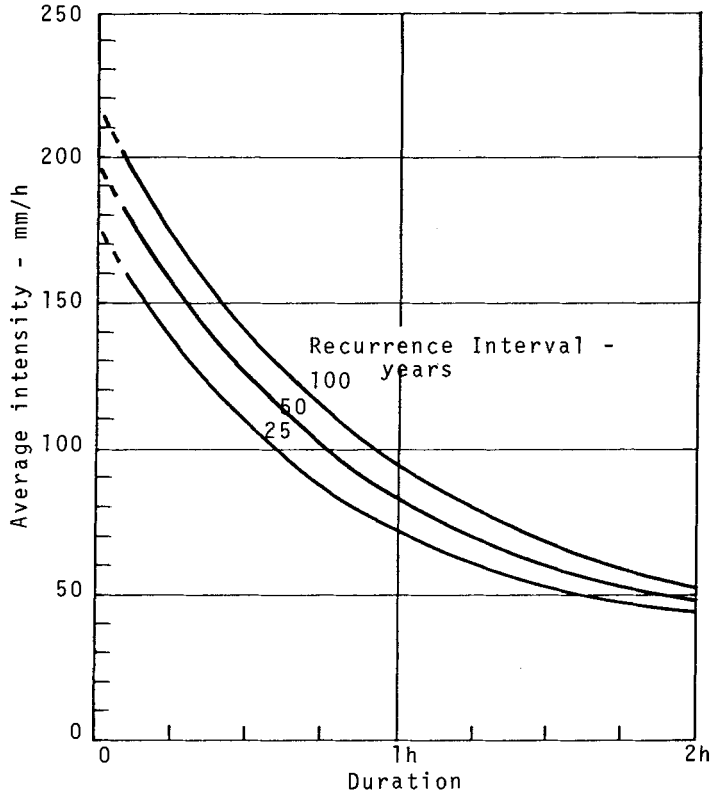


Fig. 2.2 Average Rain Intensity - Duration - Frequency Relationship for Jan Smuts Raingauge

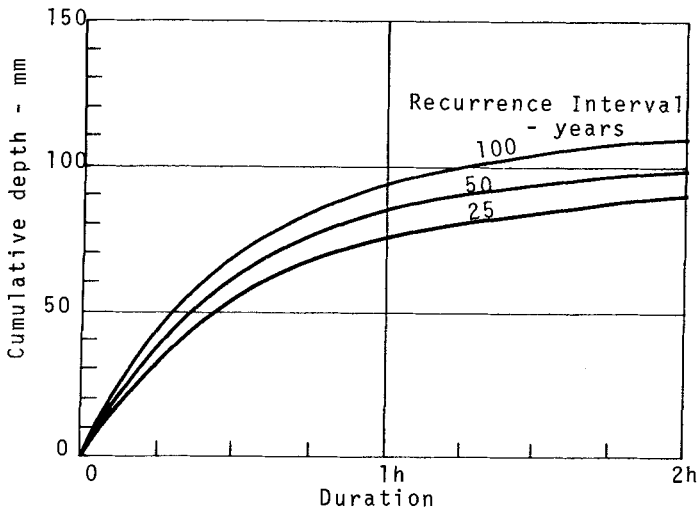


Fig. 2.3 Depth - Duration - Frequency relationship for Jan Smuts Raingauge

the average return period, or recurrence interval, of storms indicated for specific values. Recurrence interval is the average interval between events equal to or greater than the event in question. It is the inverse of the probability of exceedance. The hydrologist may have to rank the data and establish the frequency distribution by interpolation and extrapolation using an assumed probability distribution such as extreme value. Methods of assessing the recurrence interval of storm intensities, and deciding on the risk to take in designing a drainage system, are discussed in a later chapter.

SPATIAL DISTRIBUTION

The intensity of rain varies over a catchment especially in the case of convection-type storms. When studying large catchments it is thus not necessary to assume peak intensity at each point on the surface. Not only may storms have a focus and be represented by contours of equal precipitation (isohyets), but they may also move across a catchment. A numerical analysis of the effect of spatial variation in intensity, and the effect of storm movement, on peak runoff, is presented in the chapter on numerical methods for kinematic flow.

In order to assess the average rainfall over large areas, a weighted average of all the appropriate rain gauges in the catchment may be made. Thiessen (1911) proposed the catchment be divided into polygons (Fig. 2.4). Each inner side of a polygon is midway between two rain gauges and perpendicular to the line joining them. The polygon thus formed around each gauge is taken as the area within which the relevant rain falls.

Another method is to draw isohyets (lines of equal precipitation depth) over the catchment (e.g. Fig. 2.5). Then the areas between isohyets are multiplied by the average rainfall between those isohyets to obtain a total precipitation volume.

For small urban areas e.g. roofs and lots, a uniform intensity may be assumed to fall over the entire catchment, and movement of the storm may be disregarded. For successively larger catchments, a correction may be applied to reduce the average intensity over the catchment when data used are observations from isolated rain gauges. Fig. 2.6 was proposed by the Floods Steering Committee for correcting point rain intensity as a function of catchment area and storm duration for England. The factors also vary with climate, season and topography as indicated by Viessman et al. (1972).

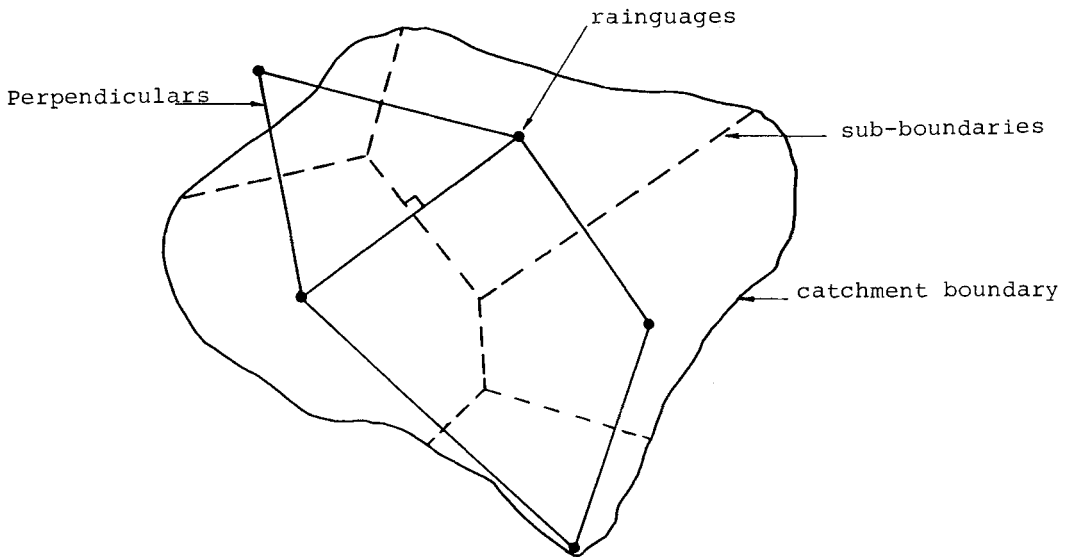
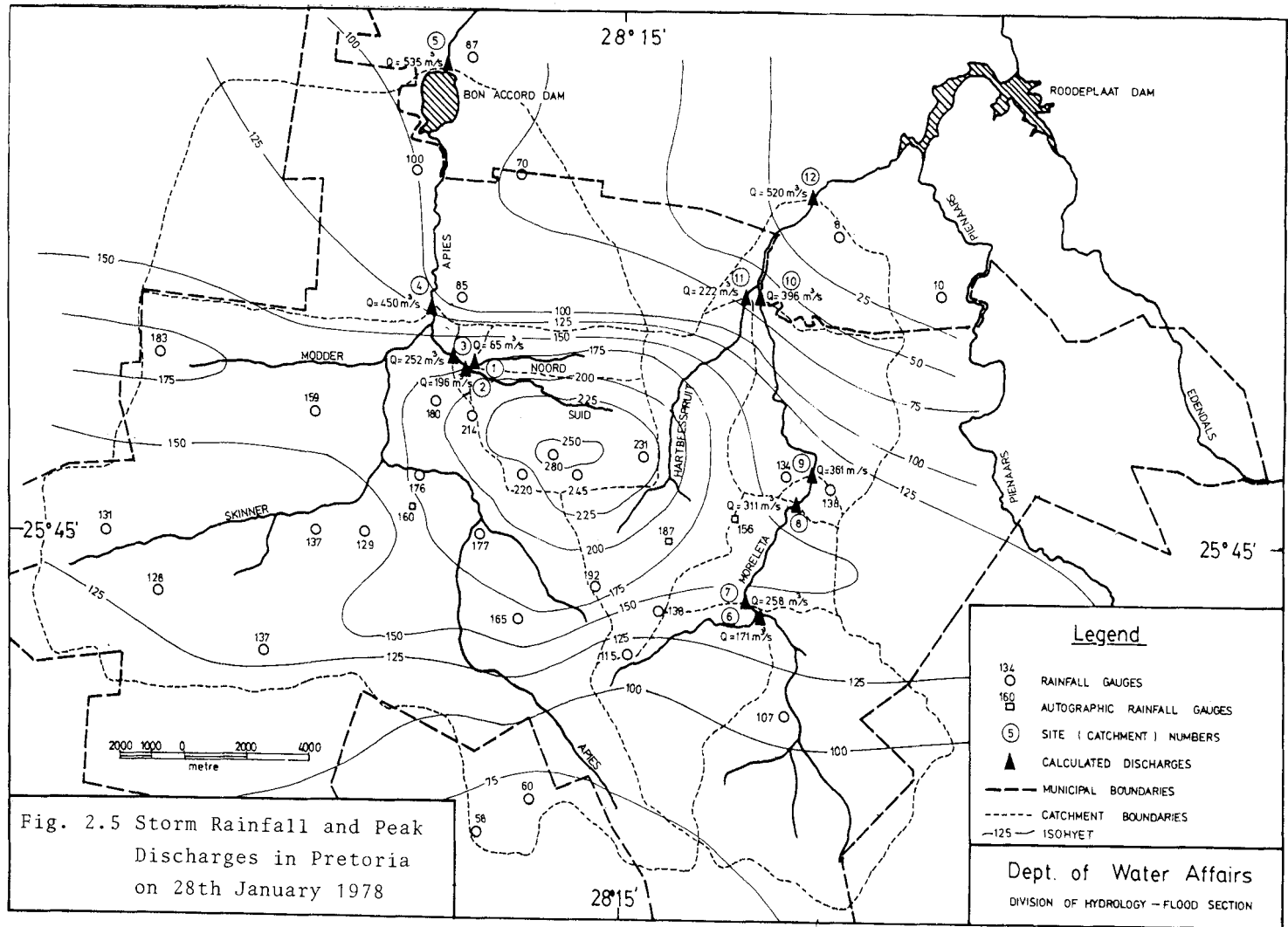


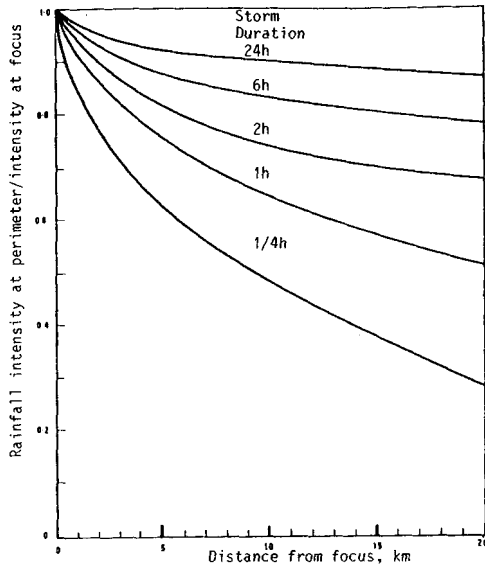
Fig. 2.4 Thiessen Polygons for averaging rainfall over a catchment.

TIME DISTRIBUTION

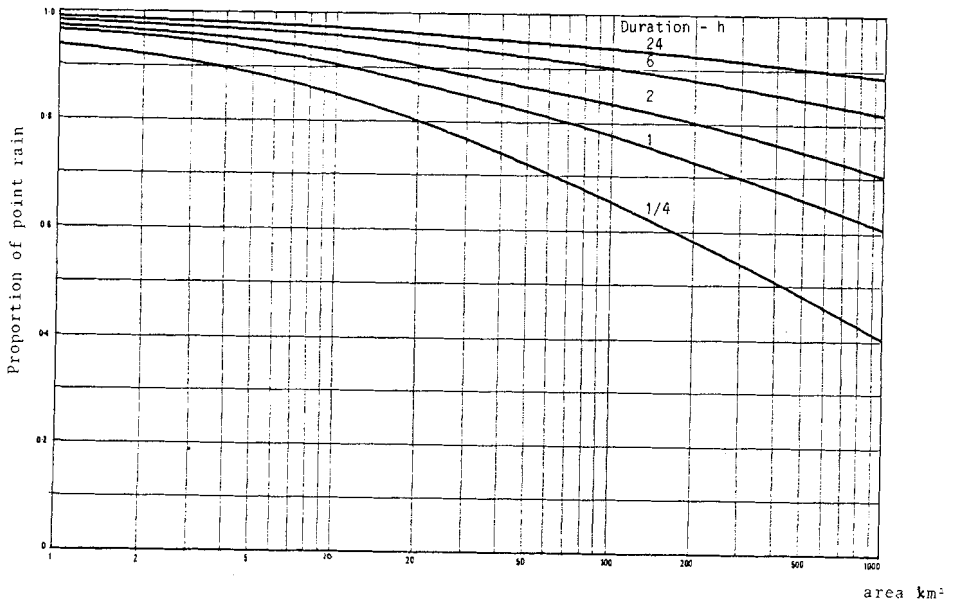
The assumption of a uniform rate of storm precipitation suffers a number of shortcomings as listed below:

- i) Peak runoff from a storm of uniform intensity is likely to be less than that for a storm of the same average intensity but varying in time, especially if it reaches peak towards the end of its duration.
- ii) Since there are initial losses, the antecedent rainfall and the rain during the beginning of the storm is likely to be used in filling depression storage and other losses. For this reason too, a storm which peaks at the beginning of its duration is therefore likely to result in a smaller peak runoff than one which peaks later.
- iii) Whatever storm intensity-duration relationship is adopted, a different storm duration must be employed in designing storm





a. Storm profile across catchment



b. Areal reduction factor

Fig. 2.6 Reduction factors for non-point rainfall

drains for each different size catchment. In fact the design storm duration should equal the concentration time of the catchment for uniform storms and maximum runoff for any selected frequency.

Analysis of storm data in the United States by Huff (1976) indicates a high proportion of a storm occurs in the first part of the storm. He categorized storms by the quartile of the duration in which the bulk of the rain fell. Fig. 2.7 indicates the distribution of precipitation for a 'first quartile' storm.

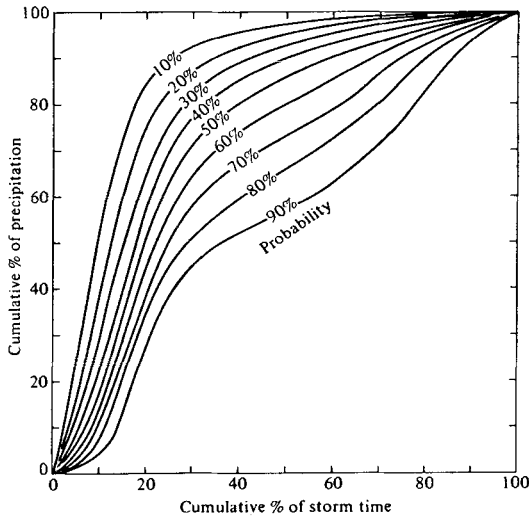


Fig. 2.7: Time distribution of first quartile storms. (After Huff, 1967)

Further analysis indicated storm patterns for differing severity. Thus 90% probability implies that 90% of storms will be more severe than that distribution i.e. will have a greater proportion occurring in the first quartile of the duration.

Chicago-type Synthetic Storm

Keifer and Chu (1957) developed a synthetic hyetograph for storm-water studies in Chicago. They proposed that a hyetograph could be developed which would have the same average intensity as a uniform storm, but it could peak at a chosen time such that the antecedent moisture conditions prior to the peak were such that they result in maximum runoff intensity. The shape of the hyetograph is also such that the average intensity is correct for any storm duration i.e. one hyetograph is sufficient to define any storm.

It is necessary to start with an empirical relationship for average storm intensity versus duration (for any chosen frequency) such as

$$i_a = \frac{a}{(b+t_d)^c} \quad (2.3)$$

where i_a is the average intensity of a storm of duration t_d and a , b and c are constants.

The total precipitation for a storm of duration t_d is:

$$p = i_a t_d = \frac{a t_d}{(b+t_d)^c} \quad (2.4)$$

Hence instantaneous rainfall rate at time t is

$$i = \frac{dp}{dt} = \frac{a[(1-c)t+b]}{(t+b)^{c+1}} \quad (2.5)$$

This is the equation of a hyetograph with the same average rate of rainfall as given by the intensity-duration curve for any storm duration.

The peak rain intensity occurs at the start of the storm, however, which may be unrealistic.

The hyetograph is therefore re-adjusted to peak at some proportion r of its duration after the start. Thus if storm duration

$$t = t_b + t_a \quad (2.6)$$

where t_b is the duration of precipitation before the peak and t_a the duration after the peak,

$$\text{then } t = \frac{t_b}{r} = \frac{t_a}{1-r} \quad (2.7)$$

$$\text{so } i_b = \frac{a[(1-c)t_b/r+b]}{[(t_b/r)+b]^{c+1}} \quad (2.8)$$

$$\text{and } i_a = \frac{a[(1-c)t_a/(1-r)+b]}{[t_a/(1-r)+b]^{c+1}} \quad (2.9)$$

One thus has a synthetic hyetograph which peaks at time rt . The hyetograph will have the same average intensity as the intensity-duration curve indicates for any storm duration. Fig. 2.8 illustrates the resulting hyetograph shape. The correct value of r to use must be determined for anticipated local antecedent moisture conditions. A figure for r of 0.375 was found applicable in Chicago.

The value of the technique lies in the fact that only one hyetograph is needed to obtain design flows for any point in a drainage system.

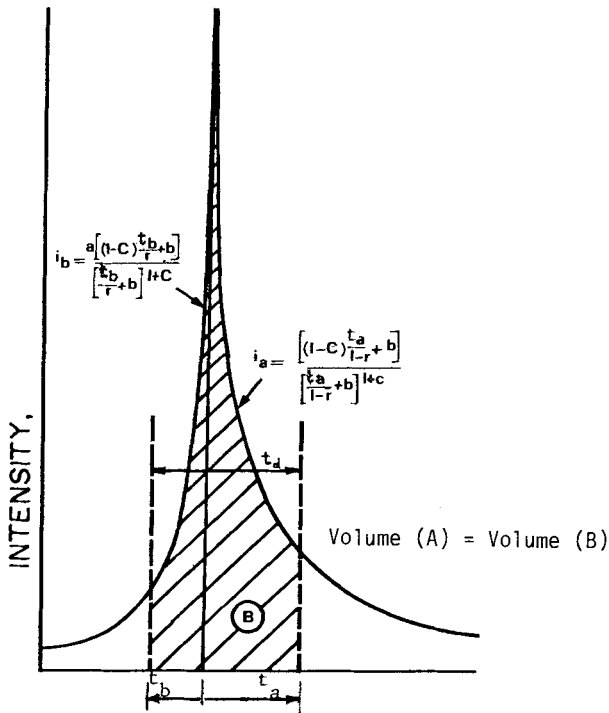
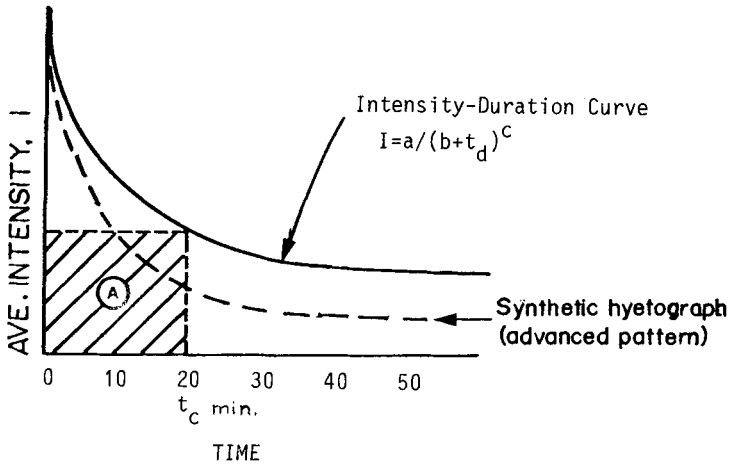


Fig. 2.8 Chicago design storm

Provided one knows the concentration time to the point at which a hydrograph is required, the mean storm intensity is correctly obtained from (2.9). The hyetograph is definitely non-uniform, but whether it represents a real rainfall pattern in all cases is doubtful.

ABSTRACTIONS AND LOSSES

Much of the water in the form of precipitation which reaches the ground does not run off. It is lost immediately or as it runs off overland and down streams. The water may be lost irretrievably such as by evaporation or transpiration, it may return to the stream, such as groundwater, or it may be stored in depressions or on surfaces. If the complete rainfall-runoff process is to be approximated, the correct abstraction and loss functions must be simulated.

Evaporation and Transpiration

Evaporation involves the vaporization of water and consequently abstraction from surface runoff or pools. The rate of evaporation depends primarily on the exposed surface area, but also on temperature, radiant sunlight, wind, atmospheric pressure and impurities in the water. The mean annual rate of evaporation can vary from 200 mm in cold damp climates to 2000 mm in hot arid areas. The peak rate may be as high as 0.3 mm per hour. The rate of evaporation from any surface depends also on the type and the properties of the surface, e.g. hard pavements, porous ground or leaves. Transpiration losses over an area of catchment are often of the same order of magnitude as evaporation from a free surface with the same overall area.

Although the evaporation rate is small in comparison with precipitation rate, (e.g. a light storm may have a rate exceeding 10 mm/h), evaporation continues after rainfall ceases, so the total loss may be significant for large basins and those with long concentration times.

Care should be taken in interpreting pan evaporation figures. Lake evaporation appears to be only about 65 to 80 percent of the corresponding pan evaporation depth. This is due largely to different radiation effects and depths.

Interception

Portion of storm precipitation will be retained on vegetation and other surface cover. The maximum amount of water which is retained will

depend on surface tension effects and the exposed surface area amongst other things. Although the amount intercepted is dependent on storm duration, common practice is to include it in initial abstractions. The total potential interception of trees varies typically from 2 mm to 10 mm.

Depression Storage

The uneven nature of most surfaces will result in some water being trapped. The maximum potential storage is dependent on the surface; thus smooth leveled concrete will retain only a fraction of a millimetre before the balance runs off, while ploughed ground may retain many millimetres of water. Water thus retained may eventually evaporate or seep away. Alternatively the storage ponds may be such that they gradually release water to contribute to the runoff. This is similar to storage routing with a relationship between depth of storage and rate of outflow. The latter form of depression storage is analogous to man-built detention ponds, but on a smaller scale, whereas the permanent storage is analogous to retention storage basins. For short duration storms the retention and detention have the same effect on the peak. In fact it is difficult to distinguish between them in many cases.

Total depression losses up to 10 mm for lawn, or even 25 mm for dense vegetation have been observed. Hicks (1944) reported for general use 5 mm for sand, 4 mm for lawn and 3 mm for clay, but the range is between 1 mm for paved areas and 10 mm for gardens.

Infiltration

Water precipitating on or flowing over porous surfaces seeps in at a rate dictated by the permeability of the surface and the ground porosity. The initial rate of infiltration will depend on the prevailing moisture content. The rate of infiltration will reduce with time during a storm as pores are filled and the water table rises. The decay in infiltration rate can be predicted with Horton's equation (1935):

$$f = f_c + (f_o - f_c)e^{-kt} \quad (2.10)$$

where f is the infiltration rate at time t , k is a decay constant, f_c is the equilibrium capacity and f_o the initial capacity. f_c may be closely approximated by the one-hour infiltration rate, which could vary from 0.2 to 2.0 mm/h for clays, 2 to 10 mm/h for loams and 12 to 25 mm/h for sandy soils. Vegetation can increase these figures many times

(Viessman et al, 1977). Thus 200 mm/h is possible for planted agricultural sandy soil. f_o may vary between 200 mm/h for bare clayey soil to 900 mm/h for planted sandy loam (Wilson, 1974).

A simplified approximation to the decaying infiltration is the constant loss assumption. This may be reasonable for large basins and long duration storms, or for deep porous soils which are unlikely to saturate. The most common nomenclature for the constant rate of infiltration is the ϕ index. It is determined by computing the average loss during a number of storms. For time-varying storm input this may be complicated (Hiemstra et al, 1976). A better approximation is to subtract initial losses and then permit a uniform rate of loss.

In reality the relationship between precipitation, losses, basin recharge and return flow are complex. The input hydrograph must be something like that in Fig. 2.9. This represents the hyetograph, or rate of rainfall together with losses. The resulting input is summated over the catchment and routed to result in an output hydrograph, to which must be added groundwater contribution. The theory of hydrographs is taken further later.

SCS METHOD FOR THE EVALUATION OF LOSSES

The amount of retention on the surface and infiltration are primarily functions of soil type and cover. The United States Soil Conservation Service (SCS) (1972) demarcated a wide range of soil types and allocated them curve numbers (CN) on the following basis.

Ground storage gradually increases after the commencement of a storm, until the ground becomes saturated. At that stage rainfall excess (i.e. runoff) rate becomes equal to the precipitation rate (see Fig. 2.10). Thus the runoff proportion of precipitation increases as the storage approaches saturation. If it could be assumed that they increase in proportion, then

$$\frac{Q}{P} = \frac{S}{S_s} \quad (2.11)$$

where Q is the volume of runoff, P is the volume of precipitation, S is the input volume to ground water storage in the basin and S_s is the input storage at saturation (all in mm or units of depth). Here it is assumed that S occurs in the form of uniform infiltration plus evaporation E plus transpiration T .

$$\text{But } S = P - Q \quad (2.12)$$

$$\text{Therefore } \frac{Q}{P} = \frac{P - Q}{S_s} \quad (2.13)$$

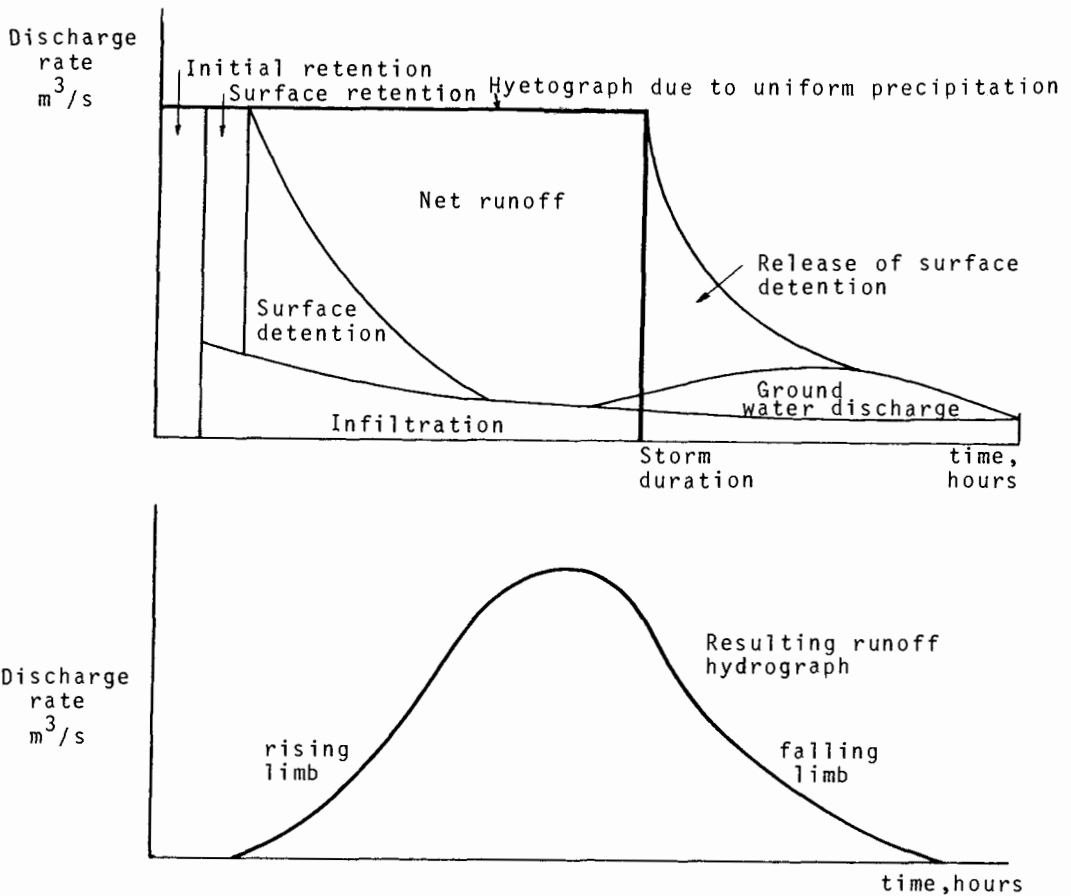


Fig. 2.9 Hydrograph and Hyetograph components.

$$\text{or } Q = \frac{P^2}{P + S_s} \quad (2.14)$$

The SCS established from a wide range of soils that the initial abstraction IA was $0.2 S_s$. Figures by others, e.g. Schulze and Arnold (1979) indicate values somewhat less than this. However, using the SCS value, then allowing for the initial abstraction one obtains

$$Q = \frac{(P - 0.2 S_s)^2}{(P + 0.8 S_s)} \quad (2.15a)$$

and if P is less than $0.2 S_s$ then

$$Q = 0 \quad (2.15b)$$

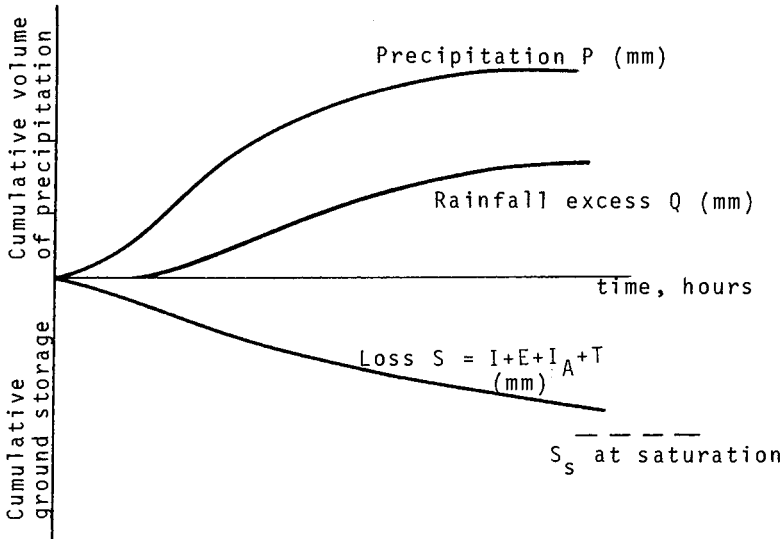


Fig. 2.10 Relationship between precipitation and infiltration losses.

The SCS also established curve numbers (CN) for different soil types, where the maximum soil storage in inches is

$$S_s = (1000/\text{CN}) - 10 \quad (2.16)$$

$$\text{or in mm, } S_s = \frac{25\,400}{\text{CN}} - 254 \quad (2.17)$$

$$\text{Hence CN} = \frac{1000}{S_s + 10} \quad (S_s \text{ in inches}) \quad (2.18)$$

The curve numbers corresponding to different ground curves are tabulated in Table 2.1. There are different numbers for different types of soil, described as groups A, B, C or D, in Table 2.2. There is also an adjustment for antecedent soil moisture (Table 2.3) and for percentage impervious area in the case of urban catchments (Table 2.4). A discussion of the effect of soil moisture on runoff is given by Hawkins (1978).

TABLE 2.1 Runoff Curve Numbers for Selected Land Uses (after Wanielista, 1978) for Antecedent moisture condition 2, and Initial abstraction $0.2S_s$.

Land Use	Hydrologic Soil Group			
	A	B	C	D
Cultivated Land				
Without conservation treatment	72	81	88	91
With conservation treatment	62	71	78	81
Pasture or Range Land				
Poor condition	68	79	86	89
Good condition	39	61	74	80
Meadow				
Good condition	30	58	71	78
Wood or Forest Land				
Thin stand, poor cover, no mulch	45	66	77	83
Good cover	25	55	70	77
Open spaces, Lawns, Parks, Golf Courses, Cemeteries, etc.				
Good condition, grass cover on 75% or more of area	39	61	74	80
Fair condition, grass cover on 50% of area	49	69	79	84
Commercial and Business Areas (85% impervious)	89	92	94	95
Industrial Districts (72% impervious)	81	88	91	93
Residential				
Average Lot Size (m ²) Average % Impervious				
< 500 65	77	85	90	92
1000 40	61	75	83	87
1500 30	57	72	81	86
2000 25	54	70	80	85
4000 20	51	68	79	84
Paved Parking Lots, Roofs, Driveways, etc.	98	98	98	98
Streets and Roads				
Paved with curbs and storm sewers	98	98	98	98
Gravel or paved with swales	76	85	89	91
Dirt	72	82	87	89
Urban Conditions:				
Bare ground	77	86	91	94
Gardens or Row Crop	72	81	88	91
Good Grass (cover greater than 75% of pervious area)	39	61	74	80
Fair grass (cover 50-75% of pervious area)	49	69	79	84
Poor grass (cover less than 50% of pervious area)	68	79	86	89
Fair Woods	36	60	73	79

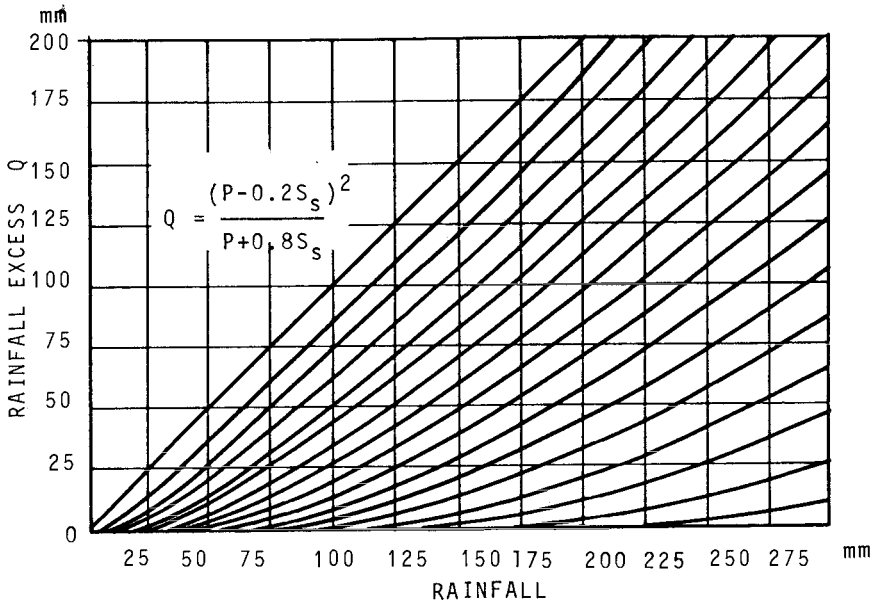


Fig. 2.11 Rainfall excess from curve numbers

TABLE 2.2 SCS Hydrologic Soil Groups

Soil Group	Description
A	Lowest Runoff Potential. Includes deep sands with little silt and clay; also deep, permeable gravel.
B	Moderately low Runoff Potential. Mostly sandy soils less deep and aggregated than A, but group has above average infiltration after wetting.
C	Moderately High Runoff Potential. Shallow soils and soils containing considerable clay and colloids, though less than those of Group D. Group has below-average infiltration after saturation.
D	Highest Runoff Potential. Mostly clays of high swelling percentage, but group also includes some shallow soils with nearly impermeable sub-horizons near surface.

HYDROGRAPHS

Discharge from a catchment following a storm will increase to a peak and then tail off. A plot of flow rate versus time produces a hydrograph. The shape of the hydrograph is a function of many factors, including

TABLE 2.3 CN Adjustments

CN for Moisture Condition 2 (average)	ADJUSTED CNs	
	Condition 1. Soil dry but not at wilting point	Condition 3. When Antecedent Moisture is high
100	100	100
98	87	98
90	78	96
85	70	94
80	63	91
75	57	88
70	51	85
65	45	82
60	40	78
55	35	74
50	31	70
45	26	65
40	22	60
35	18	55
30	15	50

TABLE 2.4 Runoff Curve Numbers for Impervious Areas in Urban Watersheds (Moisture condition 2)

% Impervious Area	Curve No.
100	98
90	97.5
80	97
70	96.5
60	96
55	95
50	94
45	93
40	92.5
35	91
<30	91

storm characteristics and basin topography. The rising limb is a function of the concentration rate of excess precipitation or runoff. Initially there will be retention storage and infiltration losses to subtract from the input. These will diminish if the storm continues until more and more precipitation manifests as runoff. The rate of flow also increases, with the result that initially the hydrograph increases exponentially. At some stage runoff from the furthest parts of the catchment will reach the mouth and a levelling off in runoff is evident. When

the input (precipitation) ceases, the hydrograph will start to fall. Runoff will decrease asymptotically. Continuing surface losses may rapidly reduce outflow to zero. Alternatively the ground water table may rise to such an extent that the aquifer discharges its load downstream to contribute to the total discharge.

Neighbouring catchments may feed into a common downstream river. Then the flows contribute to a single stream. Storage effects due to back-water at junctions is often neglected. In fact it is assumed that contributing hydrographs may be added directly for any point in time to yield a new hydrograph. That hydrograph may then be routed down the river to yield a new discharge hydrograph with the effects of channel storage and the discharge characteristics of the system accounted for.

Hydrograph theory is used to a great extent in the assessment of rural catchment runoff on a regional basis. Implicit behind the development of the theory is that the catchment rainfall-runoff response function is linear. Thus the ordinates of a hydrograph associated with 2 cm of excess rainfall of a certain duration are assumed equal to twice the ordinates of the hydrograph due to 1 cm of excess rain over the same duration. In fact unit hydrographs form the basis for derivation of the hydrographs for any storm in that catchment. Usually the unit hydrograph is prescribed for a storm of unit duration, e.g. 1hr. Then the two-hour unit hydrograph is equal to the sum of the ordinates of two successive unit hydrographs, one lagged one hour relative to the other, and divided by two to reduce it to the hydrograph due to one centimetre of rain instead of two.

By adding successive one-hour hydrographs lagged one hour, one can obtain a massed flow curve for a storm of infinite duration. The resulting curve is referred to as an 'S-curve' (Fig. 2.12).

To obtain a hydrograph for a storm of 'M' hours duration, one subtracts the ordinates the two S-curves, one lagged M hours after the other. The resulting difference should be multiplied by N/M to obtain the hydrograph for a storm of N centimetres depth falling over M hours.

The method is not suitable for small catchments. The critical storm duration is normally less than an hour, and inaccuracies in subtracting the S curves and multiplying by N/M are magnified. Oscillating S curves and even negative hydrograph ordinates may occur. The assumption of linearity is no longer acceptable. In fact the general concept of a unique unit hydrograph for any basin is a gross simplification. In view of the uncertainties and unknowns in rural catchments the techniques are often employed. Application to urban systems can lead to errors, as there is no allowance for the effect of pavements, buildings, canalization or storage.

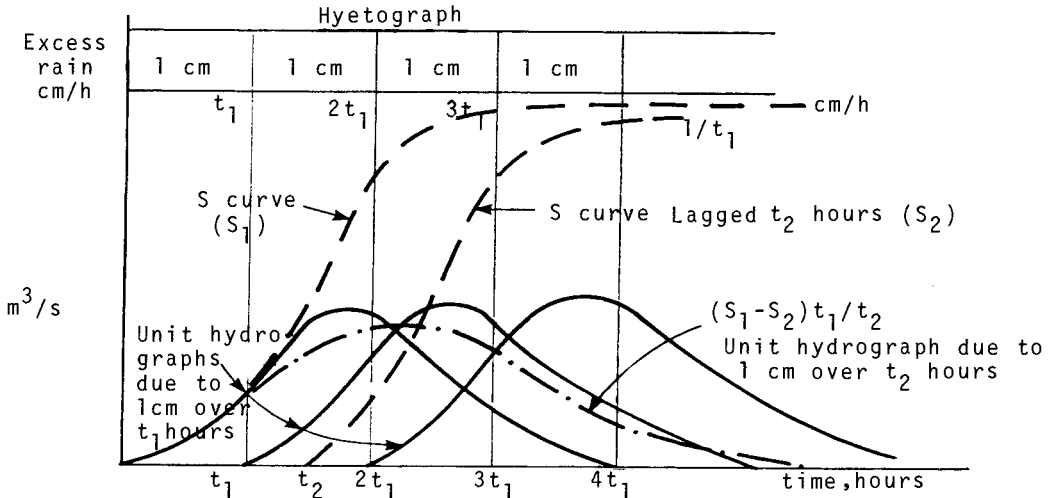


Fig. 2.12 Derivation of S-curve from unit hydrograph

REFERENCES

- Bell, F.C., January 1969. Generalized rainfall-duration-frequency relationships. Proc. ASCE, 95 (HY1), 6537, p311-327.
- Hawkins, R.H., 1978. Runoff curve numbers with varying site moisture. Proc. ASCE, Jour. Irrign and Drainage Div., 104, p.389-398.
- Hicks, W.I., 1944. A method of computing urban runoff. Trans., ASCE, 109.
- Hiemstra, L.A.V., Zucchini, W.S. and Pegram, G.C.S., 1976. A method of finding the family of runhydrographs for given return periods. J. Hydrology, 30, p95-103.
- Horton, R.E., 1935. Surface runoff phenomena, Part 1. Analysis of the hydrograph. Horton Hydr. Lab. Pub. 101 Edwards Bros, Ann Arbor.
- Huff, F.A., 1967. Time distribution of rainfall in heavy storms, Water Resources Research, 3, (4), p1007-1019.
- Keifer, C.J., and Chu, H.H., August 1957. Synthetic storm pattern for drainage design, Proc. ASCE, 83,(HY4), p1332-1352.
- Schulze, R.E. and Arnold, H., 1979. Estimation of volume and rate of runoff in small areas in South Africa based on SCS technique. Agric. Catchments Research Unit Report 8, Pietermaritzburg, S. Africa.
- Soil Conservation Service (SCS), August 1972. National Engineering Handbook, Section 4, Hydrology. Washington, D.C.
- Thiessen, A.H., July, 1911. Precipitation for large areas. Monthly Weather Review, 39, p1082.
- Viessman, W., Knapp, J.W., Lewis, G.L. and Harbaugh, T.E., 1977. Introduction to Hydrology, 2nd Ed. Harper and Row. N.Y. 704 pp.
- Wanielista, M.P., 1978. Stormwater Management, Quantity and Quality. Ann Arbor Science, Ann Arbor, 383 pp.
- Wilson, E.M., 1974. Engineering Hydrology, 2nd Edn. Macmillan, London 232 pp.
- Yarnall, D.L., 1935. Rainfall intensity - frequency data. U.S. Dept Agric. Misc. Public, 204. Washington, D.C.
- Yen, B.C., (Editor). 1978. Storm Sewer System Design, Dept. Civil Eng. University Illinois, Urbana, 282 pp.

CHAPTER 3

STANDARD METHODS OF DESIGN

INTRODUCTION

A major step in the design process is the estimation of drain sizes. To do this the engineer needs to estimate discharge rates. The methods described in this chapter are elementary methods of establishing design flows. Using locally applicable rainfall data the engineer is able to select a storm intensity and convert this to a runoff rate for a particular catchment (Jones, 1971).

The methods described here are based on certain restricting assumptions, the main one being that any catchment has a unique time of concentration equal to the travel time down the catchment. The methodology culminates in the so-called rational method. This expression is the modern version of a number of earlier formulae. Despite their limitations the methods are reputed to yield reasonable answers. (Ardis et al, 1969; Schaake, 1967). The rational method in particular is simple to apply and it is easy to visualize the reasoning behind the formula. Although it only yields an initial design, subsequent refinement by more sophisticated methods and computer modelling are always available.

THE RATIONAL METHOD

The rational formula was proposed by an Irish engineer, Mulvaney, in 1851. It was first adopted in the United States of America by Kuichling in 1889, and in England by Lloyd-Davies in 1905. Lloyd-Davies used the equation in conjunction with an empirical equation for excess rain to yield a relationship between catchment area and runoff rate. The rational equation is

$$Q = CiA \quad (3.1)$$

Q is the flow rate, i is the rainfall intensity and A is the surface area of the catchment, all in compatible units. Thus if A is in square metres and i is in metres per second then Q is in cubic metres per second. C is a dimensionless coefficient normally less than unity. Thus C is the proportion of precipitation rate which contributes to peak runoff rate. Values of C for selected catchment characteristics are indicated in Table 3.1.

The equation implies dimensional homogeneity, but also yields correct values (to within 1 percent) for Q in cubic feet per second if i is in

TABLE 3.1 Rational Coefficient C

URBAN CATCHMENTS			
General Description	C	Surface	
City	0.7-0.9	Asphalt paving	0.7 -0.9
Suburban business	0.5-0.7	Roofs	0.7 -0.9
Industrial	0.5-0.9	Lawn heavy soil, +7° slope	0.25-0.35
Residential Multiunits	0.6-0.7	2-7°	0.18-0.22
Housing estates	0.4-0.6	-2°	0.13-0.17
Bungalows	0.3-0.5	Lawn sandy soil, +7°	0.15-0.2
Parks, cemeteries	0.1-0.3	2-7°	0.10-0.15
		-2°	0.05-0.10

Frequency factor:

Recurrence interval	Multiplier
2-10 years	1.0
25	1.1
50	1.2
100	1.25

RURAL CATCHMENTS (less than 10 km²)

Ground cover	Basic factor	Corrections : Add or subtract
Bare surface	0.40	Slope < 5% : - 0.05
Grassland	0.35	Slope > 10% : + 0.05
Cultivated land	0.30	Recurrence interval < 20y : -0.05
Timber	0.18	Recurrence interval > 50y : +0.05
		Mean annual precipitation < 600mm : -0.03
		Mean annual precipitation > 900mm : +0.03

inches per hour and A is in acres. Although it may appear that C is the ratio of volume of runoff to volume of precipitation, the rational equation is not intended as such i.e. the ratio of total loss to total depth of precipitation is not necessarily (1-C). C is strictly only the ratio of peak runoff intensity of a particular frequency to average rainfall rate for the same recurrence interval assuming a hydraulic balance in the catchment. It therefore accounts for a multitude of phenomena.

The hydrograph shape may be compiled from a simple rectangular model of the catchment, (Fig. 3.1). If the rain continues indefinitely the runoff will eventually equal the excess rainfall rate multiplied by the catchment area for flow balance. Initially the runoff will increase as more and more of the catchment contributes. Thus at any time t, the length of catchment contributing is x and the runoff rate is $C_i A x / L$ where L is the total catchment length.

If the concentration time is independent of the discharge rate then $x/L = t_x / t_L$

$$(3.2)$$

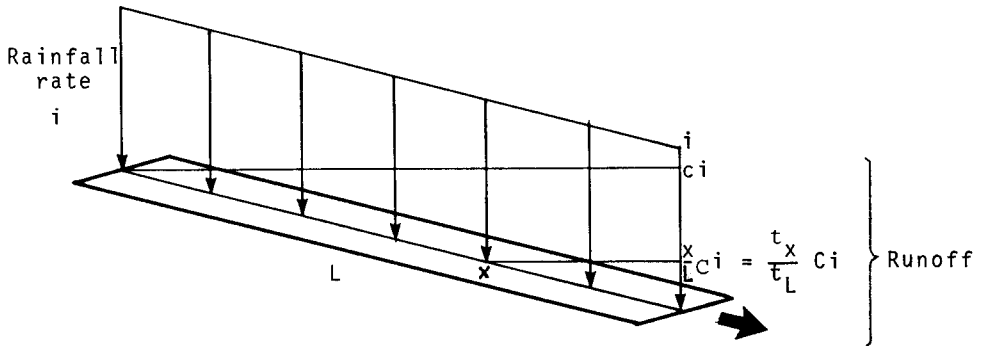


Fig. 3.1 Distribution of rainfall and flow down a simple model catchment.

where t_x is the concentration time over the length x . The hydrograph will therefore increase linearly as depicted in Fig. 3.2 until the entire area is contributing. Runoff will diminish after the rain stops. t_d is the duration of the storm. Then assuming a constant flow velocity the tail of the hydrograph will fall over a time t_c again where $t_c = t_L$ = the concentration time of the catchment.

If the storm stopped at time t_c , then the hydrograph would be triangular with a base equal to $2t_c$ (Fig. 3.3). Thus the area under the triangular hydrograph is $CiAt_c$. This indicates that C represents the ratio of the volume of runoff to volume of precipitation, as well as the ratio of peak runoff rate to precipitation rate.

It is generally accepted, however, that the falling hydrograph tail has a duration exceeding t_c and it may even exceed $2t_c$. Then C does not represent the ratio of volumes. The longer recession limb implies an acceptance that the overland flow velocity reduces as the depth of flow reduces, and casts doubts on the reasoning behind the rational method.

C accounts for initial losses due to depression storage as well as infiltration during the runoff process. It implicitly accounts for the hydrodynamics of the runoff process whereby the runoff from throughout the catchment flows down to the mouth where the discharge Q is to be computed.

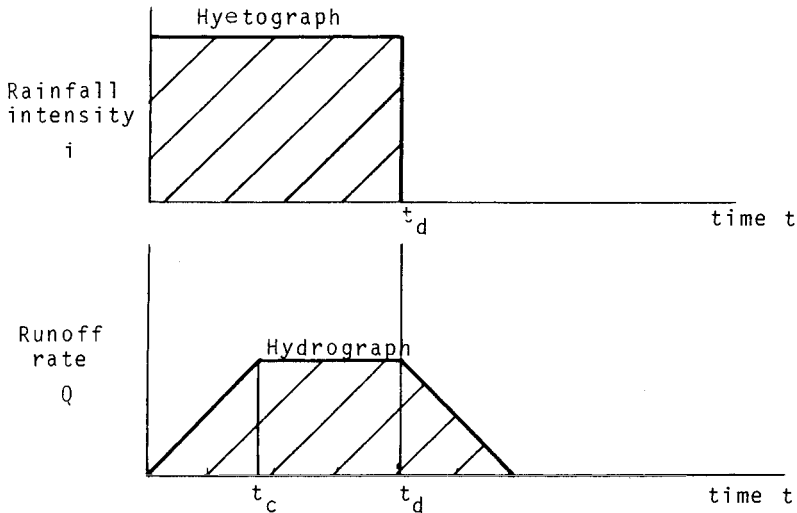


Fig. 3.2 Rainfall and runoff versus time for Fig. 3.1.

It includes the relationship between the recurrence interval of a storm and the recurrence interval of the runoff. For the way to use the formula is to select a storm of known frequency and compute the corresponding runoff assuming the same recurrence interval is applicable. Thus antecedent moisture conditions in the catchment, storm distribution and hydrograph shape are disregarded in deciding C . It is possible that different C values apply to different storms, but the C 's listed here are those found to apply to representative design storms, i.e. of the order of 10 year recurrence interval. Thus the 10 year recurrence interval runoff rate is computed from the 10 year recurrence interval storm using the given C .

Variations in storm distribution in time and space are not accounted for. The effective duration of a storm to use in the intensity-duration relationship may not be the total storm duration. Rainfall intensity may vary during a storm and the duration over which the intensity averages the design figure may be only a fraction of the total storm. Whether the design intensity occurs at the beginning or end of the storm will influence the antecedent moisture conditions which should affect C .

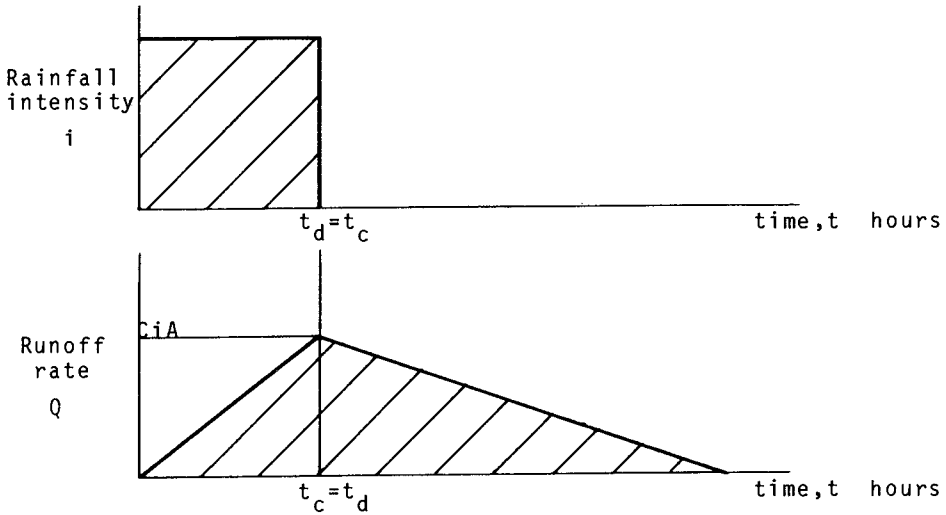


Fig. 3.3 Rainfall and runoff for design storm.

C should theoretically increase with rainfall intensity if losses are independent of intensity. Once the initial fraction is used to replenish initial abstractions, the balance occurs as runoff and the proportion of runoff to total precipitation increases the bigger the storm.

Rossmiller (1980) proposed the following empirical equation for estimating C from a variety of variables:

$$C = 7.7 \times 10^{-7} CN^3 R^{.05} (.01CN)^{-6S^{.02}} (.001CN)^{1.48(.15-I)} \left(\frac{IM+1}{2}\right)^{.7} \quad (3.3)$$

where R is the recurrence interval in years, S is the land slope in percent, I is the rainfall intensity in inches per hour, IM is the fraction of watershed which is impervious, and CN is the SCS curve number.

Now for any selected storm recurrence interval, rainfall intensity reduces with storm duration and conversely increases the shorter the storm, in a manner which can be described generally by an equation of the form

$$i = \frac{a}{(b+t_d)^c} \quad (3.4)$$

where i is the average rainfall intensity, t_d is the storm duration, and a , b and c are constants. It is therefore apparent that the storm which will result in maximum runoff rate should be as short as possible, subject to equilibrium being attained, i.e. for maximum runoff intensity

$$t_c = t_d \quad (3.5)$$

TABLE 3.2 Formulae for time of concentration for overland flow.

Name	Formula for t_c	Comments
Kerby	$3.03 \left[\frac{rL^{1.5}}{H^{0.5}} \right]^{0.467}$	$L < 0.4 \text{ km}$ $r = 0.02$ (smooth pavement) 0.1 (bare packed soil) 0.3 (poor grass or rough bare) 0.4 (average grass) 0.8 (dense grass, timber)
SCS	$\left\{ \frac{0.87L^3}{H} \right\}^{0.385}$	
Bransby-Williams	$\frac{0.96L^{1.2}}{H^{0.2}A^{0.1}}$	
Izzard	$\frac{(.024i^{3.3} + 878k/i^{6.7})L^{6.7}}{(CH^{0.5})^{6.7}}$	$iL < 3.8$ $k = 0.007$ (smooth asphalt) 0.012 (concrete pavement) 0.046 (close clipped sod) 0.06 (dense bluegrass turf)
Airport	$3.64(1.1-C)L^{8.3}/H^{3.3}$	C = rational coefficient
Kinematic	$58N^6L^9/i_e^4H^3$	N = Manning roughness

A = area, km^2

H = elevation difference, metres

i = rainfall rate, mm/h . Subscript e refers to excess (runoff)

L = length of catchment, km

t_c = concentration time, hours

There are many empirical methods for establishing the time of concentration of a catchment. Various formulae in use are summarized in Table 3.2.

The formulae apply to specific types of surface and use of an inapplicable formula should be avoided. Values of the constants in the equations are also indicated. Where compound areas are involved, the concentration time may be estimated by summing the concentration times over individual areas in series. Where the rational method is applied to compound catchments, the formula may be written as

$$Q_P = i \sum_{j=1}^m C_j a_j \quad (3.6)$$

$$\text{where } A = \sum_{j=1}^m a_j \quad (3.7)$$

LLOYD-DAVIES METHOD

Lloyd-Davies in 1905 published a paper on an approach very similar to that of the more modern rational method. It was in fact Lloyd-Davies who proposed that the storm which produces the greatest runoff of all storms of the same frequency, is the one with a duration equal to the concentration time of the catchment. It was assumed that the concentration time was equal to the travel time from the top end of the catchment to the point at which flow is to be determined. He went further in assuming the concentration time was a function of catchment area.

A relationship between excess rainfall intensity and storm duration was also produced. This could be expressed in terms of the Birmingham formula

$$i = \frac{40}{20+t} \quad (3.8)$$

where i is in inches per hour and t is the concentration time in minutes

The formula was varied slightly by others for storm duration less than 20 minutes. The formula was for rainfall in England specifically, for an acceptable recurrence interval storm, which varies from twice a year for short storms to about once in 15 months for storms over 1 hour duration. It is interesting to note that the early British formulae, and even some modern English approaches, allow for runoff off impermeable surfaces only. 100 percent loss is assumed on permeable surfaces and the formulae are quoted as being applicable to stated percentage impermeable surfaces. In fact the runoff formulae went so far as to give runoff directly in many instances (such as the Birmingham formula above). Thus incorporated in the formula is a percentage imperviousness, a storm intensity-duration relationship and a recurrence interval. The formulae are thus more of historical interest than for application. The rational method allows for many of the earlier shortcomings. Nevertheless we are also indebted to Lloyd-Davies for development of the step method of computation of drain sizes.

STEP METHOD

Although the rational method yields a design flow rate at the mouth of a catchment, it does not provide sufficient data to design

the individual drains in a catchment. In fact none of the empirical equations for time of concentration are applicable to built-up areas with impermeable surfaces, artificial channels and circular drains. The concentration time in built-up areas is reduced due to the higher volume of runoff, the smoother surfaces and canalization.

In an effort to account for the flow time through each drain in the accumulation of flow, a step-by-step method was evolved in England by Lloyd-Davies (1905). The runoff from impermeable areas is accounted for, although earlier applications ignored runoff from pervious areas. The runoff from any catchment could be accounted for by applying individual runoff coefficients to each sub-area.

The method in common with the rational method uses a basic assumption contrary to hydrodynamic principles. This is that the concentration time can be estimated from the travel time for full flow down the drains. In fact during flow concentration, flow rates will be less than the maximum, and flow velocities will be correspondingly lower than for the full pipe case. Also at design flow for any pipe, pipes upstream will not be at full flow, as they are designed for a storm of shorter duration and consequently greater intensity. This is offset by another misunderstanding. Water does not need to travel the full drainage system length before an effective equilibrium is attained. In fact reaction time of the system can be faster than flow time, as it is more a function of wave speed than water speed.

Nevertheless, the Lloyd-Davies step method yields results of satisfactory engineering accuracy. It has been found to overestimate peak flow rates for pipes over 600 mm diameter, but in order to improve on the method, more sophisticated mathematics is required, (for example the kinematic method). The Lloyd-Davies method is relatively simple to apply and drains may be sized in a systematic manner. The procedure is set out in tabular form, and calculations proceed from the top drain to successively lower drains (e.g. ASCE, 1969). Although it was common to use a rainfall intensity-duration relationship of the form

$$i = \frac{a}{b+t_c} \quad (3.9)$$

this is not a necessity for application of the method. The computations are set out with the aid of an example (Fig. 3.4) in Table 3.3.

The steps in the computations are as follows (the numbers refer to the columns in Table 3.3):

1. Mark pipe numbers on a plan, proceeding from the top pipe of each leg. In this catchment there are three levels of subdivision of the drains.

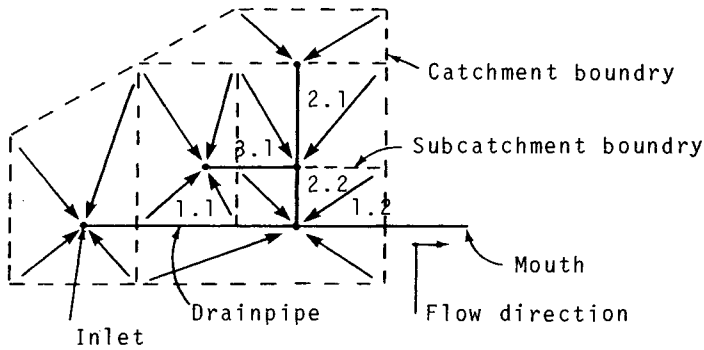


Fig. 3.4 Catchment example for Lloyd-Davies step computations

2. From the contour plan and demarcated subcatchments planimeter the area contributing to each pipe. If the inflow is along the length of the pipe it may be taken as into the head for simplicity. Alternatively (see White, 1978) it may be fed in along the pipe in which case the design storm duration depends on that pipe diameter. The pipe diameter must therefore be determined by trial in such case.
3. The proportion of runoff for each subcatchment must be estimated. The C is similar to the C in the rational formula.
4. The effective contributing area is CA .
5. Add the effective areas down to the pipe in question.
6. Measure pipe lengths from the layout plan.
7. Establish the gradient from contours. In the case of adverse ground slopes or minor drains, the minimum gradient may be dictated by minimum flushing velocity. In this case a trial and error method may be required.
8. The concentration time for upper pipes is based on the time of entry. This varies from 2 to 4 minutes for urban catchments, but may be larger for overland flow. In that case it must be established as in the rational method or the kinematic method. For lower pipes, it is necessary to compare alternative feeders and select the feeder resulting in maximum concentration time. Thus for pipe 2.2 the concentration time down route 2.1 is 153 seconds ($120 + 33$) whereas for route 3.1 it is 150 seconds.

TABLE 3.3 Step Computations

1.	2.	3.	4.	5.	6.	7.	8.	9.	10.	11.	12.	13.
Pipe No.	Contrib. area A(m ²)	Coeff. C	Effec. area CA	Total Σ CA	Length (m)	Slope S	Conc. time t _c (s)	i = $\frac{.052}{630+t_c}$ (m/s) x 10 ⁶	Q = i Σ CA m ³ /s	Dia. mm	Vel. V m/s	Incr. $\Delta t_c = \frac{L}{V}$ L/V
1.1	15000	0.5	7500	7500	180	0.01	180	64	.480	480	2.7	67
2.1	5000	0.5	2500	2500	90	0.02	120	69	.173	250	2.7	33
3.1	8000	0.7	5600	5600	80	0.01	120	69	.389	440	2.5	30
2.2	7000	0.6	4200	12300	50	0.008	153	66	.817	620	2.8	18
1.2	14000	0.3	4200	24000	100	0.0025	247	59	1.417	950	1.9	53

TABLE 3.4 Data for tangent method example

1.	2.	3.	4.	5.	6.	7.	8.	9.	10.	11.	12.	13.	14.
Pipe No.	Contr. area (m ²)	Runoff coeff. C	Effect. area (m ²)	Total Σ CA	Length (m)	Slope (m/m)	Time of entry (s)	Conc. time (s)	i = $\frac{.05}{90+t}$ 10 ⁶ m/s	Q = i Σ CA m ³ /s	Dia. mm	Vel. m/s	Incr. $\Delta t_c = \frac{L}{v}$ s
1.1	4000	0.3	1200	1200	200	0.005	140	140	217	0.261	430	1.7	117
2.1	12000	0.4	4800	4800	50	0.01	120	120	238	1.140	670	3.2	16
1.2	3000	0.5	1500	7500	50	0.008	120	257	144	1.081	690	2.9	1.7

9. The rainfall intensity is assumed to obey the relationship $i = a/(b+t_d)$ where a and b are constants, i is in m/s and t_d is the storm duration, assumed equal to travel time for maximum runoff rate.
10. Establish the peak discharge rate by multiplying i by the total effective contributing area.
11. Pipe diameter may be selected from a flow versus head loss chart, which will also yield flow velocity for (12). It is unlikely that the full-flow pipe diameter so yielded will be a standard commercially available pipe size. In such cases the nearest larger standard pipe size is selected, and the pipe may run part-full. Theoretically the flow velocity will then be different, but it is often conservative to utilize the full-pipe velocity.
12. The flow velocity at design discharge can be read from pipe charts or calculated.
13. The increment in travel time is now calculated by dividing the length of the pipe just determined by flow velocity. This increment is added to the travel time down preceding pipes to obtain travel time to the next lower pipe.

TIME-AREA DIAGRAM AND ISOCHRONAL METHODS

If travel time is assumed to be independent of storm intensity then every point in the catchment will have a unique travel time to the mouth or point of discharge. In fact one could plot isochrones on a catchment map as illustrated in Fig. 3.5. An isochrone in this context is a line of constant travel time. On a simple plane isochrones may be equidistant. Where conduits and overland flow are involved, water velocity down conduits is generally faster than over land, so the isochrones may exhibit anomalies at conduits.

For design purposes it is sufficient to mark isochrones along the conduits proceeding from the outer extremities and marking down each drain. After reaching an intersection one can correlate isochrones on each leg meeting at the intersection. By joining points of equal travel time one establishes isochrones. Ultimately the entire catchment is thus demarcated into time zones.

One could then plot a graph of area contributing to the flow at the mouth of a catchment against time. As time passed, so more and more runoff from further up-basin would reach the mouth until the entire catchment area was contributing. The time-area diagram shows the rate of build-up in contributing area (which is assumed proportional to flow) during the entire storm. It is a massed area curve. If area is

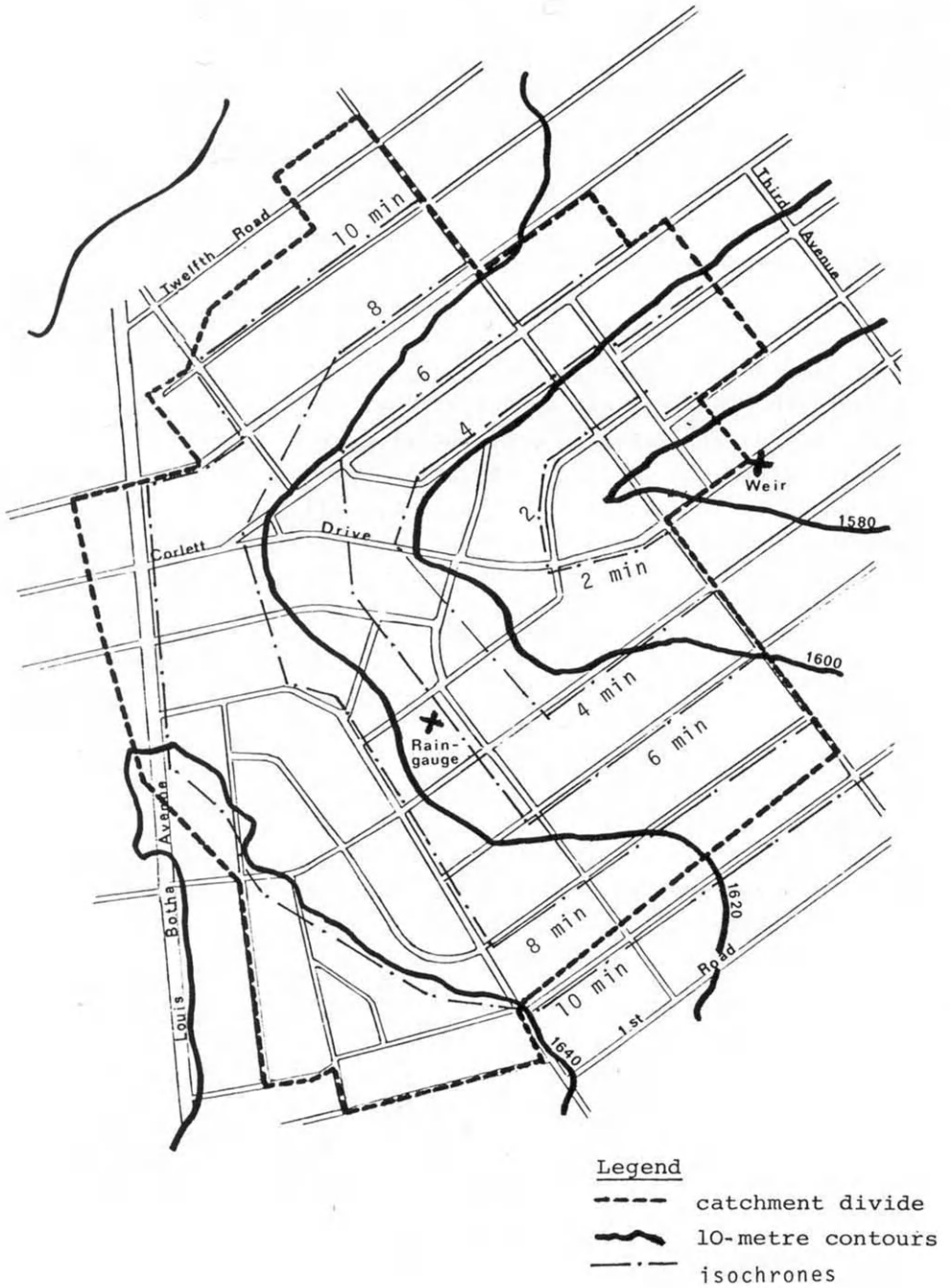


Fig. 3.5 Contour plan with isochrones

multiplied by excess rain intensity one obtains a massed flow. The slope of such a curve is proportional to flow rate. The storm intensity, however, also affects the runoff rate, and this is a function of duration. It is therefore necessary to consider the storm intensity-duration relationship together with the time-area graph and this is what the tangent method does (Watkins, 1962; White, 1978).

TANGENT METHOD AND MODIFICATIONS

The step method outlined will yield a successively larger concentration time and hence longer design storm, for successive pipes, i.e. it assumes the entire basin must contribute for the maximum runoff. This is not necessarily so, as some outlying areas of the catchment may not contribute significantly to the area, but could nevertheless add to the travel time down the catchment. For odd catchment shapes, it will be shown that the rate of runoff can exceed that calculated using the Lloyd-Davies method. This stems from the time-area diagram which uses the steepest segment to define the effective contributing area for maximum runoff intensity.

The application of the tangent method to a time-area diagram will be demonstrated with the example in Table 3.4. The example is illustrated in Fig. 3.6. Before constructing the time-area graph it is necessary to do the steps in the Lloyd-Davies calculations (Table 3.4).

In Fig. 3.7 are plotted the various contributing areas, starting on the time axis at the time at which they start to contribute and building up to the full value over the time of entry for that area. Thus the area contributing to drain 1.2 will reach the mouth first. The flow from this area will start at $t = 17s$, the travel time down the drain.

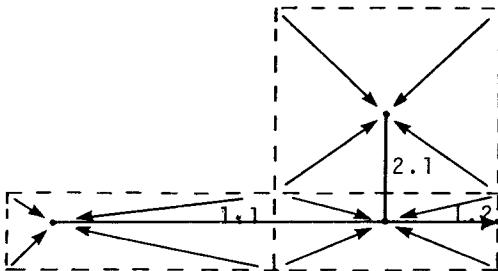


Fig. 3.6 Catchment example for tangent method.

The buildup time for each drain is its time of entry (or overland flow concentration time). If inflow were over the entire length of drain, outflow would begin immediately and built up over $t_e + t_L$ where t_e is the time of entry and t_L is the travel time for that drain. Tracing back through the drainage system, each contributing area is plotted, commencing at its time of arrival at the mouth. Each contributing hydrograph (or in this case area-graph) will rise over its time of entry and then become horizontal, implying equilibrium is reached for that sub-catchment. Each line is lagged by its travel time to the mouth. The total area graph is the sum of the individual area graphs, in the correct time positions (line OMNPQRST). It will be noted that portions of the area graph are steeper than others, in particular over the time during which the lateral contributions arrive. This fact points to the possibility that the peak discharge may result from a storm over the duration of the steeply rising portion of the area graph and not for the full concentration time of the basin. The shorter storm will be more intense and this may more than offset the reduction in area by omitting the flatter portions of the curve. If one assumes a storm intensity-duration relationship of the form

$$i = a/(b+t_d) \quad (3.9)$$

$$\text{then } Q = iA = aA/(b+t_d) \quad (3.10)$$

$$\text{Hence } Q/a = A/(b+t_d) \quad (3.11)$$

Thus discharge Q is proportional to the slope of a line with a vertical to horizontal slope of A to $(b+t_d)$. A line drawn from $-b$ on the $A=0$ axis in Fig. 3.7 and tangential to the outside of the area graph will have a slope proportional to the runoff from the entire catchment. Runoff from a portion of the catchment may, however, produce the peak flow. This will be represented by a line not originating at the base of the area diagram.

Now to find the worst (maximum) rate of runoff it is necessary to find the steepest possible tangent. This is done most easily by drawing another time-area line, a distance b in the time axis direction before the original time-area line. (Line $O' N' P' Q' R' S' T'$ in Fig. 3.7) Now draw in a straight line tangential to the convex down part of this curve and also tangential to the convex upward part of the original curve (line $N' R$). This indicates that the maximum runoff will be associated with a storm of duration $t_d = t_R - t_{N'}$, $-b = 154 - (-54) - 90 = 118\text{s}$. The corresponding contributing area is $\Delta A = A_R - A_{N'} = 6450 - 200 = 6250\text{m}^2$ and the runoff is $Q = \Delta A a / (b + t_d) = 6250 \times 0.05 / (90 + 118) = 1.50\text{m}^3/\text{s}$.

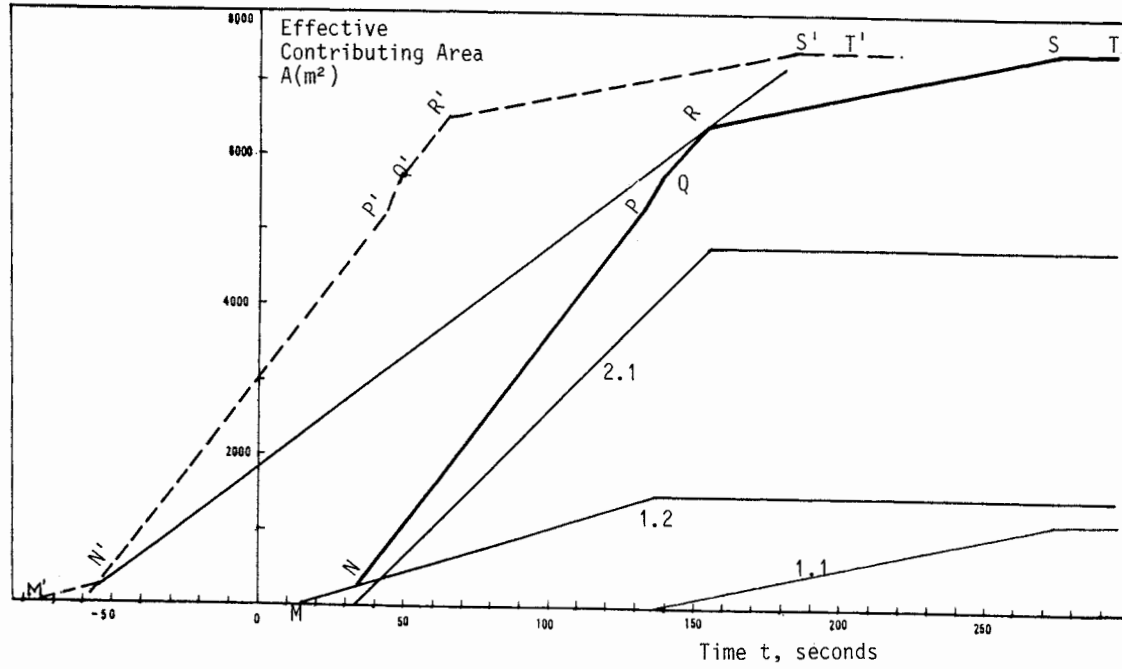


Fig. 3.7 Time-area diagram and tangent solution

An alternative method is as follows: Instead of drawing one tangent line, two parallel lines spaced b apart on the time scale are required. For maximum discharge, the left hand line should be tangential to the convex upward part of the curve as before. The right hand lower line should be tangential to the convex downward part of the area-time curve. To find the points of tangency resulting in maximum slope it is necessary to keep the right hand line tangential to the convex downward part of the curve and gradually increase the slope from the horizontal until the parallel line spaced b to the left is also tangential to the convex upward part of the curve. At this stage the maximum slope is achieved. The corresponding discharge Q is equal to the line slope multiplied by $a\Delta A/(b+t_d)$ where ΔA is the contributing area between the two points of tangency i.e. the vertical distance, and the design storm duration t_d is the horizontal distance between the same points.

The tangent method has been modified to allow for storm intensity-duration relationships not of the form suggested previously. Formulae of the following more general form have received recent recognition:

$$i = \frac{a}{(b+t_d)^c} \quad (3.12)$$

This type of formula produces curved tangent curves. Escritt (1972) proposed that transparent overlays be prepared on which a number of tangent curves of equal runoff be drawn. The method is time-consuming and not recommended. The extra effort is seldom worthwhile. If necessary the method could be replaced by numerical methods.

The tangent methods are generally time consuming and not recommended for all catchments. An inspection of the plan should reveal whether there are outlying or sparse areas not likely to contribute to the runoff but which would influence the concentration time of the basin.

Escritt (1972) suggests that a modified rational method yields reasonable results for small catchments. He recommends taking a rainfall intensity independent of storm duration for durations less than 15 minutes in England. Thus for a three-year recurrence interval storm in England he suggests a storm intensity of 1 inch (25 millimetres) per hour. This procedure does away with the need for time of concentration calculations. It is also stated that it eliminates the necessity of doing a time-area graph.

In general in order to do numerically what the tangent method does in locating the critical contributing area, it is necessary to resort to a trial and error method. Once travel times are established for all points in the drainage system, a storm of a selected duration, equal

to or less than the longest travel time is selected. By multiplying C_i by the area between any two isochrones spaced t_d apart, a runoff rate is yielded. This is repeated for different isochrones and for different storm durations. The worst storm is then selected from the results.

REFERENCES

- American Society of Civil Engineers (ASCE), 1969. Design and Construction of Sanitary and Storm Sewers. 332pp.
- Ardis C.V., Dueker K.J., and Lenz A.T., January 1969. Storm drainage practice of 32 cities. Proc. ASCE, 95(HY1), 6365, p383-408.
- Escritt, L.B., 1972. Sewerage and Sewage Disposal. Macdonald and Evans, London, 494pp.
- Jones, D.E., February 1971. Where is urban hydrology practised today. Proc. ASCE, 97(HY2), 7917, p257-264.
- Lloyd-Davies, D.E., 1905. The elimination of storm water from sewerage systems. Min. Proc. Inst. Civ. Engineers, 164(2). p41-67.
- Rossmiller, R.L., 1980. The rational formula revisited. Proc. Int. Symposium on Urban Storm Runoff. University Kentucky, Lexington.
- Schaake, J.C., Geyer, J.C. and Knapp, J.W., Nov. 1967. Experimental Examination of the Rational Method. Proc. ASCE, 93 (HY6), 5607, p353-370.
- Watkins, L.H., 1962. The Design of Urban Sewer Systems. Road Research Tech. paper 55, HMSO.
- White, J.B., 1978. Wastewater Engineering, Edward Arnold, London, 318pp.

CHAPTER 4

KINEMATIC FLOW THEORY

INTRODUCTION

Hydrological methods used regularly in practice for the design of stormwater drainage systems include the rational method and other isochronal methods. That is, they assume each point in the catchment has a unique travel time to the mouth. These methods do not account for storage in the system and the time variation in flow rates. Storage may occur on the surfaces of vegetation, roofs, walls, on the ground, in depressions and in channels. The storage may be permanent (retention) or temporary (detention). The relationship between flow depth and discharge and the effect of surface friction of the catchment are not accounted for either. The rational method and the isochronal methods are based on the assumption of uniform flow throughout the catchment. Concentration times in channels are calculated from steady-state water velocities and the dynamics of the system are not accounted for. In fact, there is a gradual increase in depth of flow with time at any point on the catchment and the depth of flow gradually increases down the catchment. The flow is therefore both unsteady and non-uniform. The time to equilibrium is therefore a function of rate of precipitation and it is not necessarily the travel time down the catchment. The kinematic method accounts for these factors in a simplified manner. It also accounts for catchment slope, roughness and infiltration.

Flow rate and velocity are related to depth according to the discharge relationships. In fact even the assumption of the steady state depth-discharge function can in some cases lead to error. Momentum and energy balance are necessary for a true representation of flow conditions through the system. Nevertheless, the full differential equations of motion, termed the Navier-Stokes equations, are complex and not warranted in most circumstances. Even the one-dimensional St. Venant equations can be simplified in many instances as will be illustrated later.

EQUATIONS OF MOTION

The differential equations describing one-dimensional flow in open channels may be derived from consideration of continuity and momentum

balance. The following assumptions are made at this stage:

- (i) Flow is one-dimensional i.e. in one direction. Acceleration in the directions perpendicular to the flow direction is therefore neglected.
- (ii) The pressure at any depth is the hydrostatic pressure.
- (iii) Depth is constant across any section, i.e. the channel is rectangular.
- (iv) Momentum transferred to the flow from lateral inflow is negligible.
- (v) The fluid is incompressible.
- (vi) The uniform flow friction equation applies to non-uniform and gradually varied flow.
- (vii) The bed gradient is small, so that $\theta = \tan \theta = \sin \theta = S_0$
- (viii) Velocity is constant across any section.

The continuity equation may be derived by considering the balance of flow across the boundaries of an element such as in Fig. 4.1.

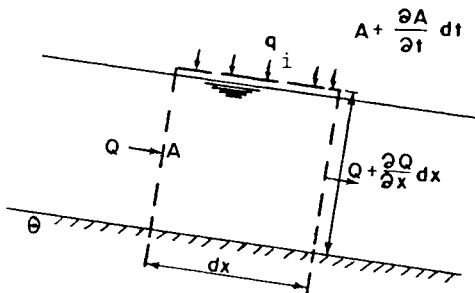


Fig. 4.1 Continuity of flow.

Equating inflow to outflow plus increase in storage produces directly

$$\frac{\partial Q}{\partial x} + \frac{\partial A}{\partial t} = q_i \quad (4.1)$$

where Q is the flow rate, A is the cross sectional area, q_i is lateral inflow per unit length in the x direction and t is time.

A dynamic balance is obtained by equating the unbalanced force across an element to the acceleration and change in momentum across the element as illustrated in Fig. 4.2.

Thus, since $F_n = \bar{w}A$ and $F_s = wA S_f dx$, we have

$$\frac{\partial}{\partial x} (w\bar{y}A) dx + wA S_f dx - wA S_o dx = - (w/g) \frac{\partial}{\partial x} (Av^2) dx - \frac{w}{g} A \frac{\partial v}{\partial t} dx - \frac{w}{g} q_i v dx \quad (4.2)$$

Re-arranging this,

$$g \frac{\partial (\bar{y}A)}{\partial x} + \frac{\partial (Av^2)}{\partial x} + A \frac{\partial v}{\partial t} = Ag (S_o - S_f) - q_i v \quad (4.3)$$

If the channel is rectangular and flow is nearly uniform, this simplifies to

$$g \frac{\partial y}{\partial x} + v \frac{\partial v}{\partial x} + \frac{\partial v}{\partial t} = g (S_o - S_f) - q_i v/A \quad (4.4)$$

Equations (4.1) and (4.4) were first published by St. Venant (1848). These can be solved numerically for various cases of unsteady flow in open channels. The equations are not simple to solve. The inclusion of the terms for acceleration and change in momentum are in some cases not worthwhile, in which case solution of the equations is simplified.

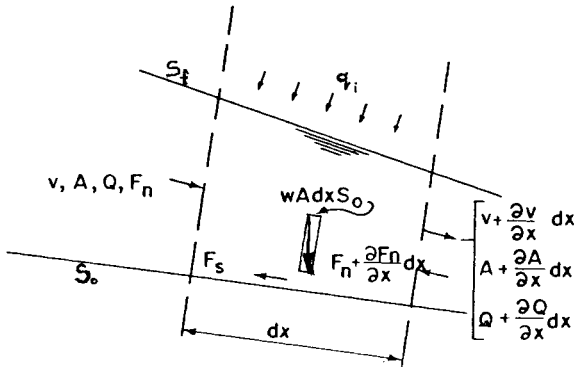


Fig. 4.2 Momentum balance in flow direction.

In the above equations, F is a force, y is the depth of flow, \bar{y} is the depth of the centroid, S_o is bed slope, S_f is friction gradient, g is gravitational acceleration, w is the unit weight of fluid, and v is the flow velocity.

KINEMATIC EQUATIONS

In many cases of overland flow and even open channel flow, the momentum change and acceleration terms can be neglected. In fact this is equivalent to assuming that the energy line is parallel to the bed, i.e.

$$S_f = S_o = S \quad (4.5)$$

It is not difficult to imagine this holds in the case of overland flow. Over a distance of 100 metres the ground surface may fall of the order of one metre whereas the difference in depth of flow over the same distance will only be of the order of a millimetre. The corresponding difference in velocity head may be of the order of 10 mm. The resulting simplified equations are termed the kinematic equations. They are equivalent to the assumption of unsteady uniform flow.

Most equations for friction gradient can be written in a form relating depth of flow y to flow per unit width q , with an equation of the form $q = z y^n$. (4.6)

Here z is a constant involving g , S_f , and the fluid and surface properties. For laminar flow n is unity, while for turbulent flow in rough conduits n is 2. Overton and Meadows (1976) indicate that in the case of overland flow the flow can be turbulent at very low Reynolds numbers (transition $Re = iL/\nu = 20$ to 2000). This is largely due to the effect of rain falling on the surface. Here i is the rainfall rate, L is the length of flow path and ν is the kinematic viscosity of the fluid, water. For rough surfaces the popular Manning equation indicates a value for n of $5/3$ and z is $KS^{1/2}/N$, where N is Manning's roughness coefficient and K is 1 in SI units and 1.486 in fps units. If the Manning roughness N is approximated by $0.13Kk^{1/6}/g^{1/2}$ the dimensionless Manning-Strickler flow equation results:

$$q = 7.7(Sg)^{1/2} y^{5/3} / k^{1/6} \quad (4.7)$$

The discharge equation must be considered together with the continuity equation (4.1) which when expressed in terms of flow per unit width, q , becomes

$$\frac{\partial q}{\partial x} + \frac{\partial y}{\partial t} = i_e \quad (4.8)$$

where the excess rainfall rate $i_e = i - f$ and i is the rainfall rate and f is the loss rate, all per unit area.

SOLUTION OF THE EQUATIONS FOR OVERLAND FLOW

General solution of the two equations (4.6) and (4.8) is possible for various situations of overland flow and sometimes conduit flow. Numerical solutions by computer are comparatively easy (Wooding, 1966; Constantinides and Stephenson, 1981) and many computer models are based on these simplified equations instead of the more rigorous differential equations. In many situations the equations are satisfactory even for conduit flow. This is the case for relatively steep gradients, but where

backwatering and rapid changes in flow or gradient occur, the rigorous equations must be employed.

Woolhiser and Liggett (1967) analyzed the rising limb of an overland flow hydrograph using both the kinematic and the complete equations. Their results indicate that the kinematic form of the equations is reasonably accurate for gh/v^2 greater than about 10 (h is the elevation difference down the length of the catchment and v is the equilibrium flow velocity at the end of the catchment).

The value of the kinematic method lies in the feasibility of obtaining analytical solutions. Thus expressions describing the shape of a hydrograph and the concentration time for different cases of overland flow and channel flow were derived by Wooding (1965) and others.

The classical method of solution of the equations for overland flow is by the method of characteristics (Henderson, 1966; Eagleson, 1970). This method involves the substitution of total differentials for partial differentials while integrating along a so-called characteristic line where x is related to t . Elements of the method can be explained without a complete mathematical background. This is attempted in the following section in order to introduce the reader to some of the resulting solutions which have been achieved.

Equations (4.6) and (4.8) may be used to derive some useful relationships in the case of constant excess rainfall rate i_e .

$$\text{Recall that } q = zy^n \quad (4.6)$$

$$\text{Then } y = (q/z)^{1/n} \quad (4.9)$$

$$\text{Now put } \frac{dx}{dt} = \frac{dq}{dy} \quad (4.10)$$

$$= nzy^{n-1} \quad (4.11)$$

$$= nq^{1-1/n} z^{1/n} \quad (4.12)$$

(i.e. consider an imaginary wave travelling at a speed

$$\frac{dx}{dt} = n z y^{n-1} \text{ down the basin}).$$

Then the total differential

$$\frac{dy}{dt} = \frac{\partial y}{\partial t} + \frac{\partial y}{\partial x} \frac{dx}{dt} \quad (4.13)$$

$$= (i_e - \frac{\partial q}{\partial x}) + \frac{q^{1/n-1}}{nz^{1/n}} \frac{\partial q}{\partial x} nq^{1-1/n} z^{1/n} \quad (4.14)$$

$$= i_e \quad (4.15)$$

i.e. the depth of flow increases at the rate of excess rain when travelling at the speed $\frac{dx}{dt} = nzy^{n-1}$ down the basin.

$$\text{Since } \frac{dy}{dt} = i_e \quad (4.15)$$

$$\text{it follows that } y = i_e t \quad (4.16)$$

Hence
$$\frac{dx}{dt} = nz(i_e t)^{n-1} \quad (4.17)$$

Integrating:
$$x = z i_e^{n-1} t^n \quad (4.18)$$

Thus water starting at the beginning of the storm at the top of the basin and travelling down the basin until $x = L$ (the length of the basin) will reach $x = L$ at a time given by

$$t_c = (L/z i_e^{n-1})^{1/n} \quad (4.19)$$

and then $q = z y^n \quad (4.20)$

$$= z (i_e t)^n \quad (4.21)$$

$$= z i_e^n L / z i_e^{n-1} \quad (4.22)$$

$$= L i_e \quad (4.23)$$

Thus the outflow equals the input at this point in time and there must be equilibrium after this time. Thus t_c is the concentration time of the basin. Note that it is not a function of the final equilibrium velocity at the mouth, but depends on the rate of flow buildup along the basin. In fact, the speed of propagation at any point is nv where the water velocity $v = q/y$ (4.24)

$$= z y^{n-1} \quad (4.25)$$

The relationship between wave celerity and flow velocity may be seen by comparing (4.11) and 4.25).

Thus the travel time at equilibrium is greater than the concentration time by the factor n (1.67 in the Manning equation). The practice of assuming that travel time equals storm duration for maximum peak runoff can therefore be unsafe as it results in an underestimate of design storm intensity.

There is some confusion between concentration time, lag time, time to equilibrium and travel time, and various authors have adopted different interpretations. The following definitions are used throughout this text:

Time to equilibrium, t_e is the time from the commencement of the storm to equilibrium flow conditions at the discharge point. It may be shown that for a plane $t_e = (L i_e^{1-n} / z)^{1/n}$ (4.19)

Travel time, t_t , is the time it takes for a drop of water to proceed from the most remote part of the catchment to the discharge point. The water velocity varies in time and space, and the custom is to assume steady-state flows and varying velocities longitudinally. It equals inlet time (from overland and roofs) plus flow time in drains. It was shown that for a plane $t_e = (1/n)t_t$.

Concentration time, is here defined as the time it takes for the flow to become steady at the discharge point. It is therefore equal to the

time to equilibrium. Overton and Meadows (1976) on the other hand define it as the travel time.

Lag time, t_L , is the time between 50% of the rainfall and 50% of the runoff. It may be shown that for a plane $t_L = \{n/(n+1)\}t_e$.

Storm duration, t_d , is the time from the commencement of the storm to the end of precipitation.

An expression for the discharge at the mouth of the basin is obtained as follows: At any time before the limiting characteristic (from the top end of the basin) reaches the mouth, then at the mouth,

$$\frac{\partial q}{\partial x} = 0 \quad (4.26)$$

This is because the depth at every point other than influenced by the upstream boundary increases uniformly at a rate i_e .

$$\text{Thus } y = i_e t \quad (4.27)$$

$$\text{and from (4.6) } q = z(i_e t)^n \quad (4.28)$$

If the rain stops at some time t_d at or after t_c , then an expression for the falling hydrograph leg may be derived as follows: Since for equilibrium at any point before the rain stops

$$q = x i_e \quad (4.29)$$

$$\text{where } x \text{ is the distance from the top end of the basin then from (4.6),} \\ x = z y^n / i_e \quad (4.30)$$

After the rain stops $dy/dx = 0$ and surface water will flow down the basin at a constant speed $dx/dt = n z y^{n-1}$ (4.11)

$$\text{Thus } x = x_0 + \frac{dx}{dt} (t - t_d) \quad (4.31)$$

$$= z y^n / i_e + n z y^{n-1} (t - t_d) \quad (4.32)$$

At the end of the basin $x = L$ so the discharge is given by the implicit relation

$$L = q / i_e + n q^{1-1/n} z^{1/n} (t - t_d) \quad (4.33)$$

The shapes of the rising and falling legs of the discharge hydrograph are illustrated in Fig. 4.5 for various cases. Three cases are illustrated. For comparison purposes the total amount of rain has been assumed constant but the storm duration is varied. Thus for a storm which stops before $t_c = (L/z i_e^{n-1})^{1/n}$, spatial equilibrium will not be reached. The rising limb will follow Equ. 4.28 until the rain stops. Then discharge will remain constant since depth will be the same over a length of basin until the effect of the upstream basin boundary reaches the mouth. Then the hydrograph will fall. The case when $t_d = 0$ is that of the instantaneous hydrograph. For the limiting case when rain duration equals the concentration time, the falling limb will immediately follow the rising limb. For longer duration storms the system will reach an equilibrium after t_c and the outflow will only fall when rain stops.

If the rain stops before $t = t_c$, then the spatial equilibrium condition would not occur and the hydrograph would tail off at an earlier stage as illustrated in Fig. 4.5.

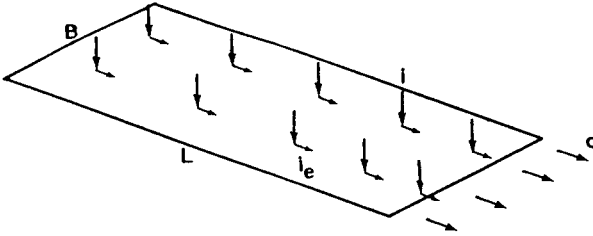


Fig. 4.3 The runoff plane with precipitation

EFFECT OF INFILTRATION

Although the preceding analysis allowed for losses during the storm, it was assumed that uniform losses ceased when rainfall ceases. In fact infiltration will continue as long as there is water on the surface.

Wooding (1966), produced an analytical solution for the shape of the hydrograph for different cases for $n = 2$. For storm durations greater than the concentration time, the rising limb and equilibrium discharge are as described previously. After the storm stops, we have

$$y = y_0 - f(t-t_d) \quad (4.34)$$

In a similar way to (4.33) it may be shown that

$$yL = (i-f)^{\frac{1}{2}} \{ i(t-t_d)^2 + t_c^2(i-f) \}^{\frac{1}{2}} - i(t-t_d) \quad (4.35)$$

The outflow stops at

$$t = t_d + t_c(i-f)/(if)^{\frac{1}{2}} \quad (4.36)$$

For storm duration less than concentration time, the falling limb will have two components. Initially the flow depth will decrease uniformly until the upstream boundary effect reaches the mouth, then the tail will decrease exponentially. The resulting different hydrograph shapes are depicted in Fig. 4.6.

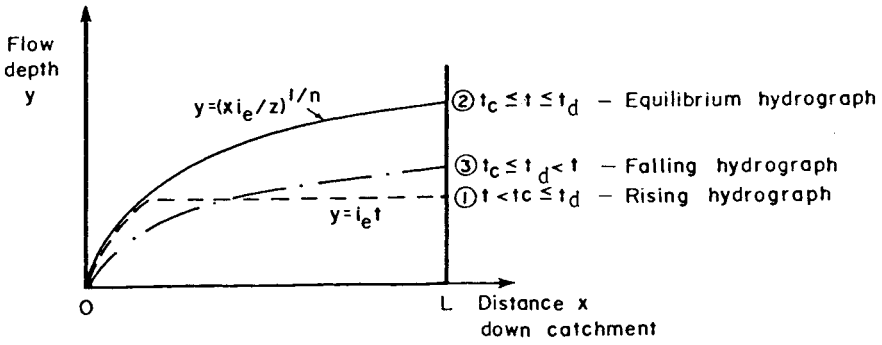


Fig. 4.4 Water depth along catchment

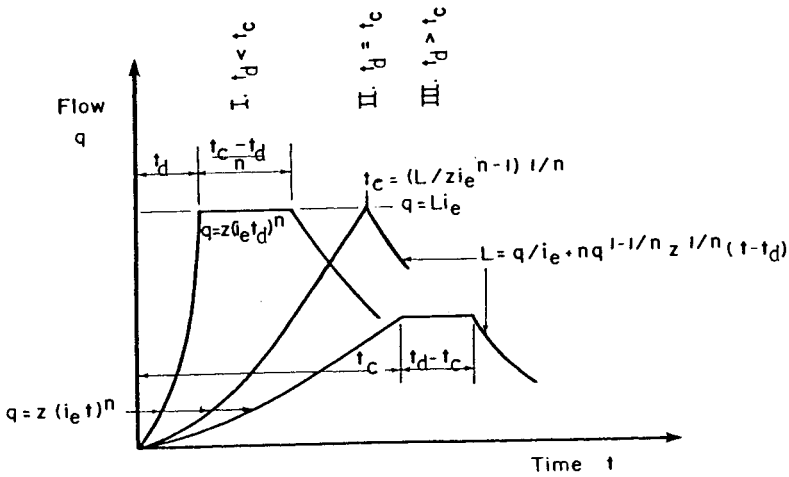


Fig. 4.5 Outflow hydrograph shape for different storm durations but similar total excess rain

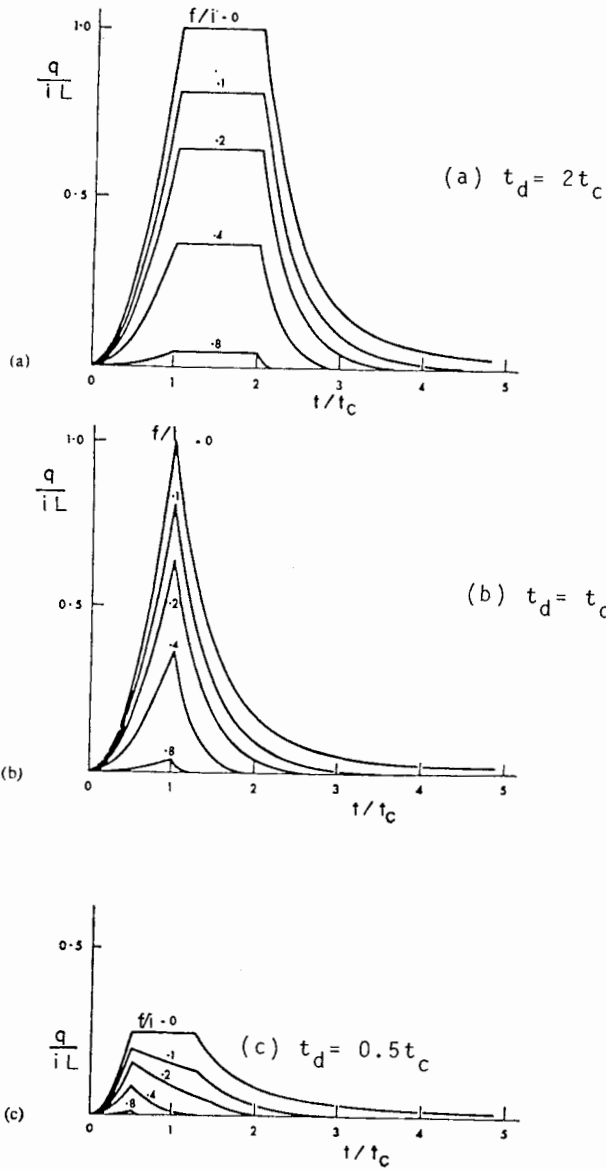


Fig. 4.6 Effects of infiltration on catchment discharge

CATCHMENT - STREAM MODEL

The assumption of a plane with uniform flow across the width is seldom a true picture. A catchment usually slopes down towards a centre channel. A more accurate representation appears in Fig. 4.7. Even this is a simplification, as overland flow will actually have a component towards the mouth and not just perpendicular to the stream.

In cases where overland flow time is negligible (e.g. a long narrow catchment with a small longitudinal fall), the channel may be taken as the catchment, with excess rain per unit length of channel equal to that per unit length of catchment. In many cases the overland flow time is not negligible and the runoff relationship becomes more complicated than for overland flow.

Analytical solutions are not feasible and numerical analysis was employed by Wooding (1965), to produce stream hydrographs.

The ratio of concentration time of the stream or channel t_s to the concentration time of the overland flow t_o per uniform stream inflow is defined as T .

Fig. 4.8 depicts the stream discharge hydrograph for different concentration time ratios. The discharge rate is expressed as a function of the uniform excess rainfall rate i_e and the total catchment area A_c . Time is expressed in terms of the overland catchment concentration time t_o . The parameter is the ratio of storm duration t_d to overland catchment concentration time t_o .

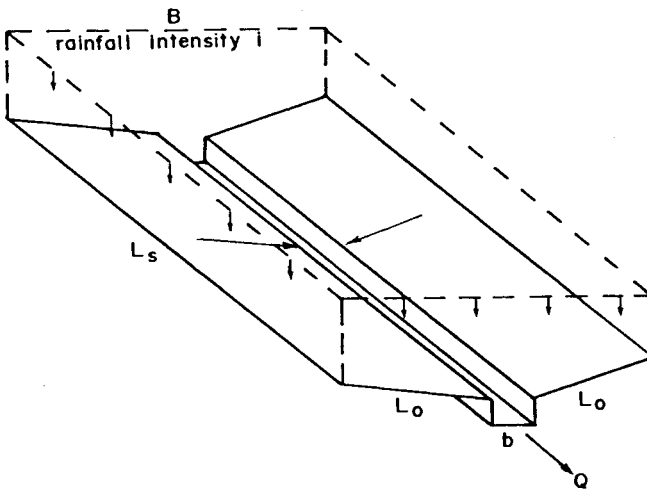


Fig. 4.7 The catchment-stream model

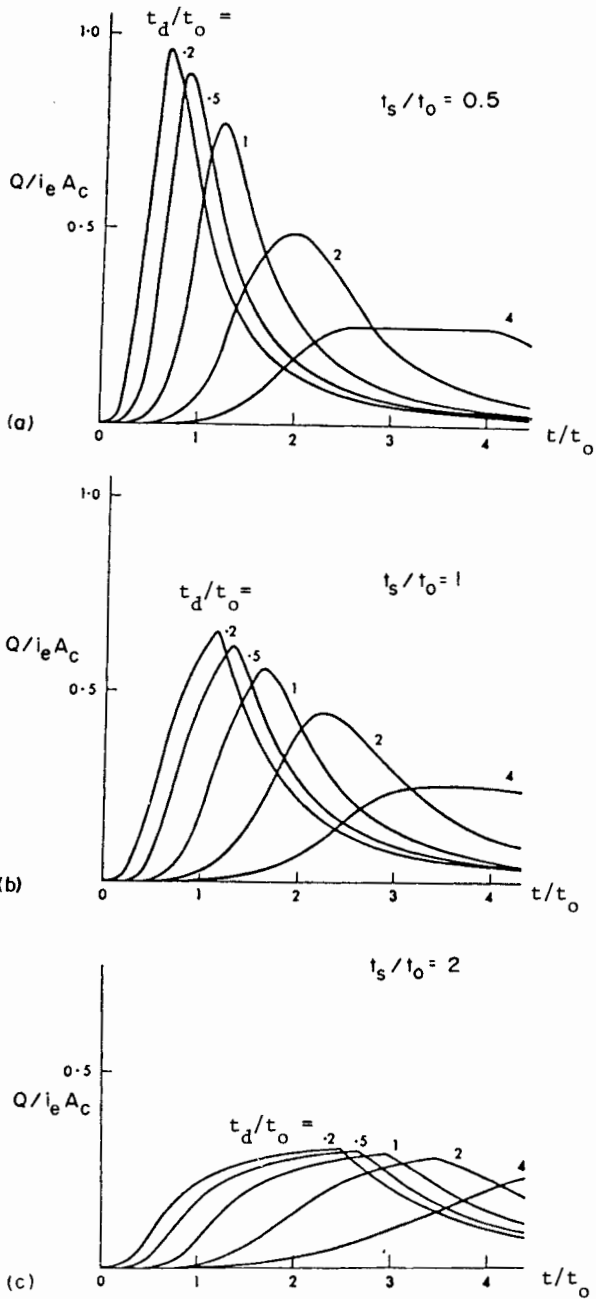


Fig. 4.8 Hydrographs for the catchment-stream model

SOLUTIONS FOR TYPICAL RAINFALL INTENSITY-DURATION CHARACTERISTICS

Rainfall data for various stations throughout the world have been analyzed to yield depth of precipitation versus storm duration and return period. The form of the results varies with the analysis and the mathematical distribution selected but essentially the average intensity of precipitation decreases with storm duration for any selected recurrence interval or return period. It is this fact which results in non-linearity between catchment area and peak runoff rate for any recurrence interval. The time of concentration, or time to peak, for any catchment is a function of the catchment size amongst other things. So it is apparent that the larger the catchment, other factors remaining constant, the longer will be the storm duration resulting in maximum runoff, even though intensity of rainfall is bound to decline the longer the storm duration, other factors being equal.

Here kinematic methods are employed together with a generalized rainfall distribution equation to estimate concentration times and peak runoff rates for a range of catchments. By rendering the results dimensionless, they may be applied globally. It is necessary to assume a rectangular catchment and uniform storm distribution. Numerical techniques must be employed for non-uniform and time-varying storms.

An attraction of the kinematic approach is that all the variables are physically measurable. No empirical factors are required. The slope, roughness and length of catchment are all measurable, although an approximate equation for friction gradient is employed. Infiltration and initial losses are still difficult to assess, but the U.S. Soil Conservation Service (SCS, 1972) has given guidelines.

The present study can be applied to cases of uniform infiltration or an initial surface retention. A combination of these will approximate to a diminishing loss with time i.e. a decay in loss rate.

t_c is referred to as the concentration time of the catchment. It was observed previously that it is a function of the catchment characteristics as well as the rate of excess rain i_e . It is therefore necessary to solve for time of concentration as a function of excess rainfall rate, which in turn is a function of storm duration for any locality and return period. The rain is assumed uniform in time and space, but the losses may not be so. Initial retention may absorb some of the rain and infiltration may vary with time and antecedent conditions.

In the following analysis two simplistic loss models are employed in deriving analytically the concentration times and runoff for rectangular catchments. One model assumes all the losses to occur at the beginning of the storm, as would occur for catchment storage. The other model assumes a uniform rate of loss for the entire storm duration. Combinations of the two types of loss may be interpolated between the two extremes, which are plotted on accompanying charts.

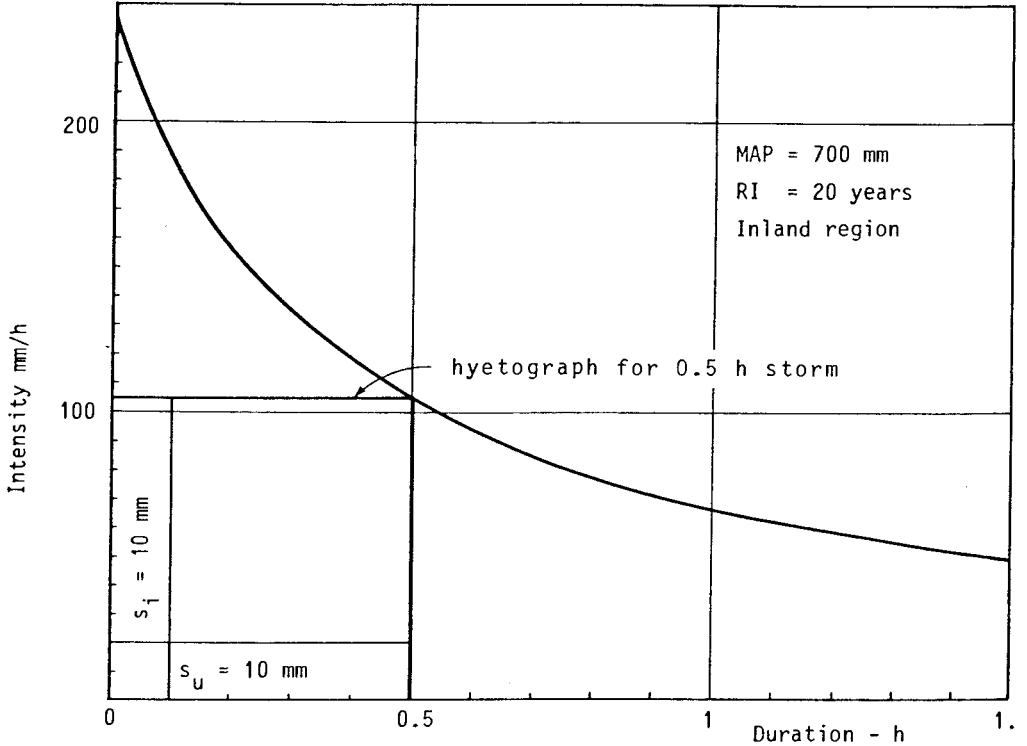


Fig. 4.9 Typical rainfall intensity-duration relationship

STORM INTENSITY - DURATION RELATIONSHIPS AND SOLUTION FOR TIME OF CONCENTRATION

For any particular locality and recurrence interval, there is a statistical relationship between storm duration and intensity. Analysis of storms through the world indicate that the storm intensity may be

predicted with reasonable accuracy with an equation of the form

$$i = \frac{a}{(b + t_d)^c} \quad (4.37)$$

where a, b and c are regionally applicable constants. Overton and Meadows (1976) and Stephenson (1980) found c to be approximately unity in some cases. Thus in many situations it is possible to approximate the relationship by one of the form

$$i = \frac{a}{b + t_d} \quad (4.38)$$

where t_d is the storm duration, and 'a' is a function of the locality and return period. It was proposed by Lloyd-Davies that the maximum peak runoff for any recurrence interval will occur if the storm lasts only as long as it takes to reach equilibrium conditions. A longer duration storm will be of lesser intensity and a shorter duration storm will not reach equilibrium. It is now realized this is not always the case. The maximum peak runoff for abnormal basin shapes can occur from a storm over portion of the catchment. The present study is confined to rectangular shaped catchments which eliminates this possibility. It may also occur that there is an initial retention loss in which case the storm duration should exceed the theoretical concentration time of the basin for maximum peak runoff. This possibility will be examined later. In that case the concentration time is measured from the time runoff commences. Whether or not initial abstraction takes place, it is possible to solve for design storm duration t_d and peak runoff i_{ep} from the equation for concentration time and the storm intensity relationship such as (4.37). The total depth of loss is designated s, in the same units as t_i , where i is the rainfall rate and t is time. Subscript i refers to initial loss and u to uniform loss rate in time.

Case I - Uniform loss rate

For a uniform loss rate over the entire storm duration

$$i_e = i - f \quad (4.39)$$

$$= i - s_u/t_d \quad (4.40)$$

In general if

$$i = \frac{a}{(b+t_d)^c} \quad (4.37)$$

$$\text{and } t_c = (L/zi_e^{n-1})^{1/n} \quad (4.19)$$

then by substitution of (4.37) into (4.39) and (4.39) into (4.19), one obtains an implicit expression for the design storm duration t_d :

$$t_d = \left[\frac{L}{z \left(\frac{a}{(b+t_d)^c} - f \right)^{n-1}} \right]^{1/n} \quad (4.41)$$

If the Manning-Strickler stage-discharge equation is employed and c is taken as unity,

$$t_d = \frac{(Lk^{1/6}/7.7\sqrt{Sg})^{3/5}}{\left(\frac{a}{b+t_d} - \frac{s_u}{t_d} \right)^{2/5}} \quad (4.42)$$

$$= \frac{F}{\left(\frac{1}{b+t_d} - \frac{U}{t_d} \right)^{2/5}} \quad (4.43)$$

$$\text{where } F = \left\{ \frac{Lk^{1/6}}{7.7\sqrt{Sg} a^{2/3}} \right\}^{3/5} \quad (4.44)$$

is defined as the catchment retardation factor and

$$U = s_u/a \quad (4.45)$$

is defined as the infiltration factor. Equ. (4.43) cannot be solved explicitly for t_d or for the peak runoff rate so the equation was solved for F as a function of t_c and U for various values of b . The results are summarized in Fig. 4.10, from which the concentration time may be read knowing the catchment characteristics, namely length L , absolute roughness k , slope S , storm characteristic a and uniform infiltration loss s_u . Unless the storm duration is known, it may be difficult to assess s_u . In many cases the infiltration rate $f = s_u/t_d$ is known instead of the total volume lost, and the dashed lines on Fig. 4.10 may therefore be of more use in estimating concentration times. Once f and t_d are established, s_u may be evaluated. The maximum storm runoff rate may now be evaluated from the equation

$$i_{ep} = \frac{a}{b+t_d} - \frac{s_u}{t_d} \quad (4.46)$$

which is plotted in Fig. 4.12 in dimensionless terms with $t_d=t_c$ evaluated from Fig. 4.10. Subscript e refers to excess rain and p to that corresponding to peak runoff rate. It will be observed that the

maximum rate of runoff per unit area does not occur for small smooth basins, except for no losses. For real losses represented by U there is some basin configuration represented by F which results in a higher rate of runoff per unit area. This is because for any U the rate of loss reduces with increasing F and hence increasing t_c , and this effect predominates over the lower storm intensity. On the other hand for short storms, the rate of loss would have to be high to produce a certain U , hence the rate of runoff is affected.

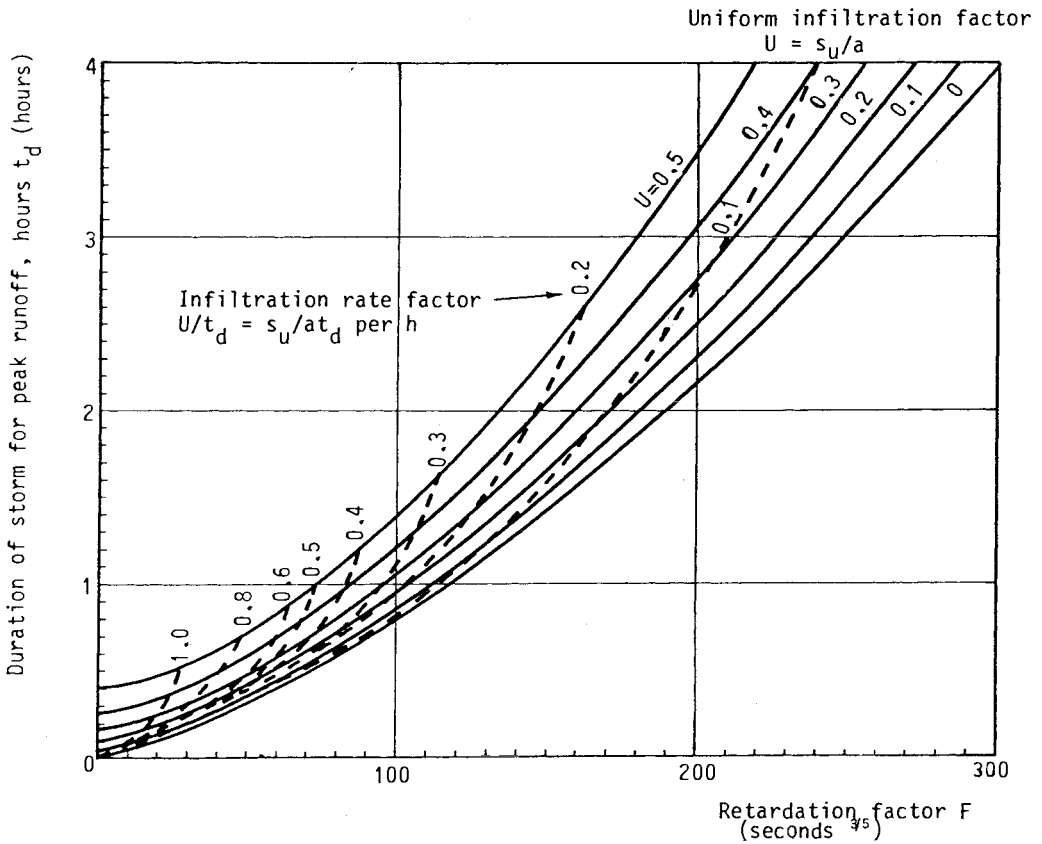


Fig. 4.10 Design storm duration for uniform losses, $b = 0.4$ h

Case II - Initial loss

If all the storm input is initially absorbed or taken up in filling depression storage, runoff will not commence until the storage is full. If the storage or loss volume is s_i per unit area, then the time until runoff commences is

$$t_i = s_i/i \quad (4.47)$$

For peak runoff,

$$\begin{aligned} t_c &= t_d - t_i \\ &= \frac{(Lk / 7.7\sqrt{Sg})^{\frac{1}{5}}}{\left(\frac{a}{b + t_d}\right)^{\frac{2}{5}}} \end{aligned} \quad (4.48)$$

$$\text{Therefore } t_d = F(b+t_d)^{\frac{2}{5}} + I(b+t_d) \quad (4.49)$$

where I is the initial retention factor, s_i/a .

This equation was solved for F for various t_d and I and the results are plotted in Fig. 4.11 for various values of I . It will be noted that the resulting storm durations for peak runoff are invariably greater for initial losses than for uniform losses.

It will be observed from Fig. 4.12 however, that the peak runoff rate is higher for initial loss than for uniform loss. For no loss both theories yield identical results as would be expected while for increasing losses the results diverge. The peak runoff per unit area for case II, however, occurs for the smallest, smoothest and steepest catchment.

For losses comprising a combination of initial storage and uniform infiltration, Fig. 4.12 may be interpolated, taking note that each line for a particular loss function is drawn assuming the other type of loss is zero.

Surface losses

The losses to be deducted from precipitation include interception on vegetation and roofs, evapotranspiration, depression storage and infiltration. The remaining losses may be divided into initial retention and a time-dependent infiltration.

The loss function is really a function of many variables, including antecedent moisture conditions and ground cover. Infiltration is time-dependent and an exponential decay curve was proposed by Horton (1939), Holton (1961), and others. The infiltration typically reduces from an

initial rate of about 50 mm/h down to 10 mm/h over a period of about an hour. The rates, especially the terminal loss rate, will be higher for coarse sands than for clays.

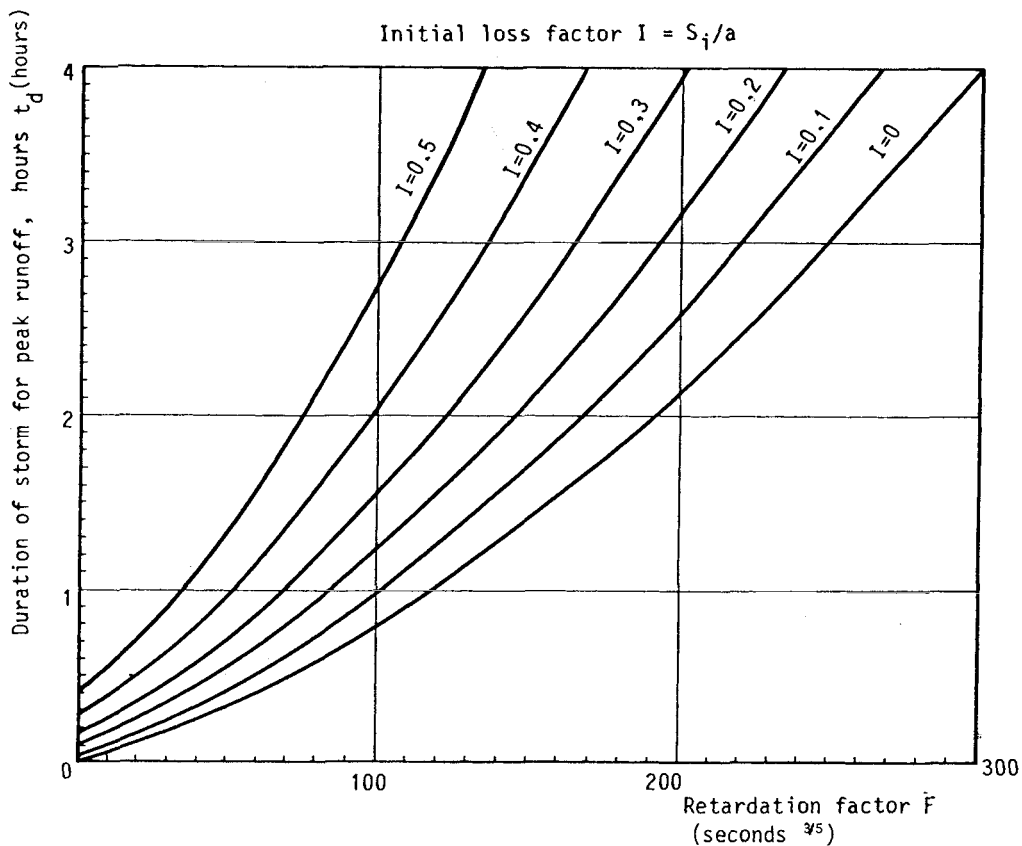


Fig. 4.11 Design storm duration for initial losses, $b = 0.4$ h

The time-decaying loss rate could be approximated by an initial loss plus a uniform loss over the duration of the storm. Values of initial and uniform losses used in the United States are tabulated in Table 4. The mean uniform loss rates are averages for storms of 30 minute duration, and the initial losses include the initial 10 minute rapid infiltration or saturation amount.

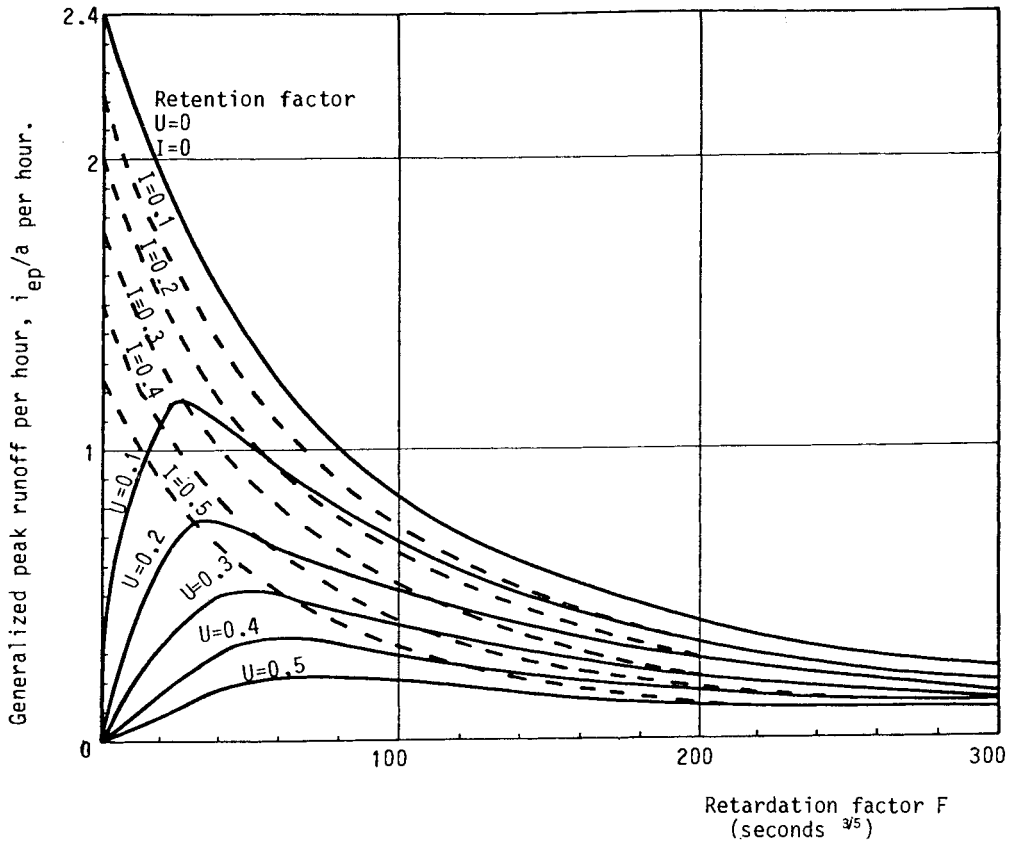


Fig. 4.12 General peak runoff, $b = 0.4$ h

TABLE 4.1 Initial and uniform loss rates

	SURFACE LOSSES		
	Initial loss - (mm)		Uniform infiltration rate - (mm/h)
	Surface Retention	Infiltration	
Paved	up to 1	-	0
Clay	" 5	20	2-5
Loam	" 5	30	5-15
Sandy soil	" 5	40	15-25
Dense vegetation	" 12	-	

In the case of ploughed lands, and other especially absorptive surfaces an additional initial loss of up to 10 mm or more may be included. Allowance must also be made for reduced losses from covered areas (paved or roofed). The values should be used with caution until more appropriate data are available.

Roughness

The Manning-Strickler drag equation is dimensionally homogeneous. By including the absolute roughness k as a variable, it loses the empiricism of the Manning equation. In fact the drag effect is very insensitive to the roughness, as it is to the power of $1/6$. Thus any inaccuracy in selecting k is masked by the equation. It is preferable to overestimate k as the drag equation tends to predict too rapid flow concentration unless this is done. This is due to the tortuosity of the flow path over rough surfaces. In fact the original form of the Manning equation and the Strickler approximation for the roughness were never intended for overland flow where the depth of flow is comparable with the roughness and Reynolds numbers are of the order of 1 000. Table 4.2 may be used as a guide for surface roughness k .

TABLE 4.2 Surface roughness

ABSOLUTE ROUGHNESS, k (mm)	
Concrete lined storm drains	0.5
Concrete paving	1
Gravel	5
Lawn, turf	20
Weeds	50
Ploughed land	150
Boulders and rubble	500
Dense vegetation	1 000+

The length of drainage path and slope influence the concentration time more than the roughness. Runoff follows a circuitous path over natural land and the ground slope along the flow path is therefore flatter than the net slope. A similar lag occurs with runoff from roofs (2 to 5 minutes lag). Allowance should be made for these effects in establishing the retardation factor F .

EXAMPLE:

The example illustrates the use of the design charts for determining design storm duration, peak runoff and the effect of canalization. The use of consistent units in the equations should be noted.

Calculate the peak 20-year runoff from a catchment which is 500 m wide and 2 000 m long with a uniform longitudinal slope of 1/500, and an effective absolute roughness of 10 mm. The infiltration rate is 20 mm per hour. Neglect overland flow time for the purposes of the example. The 20 year storm factor 'a' for the station is 90 mm and the time factor 'b' is 0.4 h.

The retardation factor is

$$F = \left[\frac{2\,000 \times 0.01^{\frac{1}{6}}}{7.7\sqrt{9.8/500} \cdot 0.09^{\frac{2}{3}}} \right]^{0.6} = 151 \text{ s}^{0.6}$$

Uniform retention factor for total loss $U/t_d = 20/90 = 0.222$ per h.

Interpolating between the lines on Fig. 4.10 storm duration = 2.2 h, therefore $U = 0.48$ and from Fig. 4.12 $i_{ep}/a = 0.16/h$. The peak excess runoff is therefore $i_{ep} = 0.16 \times 90 = 14.4$ mm/h. The peak rate of runoff is $14.4 \times 500 \times 2\,000/3\,600 \times 1\,000 = 4.0$ m³/s. The value of 'C' in the rational formula is

$$\frac{i_{ep}}{i_{ep} + s/t_d} = \frac{14.4 \text{ mm/h}}{14.4 + 20} = 0.42$$

REFERENCES

- Constantinides, D.C. and Stephenson, D. 1981. A two-dimensional kinematic overland flow model. Proc. Intl. Conf. Urban Drainage, Univ. Illinois, Urbana.
- Eagleson, P.S., 1970. Dynamic Hydrology. McGraw-Hill, N.Y., 462 pp.
- Henderson, F.M., 1966. Open channel flow. Macmillan, N.Y. 522 pp.
- Holton, H.N., 1961. A concept of infiltration estimates in watershed engineering. U. S. Dept. of Agric., Agric. Res. Service, 41-51, Washington D.C.
- Horton, R.E. 1939. Approach towards a physical interpretation of infiltration capacity. Proc. Soil Sci. Soc. Amer. 5.p 399-417.
- Overton, D.E. and Meadows, M.E., 1976. Stormwater Modelling. Academic Press, N.Y. 358 pp.
- Rossmiller, R.L., 1980. The rational formula revisited. Proc. Intl. Symp. Urban Storm Runoff. Univ. Kentucky, Lexington. p1-12.
- Saint-Venant, A.J.C. Barré de, 1848. Études Theoriques et Pratiques sur le Mouvement des Eaux Courantes. (Theoretical and Practical Studies of Stream Flow). Paris.
- Stephenson, D., 1980. Peak runoff from small areas - a kinematic approach. Water S.A., 6 (2), April. Pretoria. p 59-65.

- Wooding, R.A., 1965-6. A hydraulic model for the catchment-stream problem. (I) Kinematic wave theory, 3 (1965) p254-267; (II) Numerical solutions, 3 (1965) p268-282; (III) Comparison with runoff observations, 4 (1966) p21-37. J. Hydrology.
- Woolhiser, D.A. and Liggett, J.A., 1967. Unsteady one-dimensional flow over a plane - the rising hydrograph. Water Resources Res. 3 (3), p753-771.

CHAPTER 5

NUMERICAL SOLUTIONS TO KINEMATIC FLOW

NUMERICAL METHODS

The kinematic method has a number of advantages over other methods:

1. The mathematics are simpler than those of the comprehensive hydrodynamic equations, although hydrodynamic forces are omitted.
2. It is relatively simple to visualize the flow process described by the kinematic equations.
3. The gradual increase in water depth over a catchment during a storm can be simulated. This allowance for dynamic effects is not possible with isochronal techniques. The latter techniques use only the friction equation for steady state flow with no allowance for continuity.
4. The effect of storm intensity influences the concentration time of a catchment as it should. This is not the case with isochronal methods.
5. The equations are amenable to analytical solution in many cases.
6. Numerical solutions are feasible and simple for non-rectangular catchments, varying topography, spatial and temporal variation of storms and losses and combinations of overland and conduit flow.

Various workers (eg. Overton and Meadows, 1976) have employed the kinematic equations for catchment models.

EFFECT OF STORM DISTRIBUTION ON RUNOFF

Many hydrological studies are made on the assumption of a rectangular catchment and uniform storm distribution in space and time. Numerical simulation models such as SWMM (the overland flow components) and analytical models such as those of Wooding (1965) are based on rectangular basins. The effect of an uneven and non-planar basin can be to increase the intensity of runoff for a storm of any particular return period. A basin with its centre of gravity close to the mouth can result in a more severe runoff than a long rectangular basin or one with the centre of gravity further up the basin. Similarly a storm with a focus close to the mouth of the basin will result in a more intense runoff than a storm which is uniformly spread over the catchment.

An allowance for non-uniform storm distribution can be made with the tangent method of design. That technique, however, is based on uniform flow down the basin and the time of concentration is therefore inaccurately predicted. The true dynamic concentration of the storm in the basin must be predicted from the equations of motion. In many cases these can be approximated by the kinematic equations. These equations

are capable of analytical solution in many cases of uniform shaped plane basins and uniform storms. For irregular shaped basins and hyetographs, it is necessary to solve these or the rigorous hydrodynamic equations numerically.

It is the purpose of this section to demonstrate with the aid of the kinematic equations of flow how catchment shape and hyetograph shape affect the discharge hydrograph shape and effective time of concentration. A planar quadrilateral shaped basin is assumed and lateral flow time (perpendicular to the general direction of flow) is assumed negligible. In one case the basin is assumed to be rectangular with the slope in one direction parallel to two opposite sides. The excess rain is assumed to increase from zero to a maximum and then decrease to zero again over a defined time. The resulting hyetograph is triangular. This distribution in one extreme case could also account for a time-varying infiltration rate. In another case, the excess rain is assumed to vary spatially in a triangular fashion from zero at the top of the basin to a maximum along the basin. Thus the basin may be rectangular with the storm varying in intensity down the length of the basin (Fig. 5.4) or the storm could be of uniform intensity while the basin width varies down the length (Fig. 5.5).

GENERAL EQUATIONS

Start with the basic kinematic equations:

$$\text{Continuity} \quad \frac{\partial y}{\partial t} + \frac{\partial q}{\partial x} = i_e \quad (5.1)$$

$$\text{Dynamic equilibrium} \quad q = z y^n \quad (5.2)$$

$$\text{or} \quad q = \frac{7.7\sqrt{Sg}}{k^{1/6}} y^{5/3} \quad (5.3)$$

where $z = 7.7\sqrt{Sg} / k^{1/6}$ and $n = 5/3$ employing the Manning-Strickler equation.

Equation 5.2 is the more general equation for uniform flow but the constants are dimensionally dependent.

In these equations, z is a factor, n is a coefficient, x is distance in the flow direction, t is time, y is flow depth, g is gravitational acceleration, S is the bed slope, equal to the friction energy loss gradient, q is the discharge rate per unit width, i_e is the excess rainfall rate per unit area after subtracting infiltration and other losses, and k is a measure of surface roughness.

Substituting for y from (5.3) or (5.2) in (5.1) we get

$$\frac{1}{nz^{1/n}q^{1-1/n}} \frac{\partial q}{\partial t} + \frac{\partial q}{\partial x} = i_e \quad (5.4)$$

$$\text{or } \frac{0.6}{q^{0.4} (7.7\sqrt{Sg}/k^{1/6})^{0.6}} \frac{\partial q}{\partial t} + \frac{\partial q}{\partial x} = i_e \quad (5.5)$$

The equation may be rendered dimensionless by substituting

$$P = q/Li_{ea} \quad (5.6)$$

$$I = i_e/i_{ea} \quad (5.7)$$

$$X = x/L \quad (5.8)$$

$$T = (zi_{ea}^{n-1}/L)^{1/n} t = \frac{7.7^{0.6} (Sg)^{0.3} i_{ea}^{0.4} t}{L^{0.6} k^{0.1}} \quad (5.9)$$

where i_{ea} is the time and space averaged excess rainfall rate over the catchment and L is the length of catchment in the direction of flow.

$$\text{Now (5.5) becomes } \frac{\partial P}{\partial T} = n(pP)^{1-1/n} (I - \frac{\partial P}{\partial X}) \quad (5.10)$$

$$= 2.2P^{0.4} (I - \frac{\partial P}{\partial X}) \quad (5.11)$$

where p is the ratio of peak to average excess rain intensity i_{ep}/i_{ea} which is 2 for a triangular distribution.

It may also be proved that

$$T = t/t_c \quad (5.12)$$

where t_c is the time to equilibrium or concentration time of a rectangular plane catchment subject to uniform (in time and space) excess rain.

For that case analytical solutions to the kinematic equations are feasible. Thus the rising limb of the hydrograph at the end of a catchment is given by

$$q = i_e L (t/t_c)^{5/3} \quad (5.13)$$

$$\text{where } t_c = (L/zi_{ea}^{n-1})^{1/n} \quad (5.14)$$

$$= \frac{L^{0.6} k^{0.1}}{7.7^{0.6} (Sg)^{0.3} i_{ea}^{0.4}} \quad (5.15)$$

$$\text{hence } P = T^{5/3} \quad (5.16)$$

The falling limb of the hydrograph, beyond $t = t_c$ is given by the implicit equation

$$L = zy_L^{n-1} [y_L/i_e + n(t-t_d)/y_L] \quad (5.17)$$

which may be rewritten for the case of rain duration t_d equal to time of concentration t_c as

$$T = 1 + (1-P)/(nP^{1-1/n}) \quad (5.18)$$

$$= 1 + (1-P)\left(\frac{5}{3} P^{0.4}\right) \quad (5.19)$$

The rising and falling limbs may be plotted from (5.16) and (5.19) as in Fig. 5.3. For other cases, where rainfall is not uniform in time and space, numerical solutions are necessary. For this purpose (5.9) was solved for specific cases.

SOLUTIONS FOR NON UNIFORM AND UNSTEADY STORM INPUT

Equation (5.9) was solved iteratively using a backward difference explicit finite difference solution technique. Acceptable accuracy was obtained with $\Delta X = 0.05$ and $\Delta T = \Delta X$ gave a stable solution. The finite difference form of the equation became

$$P(X_i, T_j) = P(X_i, T_{j-1}) + 2.2 \Delta T P(X_i, T_{j-1})^{0.4} \{I - [P(X_i, T_{j-1}) - P(X_{i-1}, T_{i-1})] / \Delta X\} \quad (5.20)$$

At $T = 0$ this explicit form of (5.9) would yield zero increment in $P(x)$ so a centred explicit - implicit numerical form was employed i.e.

$$P(X_i, T_2) = 0 + 2.2 I \Delta T [P(X_i, T_1) + P(X_i, T_2)]^{0.4} / 2 \quad (5.21)$$

$$\therefore P(X_i, T_2) = (2.2 I \Delta T / 2)^{3/4} \quad (5.22)$$

The scheme was used to study two particular cases:

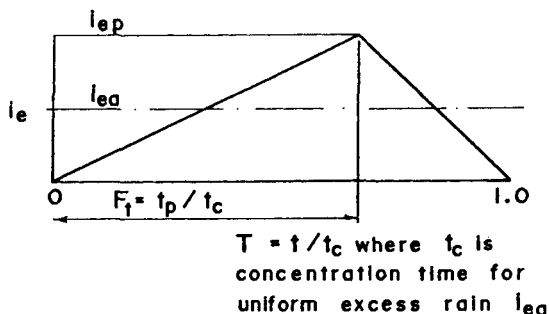


Fig. 5.1 Excess rain variation with time

I. Time varying rain intensity

A rectangular plane basin sloping in the longitudinal direction was analyzed for different cases of unsteady rainfall input. Excess rainfall was assumed to be spread uniformly over the basin, but it was

permitted to vary in time. The storm duration was set equal to the concentration time of a rectangular basin subject to uniform excess rain rate equal to the mean for the non-uniform case. A triangular hyetograph was assumed with the peak varying successively in time for different cases from the start of the storm to the end of the storm, i.e. $F = t_p/t_d = 0$ to 1 where t_d is the storm duration and t_p is the time to peak of the storm (see Fig. 5.1).

The case could be applied to the excess rain after subtracting losses, infiltration etc. Alternatively a decaying rate of infiltration could be allowed for. A rectangular storm hyetograph with a straight line decrease in losses may in some cases be approximated by a triangular excess rain hyetograph with the peak at the end of the storm (Fig.5.2).

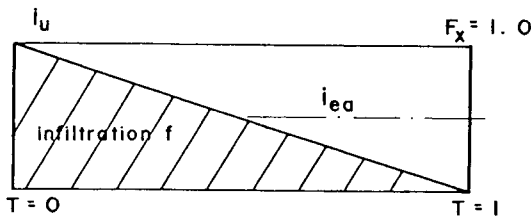


Fig. 5.2 Rectangular hyetograph with decaying losses resulting in triangular excess rain distribution with time

The resulting runoff hydrographs at the mouth of the basin are depicted in Fig. 5.3. Thus it will be observed that as F_t (the relative time to storm peak) varies from 0 to 1, so the effective concentration time of the basin increases, i.e. the time to peak of the runoff hydrograph increases. The peak runoff also increases the later the storm peak although it is always less than the peak excess rain rate which is $2i_{ea}L$ per unit width for a triangular storm distribution. In fact the worst storm distribution occurs with a storm peak at the end of the storm, and for this case the peak runoff is $1.4 i_{ea}L$ per unit width.

For comparison the runoff hydrograph for a rectangular storm is indicated in dashed lines in Fig. 5.3. The rising limbs of hydrographs for storm durations exceeding the nominal concentration time of the basin are also indicated. Here the storm intensity is assumed to increase linearly with time, reaching a maximum at the end of the storm ($t_p = t_d$).

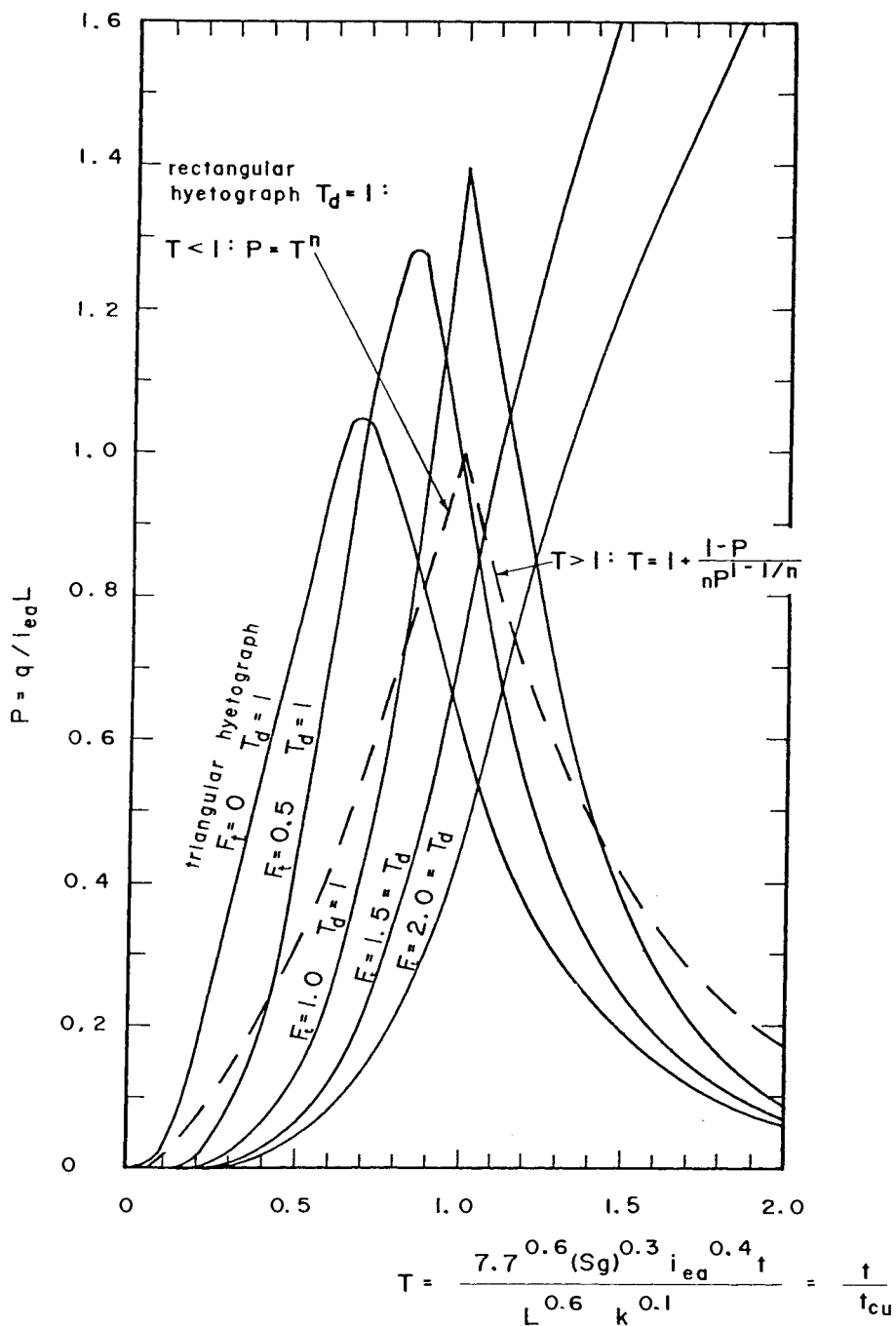


Fig. 5.3: Runoff hydrographs for triangular storm time distribution. $F_t = t_p / t_c$ where t_p = time to peak of excess rain and storm duration $t_d = t_c$ = concentration time for rectangular storm input except for $F_t > 1$

If the precipitation rate was constant over a duration equal to the concentration time of the catchment, t_c , then the peak runoff would occur at the end of the storm and would be equal to $i_{eu}L$ per unit width of catchment, where i_{eu} is the uniform excess rainfall rate. This case is generally accepted as the worst storm for any particular return period and the duration of the design storm is thus selected. In the case of an unsteady (time varying) storm it is difficult to solve directly for the storm duration which will result in the maximum peak runoff. According to Fig. 5.3 for the case of a storm peaking at the end ($F_t = 1$) the peak runoff occurs at $t = t_c$ so a storm duration equal to t_c will result in maximum peak runoff, whereas for a storm peaking at the beginning ($F_t = 0$) the peak occurs before $t = t_c$ so a shorter storm will probably result in the maximum peak runoff. Also a storm with a longer duration than t_c may result in the maximum peak runoff if the storm peak occurs at the end.

It will be apparent from Fig. 5.3 that the worst storm with duration t_c is that which peaks at the end ($F_t = 1.0$). A time decaying infiltration loss can have the same effect on a uniform storm. A rectangular hyetograph could be transformed to a triangular one with the maximum excess rain at the end. In this case the peak runoff would be 40% higher than that for a storm with a constant loss rate.

II. Space varying rain input

Consider the case of a rectangular plane basin with a steady storm intensity varying down the length of the basin. Storm intensity is assumed constant with time and the excess rain intensity is triangular with a peak somewhere along the basin, defined by $F_x = x_p/L$ between zero and one (Fig. 5.4). The rising limb of the resulting discharge hydrograph is depicted in Fig. 5.6.

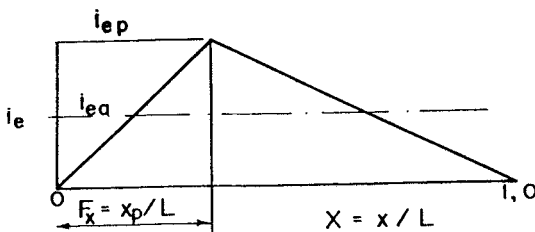


Fig. 5.4 Excess rain variation along basin

It will be observed that in all cases the hydrograph peaks near the concentration time of a uniform storm hydrograph (the dashed line in Fig. 5.6 is for a uniform storm in time and space). The hydrograph rises much faster in the case of a storm whose peak is at the mouth of the basin ($F_x = 1$) and much slower in the case of the storm with a peak at the top end of the basin ($F_x = 0$). A storm with a duration less than the nominal concentration time of the basin may therefore result in a higher peak runoff if its centre of gravity is near the mouth of the basin.

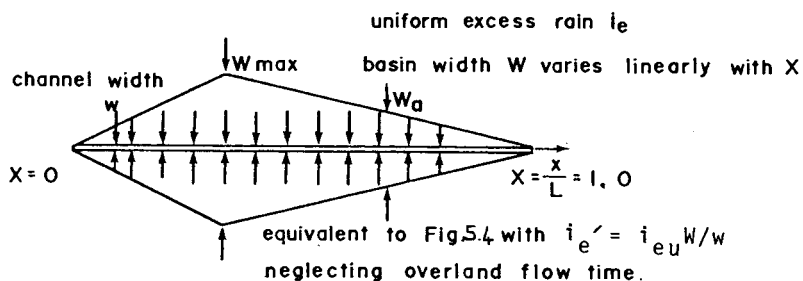


Fig. 5.5 Varying basin width

The same chart applied to the case of a basin whose width varies from zero to a maximum somewhere along the basin and then back to zero at the end (Fig. 5.5). Provided lateral flow time can be neglected, the effective excess rainfall input at any point x along the collecting channel of width w is $i'_e = i_{eu} W/w$ where i_{eu} is the uniform excess rainfall rate and W is the basin width. The mean excess rainfall is $i'_{ea} = i_{eu} W_{max}/2w$. The values of i'_e and i'_{ea} are used in place of i_e and i_{ea} respectively in Fig. 5.5 to yield the discharge q per unit width of channel. If lateral flow time is significant it is necessary to correct for this. An approximation is to move the true storm peak upbasin by the lateral flow distance.

It is evident that a basin which is wider at the mouth than upstream will result in a hydrograph which rises more rapidly initially than for a rectangular basin. Thus a storm duration less than the concentration time of the basin may result in the maximum peak runoff. It would be necessary to obtain the storm duration resulting in maximum peak runoff

by trial and error using Fig. 5.6 for calculating the peak runoff intensity corresponding to the selected storm duration.

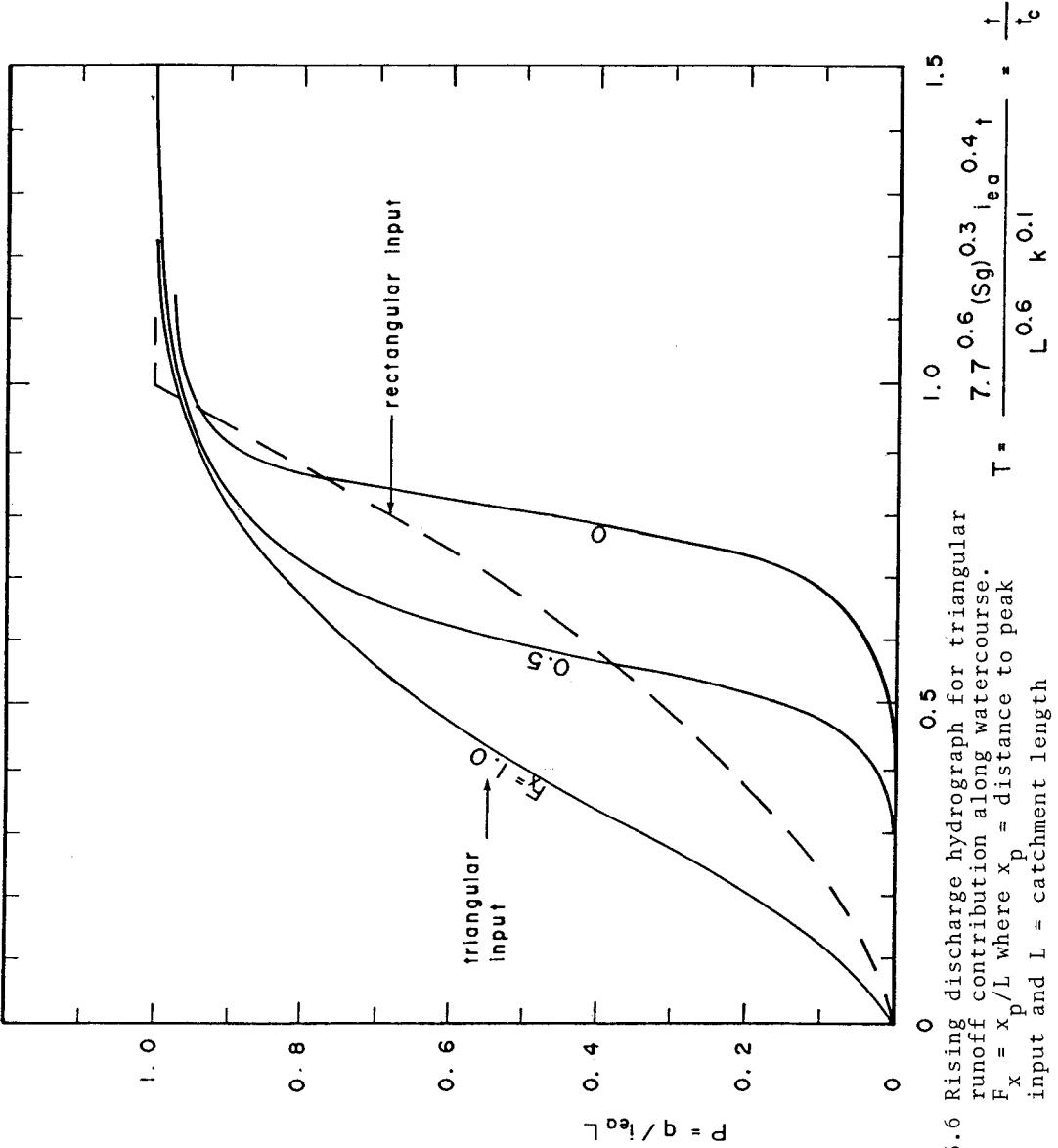


Fig. 5.6 Rising discharge hydrograph for triangular runoff contribution along watercourse. $F_x = x_p / L$ where x_p = distance to peak input and L = catchment length

Multiple variations

Fig. 5.7 applies to a storm which increases linearly in intensity towards the mouth of a rectangular catchment and also increases linearly with time. For this figure i_{ea} is taken as the excess rainfall rate occurring half way down the catchment at a time equal to half the concentration time for a uniform storm. It will be observed that the peak runoff for a storm with duration t_c would be 1.65 times the mean excess rainfall rate multiplied by basin area. This is even higher than that resulting from a time-increasing storm with even distribution down the basin (Fig. 5.3) as could be expected.

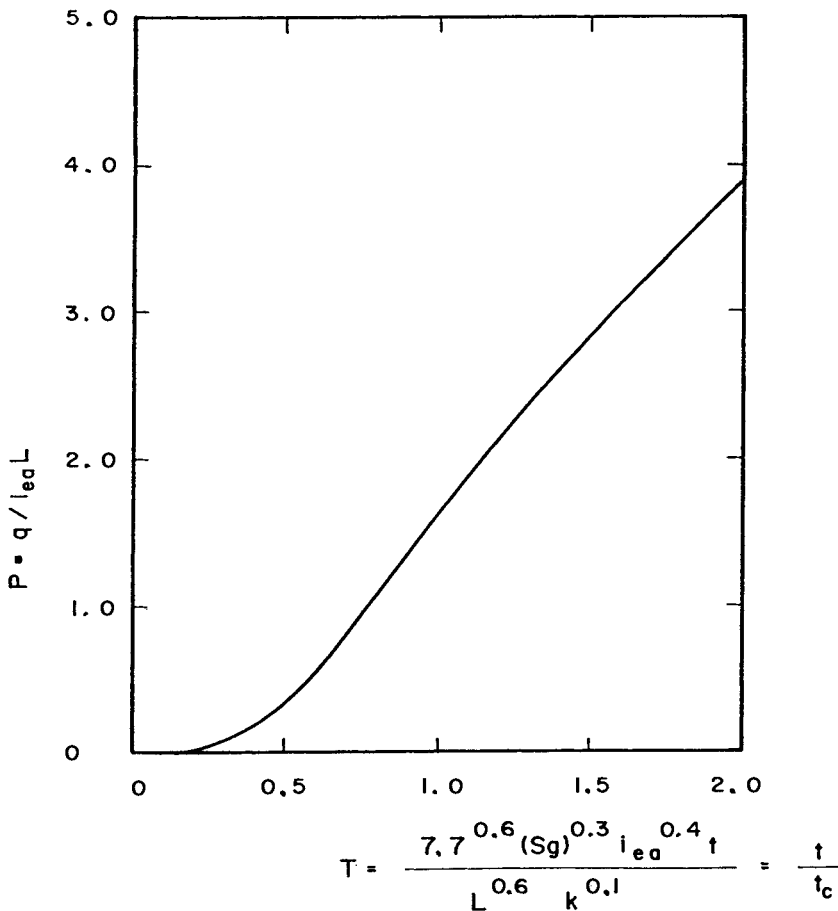


Fig. 5.7 Rising discharge hydrograph for rainfall increasing uniformly towards mouth of rectangular basin and uniformly in time. i_{ea} occurs at $X = 0.5$ and $T = 0.5$.

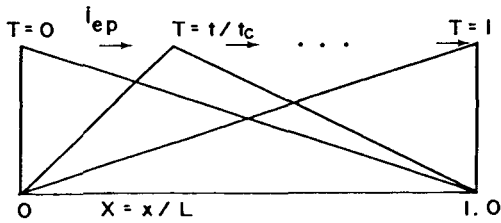


Fig. 5.8 Storm travelling along basin

Fig. 5.9 depicts the hydrographs from a rectangular basin with a travelling storm. For two cases the storm distribution down the basin is triangular. The peak of the triangle is assumed to travel at a speed L/t_c up or down the basin (see Fig. 5.8) but the storm is confined to the basin for its duration. The storm duration is taken as t_c . The peak runoff intensity for a storm travelling down the basin is more severe than for a storm travelling up the basin.

Also depicted on Fig. 5.9 are the discharge hydrographs for a rectangular storm travelling up or down the basin. The excess rain is uniform over the area of precipitation, and the storm is across the entire width of the basin, but is of limited longitudinal extent. The length of storm path is assumed equal to the length of the basin, and the storm front travels up or down the basin, starting at one end and continuing along and beyond the basin (Fig. 5.10).

SUMMARY OF EFFECTS OF STORM DISTRIBUTION

The effect of non uniform storm distribution, whether in space or time, is generally to increase peak runoff from a basin. Simple triangular storm distributions were analyzed by numerical solution of the kinematic flow equations to illustrate the effect and to produce generalized design charts.

A storm which peaks near the end of its duration can cause a runoff intensity 40 percent higher than a uniform storm of the same average intensity. The same effect manifests with a decaying infiltration rate. Storms which are more concentrated near the mouth of the basin than further upstream may result in a higher runoff than a uniformly spread

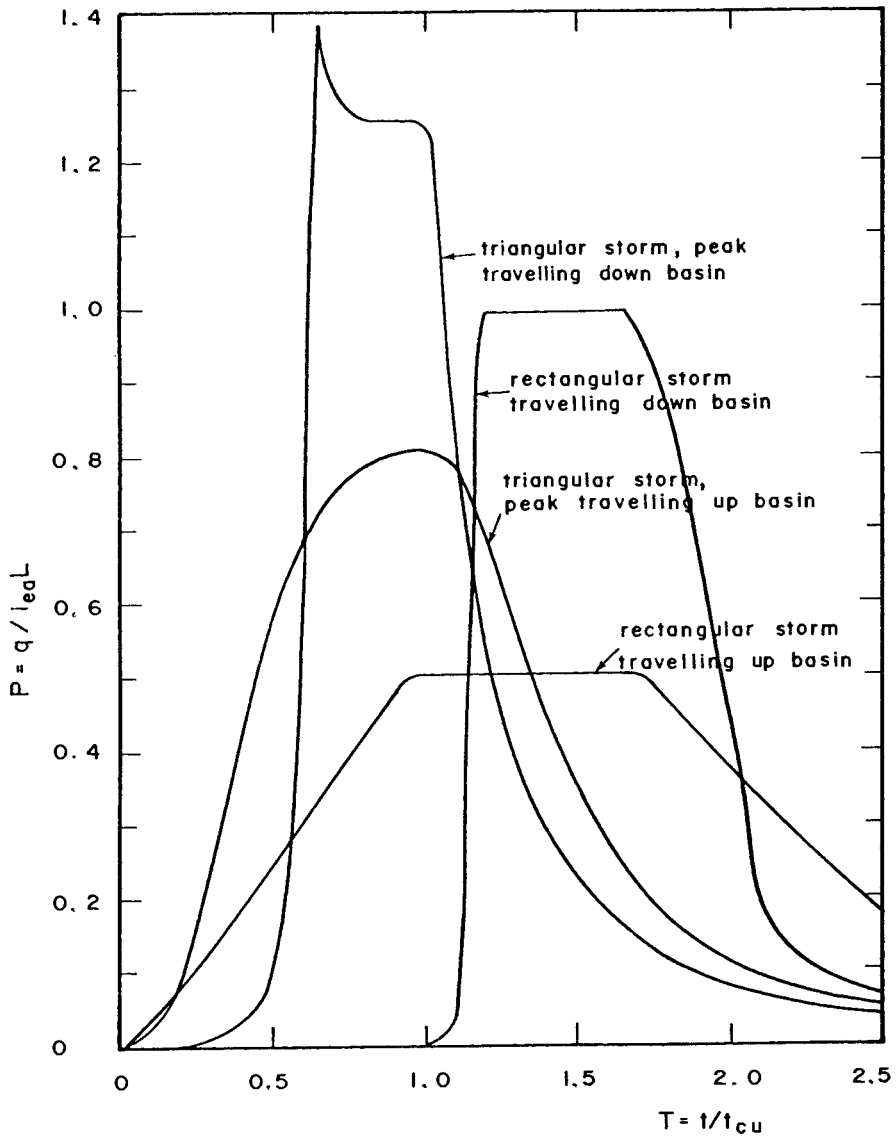


Fig. 5.9 Discharge hydrographs due to travelling storm of duration t_c

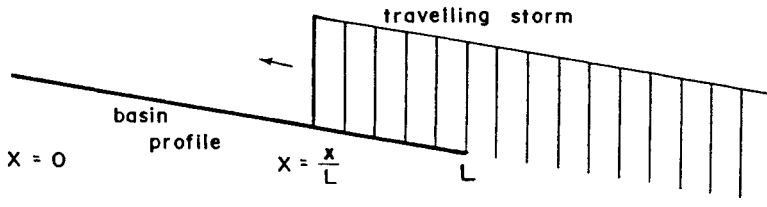


Fig. 5.10 Travelling rectangular storm

storm. Similarly basins which have the centre of gravity of the area near the mouth result in higher peak runoff than rectangular basins.

A storm travelling down a catchment will result in higher peak runoff than the same storm travelling upstream.

The assumption of uniform storm intensity and distribution can only yield average figures for any selected return period of rainfall. The number of variables contributing to the intensification of runoff imply the probability of exceedance of a particular runoff rate may be greater than is indicated by a statistical analysis of isolated rain gauge records.

TWO-DIMENSIONAL MODELS

The assumption of a one-dimensional flow off a rectangular plane catchment is often inaccurate. Many catchments vary topographically in two dimensions. Hills and valleys cause runoff to flow in varying directions. Flow will at all times be perpendicular to the contour lines under the assumption of kinematic flow. In addition to the flow path due to the lateral flow, lateral slopes may also result in flow concentrations in valleys with resulting effect on concentration time. Thus for large catchments a two-dimensional analysis is desirable.

The kinematic equations may readily be generalized for the two-dimensional case.

The continuity equation becomes

$$\frac{\partial y}{\partial t} + \frac{\partial q_x}{\partial x} + \frac{\partial q_y}{\partial y} = i_e \quad (5.23)$$

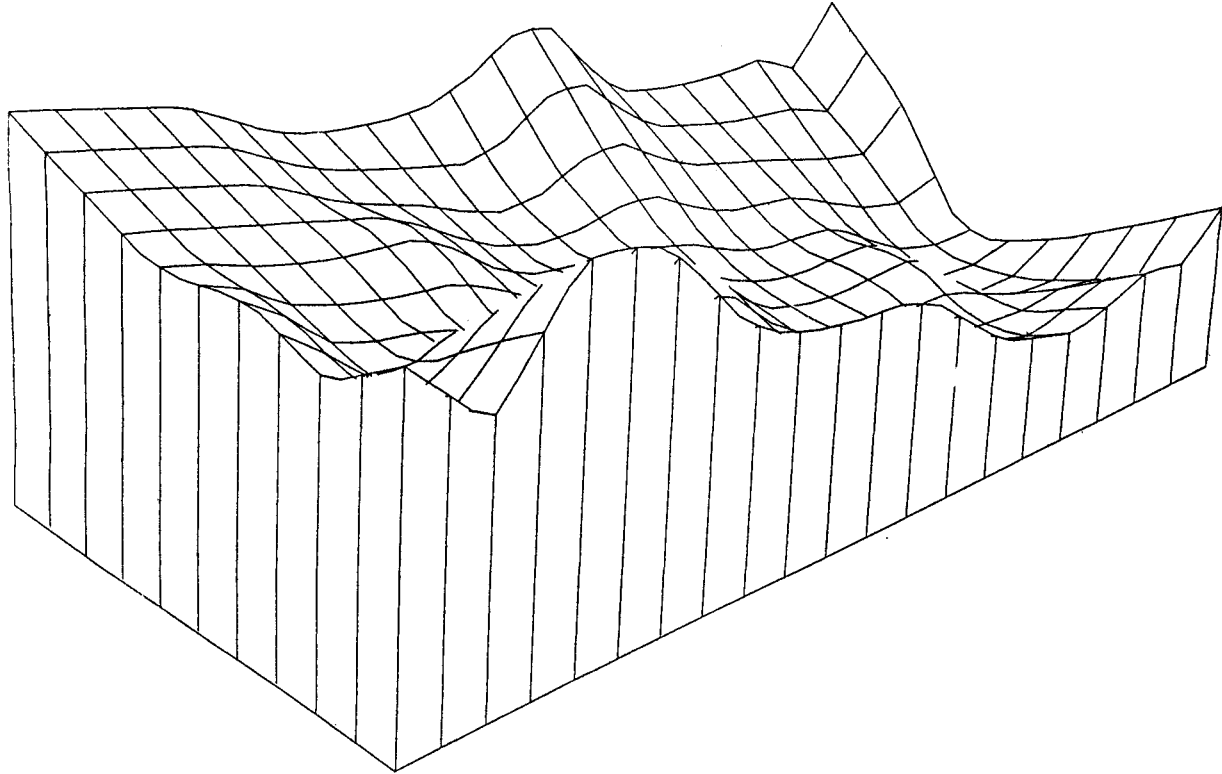


Fig. 5.11 Topography in 3-dimensions

There are two components of flow in the x and y directions, and consequently two discharge-depth equations:

$$q_x = \frac{1}{q_t} (\alpha_x y^m)^2 \quad (5.24)$$

$$q_y = \frac{1}{q_t} (\alpha_z y^m)^2 \quad (5.25)$$

where $q_t = \sqrt{q_x^2 + q_z^2}$, $\alpha_x = 7.7\sqrt{gS_{ox}}/k^{1/6}$ (similarly for α_z), and $m = 5/3$ in the Manning-Strickler equation. The resulting equations can be solved across an x-z grid at successive time increments using numerical methods Constantinides (1981) found that a backward central explicit difference scheme yielded satisfactory results with minimal computational time.

Two-dimensional models can readily be extended to allow for varying surface roughness losses, canalization and storm distributions in time and space. Where discontinuities are present such as in built up areas, it may be easier to use one of the available simplistic runoff models such as SWMM or ILLUDAS.

ANALYSIS OF FLOW IN PART-FULL PIPES

Simulation of flow in part-full circular conduits is more complicated than for overland flow. Nevertheless the same basic kinematic theory applies. It is convenient to adopt polar axes instead of cartesian axes for circular conduits. On this basis a computer program for analysing flow in pipe networks was prepared. The system is assumed to comprise overland flow planes connected to pipe inlets.

Overland flow

In analyzing the flow over the sub-catchments draining into each inlet, the assumption is made that the sub-catchment is rectangular with a width equal to the length of drain pipe into which the sub-catchment drains. This simplification is mainly to reduce data preparation to a minimum, and the relevant input line could readily be varied to feed in sub-catchment width. For overland flow the cross-sectional area per unit width of catchment is y . The concentration time of a plane is, adopting the Manning-Strickler equation for friction gradient,

$$t_c = \left\{ \frac{L k^{1/6}}{7.7\sqrt{Sg} i_e^{2/3}} \right\}^{3/5} \quad (5.26)$$

Kinematic equations for part-full circular conduits

One starts with the kinematic equations in the form

$$\frac{\partial A}{\partial t} + \frac{\partial Q}{\partial x} = q \quad (\text{inflow per unit length}) \quad (5.27)$$

$$S_o = S_f \quad (5.28)$$

Using the Manning equation to predict friction gradient,

$$Q = \frac{K}{N} \frac{A^{5/3}}{P^{2/3}} S^{1/2} \quad (5.29)$$

and from the Strickler approximation for N,

$$N = 0.13 K k^{1/6} \sqrt{g} \quad \text{therefore} \quad (5.30)$$

$$Q = \frac{7.7 \sqrt{Sg}}{k^{1/6}} \frac{A^{5/3}}{P^{2/3}} \quad (5.31)$$

No allowance for losses at manholes is made as this is usually included in the grading of successive pipes.

The cross-sectional area of flow in a circular conduit running part full (see Fig. 5.12) is

$$A = \frac{D^2}{4} \left(\frac{\theta}{2} - \cos \frac{\theta}{2} \sin \frac{\theta}{2} \right) \quad (5.32)$$

$$\text{and } P = D \frac{\theta}{2} \quad (5.33)$$

Thus if one takes θ as the variable, the continuity equation becomes

$$\frac{D^2}{8} \left(1 + \sin^2 \frac{\theta}{2} - \cos^2 \frac{\theta}{2} \right) \frac{\partial \theta}{\partial t} + \frac{\partial Q}{\partial x} = q \quad (5.34)$$

In finite difference form, solving for θ after a time interval Δt ,

$$\theta_2 = \theta_1 + \left(q - \frac{\Delta Q}{\Delta x} \right) \frac{8 \Delta t}{D^2 \left(1 + \sin^2 \frac{\theta}{2} - \cos^2 \frac{\theta}{2} \right)} \quad (5.35)$$

and in terms of the new θ ,

$$Q = \frac{7.7 \sqrt{Sg}}{k^{1/6}} \frac{D^2}{4} \left(\frac{\theta}{2} - \cos \frac{\theta}{2} \sin \frac{\theta}{2} \right) \left\{ \frac{D}{4} \left(1 - \frac{\cos \frac{\theta}{2} \sin \frac{\theta}{2}}{\theta/2} \right) \right\}^{2/3} \quad (5.36)$$

In order to simulate the flow and depth variations in the pipes, the latter two equations are applied at successive points for successive time intervals.

It will be observed that it should never be necessary to consider surcharged conditions in a design. If pipes are designed to run just full at their design capacity, then they will run part full for any other storm duration. The higher up the leg a pipe length is, the shorter will be the concentration time, or time to flow equilibrium. The design storm duration will equal the concentration time of the drains down to the pipe in question. Any subsequent pipes will have larger concentration times and consequently a lower storm intensity.

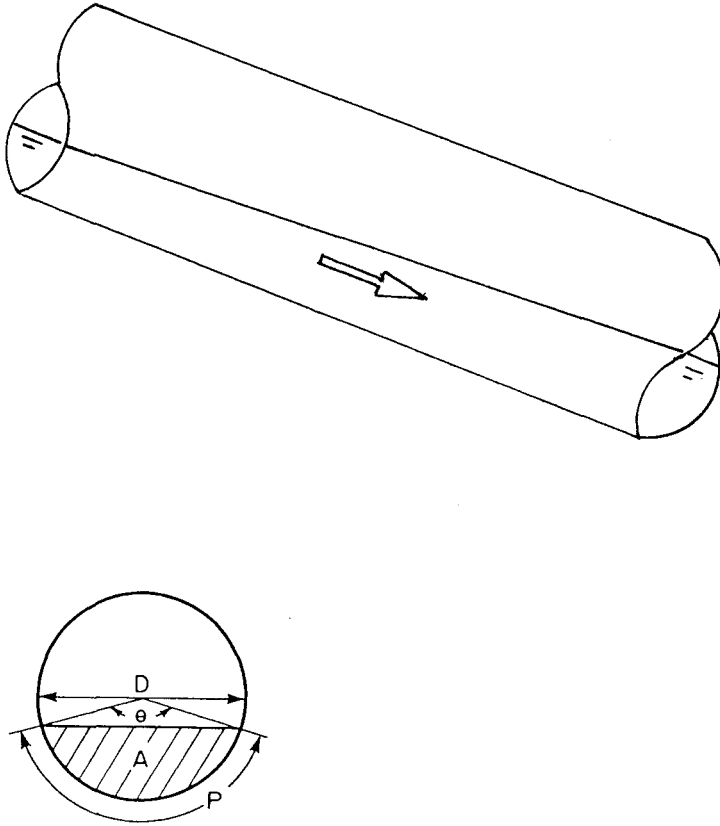


Fig. 5.12 Cross section through part-full pipe.

Pipes higher up will therefore run part-full when a lower pipe is at its design capacity and running full.

The preceding scheme was employed in a program for analyzing the flow in each pipe in a drainage network the plan which is specified by the designer. The engineer must pre-select the layout, sub-division of catchment, position of inlets and grades. The grades will in general conform to the slope of the ground.

APPLICATION IN DESIGN

Few existing storm drain design methods allow for the increase in flow in the drain until equilibrium is reached. Nor is there often allowance for the fact that upper drains are designed for a more intense storm than lower drains. The upper drains have small concentration times and consequently the design storm duration is small. Lower drains will be designed for longer duration storms. Consequently the upper drains may not flow full when the lower drains are at their design capacity.

It is in fact necessary to simulate the flow overland and in each upper drain in order to size any particular lower drain. Such analysis can only be done practically by digital computer using numerical solutions of the flow equations. Many calculations are necessary for complex networks. A limitation on the maximum time interval for numerical stability implies many iterations until equilibrium flow conditions are reached for each pipe design. In addition, a number of different storm durations must be investigated for each pipe. A simple and efficient iterative procedure was therefore sought in order to minimize computer time. The kinematic form of the flow equations was employed to ensure this. The emphasis throughout the program is simplicity of data input and minimization of computational effort. Obviously some accuracy is sacrificed hereby, but the overriding assumption of precipitation pattern is probably more important. Sensitivity analysis and refinement can, if justified, be done with more sophisticated analytical models.

The simulation proceeds for successive pipes, the diameters of which are known. The same analytical procedure may be employed for design, that is the selection of pipe diameters. Starting at the top end of a drainage system, one sizes successively lower pipes. Thus each pipe upstream of the one to be designed, is defined. It is necessary to investigate storms of different duration and intensity of flow to determine the design storm resulting in maximum flow for the next pipe.

It is assumed that the design storm recurrence interval is pre-selected. The intensity-duration relationship is assumed to be of the form

$$i_e = \frac{a}{b + t_d} \quad (5.37)$$

By selecting storms of varying duration t_d , and simulating the flow buildup down the drains, the program can select a storm which will result in the maximum peak flow from the lower end of the system. That discharge is the one to use for sizing the subsequent pipe. Thus the

program proceeds from pipe to pipe until the entire network is designed. It should be noted that the network layout and pipe grades are pre-selected.

The sophistication of gradient optimization by dynamic programming (Merrit and Bogan, 1973; Dajani and Hasit, 1974) would add considerably to the computational cost. Other optimization techniques (Argaman et al, 1973; Yen and Sevuk, 1974) also add to the computations and omit the factor of decreasing storm intensity for lower sewers.

The algorithm was employed to design the drain size for the layout depicted in Fig. 5.13 . Input data and output are appended.

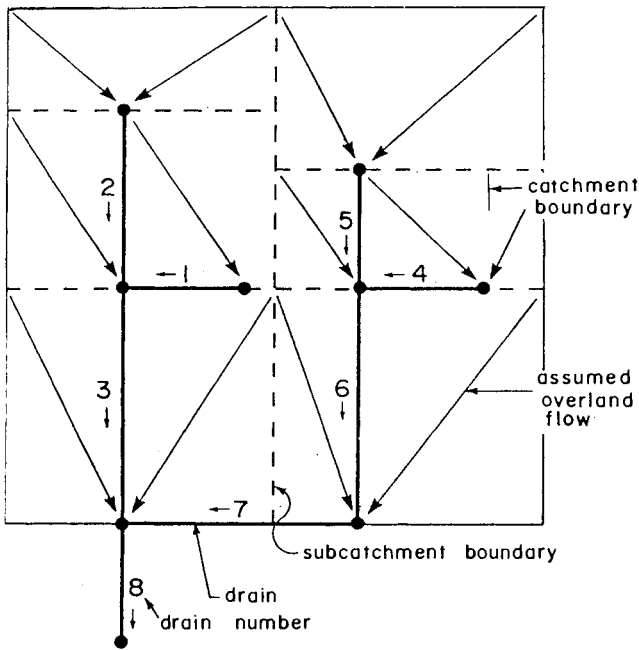


Fig. 5.13 Layout plan of drainage network sized in example.

COMPUTER PROGRAM FOR SIZING DRAIN PIPES IN NETWORKS

Assumptions in computer program

Pipes are assumed to flow initially at a depth corresponding to a subtended angle of 0.2π at the centre. The corresponding flow is very low, but this assumption avoids an anomaly for the case of zero depth when the numerical form of the equations is unrealistic.

Inflow from subcatchments is assumed to occur along the full length of the respective pipe, i.e. subcatchment breadth is assumed to be equal to pipe length. This affects overland flow time to some extent. If necessary (if flow is sensitive to storm duration) the subcatchment friction factor could be adjusted to give the correct overland flow time.

The computer program, written in FORTRAN for use in conversational mode on a terminal connected to an IBM 370 machine, is appended. The input format is described below. Data are read in free format and can be input on a terminal as the program stands.

First line of data:

M, A, B, E, IN, IR, II, G.

Second and subsequent lines of data (one line for each length of pipe):
X(I), S(I), Z(I), C(I), SO(I), EO(I), IB(I).

The input symbols are explained in the appended list and elaborated below:

- M - The number of pipes: the number of pipes should be minimized for computational cost minimization. For computational accuracy the pipes should be divided into lengths of the same order of magnitude. It is convenient to make the pipe lengths equal to the distance between inlets. Inlets between 10 and 200 m apart are normally sufficient for computational accuracy. There should be at least two pipes in the system.
- A,- Precipitation rate i is calculated from an equation of the form

$$i = A/(B + t_d)$$
 where t_d is the storm duration and B is a regional constant (both in seconds). A is a function of storm return period and catchment location and its units are in m if SI units are used, and ft if ft-lb-sec units are used.
- E - Pipe roughness. This is analogous to the Nikuradse roughness and E is measured in m or ft. It is assumed in the program that all

pipes have the same roughness. A conservative figure of at least 0.001 m (0.003 ft) is suggested to account for surface deterioration with time due to erosion, corrosion or deposits.

IN, -For each pipe sizing computation various storm durations are investigated, ranging from IU1 up to IU2 in steps of IR (all in seconds). The smallest storm duration IU1 is set equal to the overland flow time for an upper pipe or the previous pipe design storm duration for subsequent pipes down a leg. The number of storm durations investigated is specified by IN and the increment in trial storm duration is specified by IR. Thus $IU2 = IU1 + IN * IR$. The accuracy of the computations is affected by the number of trial storm durations. A value of IN between 3 and 10 is usually satisfactory. The upper limit can be estimated beforehand from experience or by trial (if all design storm durations turn out to be less than the IU2 specified then the IN selected is satisfactory).

II -The computational time and cost is affected by the time increment of computations II (seconds). The maximum possible value is dependent on the numerical stability of the computations. A value equal to the minimum value of

$$\left[\frac{B}{C(I)A} \right]^{0.4} \left[\frac{Z(I)E}{100 \sqrt{S(I)G} X(I)} \right]^{0.6}$$

will normally be satisfactory (of the order of 60 to 300 seconds).

G - Gravitational acceleration (9.8 in SI units and 32.2 in ft - sec units).

The pipe data is next read in line by line for M pipes. As the program stands, 98 individual pipes are permitted, and any number of legs subject to the maximum number of pipes.

X(I) The pipe length in metres or ft, whichever units are used. An upper limit on individual pipes of 200 m is suggested for computational accuracy and a lower limit of 10 m for optimizing computer time.

S(I) The slope of that pipe in m per m or ft per ft.

Z(I) The surface area contributing runoff to the pipe in m² or ft².

C(I) The proportion of precipitation which runs off (analogous to the 'C' in the Rational formula).

SO(I) The overland slope of the contributing area, towards the inlet at the head of the pipe.

EO(I) The equivalent roughness of the overland area in m or ft depending on units employed.

IB(I) The number of the pipe which is a branch into the head of pipe I.

For no branch, put $IB(I) = 0$

For a header pipe at the top of a leg, put $IB(I) = -1$.

Only one branch pipe per inlet is permitted.

More must be accommodated by inserting short dummy pipes between. The order in which pipes are tabulated should be obtained as follows:

After drawing out a plan of the catchment with each pipe, mark the longest leg possible starting from the outfall, then successively shorter legs on first the longest, then successively shorter pipes. Now number the pipes in the reverse order, starting at the top of the shortest leg of the shortest leg of the shortest leg, etc. Proceed down each leg with the numbering until a junction is reached. Never proceed past a branch which has not been tabulated previously. In this way all pipes leading into a pipe will have had their diameters calculated before the next lower pipe is designed.

Sample input

The data are in metres here and are taken from Fig. 5.13.

8	.075	1440	.001	3	300	60	9.8
100	.002	20000	.4	.005	.01	-1	
150	.004	20000	.4	.003	.01	-1	
200	.004	40000	.4	.003	.01	1	
100	.002	10000	.3	.005	.02	-1	
100	.004	40000	.4	.003	.01	-1	
200	.004	10000	.5	.005	.01	4	
200	.002	40000	.4	.002	.01	0	
100	.005	20000	.4	.003	.01	3	

Symbols in computer program

A Rainfall parameter in the equation:
Precipitation rate = $A/(B + IU)$. Metres or feet.

A1 Intermediate calculation variable (no significance).

A2 $AT(I)/2$

AT(I) Angle subtended at base of pipe by water surface. Radians.

B Time constant in the equation: Precipitation rate = $A/(B+IU)$.
Seconds.

C(I) Proportion of rain which runs off subcatchment I.

D(I) Diameter of pipe I. Metres or feet.

E Equivalent roughness of pipes. Metres or feet.

EO(I) Equivalent roughness of subcatchment surface I. Metres or feet.

G Gravitational acceleration 9.8 m/s² or 32.2 ft/sec².

I Pipe number.

IA(I) Feeder pipe 1 for pipe I.

IB(I) Branch pipe 2 for pipe I. If $IB = -1$, pipe I is a header.

IN Number of steps in rainfall duration.

II Increment in time between iterations. Seconds.
 IT Iteration number.
 IR Increment in storm duration. Seconds.
 IU Storm duration. Seconds
 IU1 Lower limit on storm duration. Seconds
 IU2 Upper limit on storm duration. Seconds
 IUI Concentration time for overland flow. Seconds
 J Iteration number for overland flow calculation
 M Number of pipes
 M1 M - 1
 M2 Pipe number when iterating successive pipe diameters.
 P(I) Inflow to sewer from subcatchment.

$$P(I) = Z(I) * C(I) * A / (B + IU). \text{ m}^3/\text{s or ft}^3/\text{sec.}$$

 PO Excess rain rate from subcatchment. m/s or ft/sec.
 PP1 Inflow rate from subcatchment. m³/s or ft³/s.
 Q(I) Flow rate in pipe. m³/s or ft³/s.
 QO(I) Overland flow per unit width of subcatchment. m²/s or ft²/s.
 QOV Intermediate calculation variable.
 QP(I) Flow rate in pipe for previous time interval. m³/s or ft³/s.
 QQ(I) Design flow in pipe. m³/s or ft³/s.
 Q1, Q2 Intermediate calculation parameters.
 S(I) Slope of pipe. m/m or ft/ft.
 SO(I) Ground slope of subcatchment. m/m or ft/ft.
 UU(I) Design storm duration. Seconds.
 X(I) Length of pipe. m or ft.
 Z(I) Area of subcatchment. m² or ft².

REFERENCES

- Argaman, Y., Shamir, U. and Spivak, E., 1973. Design of optimal sewerage systems. Proc. ASCE, (99), EE5, Oct., p 703-716.
 Constandinides, C. A., 1981. Numerical techniques for a 2-dimensional kinematic overland flow model, Water S.A., Pretoria.
 Dajani, J.S. and Hasit, Y., 1974. Capital cost minimization of drainage networks. Proc. ASCE, (100), EE2, April. p325-337.
 Merritt, L.B., and Bogan, R.H., 1973. Computer based optimal design of sewer systems. Proc. ASCE, (99), EE1, Feb. p35-53.
 Overton, D.E. and Meadows, M.E., 1976. Stormwater modelling. Academic Press, N.Y. 358pp.
 Stephenson, D. 1980. Direct design algorithm for storm drain networks. Proc. Int. Conf. Urban Storm Drainage, Univ. Kentucky, Lexington.
 Watkins, L.H., 1972. The design of urban sewer systems. Tech. Paper No. 55, Road Research Lab., London.
 Wooding, R.A., 1965. A hydraulic model for the catchment stream problem. J. Hydrol. (a) Kinematic wave theory, (3), 1965, p254-257; (b) Numerical solutions, (3), 1965, p268-282; (c) Comparison with runoff observations (4), 1966, p21-37.
 Woolhiser, D.A. and Liggett, J.A., 1967. Unsteady one-dimensional flow over a plane - the rising hydrograph. Water Resources Res., 3 (3), p753-771
 Yen, B.C. and Sevuk, A.S., 1975. Design of storm sewer networks. Proc. ASCE, 101, EE4, Aug. p535-553.

Computer program for sizing storm drains in a network

```

L.0001      DIMENSION P(99),Q(99),S(99),X(99),D(99),AT(99),Z(99),QQ(99),UU(99),C(99)
L.0002      DIMENSION E0(99),S0(99),QJ(99),IB(99),IA(99),JP(99)
L.0003      READ(9,5)M,A,B,E,IN,IR,II,G
L.0004 5     FORMAT(E)
L.0005 10    FORMAT(7Y)
L.0006      GO TO 15 I=1,M
L.0007      READ(9,10)X(I),S(I),Z(I),C(I),S0(I),E0(I),IB(I)
L.0008      IF (IB(I).GT.1)GO TO 13
L.0009      IF (IB(I).LT.0)GO TO 12
L.0010      IB(I)=99
L.0011      GO TO 13
L.0012 12    IB(I)=99
L.0013      IA(I)=99
L.0014      GO TO 15
L.0015 13    IA(I)=I-1
L.0016 15    CONTINUE
L.0017      Q(99)=0.
L.0018      QJ(99)=0.
L.0019      QP(I)=0.
L.0020      M1=M-1
L.0021      DO 25 I=1,M
L.0022      IF (IA(I).LT.99)GO TO 25
L.0023      PD=C(I)*A/(B+500)
L.0024      DO 20 J=1,10
L.0025 20    PD=C(I)*A/(B+(Z(I)/X(I)*EJ(I)**.167/7.7/(S0(I)*G)**.5)**.5/PD**.4)
L.0026      IU1=C(I)*A/PD-.3
L.0027      UU(I)=IU1
L.0028      PP1=PD*Z(I)
L.0029      QQ(I)=PP1
L.0030      D(I)=(PP1**E**.167/7.7/(S(I)*G)**.5/3.141**4**1.667)****.375
L.0031 25    CONTINUE
L.0032      CO 300 M2=1,M1
L.0033      IU1=IU1
L.0034      IF (IA(M2+1).GE.99)GO TO 300
L.0035      QJ(M2+1)=0.
L.0036      IU2=IU1+IN*IR
L.0037      DO 200 IU=IU1,IU2,IR
L.0038      CO 30 I=1,M
L.0039      IU=IU+I
L.0040      QJ(I)=Z(I)/10./X(I)*C(I)*A/(IU)
L.0041      AT(I)=.2*3.141
L.0042 30    Q(I)=0.
L.0043      DO 120 IT=1,IU,II
L.0044      M3=M2+1
L.0045      CO 32 I=1,M2
L.0046      COV=(7.7*(S0(I)*G)**.5/EJ(I)**.167)**.6*1.667*(I*QJ(I)**.4
L.0047      QQ(I)=QJ(I)+COV*(C(I)*A/(B+IU)-QJ(I)/Z(I)*X(I))
L.0048 32    P(I)=QQ(I)*X(I)
L.0049      DO 100 I=1,M2
L.0050 35    IF (IT.LE.1)GO TO 50
L.0051 40    A1=(P(I)-Q(I)*QP(IA(I))+QP(IB(I)))/X(I)*II*8./Q(I)/Q(I)
L.0052 45    AT(I)=A1/(1-(COS(AT(I)/2.))**.2.+(SIN(AT(I)/2.))**.2.)*AT(I)
L.0053 50    A2=AT(I)/2.
L.0054      CI=7.7*SQRT(C*S(I))/E**(1./5.)
L.0055      C2=Q1*Q(I)**2./4.*(A2-COS(A2)*SIN(A2))
L.0056 100   Q(I)=Q2*(D(I)/4.*(1.-COS(A2)*SIN(A2))**.2./3.)
L.0057      DO 110 I=1,M2
L.0058 110   QP(I)=Q(I)
L.0059 120   CONTINUE
L.0060      Q(M2+1)=Q(IB(M2+1))+J(M2)+P(M2+1)
L.0061      IF (Q(M2+1).LE.QQ(M2+1))GO TO 200
L.0062      QQ(M2+1)=Q(M2+1)
L.0063      UU(M2+1)=IU
L.0064 200   CONTINUE
L.0065      D(M2+1)=(QQ(M2+1)*E**(1./5.)/7.7/SQRT(S(M2+1)*G)/3.141**4**E**.375)**(J./3.)
L.0066      IF (IA(M2+1).LT.99)GO TO 290
L.0067      IU1=IU1
L.0068      GO TO 300
L.0069 290   IU1=UU(M2+1)
L.0070 300   CONTINUE
L.0071      WRITE(5,350)
L.0072 350   FORMAT(' STORM SEWER DESIGN')
L.0073      WRITE(5,60)
L.0074 60    FORMAT(' PIPE LENGTH DIA GRADE DSFLC/S STORM S AREA')
L.0075      DO 400 I=1,M
L.0076 400   WRITE(5,70)I,X(I),D(I),S(I),QJ(I),UU(I),Z(I)
L.0077 70    FORMAT(I6,F7.0,F6.3,F6.4,F9.3,F8.0,F9.0,F9.0)
L.0078      WRITE(5,80)M,A,B,E,IU2,IR,II
L.0079 80    FORMAT(' DATA' I6,F5.3,F5.0,F5.4,3F6.0)
L.0080 STOP
L.0081 END

```

COMPUTER OUTPUT FOR SAMPLE RUN

L.0001	STORM SEWER DESIGN					
L.0002	PIPE LENGTH	DIA	GRADE	DSFLC/S	STORM S	AREA
L.0003	1	100.	.576	.0020	.344	1014. 20000.
L.0004	2	150.	.514	.0040	.355	911. 20000.
L.0005	3	200.	.643	.0040	.462	2068. 40000.
L.0006	4	100.	.415	.0020	.102	772. 10000.
L.0007	5	100.	.574	.0040	.342	2068. 40000.
L.0008	6	200.	.619	.0040	.417	2068. 10000.
L.0009	7	200.	.853	.0020	.696	2068. 40000.
L.0010	8	100.	.905	.0050	1.287	2068. 20000.
L.0011	DATA	8	.0751440.	.0010	2963	300 60

SIMULATION PROGRAMS

ADVANTAGES OF COMPUTER MODELLING

A variety of methods has been described enabling the engineer to estimate runoff and design a drainage system accordingly. In all cases the runoff process has been simplified to some extent in order to enable design parameters to be established. In some cases there is oversimplification with the result that the effect of some variables is omitted. Simplification is invariably demanded in order to achieve a design. Once a preliminary design is achieved, however, there is no reason why the design cannot be improved by reworking and sensitivity studies. It is in the refinement of the design that computer simulation is useful.

It must be borne in mind that simulation is an analytical tool in the design process. It is also of use in management studies, and in research, but as far as the design engineer is concerned, it is a means of analyzing a system designed by some other means. Many of the urban drainage simulation programs available require data input in the form of drainage network layout, conduit sizes and grades and a complete design storm hyetograph. These features are seldom available to the design engineer, and hence analytical and simulation programs are to him a second stage in the design. There are direct design programs available based on a given layout. There are also least-cost optimization programs as outlined in Chapter 11. But these require some simplification again and the final design could be improved with more sophisticated programs.

Simulation programs are justified by the improvement they achieve with repetitive analysis. Not only do they enable discharges to be calculated with greater accuracy than the simplistic methods outlined, but they also permit sensitivity studies.

By manipulating the variables, eg. pipe diameters, the analyst is able to optimize the system to an extent. The effect of detention storage, network layout, grades and diameters and gutter capacity interact to complicate the computations and these effects justify some form of numerical computation before the design is finalized.

In cases of multiple objectives, simulation programs are valuable. Thus the concentration of flow in large conduits may reduce overall construction costs but inconvenience some ratepayers. The effect of

construction of a stormwater drainage system on the catchment may be of importance. More rapid concentration of runoff due to pavings and canalization will create higher flows downstream, possibly resulting in erosion or flooding hitherto unexperienced. Natural infiltration will be reduced, resulting in lowering of the water table. These effects can most readily be studied by modelling.

The simulation and analysis of stormwater drainage systems is therefore invariably both informative and cost effective. This does not mean that all new drainage schemes are analyzed by computer. To gain access to computer modelling facilities the designers must commit themselves to a fairly substantial outlay. The following steps indicate what is involved in modelling.

1. Programming and debugging a new model
2. Study of various models available and selection of an available computer package.
3. Selection of computer hardware and operators.
4. Mounting program on computer, debugging and adaptation to local conditions.
5. Training staff in the use of the model.
6. Study of user's manuals and familiarity with program.
7. Collection of data for modelling from records and field.
8. Interpretation of data, discretization, coding and punching.
9. Trial runs of program for calibration purposes.
10. Verification of model against existing runoff data.
11. Sensitivity analysis using alternative designs and storm input.
12. Refinement of the initial design and possibly repeat of previous steps.
13. Report back on conclusions.

There are many objectives in modelling and it would be wise to define these before committing expenditure in that subject:

1. Basic research e.g. familiarity with models and their capabilities.
2. Planning location and scale of outfalls, diversion and treatment facilities.
3. Design of conduits, diversion works and treatment facilities.
4. Refinement of designs by successive trials.
5. Catchment impact assessment i.e. the effect of drainage on the environment.
6. Selection of management and operational alternatives such as diversion rates, treatment levels.
7. Cost estimates.
8. Identification of point source pollutants.

9. Hydrological analysis of stream flooding.
10. Prediction of water quality in reservoirs and streams.

BASIS OF FLOW MODELS

Most models require data to a fairly high level of detail. Thus pipe diameters, gutter dimensions, friction factors, grades and lengths are specified to a number of significant digits. Overland flow planes can be lumped or discretized to a certain extent to the discretion of the analyst. In fact some experience in defining flow planes is useful as it affects concentration times and runoff quite markedly. Storm data (precipitation versus time) again is required to some degree of accuracy.

It is therefore important that the analyst is aware of the limitations in the programs. This may in turn influence the attention he pays to data preparation. The British Transport and Roads Research Laboratory Model (RRL) and its USA version the Illinois Urban Drainage Area Simulator (ILLUDAS) are based on isochronal methods i.e. flow velocities are independent of runoff intensity and based on full pipe conditions. Travel times are therefore only correct at design flows and dynamic effects plus the rising and falling limbs of the hydrograph are incorrectly predicted.

Unsteady flow analysis in drains is performed most efficiently by the kinematic method (e.g. the E.P.A. Stormwater Management Model, SWMM). Depth-discharge relationships are thus based on the steady flow discharge formulae such as that of Manning. Time variation in depth is also accounted for but rapidly varied flow is not correctly analysed.

Some programs are orientated towards single events whereas others perform continuous simulation i.e. they cater for the effect of previous events on the groundwater and storage state. Most simulation models are dynamic i.e. they reproduce changes with time. Optimization models on the other hand are usually static i.e. on account of the complexity of dynamic optimization they consider only one point in time. Generally the models discussed simulate flows with some theoretical basis, however simplified. Some catchment water resource models, however, and some quality models use an empirical base i.e. equations are based on limited measurement and not proven.

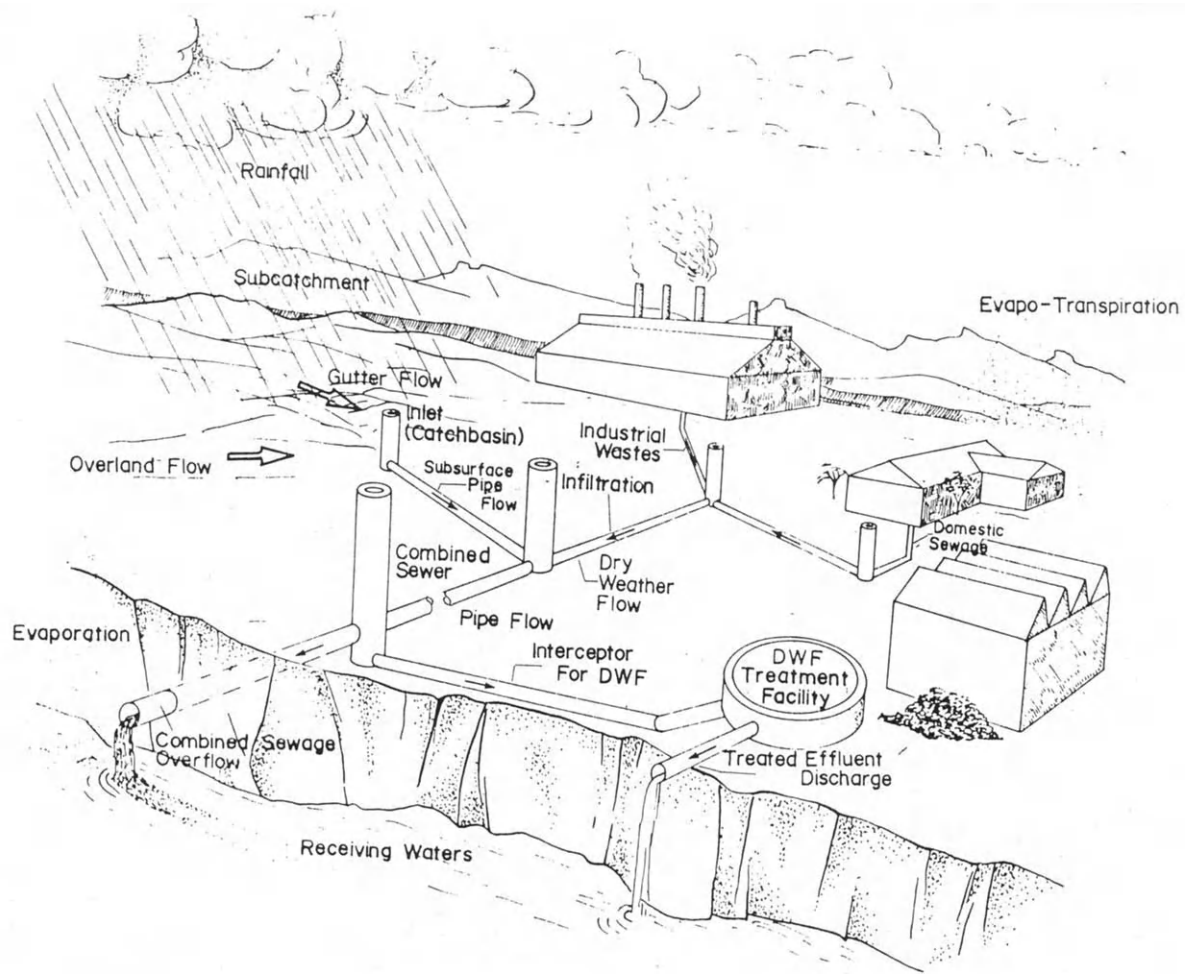


Fig. 6.1 Typical Urban Drainage System Model for SWMM - Diagrammatic

SOME MODELS

Road Research Laboratory Model (RRL)

Time-area methods have remained popular in England, and the Road Research Laboratory developed a program on the lines described by Watkins (1962). The assumption of specific isochrones, or lines of equal travel time to the mouth, is made regardless of storm intensity. Thus the dynamics and storage in the system are not simulated and single events only are studied with it.

After hydraulic properties of conduits such as cross sectional areas are calculated, flow velocities for full pipe flow and travel times are estimated. Isochrones are thus obtained and plotted to establish a time-area curve.

The model also ignores pervious areas. Interception, depression storage and evaporation are likewise omitted. Gutter flow and surcharge are not permitted. Water quality is not considered despite the fact that the model was originally intended for combined sewers.

Illinois Urban Drainage Area Simulator (ILLUDAS)

This model was developed at the University of Illinois (Terstriep and Stall, 1974) to overcome some of the shortcomings of the RRL model. Infiltration and interconnected drainage areas are permitted, but the model is also based on the isochronal method. Storage effects are simulated by routing through reservoir-type storage. Data input is straightforward and running costs are low. Quality is not considered.

The RRL and ILLUDAS models have proved satisfactory for small areas (less than 10 km²) and provided the storm is not an extreme event (with a recurrence interval exceeding 20 years).

Stormwater Management Model (SWMM)

The Stormwater Management Model (EPA, 1971) was developed by three organizations under contract to the U.S. Environmental Protection Agency. The firms Metcalf and Eddy and Water Resources Engineers originally developed parts of this model which is now maintained by the University of Florida. The model is for the study of the quantity and quality of runoff from urban catchments. It is divided into a number of blocks, some of which may be run on their own or in series with others. The blocks are described below:

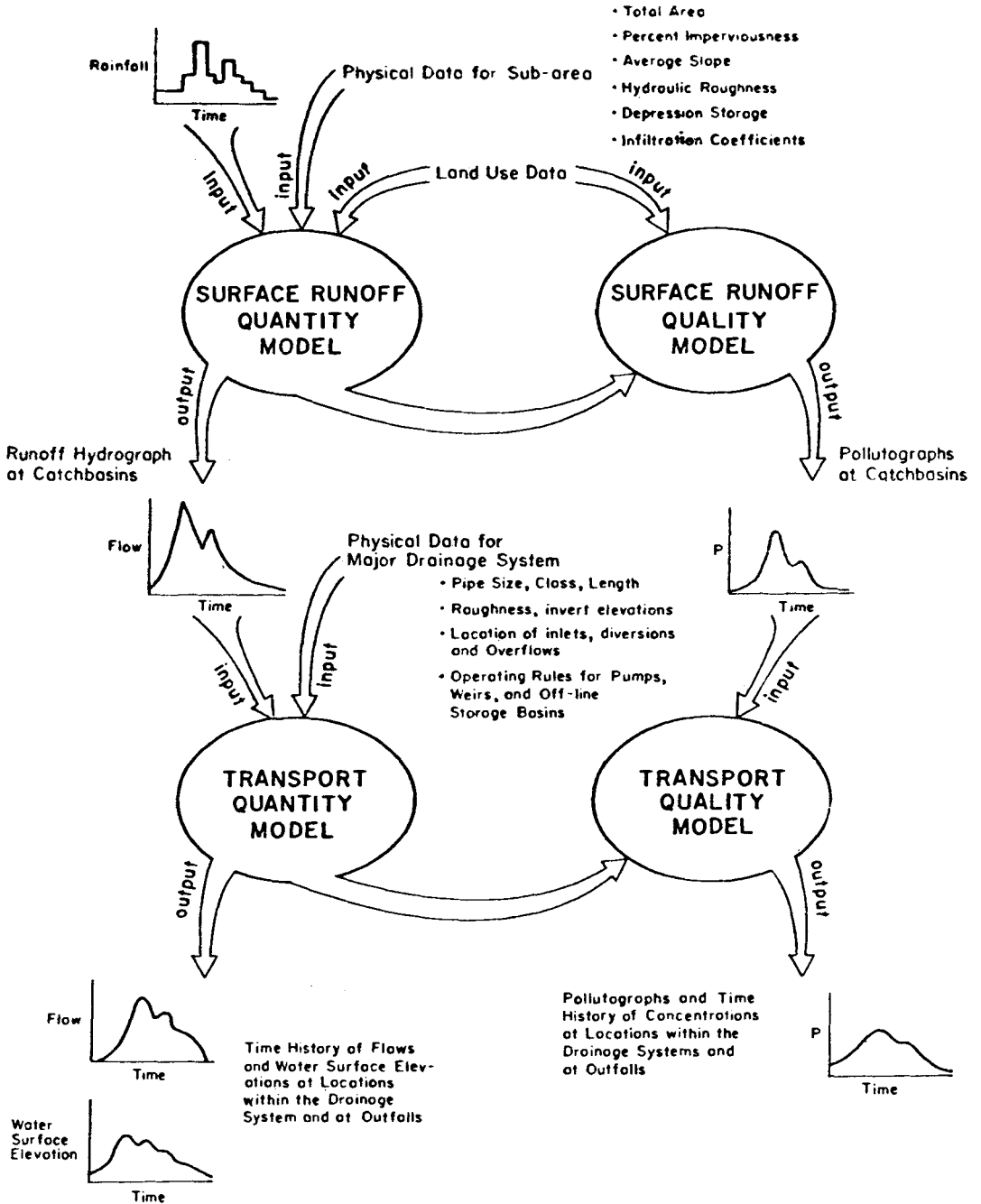


Fig. 6.2 Structure of SWMM Surface Runoff and Transport Models

1. *Executive Block*, which controls the running and links other blocks.
2. *Runoff Block*, which models flood flows off pervious or impervious ground, in gutters, drains and channels. It is based on a numerical solution of the kinematic equations so does not allow for backwater or weir storage effects. Quantity and quality may be simulated and hydrographs at any point in the system may be displayed.
3. *Transport Block*. This is a more refined routing subroutine and allows for overflowing manholes, backwatering and flow in non-uniform channels and rivers.
4. *Storage and Treatment*. The waters may be stored to alleviate floods, and treated to reduce pollutants. A sophisticated biological treatment process and solids removal system is permitted, but the number of pollutants removable is limited.
5. *Receiving Waters Block*. The circulation in lakes may be studied considering hydraulic gradients, wind effects, overflows, and numerous sources of inflow. Pollution, water levels and flows may be listed over a period of time at selected nodes.

Stormwater Runoff Model (STORM)

The U.S. Corps of Engineers (1974) developed STORM for the purpose of studying urban stormwater runoff erosion and treatment. Pollutants such as suspended solids, BOD, nitrogen and phosphorous are assumed to be conservative.

Hydrocomp Simulation Model (HYDROSIM)

The U.S. firm Hydrocomp developed a program originally for runoff simulation in non-urban areas and modified it for sewered areas. It is essentially a catchment routing model with an empirical and theoretical basis. Continuous routing on any selected time scale is possible. The program is not available to the public.

University of Cincinnati Urban Runoff Model (UCURM)

The University of Cincinnati Urban Runoff Model is not based on time-area methods, (Papadakis, 1972). It routes the flows overland and through gutters and pipes using continuity and Manning's resistance equation.

Infiltration is accounted for using Horton's equation, and surface retention is related to depression storage using an exponential equation. The drainage area is divided into subcatchments. Starting with overland flow, excess rainfall is routed through successive components of the drainage system.

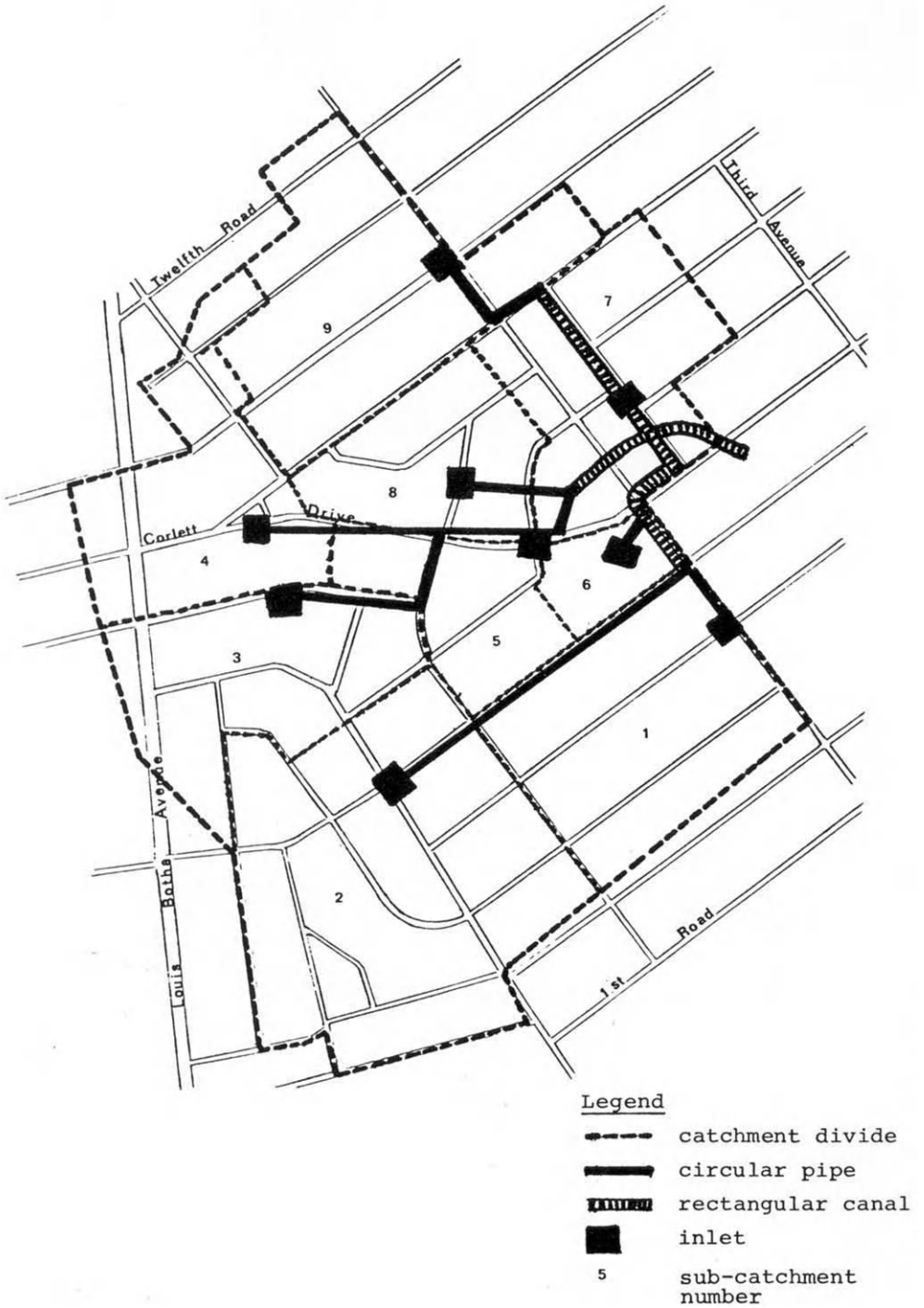


Fig. 6.3 Subcatchments and simplified drainage network

Fig. 6.4 Hyetograph plot by SWMM

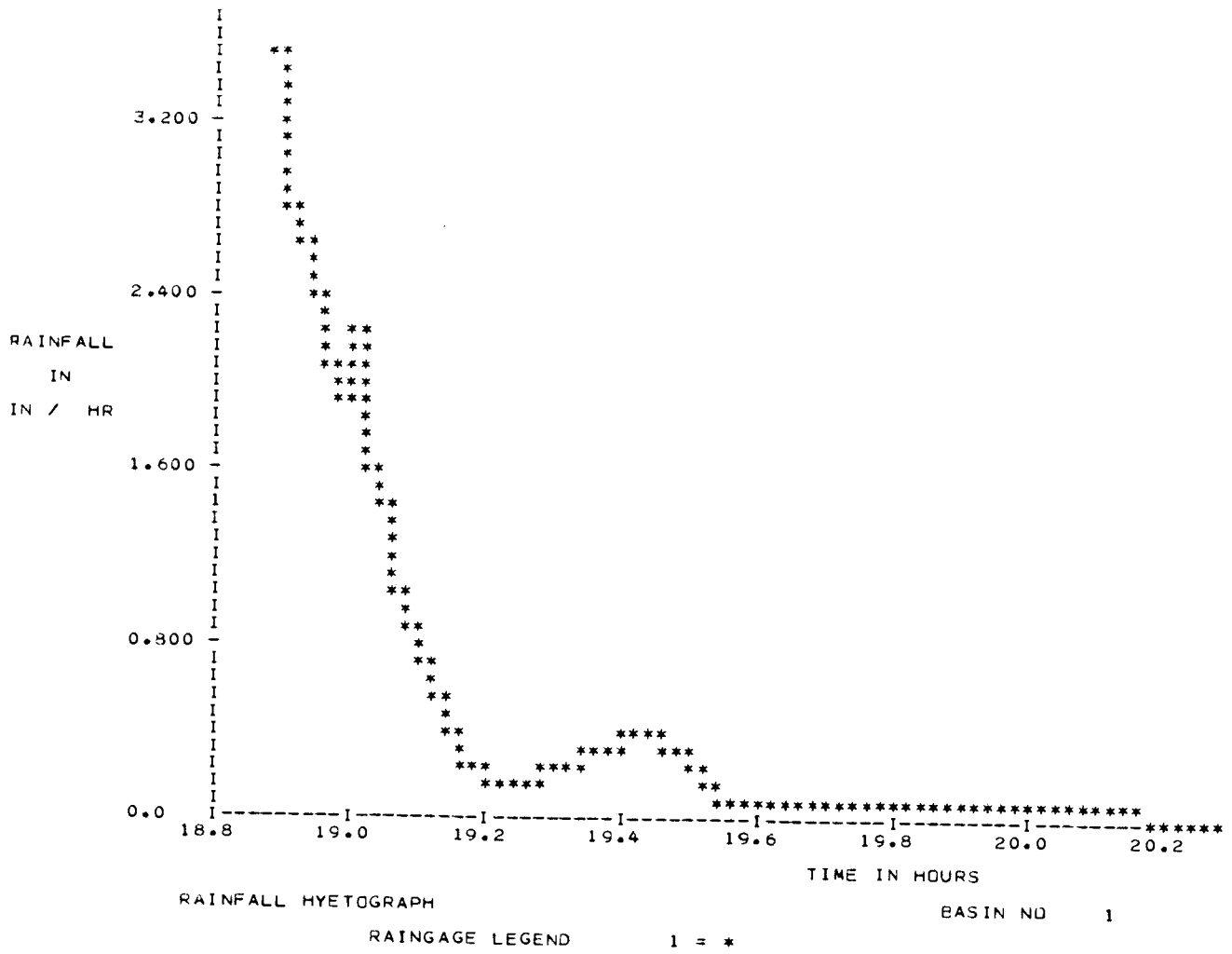
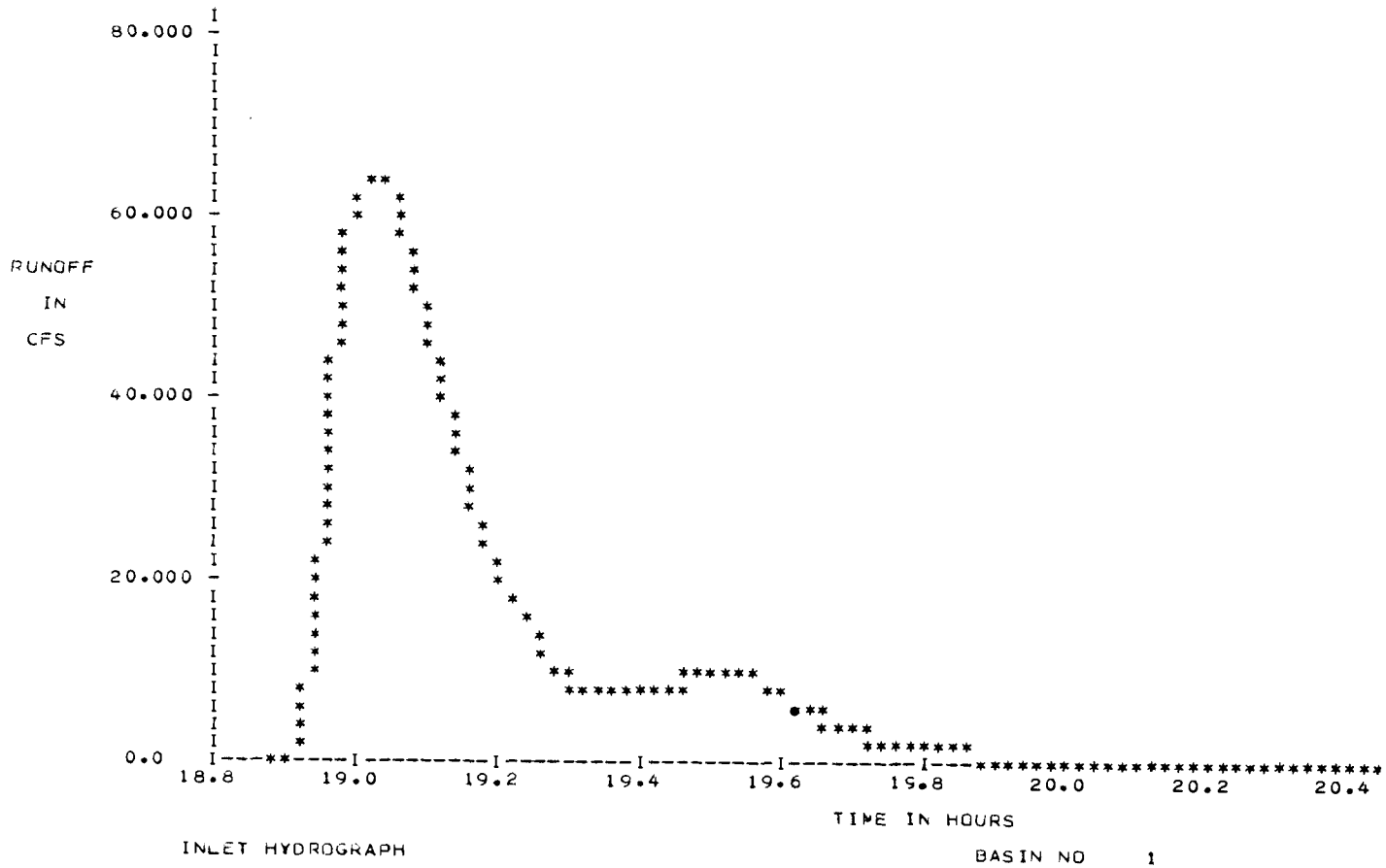


Fig. 6.5 Hydrograph plot by SWMM



Other models.

The University of Cincinnati (1970) also developed a simulation model for pollution washoff. A decay function is included but sediment transport is also permitted. Soluble pollutants are assumed to travel with the water.

Models of reservoirs include that of Chen and Orlob (1971). Their model is based on a multi-layered system, each layer which is assumed to be completely mixed.

The Texas Water Development Board (1970) developed DOSAG-1 to simulate BOD and DO in streams. QUAL-1 was developed by them to simulate temperature, BOD, DO and conservative minerals in streams, but requires more data than DOSAG-1. They are one-dimensional models but branches and a variety of options are possible. Another program, the Texas Water Yield (TWY) model, is based on the SCS curve number procedure and is primarily to estimate runoff. The Massachusetts Institute of Technology developed a program called MITCAT (MIT catchment model).

A number of comparisons of alternative models have been made (Heeps and Mein, 1974; Marsalek et al, 1975). Viessman et al (1977) list some of the urban drainage simulation programs in use and their capabilities. Their shortcomings or advantages also are set out. Wanielista (1978) concentrates on a comparison of quality simulation programs. In particular his Best Management Practices Model (BMP) evaluates the effect of diversion of stormwater for treatment. Cost effectiveness of diversion, retention and treatment are given. Runoff is calculated on the SCS curve number method.

WATER QUALITY MODELS

An in-depth study of pollution, catchment management and water purification is beyond the scope of this section, but because many simulation models handle quality as well as quantity a brief discussion of this aspect is justified. The drainage engineer is in fact just as concerned with pollution as with flooding. The protection of the environment against water problems involves a simultaneous study of both aspects. In fact as urban or industrial development grows, the pollution problem expands more rapidly than the flood problem. Pollution is difficult to prevent or control. Whereas one can predict (statistically at least) the flow off the catchment, the quality of the river may be unknown at the time of design. Illegal dumping, diffuse washoff, connections from wastewater treatment works, runoff from dirty industries

TABLE 6.1

Summary of some Runoff Simulation Programs.

Program	Prime feature	Hydraulic routing	Quality capabilities	Comprehensiveness	Ease of Use	Computer required
RRL	Combined sewers	Impervious area only. Single events	None	Limited	Reasonable	IBM
ILLUDAS	Stormwater routing	Isochronal	None	Limited	Simple	IBM
STORM	Runoff quality	Secondary	Good, conservatives	Quality balance	Reasonable	IBM, CDC, Univac.
SWMM	Routing in drains	Kinematic, continuous	Secondary	Very	Big input	IBM, CDC, Univac.
HYDROSIM	Non urban	Modified for sewers	Many	Extensive	Not available to public	IBM
UCURM	Storm sewer flow	None	None	Simple	Easy	IBM
MITCAT	Least cost simulator	Yes	None	Limited	Not available to public	
TWY	Runoff quality	SCS method	Regression	Limited	Requires calibration	IBM
BMP	Diversion and treatment	SCS	Good	Limited	Reasonable	

and from streets, all contribute to the deterioration in the quality of water in streams, rivers, lakes and even the seas.

Fortunately the pollution load is usually most severe when runoff is highest. Dilution of the pollutants may therefore render them innocuous or undetectable. On the other hand the pollution during dry periods may be severe. There may result deterioration of the ecology of rivers and lakes, killing of fish or vegetation, and even a danger to humans and animals from toxic wastes.

Water quality variations can most easily be studied with mathematical models. The analysis of pollutants in streams (Velz, 1970) has been modelled analytically (Thomann, 1972) and numerically (Rinaldi et al, 1978). Planning and optimization models have also been developed (Deininger, 1973). Reactions and circulation in large water bodies is more difficult to predict but considerable research on the modelling of water quality in reservoirs or lakes is proceeding (IIASA, 1978).

The procedures in simulating quality of runoff are very similar to those for quantity. Instead of developing hydrographs, one develops "polutographs" (Overton and Meadows, 1976). Mass balance equations are established at nodes or between reaches. The mixing, dispersion and reactions within the system are simulated. The output is in the form of pollution load and concentration over time at various points. Although some older models were empirical (black box type, requiring calibration for each situation) the modern preference is for some theoretical basis for the equations controlling reactions.

Pollutants can be categorized as organic e.g. silt, inorganic (dissolved salts affect conductivity, pH and hardness), biological (e.g. sewage), thermal (temperature) or radioactive. These classifications do not facilitate analysis and a breakdown into chemical elements is preferred. Parameters which have received most study are BOD (biochemical oxygen demand) and the coupled DO (dissolved oxygen). Nitrogen, phosphorous, TOC (total organic carbon) and silica, the constituents of algae, are suspected to be the cause of eutrophication of lakes in subtropical climates. Whereas dissolved salts and organics are usually conservative parameters requiring a mass balance only at each node, BOD and nutrients are non-conservative as they are subject to reactions and decay.

The biological reactions of even the most common pollutants are not yet thoroughly understood, so modelling techniques can only approximately predict water quality. The transport of pollutants, whether in solution or in suspension is more easily modelled. Even dispersion (turbulent mixing and molecular diffusion) can be modelled. Temperature

and density gradients, resulting in upward or downward transport and wind movements can also be accounted for. Groundwater movement in non-homogeneous and anisotropic aquifers has received considerable attention (Fried, 1975).

Models for predicting pollutant washoff used in the United States are generally of the form

$$P = M (i - e^{-kR\Delta t}) \quad (6.1)$$

where P is the mass of pollutant washed off the catchment in a time increment Δt , M is the available pollutant mass at the start of the time step, k is a washoff decay coefficient and R is the runoff rate per unit area. The equation is used in a step-wise manner to simulate the pollutant washoff rate.

Available pollutant accumulation between streams depends on the pollutant, winds, and type of ground cover. Jewell et al (1980) quote 10 pounds per acre per day (10kg/ha/d) total buildup in US cities, and k about 1 per inch (40 per m). A frequently used figure for k is 4.6 per inch, based on a runoff of 0.5 inches per hour removing 90% of the constituent.

REFERENCES

- Chen, C.W., and Orlob, G.T., Aug. 1971. Ecological Simulation for Aquatic Environments. Annual Report, OWRR Project No. C-2044, U.S. Dept. Int., Office Water Resources Research.
- Deininger, R.A., 1973. Models for Environmental Pollution Control. Ann Arbor Science, Ann Arbor, 448 pp.
- EPA (Environmental Protection Agency), 1971. Stormwater Management Model Vol. 1. Washington D.C.
- Fried, J.J., 1975. Groundwater Pollution, Elsevier, Amsterdam, 330 pp.
- Heeps, D.P. and Mein, R.G., July, 1974. Independent comparison of three urban runoff models. Proc. ASCE, 100, HY7, p995-1010.
- IIASA (International Inst. of Applied Systems Analysis), 1978. Modelling the Water Quality of the Hydrological Cycle, Proc. Joint Symp. Intl. Assn. Hydrol. Science, Baden, 382pp.
- Jewell, T.K., Adrian, D.D., Horner, D.W., 1980. Analysis of stormwater pollutant washoff estimation techniques, Proc. Int. Symp. Urban Storm Runoff, Univ. Kentucky, Lexington.
- Marsalek, J., Dick, T.M., Wisner, P.E., and Clarke W.G., April 1975. Comparative evaluation of three urban runoff models. Water Resources Bulletin, AWRA, 11 (2), p306-328.
- Overton, D.E. and Meadows, M.E., 1976. Stormwater Modelling, Academic Press, N.Y. 358 pp.
- Papadakis, C.N., and Preul, H.C., Oct. 1972. University of Cincinnati Urban Runoff Model, Proc. ASCE, 98 (HY10), p1789-1804.
- Rinaldi, S., Soncini-Sessa, R., Stehfest, H., and Tamura, H., 1978. Modelling and Control of River Quality, McGraw Hill, N.Y., 380 pp.
- Terstriep, M.L. and Stall, J.B., 1974. The Illinois Urban Drainage Area Simulator, ILLUDAS, Illinois State Water Survey Bulletin 58.
- Texas Water Development Board, 1970. DOSAG-1. Simulation of Water Quality in Streams and Canals. Program Documentation and Users Manual, National Tech. Inform. Service, Springfield, V.A.

- Thomann, R.V. 1972. Systems Analysis and Water Quality Management. McGraw Hill, N.Y. 286 pp.
- University of Cincinnati, 1970. Div. of Water Resources, Dept. Civil Eng., Urban Runoff Characteristics.
- U.S. Army Corps of Engineers, Oct. 1974. Urban Stormwater Runoff, Program 723-58-L2520, Hydrological Engg. Centre.
- Veissman, W., Knapp, J.W., Lewis, G.L., and Harbaugh, T.E., 1977. Introduction to Hydrology, 2nd Ed. Harper and Row, N.Y. 704 pp.
- Velz, C.J., 1970. Applied Steam Sanitation. Wiley Inter-science, N.Y. 619 pp.
- Wanielista, M.P., 1978. Stormwater Management, Quantity and Quality, Ann Arbor Science, Ann Arbor, 383 pp.
- Watkins, L.H., 1962. The Design of Urban Sewer Systems. Road Research Tech. Paper 55, Dept. Scientific and Industrial Research, London, HMSO.

CHAPTER 7

PROBABILITY AND RISK

DESIGN STORMS

Storms and floods are unpredictable. The magnitude and frequency of floods cannot be calculated in advance, although a statistical assessment is possible. The question thus arises as to what discharge rate to design any drainage structure for. The design flow may seldom, if ever, occur during the life of the structure. Fortunately the flow rate at other times will usually be less than the capacity of the system. For extreme events the drain may overflow. This may cause damage or inconvenience and is to be avoided. The decision as to what discharge to design a structure for is usually based on an economic risk analysis. The cost of a larger structure is balanced against the probable cost of damage due to larger floods than the structure can accommodate.

The probability of different storm magnitudes and durations occurring must be obtained from a statistical analysis. The ideal situation for a hydrological analysis would be one where a continuous flow record over many years was available. A direct analysis of peak flows could then yield probabilities of different flow rates at the site.

Unfortunately adequate flow records are seldom available at the site in question, or even anywhere in the catchment in question. Even if there were historical records, it is likely that the catchment has undergone, or will undergo, changes in surface cover and drainage patterns. The hydrologist will therefore need to resort to rainfall records, and from these synthesize the necessary runoff pattern at the site of the proposed drain, culvert or conduit. Regional or local rainfall records are usually come by and are independent of development in the basin. There may, however, be a change in the method of recording at some stage, and tests for stationarity in the records should be done.

Many standard hydrological techniques, such as the rational method, the Lloyd-Davies method and the tangent method, are based on the assumption that the probability of a storm of a particular duration is the same as that of the runoff computed using the method. Any discrepancy in the correspondence is supposedly built into the runoff coefficient. The assumption is suspect as there are many variables likely to affect runoff besides the storm intensity. These include antecedent moisture conditions in the catchment, including the state of the surface or retention storage and soil saturation. The storm distribution

in space and its variation in time will also affect the peak rate of runoff. The length of record will also affect the distribution pattern especially if recurrence intervals are extrapolated. Beard (1978) indicated that risk is traditionally underestimated with short records.

There is a tendency to design drainage structures to discharge safely the flood which will be exceeded on an average of once in a specified number of years. Thus mean storm return periods of 2, 5, 10, 20, 50 or 100 years, depending on the severity of exceedance, are often used as the basis for the design flood. In general areas subject to more extreme events plan for more remote possibilities. Whereas such rules of thumb are useful design guides it is invariably worthwhile selecting a probability of exceedance based on hydro-economic risk analysis.

PROBABILITY DISTRIBUTIONS

Although rainfall and runoff are to some degree random they have limits imposed by the climate and environment and even follow some trend. Rainfall or storm intensity generally follows a distribution pattern with a mean and variation. Total storm precipitation depth for any selected storm duration can be correlated with probability as in Fig. 7.1.

Rainfall follows a more distinctive probability distribution than runoff. Runoff or stream flow can be described with a distribution curve but the parameters are more complex than for storm distribution. No mathematical expression can be fitted to runoff distribution or even the relationship between runoff and rainfall, on account of such factors as antecedent ground water conditions, alternative sources of flow (groundwater, surface runoff, unnatural discharges), changing land use, storage-discharge relationships for the catchment, and complex topography, all of which result in a non-linear rainfall-runoff relationship

Various mathematical approximations have been attempted to fit flood discharges (and, not of interest in this context, drought flows). Instantaneous runoff has some frequency distribution (e.g. Fig. 7.2) which may or may not coincide with a mathematical function. Parameters which describe mathematical or other distributions are indicated below. The storm drain designer is primarily interested in the upper extreme values of flow.

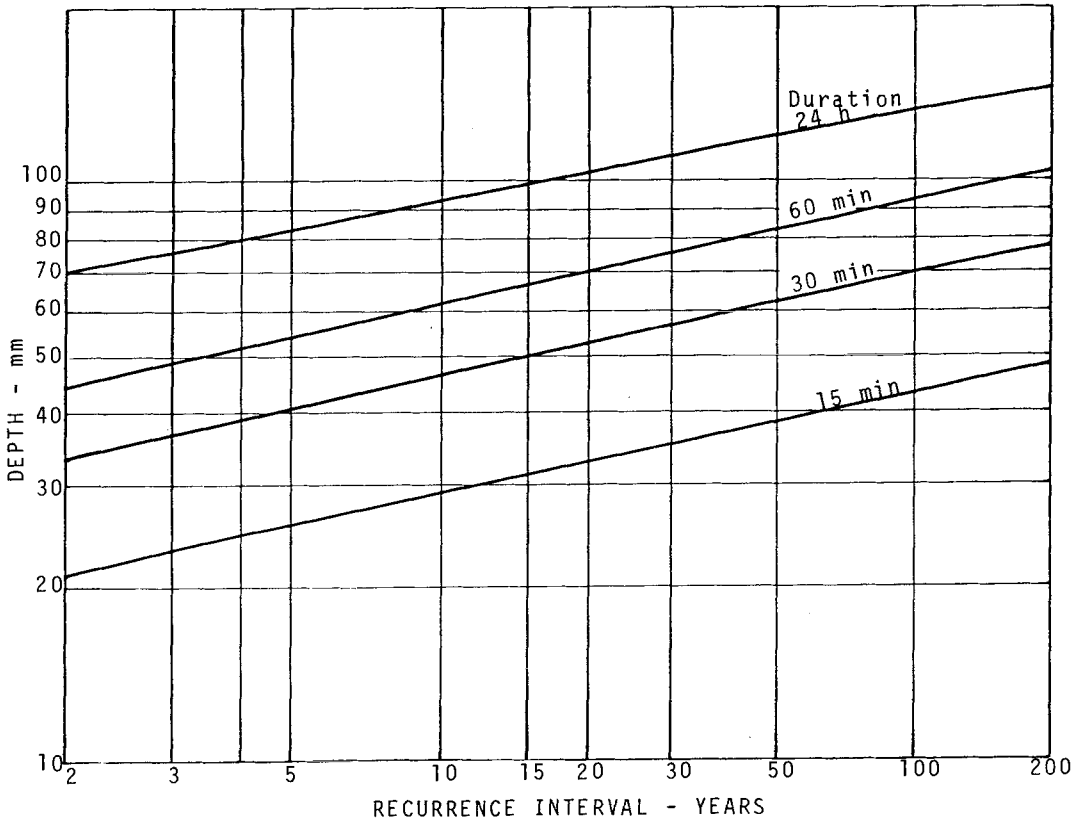


Fig. 7.1 Rainfall depth - Duration - Frequency relationships

In the expressions, the following terms are employed.

Arithmetic mean or mean: The centre of gravity of the distribution. The population mean is designated μ , and the sample mean \bar{x} .

$$\text{Population mean } \mu = \int x dp \quad (7.1)$$

$$\text{Sample mean } \bar{x} = \frac{\sum x}{N} \quad (7.2)$$

where x is the variate and N the number of observations and p is the expectance of x .

Median: Middle value of variate, such that it divides the frequency distribution into two equal portions.

Mode: Value of variate which occurs most frequently.

Standard deviation: A measure of variability. Variance is the square of the standard deviation.

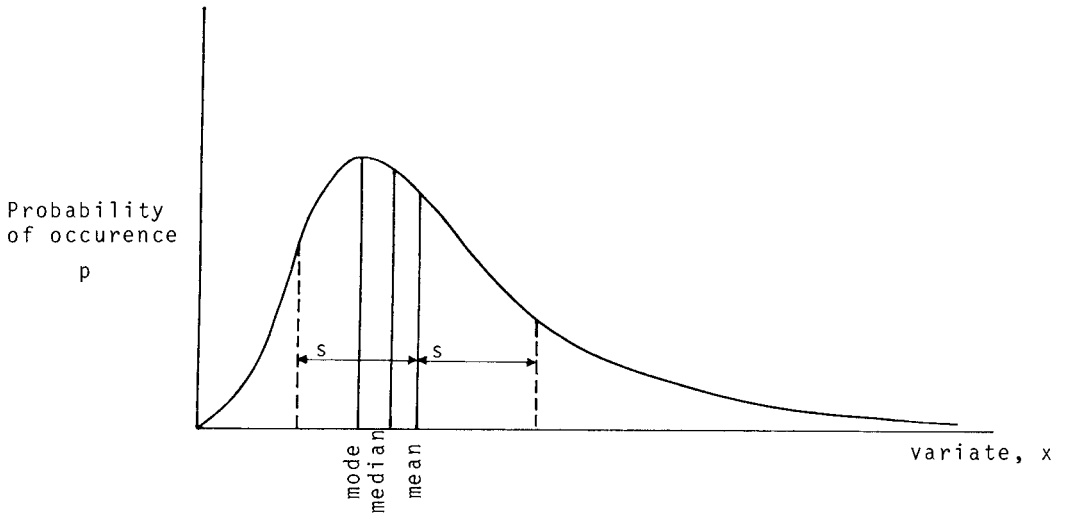


Fig. 7.2 A probability distribution

Population standard deviation $\sigma = \sqrt{\frac{\Sigma(x-\mu)^2}{N}}$ (7.3)

Sample estimate $s = \sqrt{\frac{\Sigma(x-\bar{x})^2}{N-1}}$ (7.4)

Skewness:

Population skewness $\alpha = \frac{1}{N}\Sigma(x-\mu)^3$ (7.5)

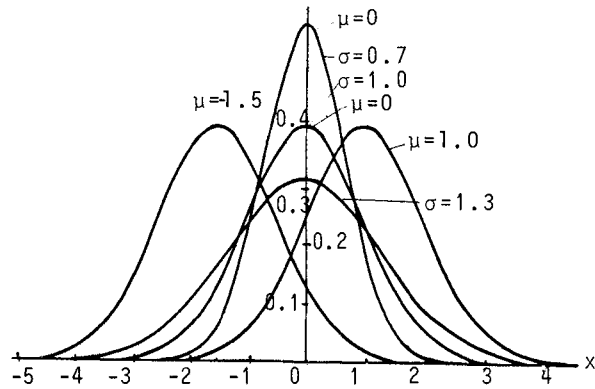
Sample estimate $a = \frac{N}{(N-1)(N-2)}\Sigma(x-\bar{x})^3$ (7.6)

The distributions in Fig. 7.3 are often used in hydrological analysis (Haan, 1977, Yevjevich, 1972a, Bury, 1975).

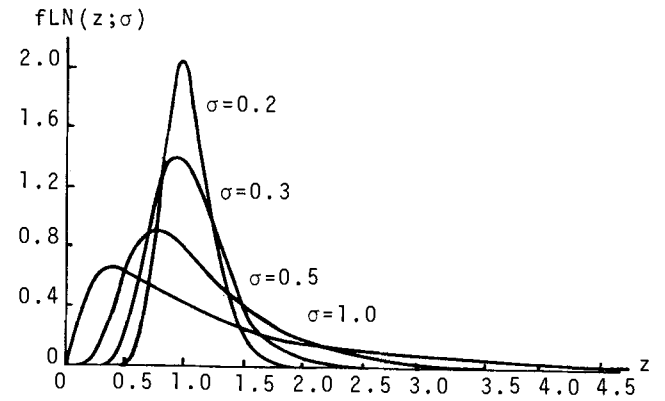
The *Normal distribution* represents the distribution of a completely random number about a mean. It is a symmetrical bell-shaped distribution with the area under the curve equal to unity.

The *Log Normal distribution* represents a similar distribution of the log of the variate.

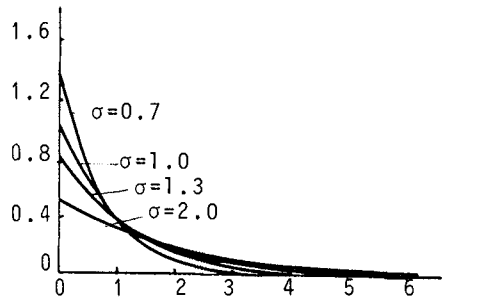
The *Gamma distribution* has a skewness and passes through zero. It is used in draught flow analysis in particular for estimating reservoir capacity.



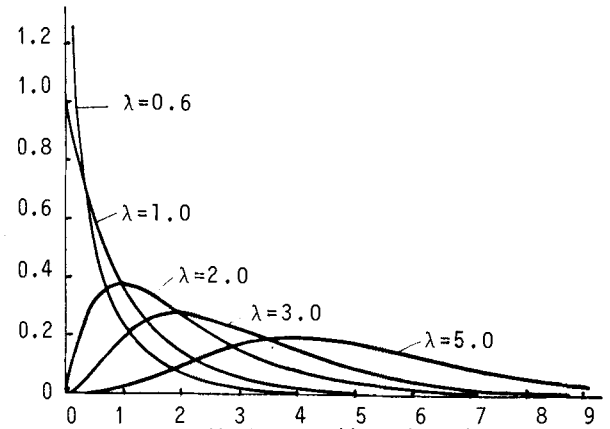
a) Normal distributions with different means and variances



b) Log-Normal distribution



c) Exponential distribution



d) Gamma distribution

Fig. 7.3 Shapes of various mathematical probability distributions

Pearson distributions (types I, II and III) were devised by Karl Pearson (1930) to fit virtually any distribution and are of an exponential type. Log Pearson distributions are also used.

Extreme value distributions (types I, II and III). Fisher and Tippet (1928) found that the extreme values of many distributions approached a limiting exponential form as the number of points in the sample increased. They fitted equations to the upper extremes. Gumbel (1941) first applied the Type I extreme value theory to floods. His work is now standard in the analysis of hydrological extremes (1958).

The distribution is of the form

$$p = 1 - e^{-e^{-y}} \quad (7.7)$$

where p is the probability of the flood being equalled or exceeded, e is the base of Napierian logarithms and y is a mathematical function of probability. The equation for the extreme value of the variate as a function of recurrence interval T resulting from Gumbel's theory is

$$x = \bar{x} - \frac{\sqrt{6}}{\pi} s \{0.5772 + \ln[-\ln(1-1/T)]\} \quad (7.8)$$

Gumbel went so far as to prepare graph paper which causes the variate (flood peaks), to plot as a straight line against probability or its inverse, return period (e.g. Fig. 7.4). Alternatively the variate may be plotted to a log scale (Fig. 7.1). The distribution, together with the log Pearson type III is often applied in flood hydrology.

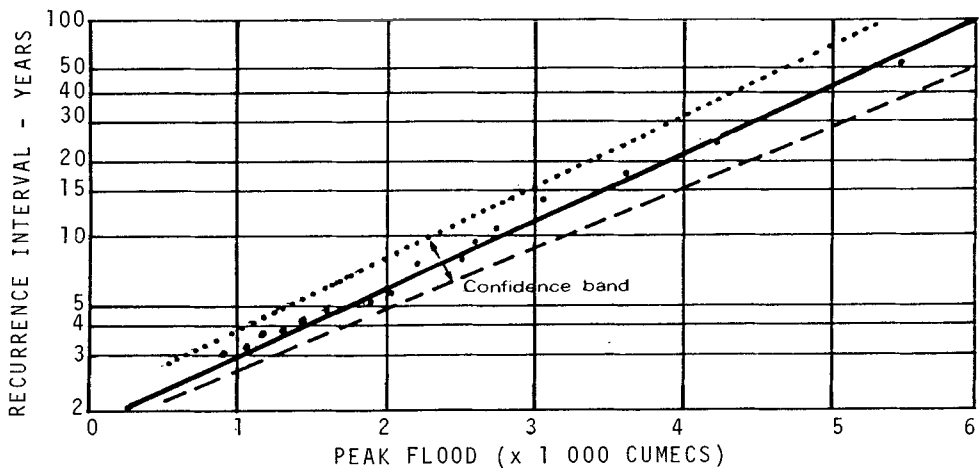


Fig. 7.4 Frequency distribution of flood peaks

ANALYSIS OF RECORDS

Presuming that flow records are available or can be synthesized (e.g. Yevjevich, 1972b; Fiering, 1967), then the extreme flow distributions can be analysed by means of the following procedure. The record is usually produced in chronological order as a complete duration series with peak flows for each day or month or year identified. The record should be divided into years (with the beginning of the hydrological year preferably at the start of the wettest season). The annual maxima should be selected and ranked, taking only the maximum flood in any one year. If the annual flood peaks are arranged in order of magnitude (Fig. 7.5b) we have an extreme value exceedance distribution. One thus has what is termed an annual partial series. If every flood on record was included we would have a complete series. The difference is only of interest for low recurrence intervals giving a lower recurrence interval for partial series than for annual series. For recurrence intervals over 10 years both series yield practically the same results.

The probability of a flow being equalled or exceeded in any hydrological year is the inverse of the frequency of it occurring. Thus a flood which is equalled or exceeded on an average once every 50 years has a two-percent probability. It is common to use the frequency, or recurrence interval or return period in hydrological analysis, in preference to probability. Thus

$$P(X > x) = \frac{1}{T} \quad (7.9)$$

So the probability that the annual maximum flood X is less than x is

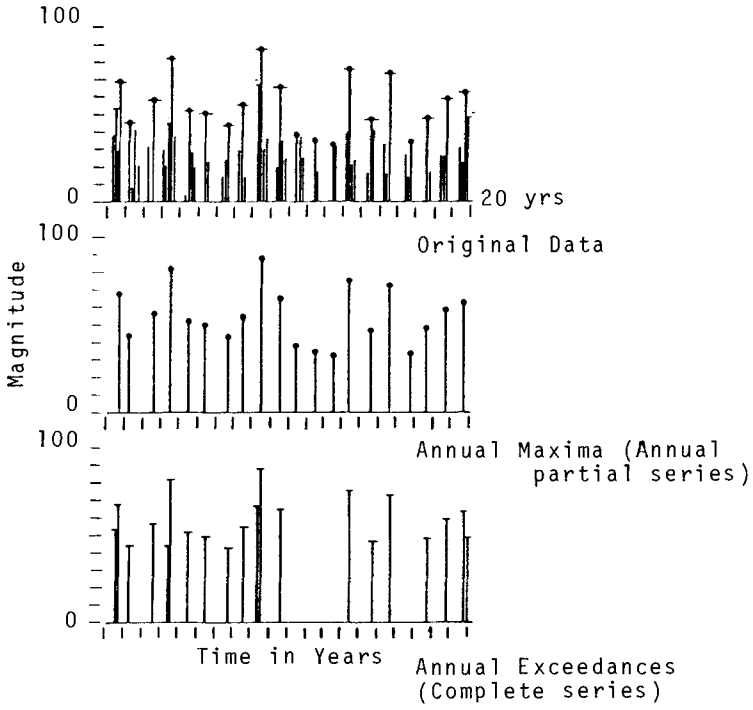
$$P(X < x) = 1 - \frac{1}{T} \quad (7.10)$$

where T is the recurrence interval of the flood of magnitude x .

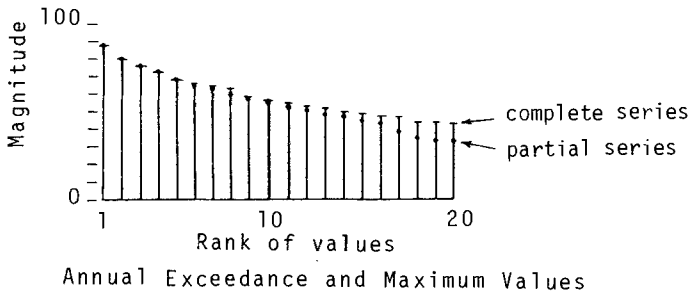
The estimation of T from the ranked sample has been done in different ways. Once a sample has been ranked in descending order of magnitude, the recurrence interval T may be estimated from the Weibull formula

$$T = \frac{N+1}{m} \quad (7.11)$$

where N is the number of events (or years of record) and m is the rank proceeding from 1 for the highest value. Some other formulae for estimating recurrence interval and the corresponding origin are indicated in Table 7.1.



a. Arranged in the order of occurrence



b. Arranged in the order of magnitude

Fig. 7.5 Hydrological data series.

TABLE 7.1 Formulae for recurrence interval T

Formula	T	Distribution	T for N=50, m = 1
California (1923)	$\frac{N}{m}$		50
Hazen (1930)	$\frac{2N}{2m-1}$		100
Weibull (1939)	$\frac{N+1}{m}$	Normal & Pearson III	51
Blom (1958)	$\frac{N+0.25}{m-0.375}$	Normal	80.4
Beard (1962)	$\frac{N+0.4}{m-0.3}$	Pearson III	72
Gringorten (1963)	$\frac{N+0.12}{m-0.44}$	Exponential, Extreme Value I	89.5

The constants in Gringorten's equation actually vary slightly depending on length of record.

The resulting recurrence intervals or so-called plotting positions may be plotted on a suitable graph such as in Fig. 7.4. The process of fitting a smooth curve through the resulting data will then eliminate many deviations. It should be borne in mind that values will deviate from the distribution near the mean, as extreme value theory as its name implies, is inapplicable there. In fact different distributions apply on either side of the mean.

CONFIDENCE BANDS

An infinite length of record only, will yield a true distribution with a very low minimum and an extremely high maximum. Any record of finite duration will have a more limited range and can only approximate the true distribution. The shorter the record, the less representative of the true distribution it is likely to be. In fact the variation of a number of sample means about the true mean will be distributed as a normal distribution with a mean μ and variance σ^2/N .

The possible extent of the true distribution each side of the available data can be described in terms of confidence limits. There will be a confidence band above and below the plotted line on an extreme value plot such as Fig. 7.4. The width of the band will depend on the degree of confidence accepted and on the scatter and sparseness of the data.

Confidence limits can be estimated in the case of a normal distribution from the data set (Haan, 1977). Thus there is a 68% probability that a sample mean will be within $\pm\sigma/\sqrt{N}$ of the true population mean. The probability of lying within a certain band about the mean, $F(c)$ for different c is given in Table 7.2.

TABLE 7.2 Confidence band factors

Degree of confidence, c (%)	95	90	80	68
F(c) (about mean)	2.0	1.7	1.3	1.0
Recurrence interval, T(years)	2	10	100	1000
G (T)	1.0	1.5	2.2	2.7

For other plotting positions the band width increases in accordance with a factor G. The factor is dependent on the population distribution, length of record and recurrence interval. It may be deduced that G is dependent primarily on recurrence interval T, and the values in Table 7.2, apply for over 20 years of record. Thus the confidence band width about the line drawn through the plotted positions is very approximately

$$BW = F(c)G(T)s/\sqrt{N} \quad (7.12)$$

As an approximation the band width on the upper side of the line is 0.6BW and on the lower side 0.4BW. For example for a sample of 20 peak flows with a standard deviation of 200 m³/s, then the width of the 90% confidence band about the 100 year value plotted is $BW = 1.7 \times 2.2 \times 200/\sqrt{20} = 168$ m³/s. For plotting positions below the mean the band width again expands but these positions are normally of little interest to the drainage engineer. More accurate figures for the 90% confidence band are presented by Viessman et al (1977) and Beard (1978).

Yen (1974) presented a chart from which it is possible to read the probability of an event of rank $m = 1, 2$ or 3 in n years of record corresponding to an event of average return period T.

DESIGN DISCHARGE

The construction of a culvert, bridge waterway or even drain to pass a flood of a selected recurrence interval, involves some risk. The probability of the discharge capacity being exceeded at least once during the operation of the structure is greater than $1/T$ where T is the recurrence interval of the design flood.

Although a minor overtopping may result in only inconvenience, a severe overflow of an embankment could cause scour and wash-away. This would cause economic damage as well as risk to traffic and life. A probabilistic approach to the selection of design capacity is therefore desirable. Young et al (1974) applied risk analyses to the design of highway culverts and indicated damage costs. Allowance for cost uncertainty and interaction between culvert capacity and flood magnitude was studied in detail by Mays (1979).

SPREAD RISK

The simplest approach to the computation of design flood in the case of a structure which is to function over a long time or indefinitely is on an annual basis. The costs of the structures which can discharge different flood magnitudes are added to the corresponding probable cost of damage. All cost figures are converted to a common time basis, eg. annual costs. The method is explained with an example below.

Example

A highway authority is to construct a low bridge over a river. The flood frequency distribution is indicated in Fig. 7.4. The capital cost of the bridge is a function of the discharge capacity of the waterway beneath. The capital cost corresponding to various design discharge rates is converted to an annual amount representing interest and redemption on the loan to meet the cost, and added to annual maintenance cost. Annual interest plus redemption figures can be obtained from interest tables or from a formula (Institution of Civil Engineers, 1969). The capital cost is multiplied by the factor

$$\frac{r(1+r)^n}{(1+r)^n - 1} \quad (7.13)$$

where r is the interest rate (a fraction) on the loan, assumed here equal to the interest rate on the redemption or sinking fund, and n is the loan period in years. To get a true picture the loan should be renewed for as long as the economic life of the structure.

The resulting annual cost, as a function of waterway capacity, is plotted in Fig. 7.6 (curve A). Now corresponding to each of the trial waterway design capacities is a probability of exceedance in any year, as indicated in Fig. 7.4. There is a different probability corresponding to either the best estimate or the upper confidence limit of the flood frequency curve.

The probabilities of each flow being exceeded are multiplied by the cost of a flooding. This may include repair costs to the bridge, damage to surroundings, and interference with transport. Assuming in this case that the cost of exceeding the design capacity is \$100 000, the probably cost is this figure multiplied by the probability of exceedance of the discharge. The resulting annual costs are plotted in Fig. 7.6 as curve B, for both best estimate and upper confidence limit.

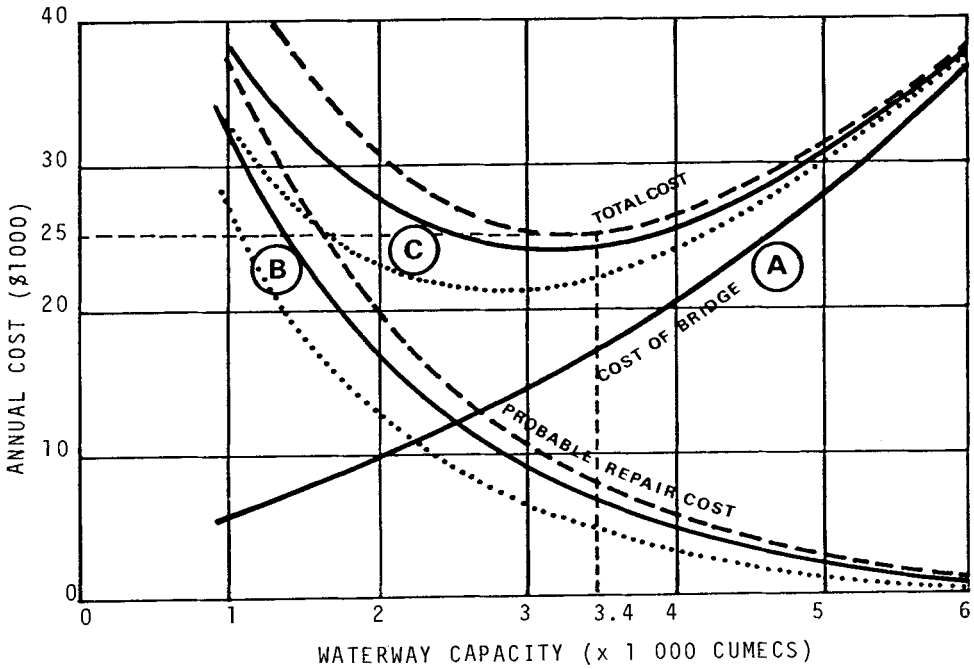


Fig. 7.6 Overall costs for spread risk example

The total average annual cost is the sum of A and B and this is indicated as curve C. The minimum cost corresponds to a waterway capacity of 3400 m³/s, provided the upper flood curve is chosen. This is the usual procedure as it provides a margin for uncertainty in flood estimates. It will be observed however that the best estimate curve will result in a slightly smaller optimum waterway capacity. Thus the effect of uncertainty in hydrological data is to increase expenditure.

In real situations the computations will be more complicated. There is always the risk to human life which is difficult to evaluate. The damage costs may very well increase with increasing flood magnitude above the design capacity. In this case the probable economic loss must be evaluated. It is the integral of the probability of various extreme floods occurring multiplied by the corresponding cost, i.e.

$$\text{probable annual cost} = \sum P C \quad (7.14)$$

where P is the probability of the flood being in a certain range and C is the corresponding damage cost.

The aspect of cost escalation also arises. If damage costs are likely to increase over the years, they should be evaluated separately for successive years, and discounted to a present value. Thus each annual cost is multiplied by

$$\frac{1}{(1+R)^n} \quad (7.15)$$

where R is the inflation rate as a fraction. The total of the present values for each year is obtained and this may be added to the capital cost of the bridge. Again the capacity with least total cost is selected.

ISOLATED RISK

A flood with a return period of T will occur or be exceeded in any year with a probability of 1/T. The probability that it will occur at least once in n years is greater than 1/T since there is more chance for it to occur. The actual probability of the flood being equalled or exceeded at least once in a year may be evaluated as follows:

The probability that it will not occur in any one year is $1-1/T$. Hence the probability that it will not occur in n years is the product of n such probabilities or $(1-1/T)^n$.

The probability that it will occur at least once in n years is therefore

$$P(Q \geq Q_T) = 1 - (1-1/T)^n \quad (7.16)$$

This probability represents the risk that a flood with return period T will occur or be exceeded at least once in n years. If the life of a structure is n years, there is a risk P that the capacity of the structure will be exceeded sometime in its life. P is greater than 1/T but less than n/T except for very high recurrence intervals, when P approaches n/T. It can be calculated that for large T there is a 63% chance that a flood of any recurrence interval T will occur in T years.

The application of (7.16) is in short-term projects such as temporary diversion works eg. bypass culverts or cofferdams (see eg. Linsley et al, 1975). An overtopping could result in damages of greater order than the actual cost of the diversion works and may in fact entail a completely new start. Thus the average loss is not so much of concern as the risk of overtopping. Nevertheless in view of the short useful life a more frequent design flood may be selected than for permanent structures.

The constructor of a temporary diversion works or cofferdam will be not so much interested in whether the structure will be overtopped

during its useful life at all, as to what the probability is of it being overtopped once, twice or any other number of times. Each flooding will cause damage and he needs to know the total probable damage. The partial series method of ranking the floods excludes the investigation of more than one flood in any year though (unless the n worst events are selected in strict order of magnitude without only selecting one maximum a year i.e. a complete series).

The probability that a flood Q_T of recurrence interval T will be exceeded exactly r times in n years ($r \leq n$) can be calculated from the expression

$$P(Q > Q_T)_r = \frac{n!}{r!(n-r)!} \left(\frac{1}{T}\right)^r \left(1 - \frac{1}{T}\right)^{n-r} \quad (7.17)$$

This equation is derived using the binomial distribution describing the probability of occurrence of independent events, and was solved by Yen (1970) for various cases.

Use of the equation is demonstrated by way of an example involving the construction of a temporary diversion culvert. Assuming the flood frequency distribution in Fig. 7.4 again, the probable damage costs associated with a 5-year design life are to be investigated. The total cost of exceeding the design capacity or overtopping the embankment is estimated to be \$100 000 per flooding. The cost of the culvert and embankment for various capacities is indicated in Fig. 7.7, line A. The risk of exceeding the diversion works capacity 1, 2 or 3 times is computed from (7.17) and tabulated in Table 7.3.

TABLE 7.3 Risk of flooding for a 5-year diversion works

Recurrence interval, years		5	10	20	30	50
Discharge capacity, m ³ /s:		1700	2800	3800	4500	5300
No. of failures	Total cost of failures					
0	0	0.33	0.59	0.77	0.85	0.90
1	\$100 000	0.39	0.32	0.20	0.135	0.09
2	\$200 000	0.20	0.075	0.025	0.013	0.009
3	\$300 000	0.07	0.014	0.005	0.001	0.001

The cost of failures multiplied by the corresponding risk is indicated in Fig. 7.7 (lines marked B are filled in after plotting the individual risks).

The total cost of construction and the associated risk of damage is then computed and plotted at the top of Fig. 7.7 (curves C). This figure presents more information than the average cost data derived in the example under the spread risk approach. In fact it gives the

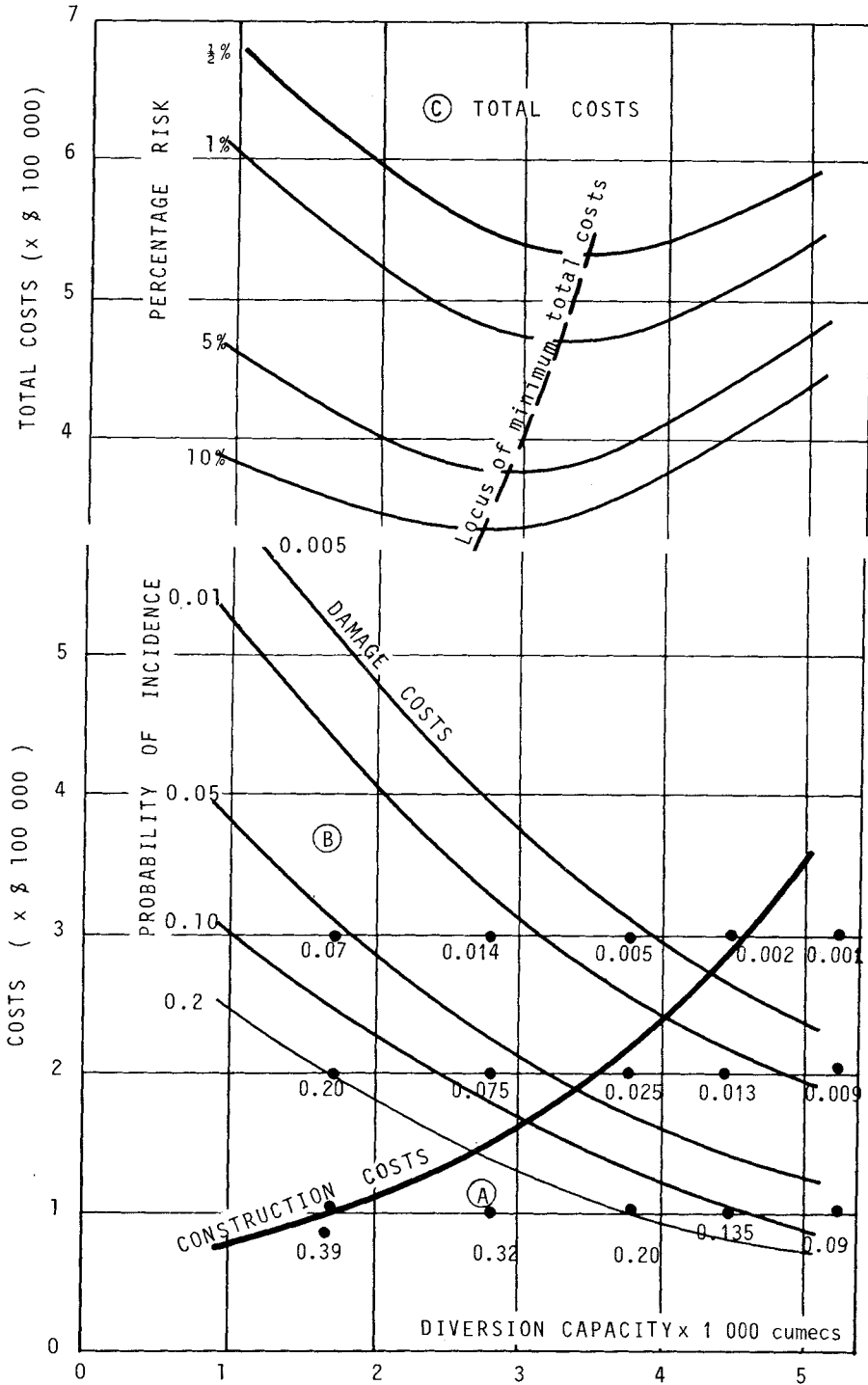


Fig. 7.7 Hydro-Economic analysis of diversion works; isolated risk example

risk of different expenditures corresponding to various design capacities. Thus for a design capacity of 3000 m³/s there is a 1% risk that the cost will be as high as \$480 000.

The additional or marginal information is useful in cases where the contractor or constructor must bear an excess on insurance premiums. In particular the constructor may have \$400 000 available to cover cost of construction and damage, and the balance of damage must be covered by insurance. If the works was constructed to a capacity of 3000 m³/s (corresponding to minimum total cost of \$400 000), then there is a 4% chance the insurance company will have to meet a proportion of costs.

REFERENCES

- Beard, L.R., Nov., 1978. Impact of hydrological uncertainties on flood insurance. Proc. ASCE, 104(HY11), 14168, p1473-1484.
- Bury, K.V., 1975. Statistical Models in Applied Science. John Wiley & Sons. N.Y.
- Fiering, M.B., 1967. Streamflow Synthesis. Harvard Univ. Press, Cambridge, Mass., 139pp.
- Fisher, R.A. and Tippett, L.H.C., 1928. Limiting forms of the frequency distribution of the smallest and largest members of a sample. Proc. Cambridge Phil. Soc., 24, p180-190.
- Gringorten, I.I., Feb. 1963. A plotting rule for extreme probability paper. J. Geophys. Res., 68(3), p813-814.
- Gumbel, E.J., June, 1941. The return period of flood flows. Ann. Math. Statist., XII (2), p163-190.
- Gumbel, E.J., May, 1958. Statistical theory of floods and drought, J. Inst. Water Engrs. 12 (3), p157-184
- Haan, C.T., 1977. Statistical Methods in Hydrology Iowa State Univ. Press, Iowa. 378pp.
- Institution of Civil Engineers, 1969. An Introduction to Engineering Economics, London. 182pp.
- Linsley, R.K., Kohler M.A., and Paulus J.L.H., 1975. Hydrology for Engineers, 2nd Ed. McGraw Hill, N.Y. 482pp.
- Mays, L.W., May, 1979. Optimal design of culverts under uncertainties. Proc. ASCE, 105(HY5), 14572. p443-460.
- Pearson, K., 1930. Tables for Statisticians and Biometricians, 3rd Ed. Part I. The biometric Lab., Univ. College, Cambridge Univ. Press, London.
- Viessman, W., Knapp, J.W., Lewis, G.L. and Harbaugh, T.E., 1977. Introduction to Hydrology, 2nd Ed. Harper & Row, N.Y. 704pp.
- Yen, B.C., April, 1970. Risk in hydrologic design of engineering projects. Proc. ASCE., 96(HY4), 7229, p959-966.
- Yevjevich, V., 1972a. Probability and Statistics in Hydrology. Water Resources Publications, Fort Collins, 302pp.
- Yevjevich, V., 1972b. Stochastic Processes in Hydrology. Water Resources Publications, Fort Collins, 276 pp.
- Young, G.K., Childrey, M.R., and Trent, R.E., July, 1974. Optimal design for highway drainage culverts. Proc. ASCE, 100(HY7), 10676, p971-993.

CHAPTER 8

ROOF DRAINAGE

(from a paper by Schartz and Culligan, 1976)

INTRODUCTION

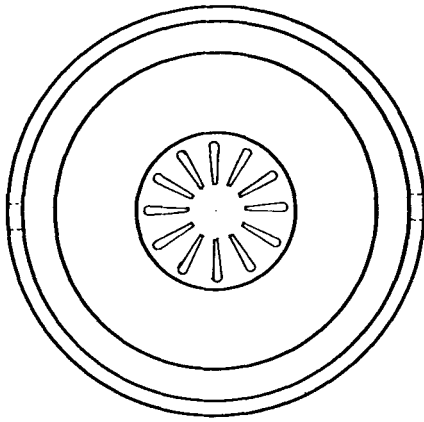
The number of reports of substantial damage to stock and installations in buildings as a result of the inadequate capacity of roof drainage facilities suggests that closer attention should be paid to the provision of waterproofing and storm-water control systems. The inconvenience of water flowing in and the resulting need to redecorate often detract from the prestige value of buildings and reduce the rate of return on the investment concerned.

Where high intensity rainfalls are experienced frequently it would appear acceptable to size eaves gutters so that they became periodically surcharged, provided of course that excess water can safely be discharged clear of the building. Internal or valley gutters or flat roofs should, however, be designed in such a manner that the consequences of functional failure are taken into account. The sizing of components can be rationally assessed only on the basis of a full consideration of the economic, hydrologic and hydraulic factors.

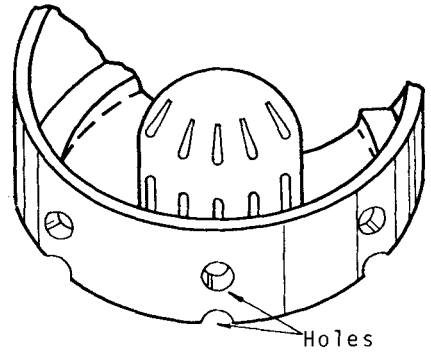
Steel-framed buildings with sloping roofs usually have gutters that are not integral with the roof so that a surcharge results in an overflow of the gutters. Concrete buildings, on the other hand, generally have horizontal or slightly sloping roofs and the problems that arise are due to the penetration of water through flaws in waterproofing membranes or inadequate flashing.

The high cost of ensuring lasting protection of flat roofs against moisture penetration is such that it is generally not wise to rely on a reduction of peak flows by roof-ponding (Fig. 8.1), a practice which in America has occasionally been enforced on property owners in order to reduce the surcharge on existing overloaded stormwater collection systems in the streets (Poertner, 1973).

In low and medium rainfall areas there seems little doubt that provision for storage is not warranted and most designers regard peak reduction by detention simply as an additional safety margin. Should it be decided to investigate the effect of storage then Fig. 8.2 after Pagan (1975) can be used to yield a preliminary estimate of the reduction likely to be achieved. Some suggestions for waterproofing regulations are contained in a paper by Lardieri (1975) on flood proofing.



PLAN



ELEVATION

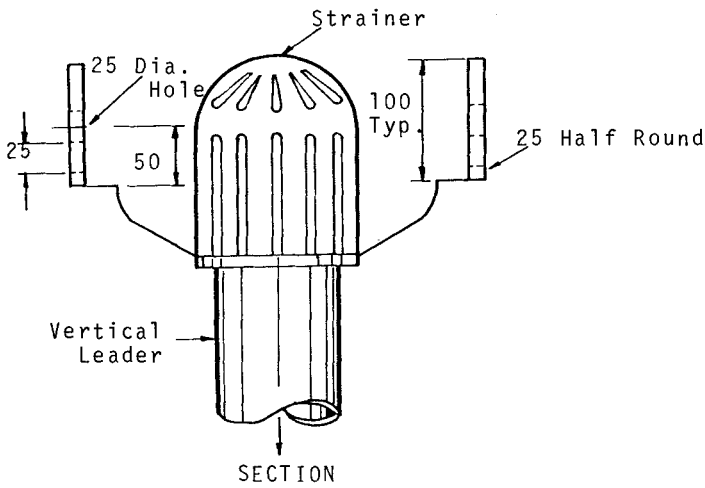


Fig. 8.1 Rainfall Detention Ponding Ring for Flat Roofs

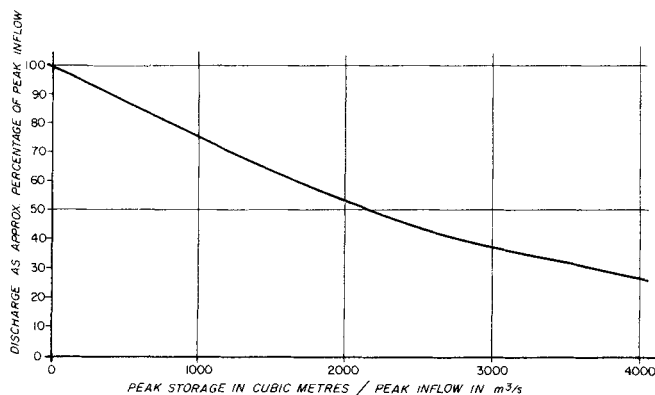


Fig. 8.2 Discharge attenuation due to storage (after Pagan, 1975)

It is practice in places to place downpipes in the centre of the columns of reinforced concrete buildings. This leads to certain difficulties in that the capacity of a down-pipe almost invariably depends on the design of its inlet. The concentration of beam or slab steel required at the top of a column often precludes the use of a hopper at that point. It may therefore be worth considering American practice of placing downpipes entirely clear of the columns.

In large buildings stormwater can be discharged internally into large conduits or culverts below ground level. An alternative approach sometimes adopted for large steel-framed industrial buildings is to place outlets at regular intervals in the floor of gutters and to collect the discharge from them in a suspended closed sloping launder or collector pipe which discharges at the perimeter of the building.

In 1973 the Division of Building Research of the CSIRO in Australia published a paper by Martin (1973) entitled 'Roof Drainage'. The paper presents a method of design which is essentially a modified version of a series of research digests published over a decade or more by the Building Research Station in England. The methods were adapted for Australian conditions where rainfall intensities are generally far higher than those of the United Kingdom. In addition, Martin investigated certain aspects such as the influence of slope on gutter capacity.

In April 1974 the British Standards Institution (BSI) issued a comprehensive code of practice which deals with the drainage of roofs and also of paved areas. Design procedures are given together with helpful notes on the practical considerations of the choice and disposition of elements of a drainage system. Special mention is made of the effects of mining subsidence. The publication contains diagrams giving roof

areas served by rainwater pipes and gutters for design intensities of 75 mm/h. The diagrams may, however, be modified for other intensities

GUTTER CAPACITY

Optimum proportions of rectangular gutters

The depth of a valley gutter is generally limited by structural considerations such as the size of purlins or by other space limitations, but it is considered instructive to ascertain the optimum proportions of a level box gutter discharging freely at one end.

By application of the momentum principle it can readily be shown that if friction effects are ignored the maximum depth y at the upstream end of a level box gutter is $\sqrt{3}$ times the critical depth h_c (that is $y = 1.73h_c$). This theoretical relationship holds regardless of the length of gutter.

When frictional losses are included then an analysis similar to that developed by Hinds (1926) for side-channel spillways indicates that the maximum depth for the normal range of gutter lengths varies from about 1.8 to 2.1 times the critical depth.

In CP 308 (BSI, 1974) a value of twice the critical depth is advocated for design purposes. If the ratio of maximum depth to critical depth can be accepted as being constant then it can readily be shown that when a flat metal sheet of width W is to be bent into a rectangular horizontal gutter of any length then if an allowance is made for freeboard and lips, the remainder of the sheet should be bent in such a way that the maximum depth of flow y is three quarters of the gutter width b . Any other proportion would imply that the capacity of the gutter is less than the optimum for the material employed and the constraints specified. If the width of a rectangular gutter is chosen to be not less than 300mm in order to facilitate maintenance it follows that for flows less than 0.035 m³/s it is not feasible to maintain optimum proportions.

If a strip of metal is bent into a rectangular gutter in such a way that the maximum depth of flow is one half of the width then for spatially varied flow the maximum discharge will be about five percent less than that of a gutter with optimum proportions.

Fig. 8.3 shows the width of gutter needed for a maximum depth to width ratio of both 0.75 and 0.5 and allows the designer to select a suitably sized gutter for various rainfall intensities. It must be borne in mind that the diagram is valid only if the water at the outlet discharges freely, say into a rainwater head.

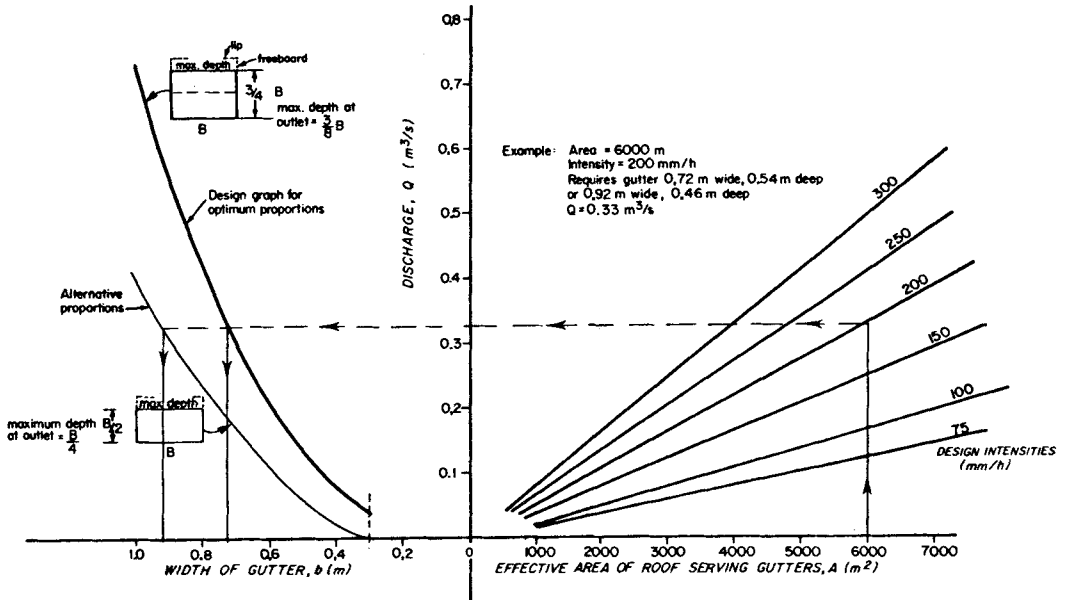


Fig. 8.3 Graph for design of level gutters

Sloping gutters

Sloping gutters carry more than horizontal gutters but unless the gutter is steep the additional discharge can generally be regarded only as an extra safety margin. Martin (1973) published a graph showing that when the slope of a drainage channel is about 2° the discharge capacity is doubled. If the flow should become supercritical then special care would have to be taken because water flowing supercritically would not readily negotiate bends.

A comprehensive computer analysis of flow in variously shaped horizontal gutters from 3 to 25 m long, established the effect of gutter length on maximum flow depth. Using the Hinds momentum equation it was found that the following empirical relationships accurately predict discharge capacity:

For rectangular gutters:

$$QL^{0.05} = 1.429 (y b^{0.67})^{1.614} \quad (8.1)$$

where Q is the discharge in m^3/s , y , b and L are maximum flow depth, gutter width and gutter length respectively (all in meters).

For trapezoidal gutters:

$$Q = 0.697 \frac{(A \theta^{0.25})^{1.338}}{(b^{0.09})} \quad (8.2)$$

where Q is the discharge in m^3/s , A is the cross-sectional area of the gutter in m^2 , b is the bottom width in m , and θ is the side slope in radians measured from the horizontal. For trapezoidal gutters the maximum depth including an allowance for freeboard can be taken to be approximately 2.3 times the critical depth.

For half-round gutters:

To take account of length effects the Building Research equation should be modified to read as follows:

$$Q = 2.26 \frac{0.8433A^{1.25}}{L^{0.47}} \quad (8.3)$$

where Q is the discharge in m^3/s , A is the cross-sectional area of the gutter in m^2 and L the gutter length in metres.

Box receivers :

Where possible gutters should discharge freely into a box-receiver, the depth of which can be selected so as to match the use of a downpipe of convenient size. The receiver should be at least as wide as the maximum gutter width and should according to CP 308 be long enough to prevent the flow from overshooting the box. The horizontal distance m travelled by a particle leaving a horizontal gutter is given by the equation $m = 2\sqrt{ny}$ where y is the depth of flow at the outlet and n the vertical drop of the particle.

If one assumes that the jet is not to strike the far wall of the receiving box then the box could turn out to be unduly long and when loaded have a total mass of several hundred kilograms or more. It is therefore suggested that for large buildings the box be limited in size by the introduction of baffles even if the impact force has to be catered for in the structural design. The importance of placing the downpipe asymmetrically to prevent swirl which decreases effectiveness is worthy of note. External boxes should be provided with overflow weirs.

FLAT ROOFS

Flat roofs should have a slightly sloping upper surface to shed water to drains or outlets and it is recommended that ponding be minimized to restrict the ingress of water through waterproofing membranes that might for some reason have suffered damage. The depth of water on the roof will depend mainly on critical depth at overflow and thus a gutter or large depressed outlet is desirable. Fig. 8.4 gives for a series of representative rainfall intensities the area of flat roof served per metre of free overfall for selected depths of flow approaching the

brink. For a limiting depth of 20 mm the critical depth would be 13.3 mm. The design of the downpipe and its inlet would have to be taken into account in establishing the depth of water likely to occur on the roof and this aspect is dealt with separately.

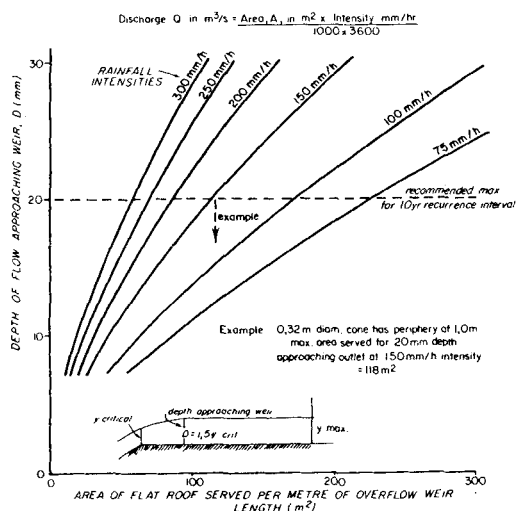


Fig. 8.4 Area of roof for unit length of free overfall available

DOWNPIPES

Martin (1973) found in Australia that the optimum size of downpipes to serve a gutter is given by the rule that the cross-sectional area of the downpipe should be half the cross-sectional area of the gutter. The rule is advocated by him as it has been found satisfactory in practice. Application of the rule presupposes, however, that a rain-water head of sufficient depth is available to avoid surcharge at the upper end of the gutter. Care must therefore be exercised in applying the rule. The British Code quite rightly lays stress on the design of the inlet and indicates that the size of the downpipe may be reduced once the water has entered it effectively.

For downpipes fed by flat areas and not gutters Martin limits the effective velocity to 1.78 m/s and produces a diagram (Fig. 8.5) which gives an indication of the roof area served by downpipes for various intensities of rainfall. It is important, however, to note that the capacity of a downpipe is normally controlled by inlet conditions and designers should avoid making the error of selecting a down-pipe size

from the chart without ensuring that the water build-up at the entrance to the pipe necessary to feed the pipe at the design rate of flow can safely be accommodated. It should perhaps be emphasized that downpipes seldom run full. In fact, when the water reaches its maximum velocity in a vertical stack the pipe usually runs only about one-quarter full. Thus, down-pipes could be reduced in size but not without causing considerable noise and vibration due to pneumatic effects.

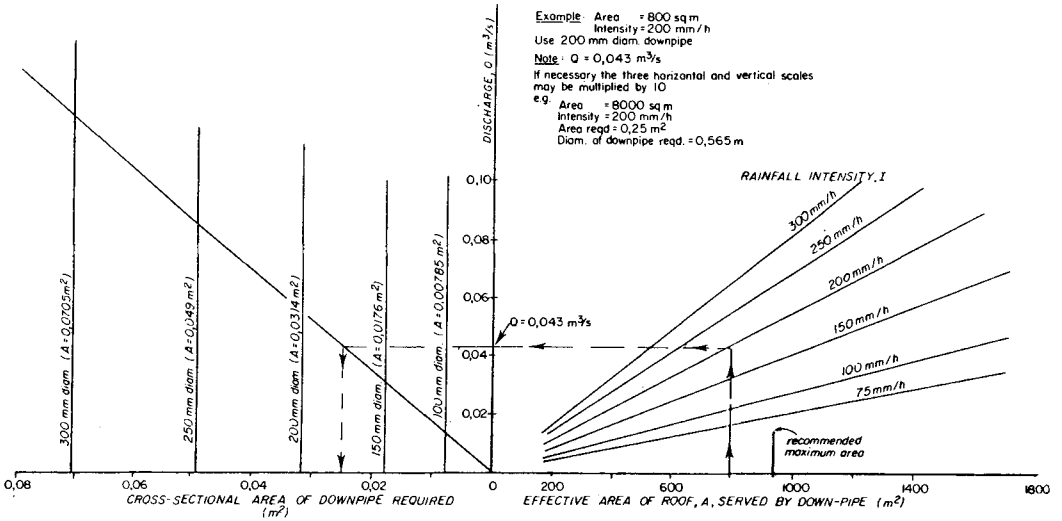


Fig. 8.5 Preliminary downpipe selection graph (inlet conditions to be checked)

Dawson and Kalinske (1939) showed that for ordinary plumbing stacks the maximum velocity is attained in about 3 to 6 m of fall. It follows that for multi-storied buildings the water velocity at ground-level would be no greater than that for a two-storey building. The maximum velocity measured in experimental stacks was of the order of 7 m/s and therefore Martin's rule of sizing downpipes by assuming that the nominal velocity based on the full cross-sectional area is 1.78 m/s appears reasonable.

The size of a downpipe fed by a gutter should also be selected from Fig. 8.5 and the inlet designed to provide sufficient head to ensure that the water enters without causing distress elsewhere.

Inlet conditions for downpipes

For a pipe flush with a flat roof or gutter floor the weir formula $Q = k_1 h^{3/2}$ (8.4)

is applicable for low flows (i.e. when the head h on the weir overflow is less than about one-third of the diameter). For greater heads the orifice relationship

$Q = k_2 h^{1/2}$ (8.5)

is applicable. In these formulae Q is the discharge in m^3/s , h is the head in metres and k_1 and k_2 are appropriate constants.

If conical outlets are used then the origin of the orifice equation for the pipe entrance is below the roof or gutter level and as the discharge increases the control may shift to a lower level. If a protective grill is used due allowance should be made for its presence. Fig. 8.6 illustrates the concepts involved and it is immediately apparent from the figure that the design of an inlet is by no means a straight-forward matter.

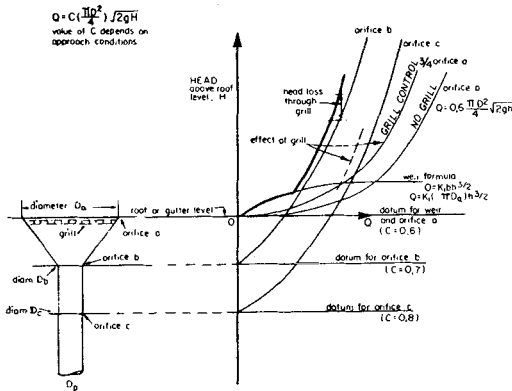


Fig. 8.6 Diagram showing method of determination of inlet control

If the downpipe is fed by a level rectangular gutter then (if surcharge is to be avoided) the depth of flow in the gutter at the outlet should not exceed 80 percent of the depth at the upstream end. For design purposes the more conservative rule that the water depth at the outlet should not be more than 50 percent of the effective gutter depth is recommended. If, on the other hand, the downpipe is fed directly from a flat roof then the approach head should be limited to about 25 mm and this severely restricts the discharge.

Calculations, supplemented by some laboratory tests for selected sizes, indicate that the chart given as Fig. 8.7 can be used for inlet design. Similar reasoning may be applied to ascertain the depth of water required in receiving boxes.

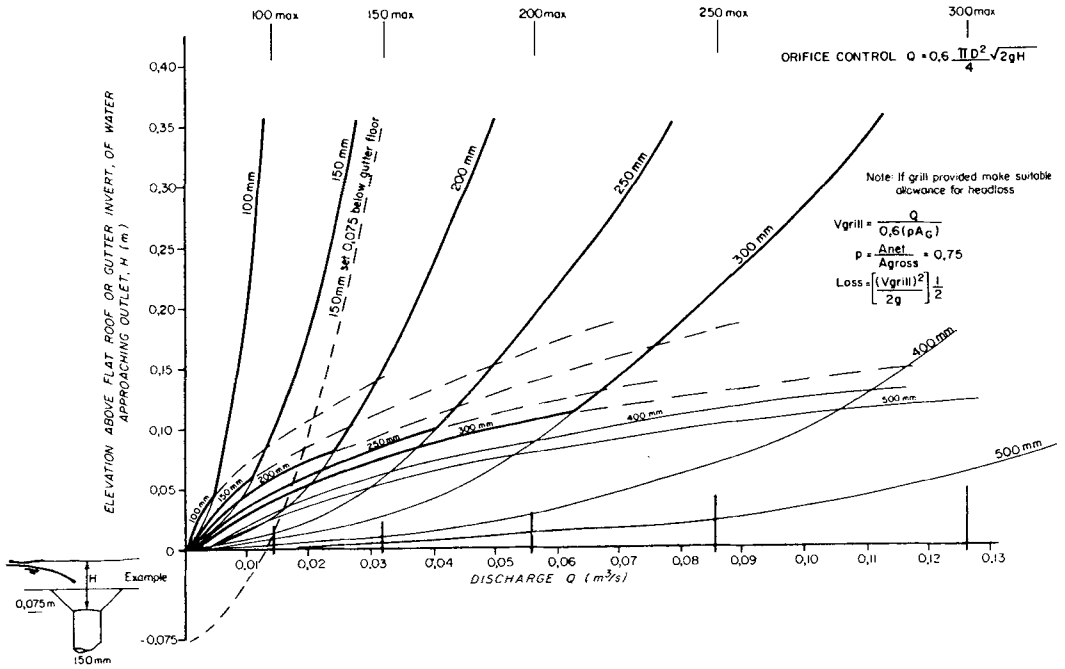


Fig. 8.7 Inlet design diagram

A useful technique for the design of conical outlets and tapers is to plot orifice relationships on a transparent overlay and then to slide the overlay vertically over a diagram such as Fig. 8.7 to establish optimum conditions.

A grill in a conical outlet acts as a control for low discharges and as an obstruction for larger discharges. Generally the open area of the grill is about 75 percent of the gross area A, and the head loss can be approximated by taking half the velocity head at each vena-contracta. The total effective area is then about 60 percent of the 75 percent mentioned above. Thus, the head loss, h, across the grill, may be approximated by the expression

$$h = 0.5 \left(\frac{Q}{0.6 \times 0.75 \times A_1} \right)^2 \frac{1}{2g} \tag{8.6}$$

where Q is the discharge in m^3/s and A_1 the gross grill area in m^2 .

Fig. 8.8 may be used for the final selection of downpipe size depending on the value of available head. Where receivers are used the depth of receiver required for a selected downpipe diameter may be determined from the diagram.

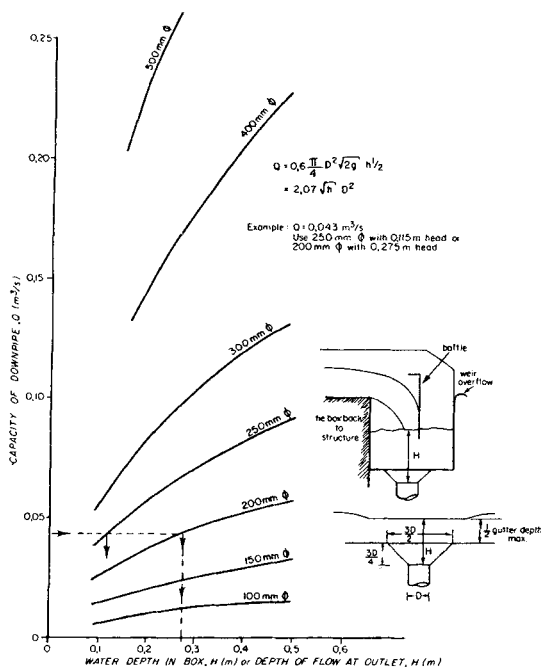


Fig. 8.8 Downpipe selection for different available heads

REFERENCES

- British Standards Institution, 1974. Code of Practice for drainage of roofs and paved areas, CP 308, London.
- Dawson, F.M., and Kalinske, A.A., 1939. Report on hydraulics and pneumatics of the plumbing drainage systems, Technical Bulletin No. 2. National Association of Plumbing, Heating, Cooling Contractors, Washington DC, 38pp.
- Hinds, J., 1926. Side channel spillways, Trans., ASCE, 89, p 881-927.
- Lardieri, A.C., Sept. 1975. Flood proofing regulations for building codes, Proc. ASCE, 101 (HY9), p1155-1169
- Martin, K.G., 1973. Roof drainage, Division of Building Research, Technical Paper (Second Series) No. 1, CSIRO, Australia, 16pp.

- Pagan, A.G., Oct. 1975. Usefulness of the storage parameter, Civ. Eng. ASCE, 45 (10), p 82-83.
- Poertner, H.G., 1973. Better Storm drainage facilities - at lower cost, Civ Eng, ASCE, 45 (10), p 67-70
- Schwartz, H.I. and Culligan, P.T., Aug. 1976. Roof Drainage of large buildings in South Africa. Trans. S.A. Instn. Civil Engrs., 18(8), p 171-176. Discussion March, 1977.

CHAPTER 9

ROAD DRAINAGE

INTRODUCTION

Despite the fact that roads cover a relatively small proportion of the earth's surface, the drainage of roads is one of the more important of the drainage engineer's responsibilities. The popularity of road transport has resulted in a public awareness of road design. Poor geometric designs from the point of view of drainage, whether to take away precipitation falling on the road surface, or to divert stormwater approaching the road, will receive public condemnation. In fact, there is reason for this. Water on road surfaces poses a serious hazard to safety and interruptions of traffic can disrupt commerce.

ROAD SURFACES

The depth of water on a road surface has a direct bearing on the safety of vehicles. There is a water film depth beyond which tyres tend to skid or plane when braking. Steering and acceleration are also affected. The friction factor of wet surfaces is lower than that of dry surfaces, but this feature cannot be avoided if it rains. The engineer can however, control the depth of water on the road.

Splashing of water affects visibility and comfort of passengers and the noise can impair driving. Although there have been advances in tyre tread design to reduce skidding, these designs can only go so far without adding to drag resistance on dry roads.

The road surfacing affects the skid resistance in a number of ways. A good surface will be rough as well as quick-drying. One way of doing this is to provide a permeable surface so that water may seep through the upper layer. Another method is to provide a camber or cross-fall. The latter can be uncomfortable and dangerous especially near the edge where camber is the greatest.

Factors affecting the permissible depth of water on a road include:

- Traffic speed
- Tyre tread design
- Weight of vehicles
- Tyre compound
- Road surfacing material
- Road crossfall
- Deposits such as oil and dirt on the road
- Flow velocity of water

Water depths less than 1 mm are rarely conducive to hydroplaning, but between 1 and 2 mm the water film can significantly affect the grip. For greater depths other factors such as visibility usually limit driving speed anyway. For depths over 5 mm, driving can be dangerous.

Stopping distances at 70 km/h on wet roads vary from 60 m on rough asphalt to 120 m on smooth asphalt, in the case of new tyres. The distances can become 80 m on wet rough asphalt and 160 m on wet smooth asphalt in the case of smooth tyres. These distances are about double those for dry roads. In the case of inundated roads the stopping distances may be much greater. It should be noted that the coefficient of friction on wet roads drops with speed, from 0.6 at 20 km/h to 0.1 at 45 km/h, for smooth wet asphalt (Visser, 1976, Jackson and Rogan, 1974).

The cross-sectional profile of a road may be calculated assuming a certain permissible depth of water. Apart from the flow in the gutter adjoining the kerb, the camber may be designed to result in uniform depth across the road. Consider the road depicted in Fig. 9.1. It is assumed the road drains laterally to either side, i.e. there is a hump in the centre. Precipitation rate is assumed uniform without any losses, (alternatively the excess rainfall rate is used) and the flow depth is assumed to have reached equilibrium and be the same at all points. Consider a strip 1 metre wide across the road. Then the discharge per unit width is

$$q = ix \quad (9.1)$$

where i is the precipitation rate and x is the distance from the crown. According to the Manning equation

$$q = \frac{K}{N} y^{5/3} S^{1/2} \quad (9.2)$$

where K is 1.0 in metre units and 1.486 in feet units, S is the cross-fall slope, N is the Manning roughness coefficient and y is the flow depth. According to Strickler $N = 0.13Kk^{1/6}/\sqrt{g}$ where k is the equivalent roughness. Solving the previous two equations for cross-slope in terms of permissible depth of flow y ,

$$\frac{dZ}{dx} = S = 0.0169 \frac{i^2 x^2 k^{1/3}}{gy^{10/3}} \quad (9.3)$$

Integrating this with respect to x we get an expression for cross-fall from the crown:

$$Z = 0.0056 \frac{i^2 x^3 k^{1/3}}{gy^{10/3}} \quad (9.4)$$

Thus if roughness $k = 10$ mm, $g = 9.8$ m/s², permissible water depth $y = 1$ mm, and design precipitation rate $i = 100$ mm/h, then

$$Z = 0.95 x^3 / 10^3 \quad (9.5)$$

Thus for a road width of 6 m, $x = 3$ m and the crown rise must be $Z = 25$ mm.

GUTTER FLOW

Water flowing laterally off the road surface may either discharge into the countryside or into a lateral ditch, or be collected in shoulder drains. The latter may be trapezoidal formed ditches running beside the road, or may be formed between the cross sloping road surface and a near-vertical kerb. The water will flow longitudinally until diverted by an inlet to an underground drain. The longitudinal slope of the road as well as the lateral slope therefore influence the gutter flow.

The discharge rate in a trapezoidal channel may be related to depth of flow according to an equation such as the Manning equation:

$$Q = \frac{KA}{N} R^{2/3} S_o^{1/2} \quad (9.6)$$

where S_o is the longitudinal slope.

$$R = A/P \quad (9.7)$$

$$A = \frac{y^2}{2} \left(\frac{1}{S_1} + \frac{1}{S_2} \right) \quad (9.8)$$

$$P = y\sqrt{1 + 1/S_1^2} + y\sqrt{1 + 1/S_2^2} \quad (9.9)$$

and for turbulent flow

$$N \doteq 0.13 Kk^{1/6}/\sqrt{g} \quad (9.10)$$

y is the water depth in the triangular shaped channel with side slopes S_1 and S_2 respectively and k is the equivalent roughness.

For a channel with one side a vertical kerb and the other side the road camber S_c , the flow equation becomes:

$$Q = 0.32 y^{8/3} S_o^{1/2} / S_c N \quad (\text{SI units}) \quad (9.11)$$

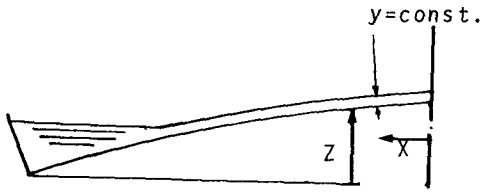
On the other hand if the gutter is treated as a lot of strips each with $A/P = y$, then integrating over the width results in

$$Q = 0.375 y^{8/3} S_o^{1/2} / S_c N \quad (\text{SI units}) \quad (9.12)$$

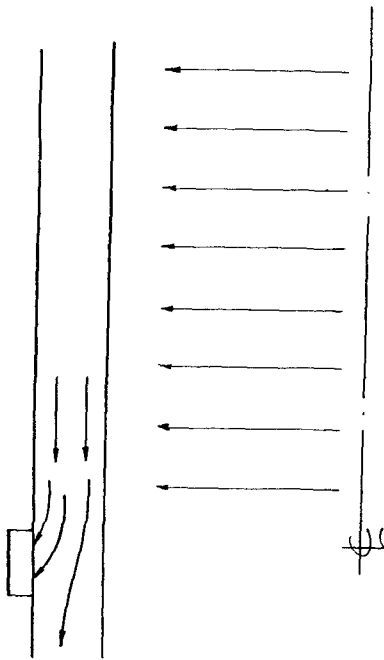
Here the longitudinal momentum of the water off the road is neglected and the discharge rate at any point is the rate of runoff from the area draining to that point. Again, owing to the limited areas usually involved, equilibrium conditions are assumed and the design flow is that corresponding to the maximum rainfall intensity for the selected recurrence interval.

RURAL ROADS

In the country it is rare to have gutters or kerbs. Runoff may run directly into adjacent lands. Alternatively it may be collected in



Exaggerated cross section through road



Plan of Road

Fig. 9.1 Road Drainage

mitre channels excavated alongside the road. Lateral channels will lead the water into fields in a herringbone pattern.

LATERAL INFLOW

The analysis of the flow profile along a channel with inflow along the length must be made using momentum principles, (Henderson, 1966). There is a loss of energy due to the inflow mixing with the water in the channel. The incoming flow is assumed to have no momentum in the longitudinal direction so one can write

$$M = \frac{Q^2}{gA} + A\bar{y} = \text{constant} \quad (9.13)$$

If there is a bed slope and bed resistance then one has

$$\frac{dM}{dx} = A(S_o - S_f) \quad (9.14)$$

This equation must be solved numerically, starting at a known control point. A problem may arise if the channel is steep and flow is supercritical at some point. In that case the critical flow section must be located.

INLET CONFIGURATION

Stormwater off the road will flow down the edges confined by a kerb to a channel with a triangular cross section formed by the camber on the road on one side and the kerb on the other side. The water may be intercepted at intervals by stormwater inlets leading to buried stormwater drains. The spacing and size of the inlets will depend on the design runoff rate. Details of the design of the inlet vary according to standard practice in different towns. A number of practical considerations should affect the selection of inlet type. Some of the configurations adopted are shown in Fig. 9.2. Vertical inlets into the kerb, termed kerb inlets, offer practical advantages to traffic, but are less efficient hydraulically unless special attempts are made to divert the flow laterally. Horizontal screens, termed gutter inlets, set in the road are liable to damage by heavy vehicles. Longitudinal slots in gutter inlets are more efficient than perforations, but pose a danger to bicycle traffic. Small perforations are also liable to blockage by litter or grass cuttings from verges.

In general, the cross-fall towards the inlet should be as steep as practical with depressions at the inlet adding to the efficiency. A small amount of carry-over to the next inlet is acceptable as the inlet capacity improves the deeper the flow.

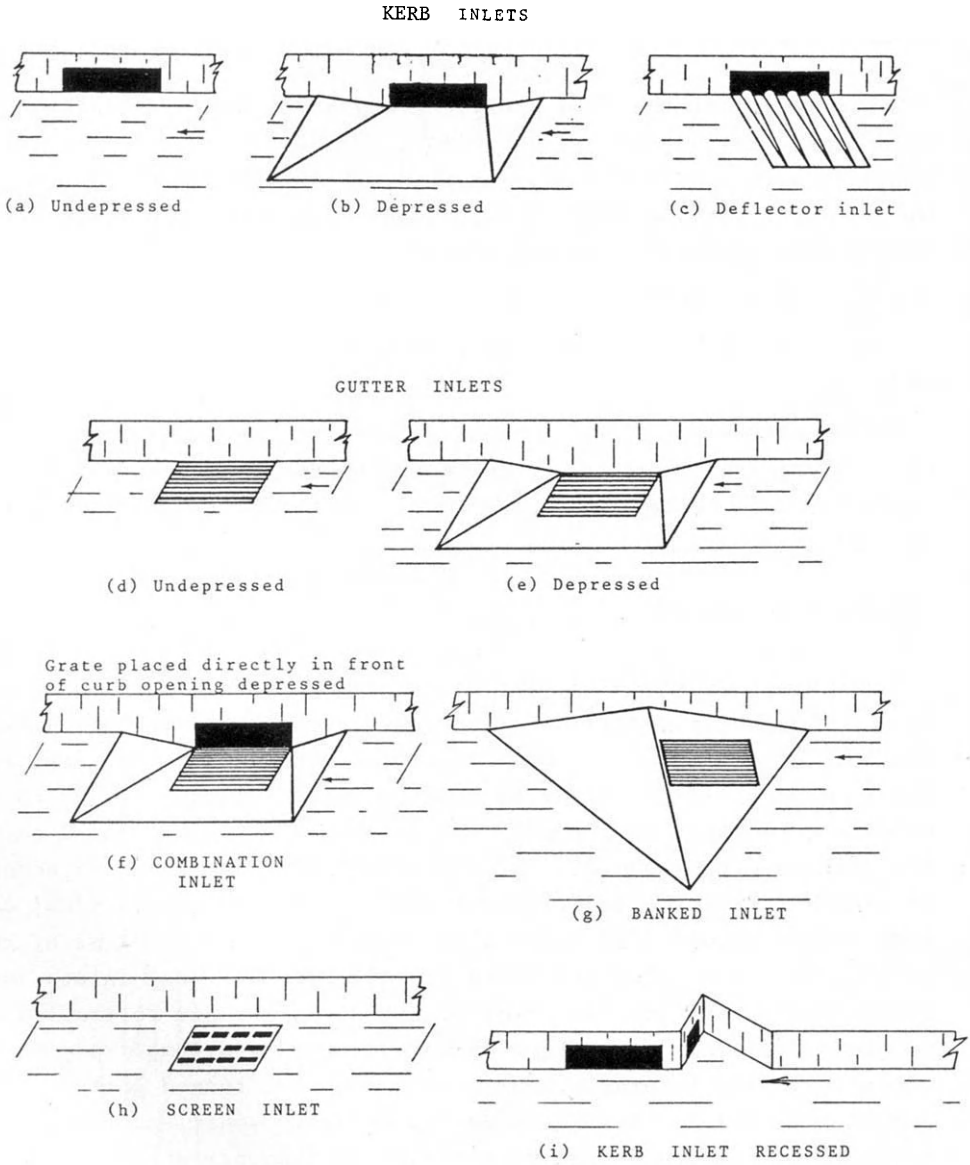


Fig. 9.2 Kerb and gutter inlets

SIDE WEIRS

In the case of lateral flow out of a channel, momentum is lost along the length, and energy principles must be employed for analysis. The specific energy or energy per unit mass of the water in the channel is assumed to remain intact, whence one may write

$$\frac{dE}{dx} = S_o - S_f \quad (9.15)$$

$$\text{but } E = y + \frac{Q^2}{2gA^2} + Z_1 \quad (9.16)$$

Hence it may be shown

$$\frac{dy}{dx} = \frac{S_o - S_f - \frac{2Q}{gA^2} \frac{dQ}{dx}}{1 - F^2} \quad (9.17)$$

where $F^2 = Q^2B/gA^3$, B is the channel width, Q is the flow rate, A is the cross sectional area of flow, y is depth, x is the longitudinal direction, S_o is bed slope, and S_f is friction gradient. dQ/dx is given approximately by

$$-\frac{dQ}{dx} = C_1 \sqrt{2g} (y - H)^{3/2} \quad (9.18)$$

where H is the weir height and C_1 is about 0.51 if y, the depth at the crest is used on the right hand side, not E (see Ackers, 1970).

The discharge in the main channel is, where b is the width,

$$Q = by \sqrt{2g} (E - y) \quad (9.19)$$

The last three equations may be solved numerically for outflow rate dQ/dx , discharge Q and depth y at any point x along a side weir. An analytical solution is possible for $S_o = S_f = 0$:

$$\frac{x C_1}{b} = \frac{2E - 3H}{E - H} \sqrt{\frac{E - y}{y - H}} - 3 \sin^{-1} \sqrt{\frac{E - y}{y - H}} + \text{constant} \quad (9.20)$$

The variations in possible water surface profiles are shown in Fig. 9.3.

KERB INLETS

The kerb inlet, i.e. a slot into the side of the kerb, remains preferable to the bottom or gutter inlet in many towns and centres despite its low hydraulic efficiency. A substantially larger hole is required than for a gutter inlet in most cases. Nevertheless as holes do not cost much more than curb, they are less susceptible to traffic damage, and as they are less of an obstacle to traffic than gutter grates, they remain popular in high density traffic zones.

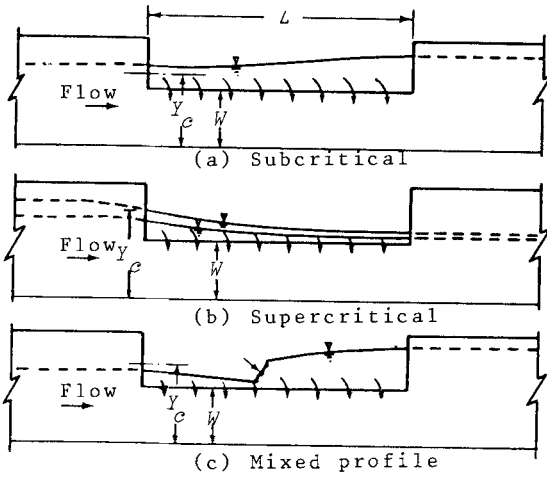


Fig. 9.3 Typical Flow Profiles at Side-Discharge Weirs.

The efficiency of kerb inlets is measured in terms of the amount of water diverted. Associated with the inlet or hole there may be means of improving the lateral diversion of the flow. This may include a steeper cross-fall than the general road cross-fall, a depression, or diagonal diverter ribs on the road surface.

Hydraulic analysis of the flow into a side inlet is difficult as explained previously. The research by the John Hopkins University (1956), also summarized by Li et al (1951-4) employed a semi empirical approach. They grouped the basic variables into significant dimensionless parameters, as follows: For a plain rectangular kerb opening without a gutter depression:

$$\frac{Q}{Ly \sqrt{yg}} = f \left(\frac{v}{\sqrt{gy}}, \frac{q}{Q}, \theta \right) \tag{9.21}$$

From tests it was established that

$$\frac{Q}{Ly_0 \sqrt{y_0 g}} = K(\theta) \tag{9.22}$$

where $K = 0.23$ for $\tan\theta = 12$, and $K = 0.20$ for $\tan\theta = 24$ and 48 .

Here Q is the abstraction through the inlet, L is the inlet length to catch discharge rate Q , y is the depth, v the flow velocity in the longitudinal direction, and q the carry-over flow bypassing the inlet. θ is the road cross-slope angle from the vertical (see Fig. 9.4 for underessed inlet and Fig. 9.5 for depressed inlet arrangement).

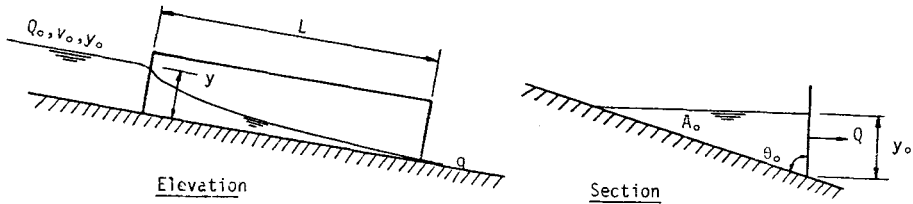


Fig. 9.4. Undepressed Kerb Inlet Notation.

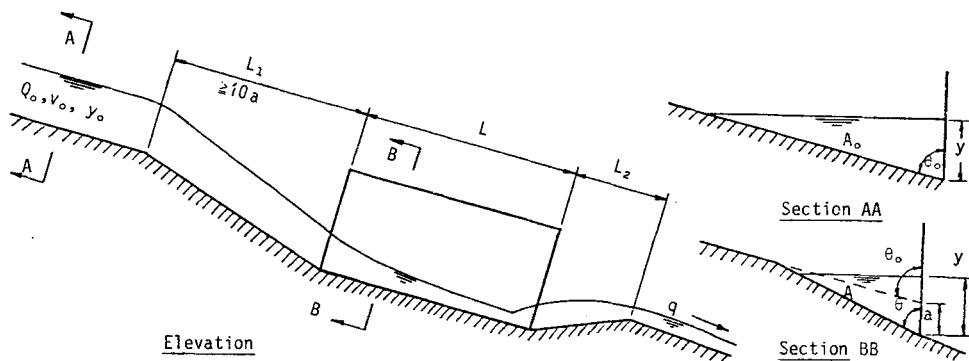


Fig. 9.5 Depressed Kerb Inlet Notation.

The depth of flow y in the depression and the corresponding velocity should be established from an energy balance using the Bernoulli equation

$$\frac{v_o^2}{2g} + y_o + Z_o = \frac{v^2}{2g} + y + Z + S_f L_1 \quad (9.23)$$

assuming normal flow depth y_o upstream of the depression. Z is elevation and S_f is the friction loss gradient over length L_1 . It was established that the inflow could be predicted by the equation

$$\frac{Q}{Ly \sqrt{gy}} = K + C \quad (9.24)$$

where K is as for (9.22) and

$$C = \frac{0.45}{1.12 (v^2 L / g y a \tan \theta)} \quad (9.25)$$

a is the projected gutter depression (see Fig.9.5)

Li et al (1955) provide curves for quick estimation of y , C or θ for any given design flow. ASCE (1969) present charts some of which are here translated to metric units. Fig. 9.6 and 9.7 are based on a two-dimensional depiction of the streamlines assuming uniform flow in the gutter.

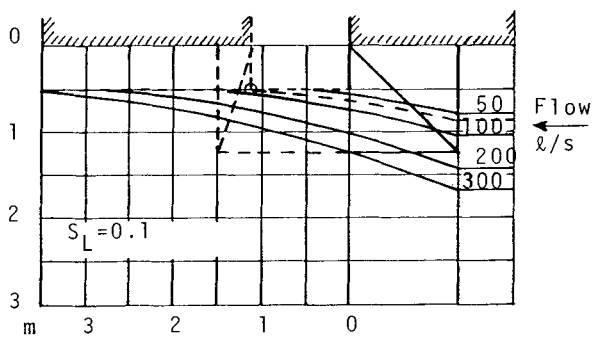
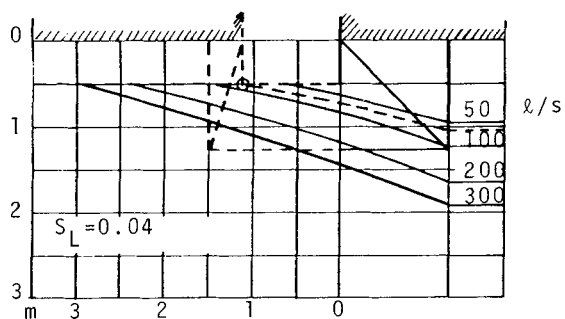
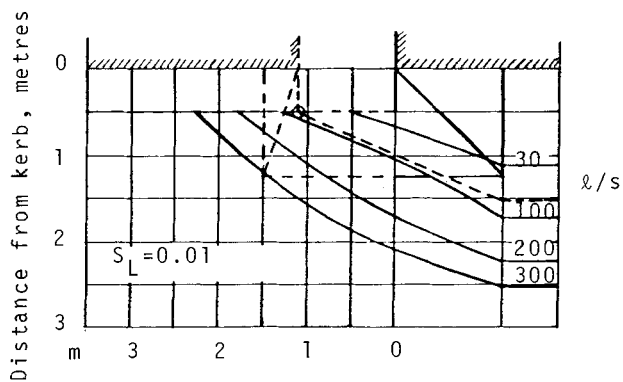
Zwamborn (1966) used model and prototype studies to establish design equations for gutter flow, inlet capacity and optimum gutter depression. He employed the Chezy equation to express flow rate as a function of slope etc. as he was thus able to scale down roughness for model tests. He presented charts (in feet units) for gutter flow as a function of cross-fall and longitudinal slope of the road. From tests he determined that the water depth decreased linearly along the length of an undepressed gutter opening, although the depth y (see Fig. 9.4) is a fraction of the normal flow depth, as determined by experiment. Starting from the free-fall equation $Q/L = K g^{1/2} y^{3/2}$ where L is the weir length, and integrating over the length L where depth y_o decreased linearly to zero, one obtains an equation similar to

$$Q/L = 0.33y^{1.25} \text{ (metre units)} \quad (9.26)$$

where the coefficients were determined experimentally. Zwamborn also recommended that side inlets should be dropped 60 mm to give an increase in inlet capacity. For partly intercepted flow Zwamborn derived the equation

$$\frac{Q'}{Q} = 1 - \left(1 - \frac{L'}{L}\right)^{5/2} \quad (9.27)$$

where L' is the actual inlet length to catch Q' and L is the length required to catch the full flow Q .



Distance from upstream edge of grate, metres

Fig. 9.6 Flow pattern for simplified design of combination inlets. Crown slope 1/18, $N=0.013$, Depression 65mmx1.2m

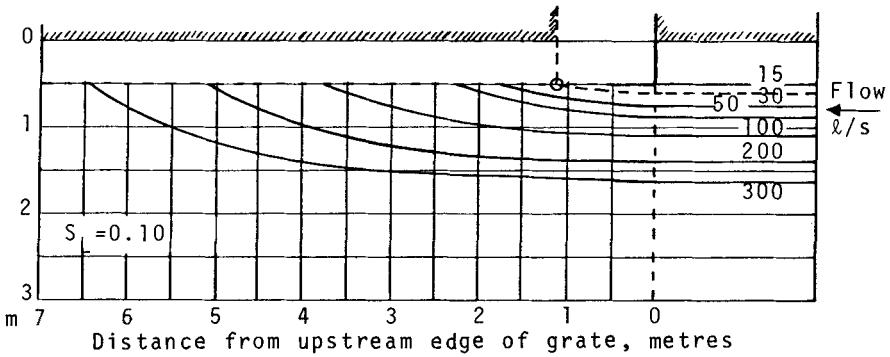
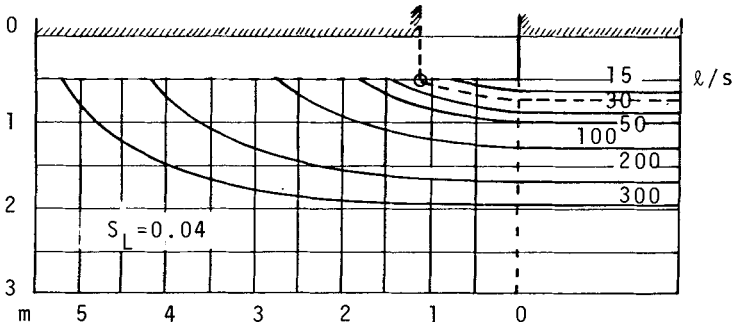
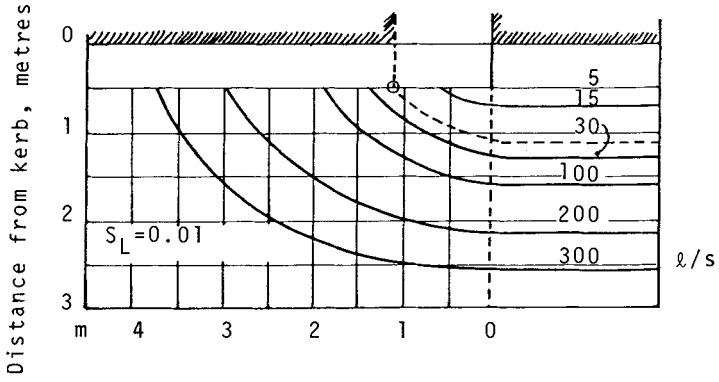


Fig. 9.7 Flow pattern for simplified design of combination inlets. Crown slope 1/18, $N=0.013$, Undepressed.

For ponded flow, however, it is recommended to use the equation

$$Q/L = 1.66 y^{3/2} \text{ (metre units)} \quad (9.28)$$

Forbes (1976) later recommended a standard drop of 75 mm and drop width of 300 mm (Fig. 9.8 and 9.9).

Zwamborn mentions that grooves 100 mm wide, 50 mm deep and 50 mm apart at 45° to the kerb over 500 mm wide, increase gutter capacity up to 20%, but they may get damaged and become clogged.

Forbes noted that Zwamborn's results were based on tests on 0.9 m long inlets only, and that they were of limited use for steep gradients. Using approximations, he analyzed the flow pattern in the vicinity of the inlet. He considered successive cross sections, solving simultaneously the Manning equation in the direction of flow, the weir equations in the lateral direction and the continuity equation in steps using a desktop calculator. It was necessary to apply a correction factor of 0.48 to the computed results to conform to other published data.

Fig. 9.10 was prepared by Forbes to indicate the capacities of inlets for various road gradients, cross falls and inlet lengths. The charts also indicate the required upstream gutter length and flooded road width.

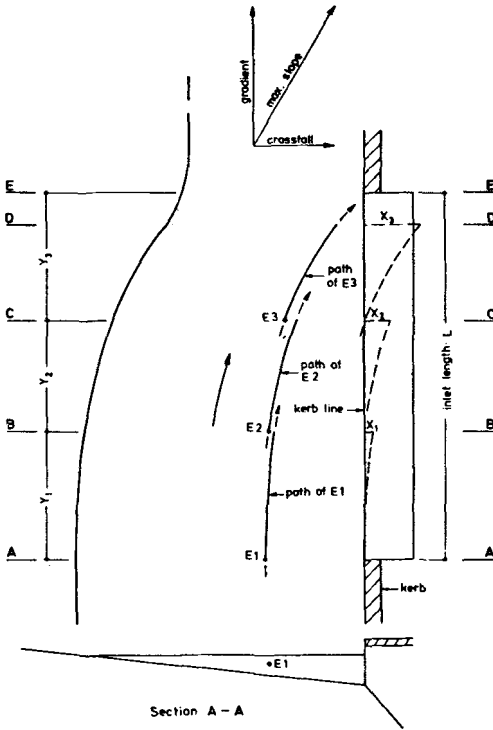
BOTTOM OPENINGS

In the case of flow over a longitudinal bar screen (Fig. 9.11) the outflow velocity head is equal to the specific energy. The discharge coefficient has been found to vary between 0.44 and 0.50 for bed slopes between 0.2 and 0.

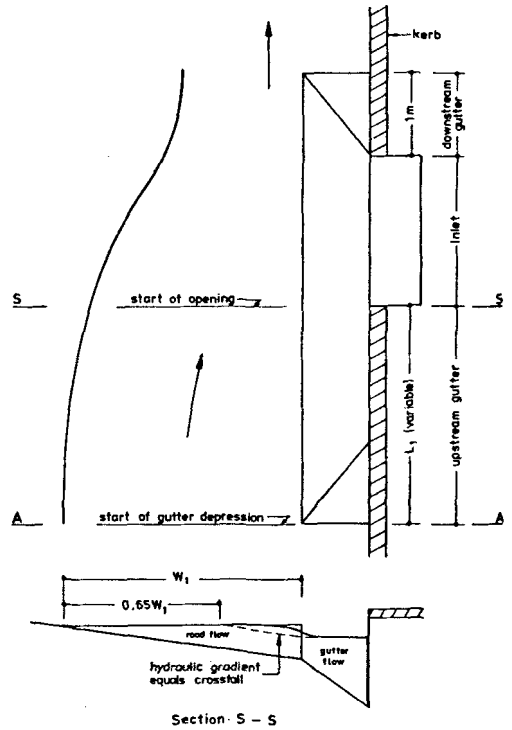
If there are openings in a perforated screen, the outflow velocity head is equal to the overlying water depth. There is a change in energy due to the change in direction. The corresponding discharge coefficient varies from 0.75 to 0.80 for bottom slopes from 0.2 to 0.

GUTTER INLETS

Although horizontal inlets on the road surface are attractive in that they do not require kerbs, they suffer a number of disadvantages (ref. also U.S. Dept. Transport, 1969). Bars or perforated screens are required to prevent traffic falling in the hole. The inlet capacity is reduced by the screens or bars. In particular longitudinal bars which are most efficient hydraulic-wise, are a danger to bicycles unless narrowed down below 25 mm. The bars or screens are prone to blockage.



Section A - A



Section S - S

Fig. 9.8 Road flow, undeepressed gutter for kerb inlet

Fig. 9.9 Road flow, depressed gutter for kerb inlet

The screens or bars are liable to break under heavy loads. Gutter inlets, like vertical kerb inlets, are susceptible to overshoot unless angled into the flow path (see Fig. 9.2c). The most efficient system appears to be longitudinal bars unrestricted by laterals. The length of grate required to fully capture the gutter flow may be estimated using free fall theory. If the approach depth is y_0 and discharge per unit width of gutter q_0 , then the locus of the water surface beyond the upstream edge of the gutter is given by the equations

$$y = gt^2/2 \therefore t = \sqrt{2y/g} \tag{9.29}$$

$$x = vt = qt/y = \sqrt{2q^2/gy} \tag{9.30}$$

i.e. the length of gutter grate to catch a flow q per unit width is $L_0 = (2q^2/gy_0)^{1/2}$ where y_0 is the depth of gutter flow.

This equation was found by the John Hopkins University (1956) to apply irrespective of whether there are bars obstructing the flow provided $a/b > 1$ (Fig. 9.12) where a is the gap width and b the bar width.

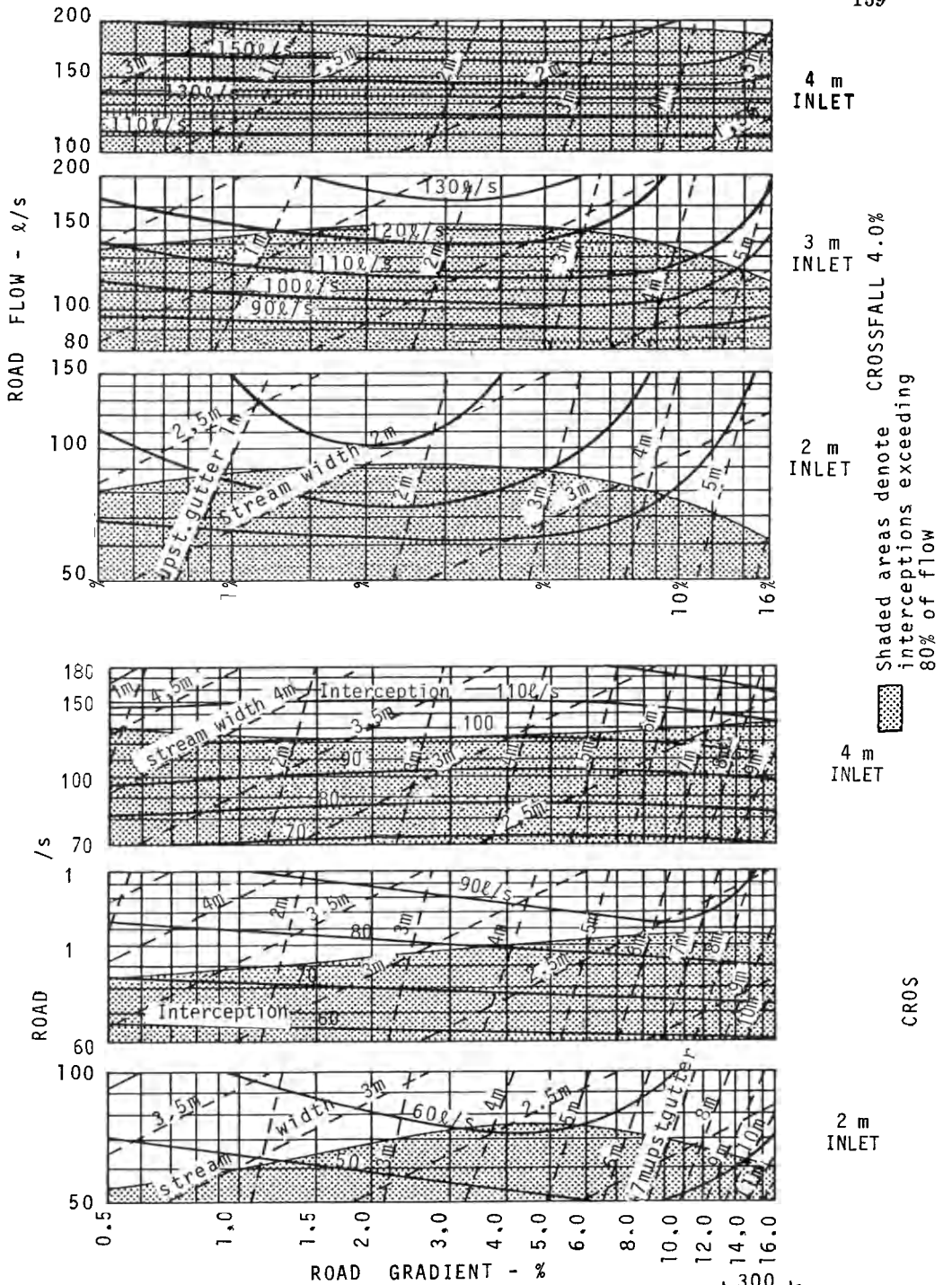
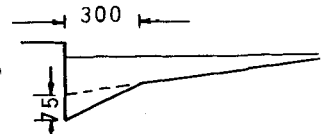


Fig. 9.10 Capacities of kerb inlets (Forbes, 1976)



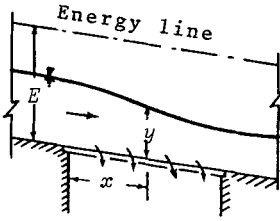


Fig. 9.11 Withdrawal of flow through a bottom rack

If the gutter flow is subcritical on account of a flat longitudinal slope then the flow depth at the grate crest may be assumed to be critical and

$$y_o = \sqrt[3]{q^2/g} \quad (9.31)$$

$$\text{hence } L_o = \sqrt{2} y_c \quad (9.32)$$

By plotting the water surface (which is an inverted parabola) from (9.30) where y is the fall in water surface level over a distance x , one may also estimate the length of inlet required for sloping grates. If the grate is tilted up slightly (at 5 to 10 degrees to the horizontal) the capacity increases considerably, or conversely a shorter grate length is required.

If there is overshoot, i.e. not all the flow is captured, then the orifice equation may be employed to estimate the inlet capacity. The inflow per unit width is

$$q = C_c L \frac{a}{a+b} \sqrt{2gy} \quad (9.33)$$

where C_c is a contraction coefficient, about 0.6 for square edges and nearly 1.0 for round bar grating. y is the flow depth here, and if this varies over the length of inlet then the equation must be integrated to obtain the total inflow.

The number of possible water surface profiles is, however, large. Downstream water depth is in turn dependent on discharge, so that it is difficult to solve the equation. The John Hopkins University (1956) therefore resorted to empirical tests.

Transverse bars increase the length of inlet required considerably. Thus three bars (at 1/4 points) will double the required length. An alternative to transverse bars which has not been tested is diagonal bars.

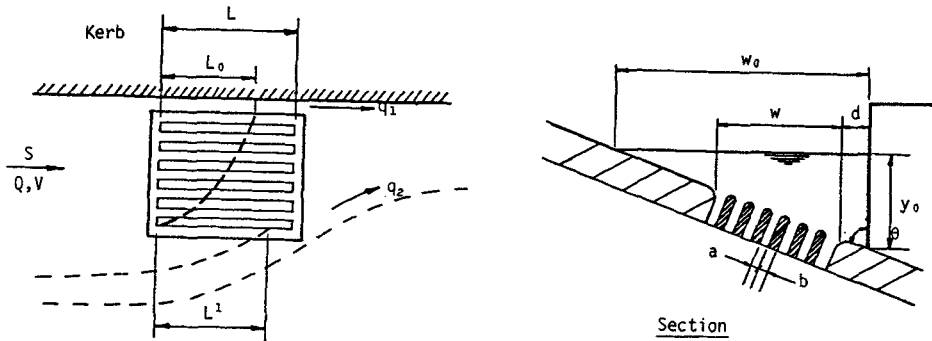


Fig. 9.12 Gutter Inlet Notation

For very wide road flow ($W_0 \gg W$ where W is the width of grate and W_0 the width of gutter), then for complete capture of the outer portion of the flow,

$$\frac{L'}{V_0} \sqrt{\frac{g}{y_0 - W/\tan\theta}} = 1.2 \tan\theta \quad (9.34)$$

and if the inlet length is less than this (i.e. $L < L'$), the carry-over is

$$q_2 = \frac{1}{4} (L' - L) \sqrt{g} (y_0 - W/\tan\theta)^{3/2} \quad (9.35)$$

In the case of bar or perforated inlet screens, the coefficient of discharge is fairly low due to a vena-contracta of about 0.6 times the hole opening width (or each edge length in the case of perforations).

DROPS

Water entering an inlet from the road falls into a drain pipe. Apart from sizing the drop structure for ease of access, it should also take the design flow with minimum impedance. The drop inlet is normally free-fall so that the length of lip is the flow-limiting criterion. In fact, the vertical drop could be constricted without restricting the capacity.

The falling water tends to draw in air and this aerates the water in the drain beneath. This action can reduce the capacity of the drain. There is also a head loss in the drain due to the incoming flow

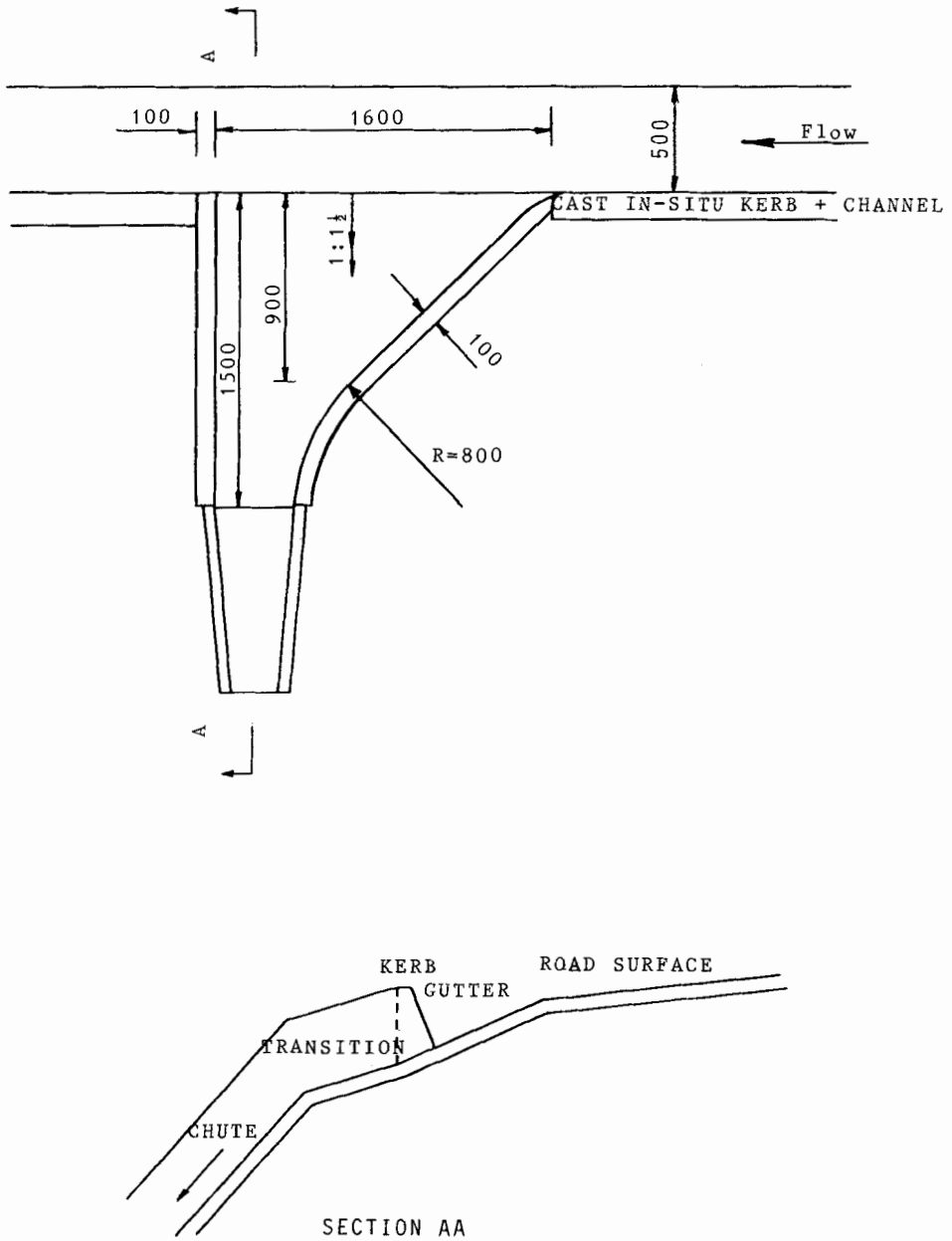


Fig. 9.13 Typical highway gutter transition

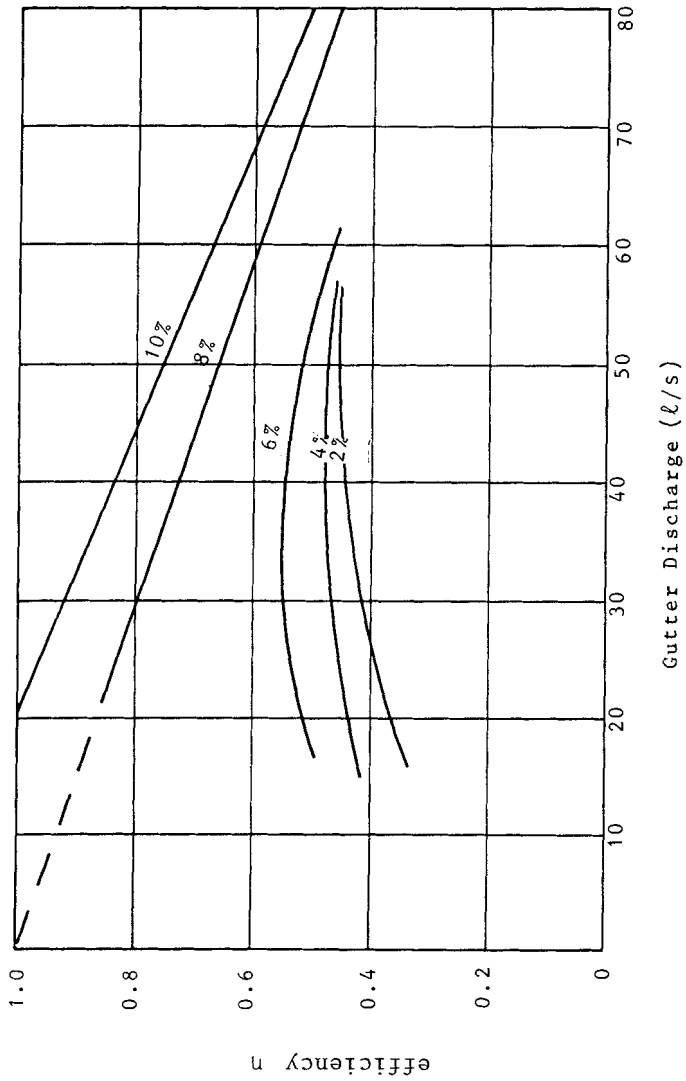


Fig. 9.14 Chute take-off efficiency curves for constant 1% longitudinal slope and variable cross slope

(Townsend and Prins, 1978). The losses may be assessed using momentum principles.

Devices for minimizing head losses and air entrainment have not been used extensively probably due to the complexity of construction. Spiral drops, (e.g. Ackers and Crump, 1960), chutes and tapered drops are some of the possibilities.

HIGHWAY CHUTE TAKE-OFFS

Where the road is on an embankment, stormwater will naturally run off laterally. Unless constrained, the runoff may erode the embankment, washing away vegetation and soil. It is common to provide shoulder gutters to collect the flow, and discharge down the embankment at suitable intervals. The design of chutes to take the flow down the embankment is discussed here.

The means of diverting the flow laterally is normally the restriction on the capacity of the system. Transitions of the type shown in Fig. 9.13 are used.

The chute itself can be made of precast concrete units. The base should receive particular attention as flow down the chute is supercritical and liable to erode unless some form of energy dissipation works is provided. Fig. 9.14 indicates that cross-fall plays a significant role in the catch-efficiency of take-offs.

REFERENCES

- Ackers, P., Feb. 1957. A theoretical consideration of side weirs as stormwater overflows. Proc. Inst. C.E. (London) 6, p 250.
- Ackers, P. and Crump, E.S., Aug. 1960. The vortex drop. Proc. I.C.E., 16, p 443-444.
- A.S.C.E., 1969. Design and construction of sanitary and storm sewers. N.Y.
- Forbes, H.J.C., Sept. 1976. Capacity of lateral stormwater inlets. Trans. South African Instn. Civil Engrs., 19(9). Also discussion May, 1977.
- Henderson, F.M., 1966. Open Channel Flow. Macmillan, London, 522pp. P 269-275.
- Jackson, T.J., and Rogan, R.M., Dec. 1974. Hydrology of porous pavement parking lots. Proc. ASCE, 100, HY12, 11010, p 1739-1752.
- John Hopkins University, 1956. The Design of Storm Water Inlets. Dept. Sanitary Engineering and Water Resources, Baltimore,
- Li, W.H., Geyer, J.C. and Burton, G.S., Jan. 1951. Hydraulic behaviour of stormwater inlets. Sewage and Industrial Wastes, Part I Jan., 1951, Flow into gutter inlets in a straight gutter without depression. 23 (1). Part II, June 1951, Flow into kerb opening inlets, 23 (6). Part III, July, 1951. Flow into deflector inlets, 23 (7), Part IV, Aug. 1954, Flow into depressed combination inlets. 26 (8).

- Townsend, R.D., and Prins, J.R., Jan., 1978. Performance of model storm sewer junctions. Proc. ASCE., 104 (HY1), p 99-104.
- U.S. Dept. Transportation, Federal Highway Admin., 1969. Drainage of Highway Pavements. Hydraulic Eng. Circular 12.
- Visser, A.T., Aug. 1976. Design and maintenance criteria for improved skid resistance of roads, Trans. South African Instn. of Civil Engineers., 18 (8). p 177-182.
- Zwamborn, J.A., May 1966. Stormwater inlet design. Proc. Annual Municipal Conf., Johannesburg. p 61-70.

CHAPTER 10

FLOW IN CIRCULAR DRAINS

ADVANTAGES OF PIPES

Pipes are in many ways a very convenient means of removing stormwater. They are buried so that they are unobtrusive, they are structurally strong, and the hydraulic properties of circular pipes are favourable in comparison with other types of closed conduits.

In regions sewerred many years ago and where storm runoff is relatively low, wastewaters and storm drainage are transported in the same pipes. In those situations closed conduits were essential for health. This is not always done nowadays, although surplus capacity is often allowed in sewers for stormwater which may enter the system at gulleys or leaking manholes or joints. Waste sewers are rarely designed to run full, whereas stormwater drains are. The hydraulic grade line ideally runs along the soffit of stormwater drains at design flow so that manholes are not surcharged.

Although the design of pressure pipes is beyond the scope of this section, basic principles of hydraulics of circular pipes are presented together with some design rules.

HEAD LOSS IN FULL PIPES

The energy of a flowing fluid expressed per unit weight of fluid, is termed the head. It comprises elevation head, pressure head and velocity head. In accordance with Bernoullis's equation for an ideal fluid the total energy at one section is equal to that at another section:

$$z_1 + \frac{p_1}{w} + \frac{v_1^2}{2g} = z_2 + \frac{p_2}{w} + \frac{v_2^2}{2g} \quad (10.1)$$

where v = mean velocity across a section

$\frac{v^2}{2g}$ = velocity head (units of length)

g = gravitational acceleration

p = pressure

p/w = pressure head (units of length)

w = unit weight of fluid

z = elevation above selected datum

If there occurs head loss due to friction and turbulence between sections 1 and 2, then the term h_f (head loss) should be added to the

right hand side of (10.1). Strictly the velocity head should be multiplied by a coefficient to account for the variation in velocity across the section of the conduit. The average value of the coefficient for turbulent flow is 1.06 and for laminar flow it is 2.0. For the Bernoulli equation to apply the flow should be steady, i.e. there should be no change in velocity with time at any point. The flow is assumed to be one-dimensional and irrotational and the fluid should be incompressible.

The respective total energy head and hydraulic grade line are illustrated in Fig. 10.1 (Stephenson, 1979). For most practical cases the velocity head is small compared with the other components, and it may be neglected.

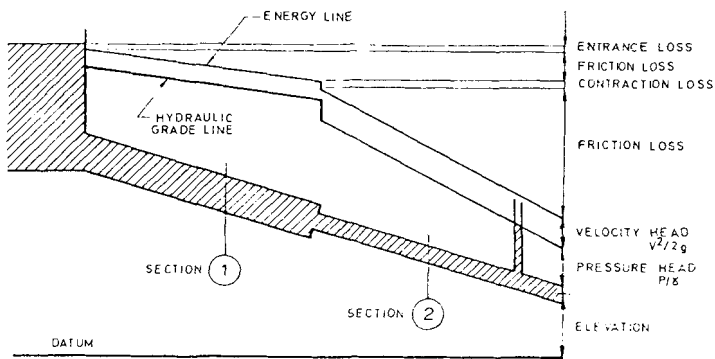


Fig. 10.1 Heads along a pipeline

The throughput or capacity of a pipe of fixed dimensions is controlled by the total head difference between the ends. This head is consumed by friction and other turbulence losses. The losses at bends, junctions, changes in diameter and at manholes (sudden expansions) are usually less than the friction loss. Gravity or free flowing pipelines are laid to the friction gradient, with additional allowances at changes in section. The head loss at such a section is a fraction of the velocity head;

$$h_L = K_1 v_1^2 / 2g \quad (12.2)$$

$$\text{where } K_1 = (1 - A_1/A_2)^2 \quad (10.3)$$

for a sudden expansion from area A_1 to A_2 .

TABLE 10.1 Nikuradse Roughness for Pipe Materials

Value of k in mm for new, clean surface unless otherwise stated.

Finish:	Smooth	Average	Rough
Glass, drawn metals	0	0.003	0.006
Steel, PVC or A C	0.015	0.03	0.06
Coated steel	0.03	0.06	0.15
Galvanized, vitrified clay	0.06	0.15	0.3
Cast iron or cement lined	0.15	0.3	0.6
Spun concrete or wood stave	0.3	0.6	1.5
Riveted steel	1.5	3	6
Foul sewers, tuberculated water mains	6	15	30
Unlined rock, earth	60	150	300

TABLE 10.2 Hazen-Williams Friction Coefficients C

Type of Pipe	Condition			
	New	25 years old	50 years old	Badly corroded
PVC	150	140	140	130
Smooth concrete, AC	150	130	120	100
Steel, bitumen lined				
galvanized	150	130	100	60
Cast iron	130	110	90	50
Riveted steel				
vitrified, woodstave	120		80	45

FRICTION EQUATIONS

Darcy-Weisbach equation

A number of empirical relationships for friction head loss in terms of pipe diameter and discharge were developed for specific use in water works practice. These equations (such as that of Hazen-Williams) were applicable within their sphere of development but cannot be extrapolated heedlessly. Following research by Reynolds, van Karman and others into turbulence, boundary layer theory was developed to yield a flow-head loss relationship for a range of flows in pipes. The Darcy-Weisbach friction equation is one equation resulting from this research:

$$S = \lambda v^2 / 2gD \quad (10.4)$$

This equation together with the associated Moody diagram (Fig. 10.2) or the Colebrook-White equation for the friction factor λ (or f in USA practice) is slowly gaining acceptance as the most rational method for estimating friction head losses in pipes. S is the head loss gradient, and D is the pipe internal diameter. For non-circular conduits or partly

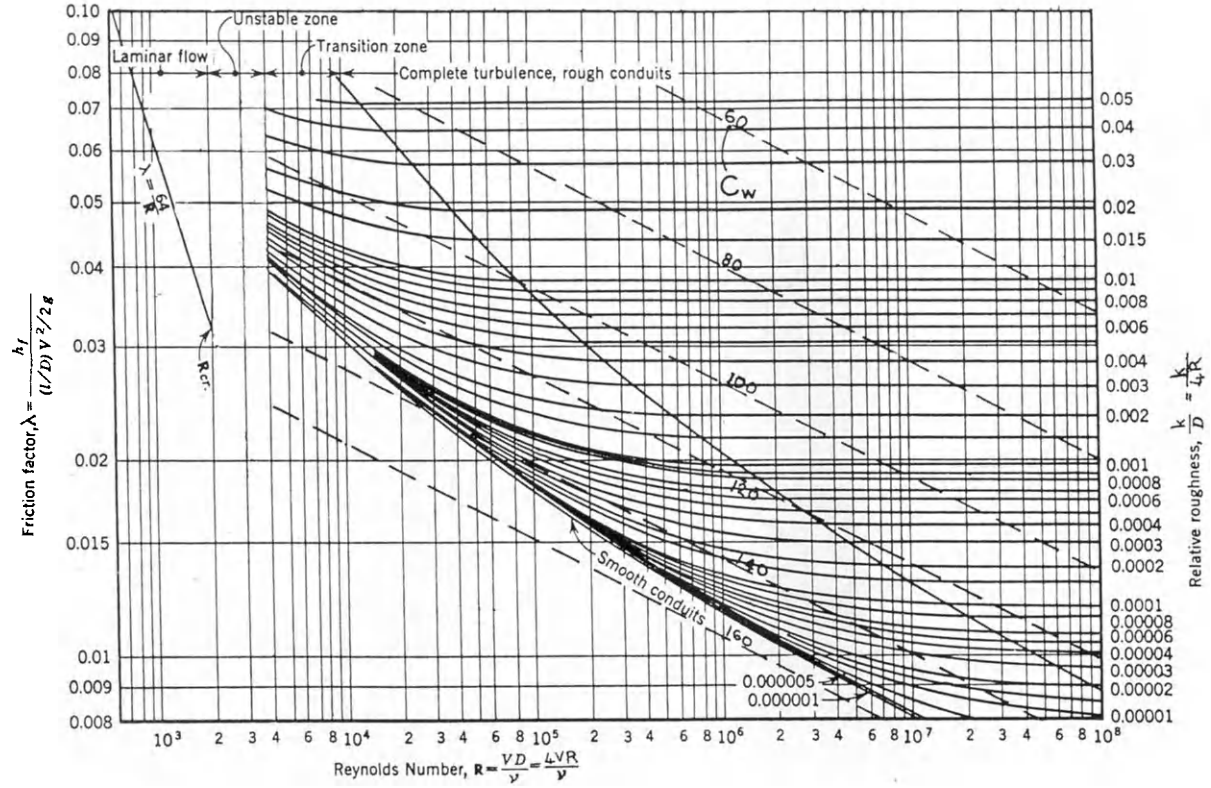


Fig. 10.2 Friction factors as a function of Reynolds number and relative roughness

full conduits D may be replaced by $4R$, where R is the hydraulic radius A/P , A is the cross-sectional area of flow and P is the wetted perimeter

The Darcy friction factor is yielded by the Colebrook-White equation (1939):

$$\frac{1}{\sqrt{\lambda}} = -2 \log \left(\frac{k}{3.7 D} + \frac{2.5}{R_e \sqrt{\lambda}} \right) \quad (10.5)$$

In view of the complicated relationship between the Darcy friction factor λ , Reynolds number R_e and the relative roughness k/D , explicit head loss charts have been prepared (Ackers, 1969; Watson, 1979). Such a chart is given as Fig. 10.3. k is a measure of the boundary roughness, termed the Nikuradse roughness (see Table 10.1). The Reynolds number is $R_e = vD/\nu$ or $4vR/\nu$ for part-full pipes (10.6) where ν is the kinematic viscosity of the fluid

Hazen-Williams equation

Despite its sound background and apparent simplicity the Darcy-Weisbach equation does not directly yield discharge rate for any given pipe and head loss gradient except in the turbulent rough zone of the Moody diagram. Equations such as that of Hazen-Williams and Manning remain in use because they can be solved directly for discharge rate. The bounds of applicability of these equations requires clarification. The equations also appear in specific units, and a dimensionless rendering would be welcome. Diskin (1960) presented a useful comparison of the friction factors from the Hazen-Williams and Darcy Equations.

The Hazen-Williams equation is widely used in water engineering practice. The equation is

$$v = K_w C_w D^{0.63} S^{0.54} \quad (10.7)$$

where K_w is 0.354 in metre units and 0.550 in foot units. C_w is the Hazen-Williams coefficient (see Table 10.2). The Hazen-Williams equation may be rewritten in the following dimensionless form:

$$v = 0.044 C_w (R_e/C_w)^{0.075} \sqrt{gDS} \quad (10.8)$$

The Hazen-Williams coefficient C_w is a function of λ and R_e and values may be plotted on a Moody diagram (see Fig. 10.2). It will be observed from Fig. 10.2 that lines for constant Hazen-Williams coefficient coincide with the Colebrook-White lines only in the transition zone. In the completely turbulent zone for non-smooth pipes the coefficient will actually reduce the greater the Reynolds number. The Hazen-Williams equation should therefore be used with caution for high Reynolds numbers and rough pipes.

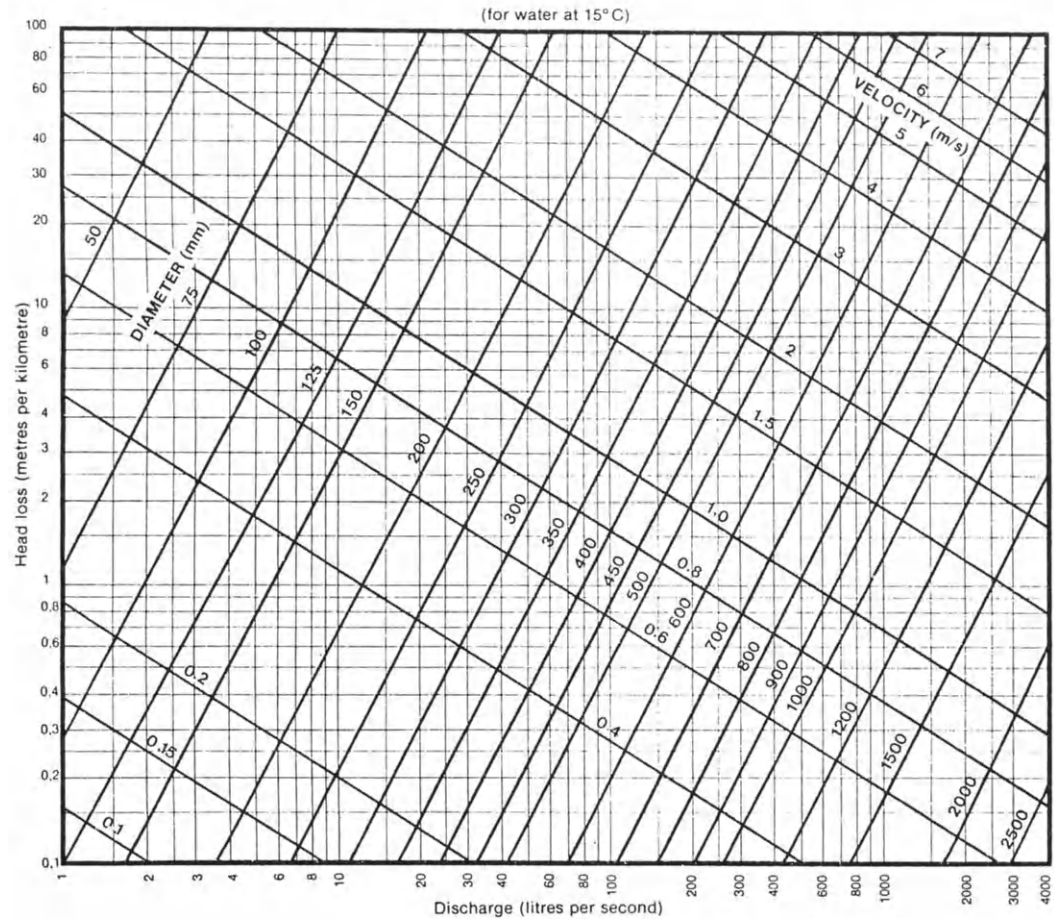


Fig. 10.3 Friction loss chart for pipes flowing full, $k = 0.3$ mm

Manning equation

The Manning equation is widely used for head losses in open channel flow calculations and for part full pipes.

The equation is

$$v = \frac{K_n}{N} R^{2/3} S^{1/2} \quad (10.9)$$

where K_n is 1.0 in S.I. (metre) units and 1.486 in ft units.

Strickler proposed the following relationship between the Manning coefficient N and the effective size of boundary roughness k :

$$N = 0.13 K_n k^{1/6} / \sqrt{g} \quad (10.11)$$

$$\text{thus } v = 7.7 (R/k)^{1/6} \sqrt{SRg} \quad (\text{all units}) \quad (10.12)$$

i.e. the Manning coefficient depends only on the boundary roughness, k .

The Manning equation is therefore only applicable to turbulent flow with a rough boundary. It is however easier to use than the Darcy equation and has thus retained popularity despite its limitations. Typical values of N are given in Table 10.3 and a relationship between N and k is given in Table 10.4. In fact Strickler's equation is analogous to the Darcy equation with a simpler 1/6th power equation for λ instead of the Colebrook-White log equation.

TABLE 10.3 Manning's N

Smooth glass	0.010
Concrete, galvanized or lined steel	0.011
Cast iron	0.012
Slimy or greasy sewers	0.013
Rivetted steel, vitrified	0.015
Rough concrete	0.018

TABLE 10.4 Relationship between Manning Coefficient N and roughness k .
($n = 0.13K_n k^{1/6} / \sqrt{g}$)

N	k (m)	k (ft)
0.01	0.0002	0.0006
0.012	0.0006	0.0019
0.015	0.0022	0.0072
0.02	0.012	0.039
0.025	0.048	0.156
0.03	0.142	0.466
0.04	0.80	2.625
0.05	3.05	10.00

NON-CIRCULAR CROSS SECTIONS

A circular pipe is normally the most economic if it is to be designed to resist internal pressures. A circular shape has the shortest circumference per unit of cross sectional area, consequently it requires least wall material, as well as being easy to manufacture.

Elliptical or horseshoe shapes are often adopted for sewers or drains. They have different strength and hydraulic characteristics to circular pipes. Vertical elliptical pipes (major axis vertical) have smaller wetted perimeters when running partly full with low flows, consequently the velocity is higher than for a circular pipe, which assists in flushing. The vertical load on a vertical elliptical pipe is less than on a circular pipe with the same cross sectional area, and the strength is greater because the curvature is sharper at the top.

Horizontal elliptical pipes (major axis horizontal) are sometimes used where vertical loads are low or clearance is limited. Running partly full they will discharge relatively high flows at small depths of flow which may be an advantage if head is limited.

Arch shapes with flat bottoms have similar hydraulic characteristics to horizontal elliptical shapes for low flow under partly full conditions. The arch shape is usually the most practical shape in tunnelling.

Provided the cross-sectional shape does not differ much from circular i.e. it could be elliptical or even rectangular, the Darcy equation is applicable. $4R$ is substituted for D in the equation and in the Reynolds number.

UNIFORM FLOW IN PART-FULL CIRCULAR PIPES

Most friction formulae for full pipe flow have been used for part-full flow. For a circular pipe of diameter D running at depth y , the cross-sectional area of flow is:

$$A = \frac{D^2}{4} \cos^{-1} \left(1 - \frac{2y}{D} \right) - \left(\frac{D}{2} - y \right) \sqrt{yD - y^2} \quad (10.13)$$

The wetted perimeter is:

$$P = D \cos^{-1} \left(1 - \frac{2y}{D} \right) \quad (10.14)$$

Using these equations charts may be prepared yielding a dimensionless relationship between flow depth and cross sectional area and hydraulic radius as a proportion of the full depth value, i.e. A/A_f and R/R_f versus y/D , as given as Fig. 10.4.

Also indicated on the chart are lines indicating the velocity ratio v/v_f and the discharge ratio Q/Q_f versus y/D for uniform flow. For non-uniform flow the ratio of friction gradient S_f/S versus y/D is indicated assuming $Q/Q_f=1$. These lines are dependent on the assumed friction loss equation. If Manning's equation is used with roughness N independent of depth, then the resulting relationships are as indicated. In

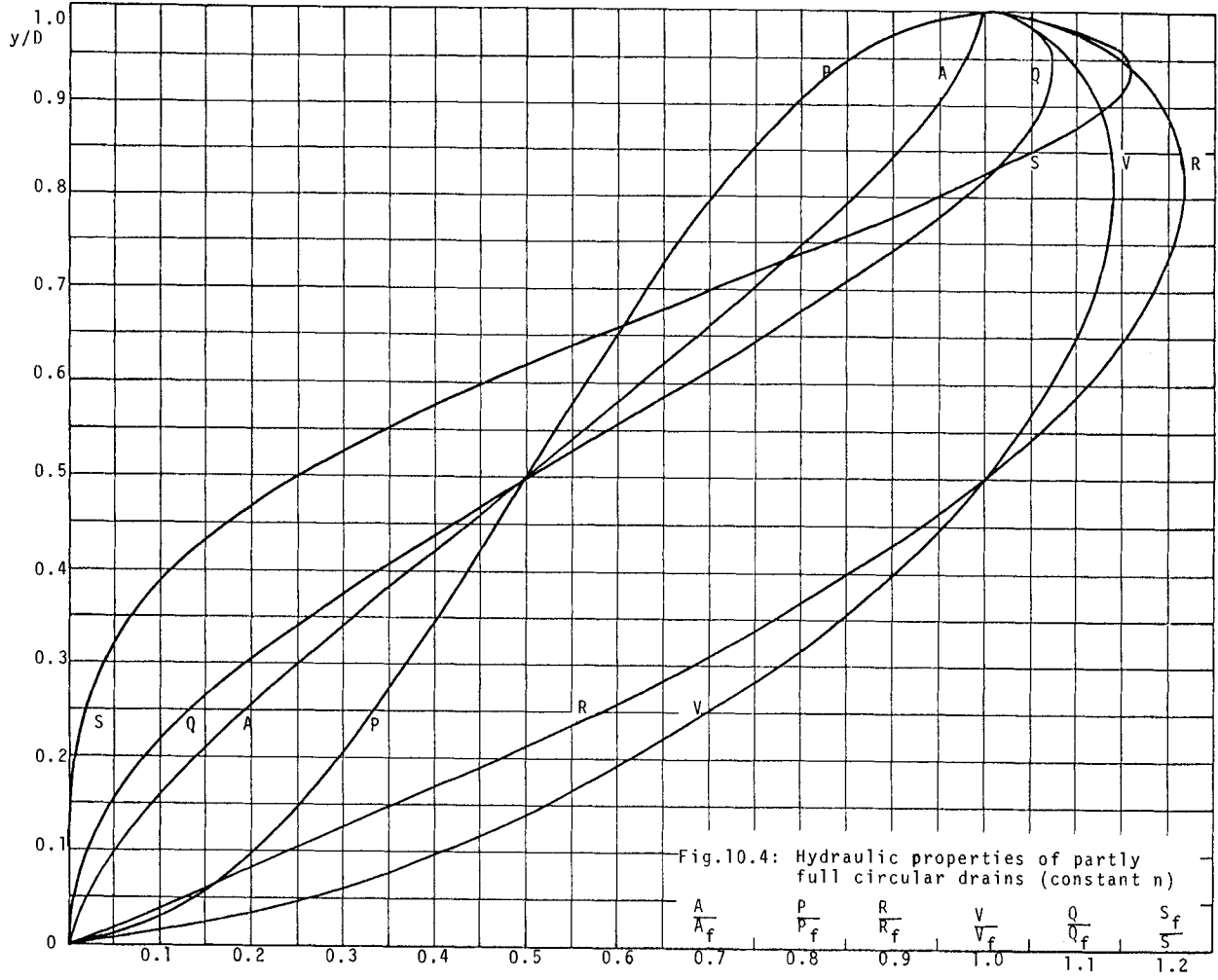


Fig.10.4: Hydraulic properties of partly full circular drains (constant n)

fact if Strickler's approximation for N is used, then N is independent of flow depth and dependent only on boundary roughness. If the Darcy-Weisbach equation is adopted, then assuming a constant friction factor λ i.e. independent of depth of flow, similar relationships could be plotted. The friction factor λ is known to vary with Reynolds number though, especially for shallow depths and correspondingly low Reynolds numbers. In such cases the relationships between v/v_f , Q/Q_f and y/D are not unique unless a varying λ is used i.e. λ is a function of two variables, k/R and Reynolds number, so a different line will apply for each case.

Camp (1946) performed tests to determine the variation of N and λ with depth. His charts are presented by ASCE (1969), but it should be borne in mind those relationships are not completely in accordance with the Colebrook-White equation for the reasons indicated above.

Using Figs. 10.3 and 10.4, given any three of the five variables Q , D , S , v and y , the other two may be determined. The flow conditions for full-bore flow ($y/D = 1$) are yielded simultaneously. Designate Q_f = flow at full bore and v_f = velocity at full bore. Now assume the flow, pipe diameter and slope (Q , D and S) are known, and y/D and v are to be determined. Read Q_f and v_f from Fig. 10.3 and using the ratio Q/Q_f , read y/D from Fig. 10.4. Hence also read v/v_f from Fig. 10.4 and calculate v knowing v_f .

As another example, given $Q = 50$ l/s, $S = 0.0005$ and $y/D = 0.25$, find the necessary diameter D and corresponding velocity: From Fig. 10.4, $Q/Q_f = 0.135$ so $Q_f = 370$ l/s and from Fig. 10.3 $D = 525$ mm and $v_f = 1.7$ m/s. Now from Fig. 10.4, $v/v_f = 0.7$ hence $v = 1.2$ m/s.

An interesting fact is illustrated in Fig. 10.4. The flow for a partly full pipe is greater than the flow through a fully charged pipe if the depth of flow is between 82% and 100% of the diameter. The reason for this is that the wetter perimeter increases rapidly but the area does not, as the pipe fills up over the last portion. The additional capacity should not be relied upon however as the slightest irregularity may cause the pipe to run full.

CRITICAL DEPTH AND HYDRAULIC JUMPS IN PIPES

Bernoulli's energy equation applies to the flow in circular drains running full or part full. Thus for no friction or energy losses,

$$z + y + \frac{v^2}{2g} = \text{constant} \quad (10.15)$$

or

$$z + y + Q^2/2gA^2 = \text{constant} \quad (10.16)$$

where z is bed elevation, y is water depth and v is mean velocity. In accordance with this equation, the specific energy is a minimum at some depth y_c termed the critical depth. It is derived in implicit form by differentiating the energy equation with respect to depth and setting the differential equal to zero. Then

$$Q_c = (gA_c^3/B_c)^{1/2} \tag{10.17}$$

or in dimensionless numbers

$$\frac{Q_c}{(gD^5)^{1/2}} = \frac{(A_c/D^2)^{3/2}}{(B_c/D)^{1/2}} \tag{10.18}$$

Both area A and surface width B are functions of flow depth y . Thus

$$A/D^2 = \frac{1}{4} \cos^{-1} (1-2y/D) - (\frac{1}{2}-y/D)(y/D-y^2/D^2)^{1/2} \tag{10.19}$$

$$\text{and } B/D = 2(y/D-y^2/D^2)^{1/2} \tag{10.20}$$

TABLE 10.5 Flows for Varying Values of Critical Depth in Circular Channels

y/D	A/D^2	B/D	\bar{y}/D	$Q_c/(gD^5)^{1/2}$
0.00	0.0000	0.0000	0	0.000
0.05	0.0147	0.4359	0.017	2.699 x 10 ⁻³
0.10	0.0409	0.6000	0.039	10.68 ..
0.15	0.0739	0.7141	0.061	23.77 ..
0.20	0.1118	0.8000	0.082	41.80 ..
0.25	0.1535	0.8660	0.103	64.64 ..
0.30	0.1982	0.9165	0.122	92.18 ..
0.35	0.2450	0.9539	0.146	124.16 ..
0.40	0.2934	0.9798	0.168	160.55 ..
0.45	0.3428	0.9950	0.190	201.18 ..
0.50	0.3927	1.0000	0.212	246.11 ..
0.55	0.4426	0.9950	0.236	295.17 ..
0.60	0.4920	0.9798	0.260	348.63 ..
0.65	0.5404	0.9539	0.284	406.76 ..
0.70	0.5872	0.9165	0.310	470.00 ..
0.75	0.6318	0.8660	0.336	539.68 ..
0.80	0.6736	0.8000	0.364	618.09 ..
0.85	0.7115	0.7141	0.393	710.22 ..
0.90	0.7445	0.6000	0.424	829.29 ..
0.95	0.7707	0.4359	0.459	1001.8 x 10 ⁻³
1.00	0.7854	0.0000	0.500	∞

Employing these relationships values of A/D^2 , B/D and the corresponding value of $Q_c/(gD^5)^{1/2}$ are given in Table 10.5 as functions of y/D .

Diskin (1958 and 1962) indicates that the following experimental equation fits the relationship between y_c/D and $Q/(gD^5)^{1/2}$ for y/D

$$y_c/D = \{1.05Q/(gD^5)^{1/2}\}^{0.513} \tag{10.21}$$

The minimum specific energy corresponding to critical depth is (Jenker, 1962)

$$H_{\min} = Y_C + A_C / 2B_C \quad (10.22)$$

This may be evaluated from the functions of A/D^2 and B/D versus y/D previously tabulated. In general whether the depth is critical or not, the relationship between depth and specific energy can be plotted in non-dimensional form (Fig. 10.5), from

$$\frac{E}{D} = \frac{y}{D} + \frac{Q^2 / gD^5}{2(A/D^2)^2} \quad (10.23)$$

It should be noted that for high specific energy the pipe may be surcharged in the subcritical condition in which case the term y/D represents the depth plus pressure head. In this case the lines above $y/D = 1$ in Fig. 10.5 extend at 45 degrees above the soffit of the pipe.

The specific momentum of the flow may likewise be evaluated in dimensionless terms. The total momentum per unit weight of water is

$$M = \frac{Q^2}{gA} + A\bar{y} \quad (10.24)$$

or in dimensionless terms

$$\frac{M}{D^3} = \frac{Q^2}{gD^5} \frac{D^2}{A} + \frac{A}{D^2} \frac{\bar{y}}{D} \quad (10.25)$$

where \bar{y} is the depth from the top water surface to the centroid of the section. \bar{y}/D as a function of y/D was evaluated numerically and is given in Table 10.5. It may be shown (Henderson, 1966, p 84) that

$$A\bar{y} = \frac{D^3}{24} \left(3 \sin \frac{\theta}{2} - \sin \frac{3\theta}{2} - 3 \frac{\theta}{2} \cos \frac{\theta}{2} \right) \quad (10.26)$$

$$\text{where } \cos \theta = 1 - 2y/D \quad (10.27)$$

The dimensionless specific momentum function is plotted in Fig. 10.6. In many cases the sequent depth should exceed the diameter of the conduit. In this case the conduit will run full and pressurized. The corresponding specific momentum is

$$\frac{M}{D^3} = \frac{Q^2}{gD^5} \frac{4}{\pi} + \frac{\pi}{4} \frac{\bar{y}}{D} \quad (10.28)$$

where \bar{y} is the pressure head above the centre-line of the conduit. A limited range of values is plotted in Fig. 10.6.

A hydraulic jump in a conduit can entrain air which causes additional complications. The air is likely to be released from solution and small bubbles will rise to the top of the pipe, creating a part-full pressurized flow situation. Whether the air is in the form of bubbles or a pocket along the soffit of the conduit, the head losses will be higher than for pure water flowing at the specified rate. The volume occupied by entrapped air can be as great as 25% for low pressure systems (Mussalli, 1978).

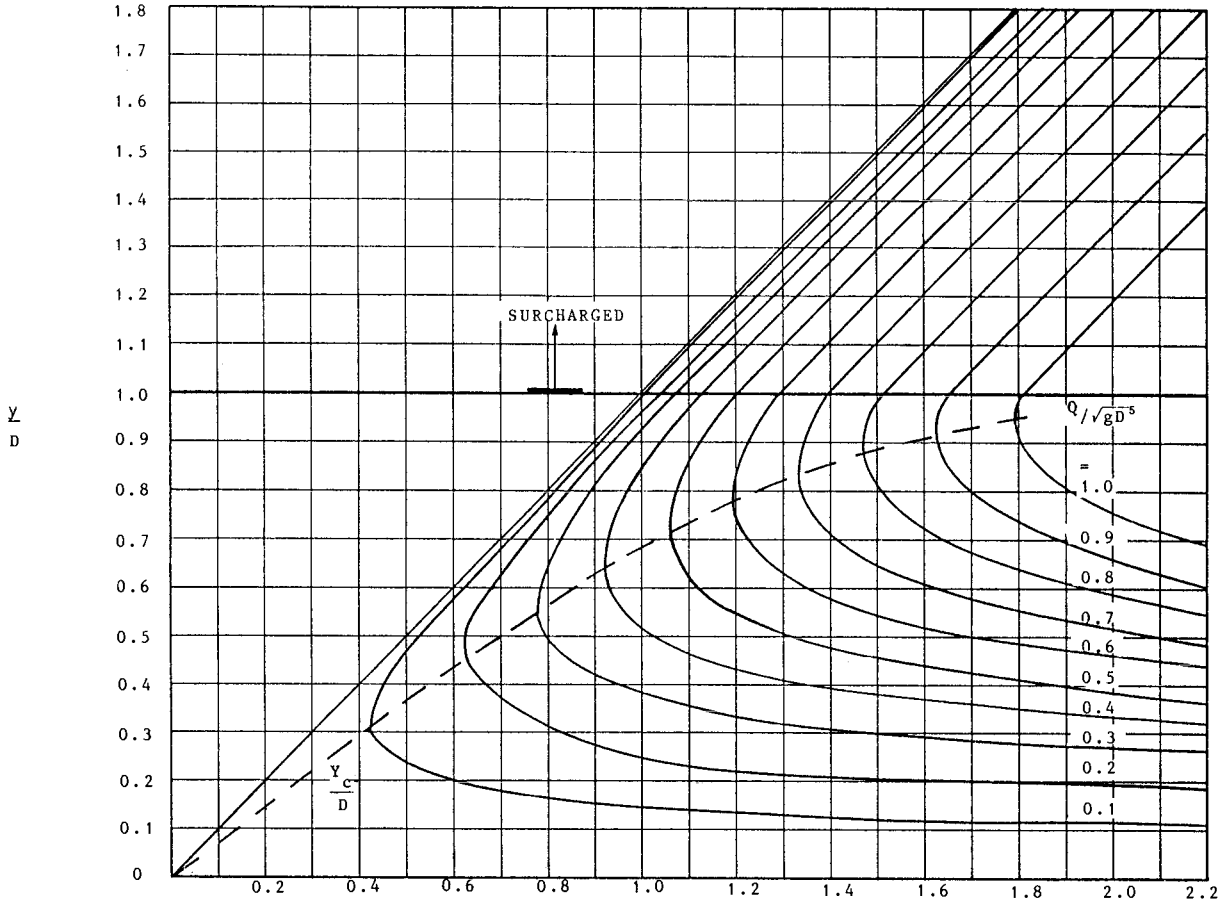


Fig. 10.5 Specific energy function for circular conduits

$$\frac{E}{D} = \frac{y}{D} + \frac{Q^2}{2gD A^2}$$

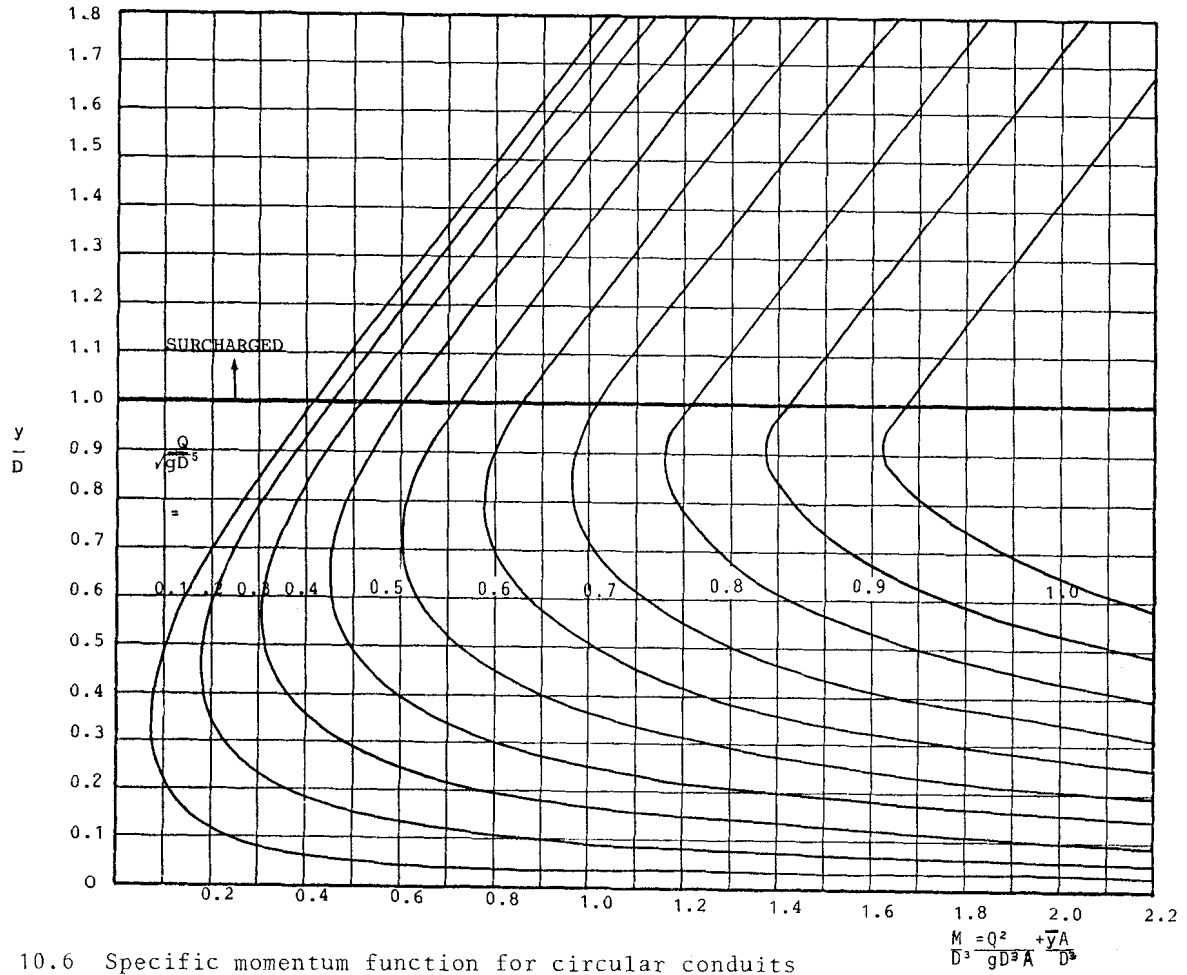


Fig. 10.6 Specific momentum function for circular conduits

The rate of air entrainment of a free hydraulic jump in a rectangular channel was determined from model experiments by Kalinske and Robertson (1943). Recent tests on jumps in pipes indicate this equation underpredicts the air entrainment rate. An equation of the following form is indicated

$$Q_a/Q_w = 0.03 (F-1) \quad (10.29)$$

where Q_a is the volumetric air entrainment rate and F is the upstream Froude number $(Q^2 B/gA^3)^{1/2}$. Wisner et al (1975) also advocate the removal of air by hydraulic means.

The total volume of discharge immediately downstream of the jump before the air has had time to dissolve, is therefore $Q + Q_a$ and the friction loss is a function of this total flow. Air may subsequently be released at manholes in gravity lines or by air valves in pressure lines. In fact air is a nuisance in many cases as it results in head losses which restrict the capacity of the pipe.

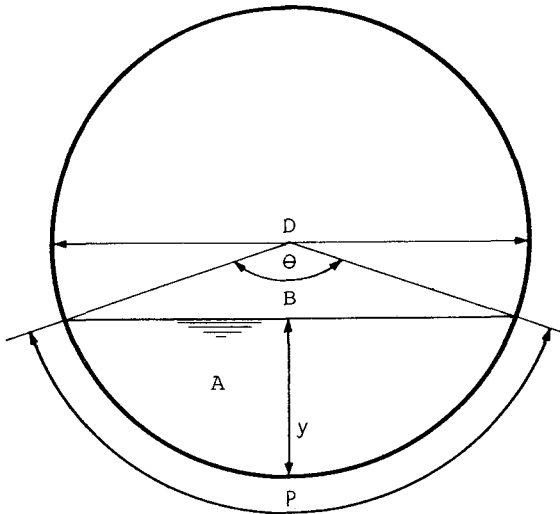


Fig. 10.7 Circular pipe part full

FLOOD ROUTING

Although the kinematic method of routing, ignoring dynamic terms, is sufficiently accurate for most drains (Stephenson, 1980), for large drains the full hydrodynamic equations can be employed for greater accuracy. Harris (1970) found the characteristic method expensive on computer time and preferred a progressive average lag method. In many cases the kinematic equations enable routing to be performed easily. The cross sectional area of flow in a circular conduit running part full (see Fig. 10.7) may be written as

$$A = \frac{D^2}{4} \left(\frac{\theta}{2} - \cos \frac{\theta}{2} \sin \frac{\theta}{2} \right) \quad (10.30)$$

$$\text{and } P = D \frac{\theta}{2} \quad (10.31)$$

Thus if we take the angle θ subtended at the centre as the variable the continuity equation becomes

$$\frac{D^2}{8} \left(1 + \sin^2 \frac{\theta}{2} - \cos^2 \frac{\theta}{2} \right) \frac{\partial \theta}{\partial t} + \frac{\partial Q}{\partial x} = q \quad (10.32)$$

where q is the inflow per unit length and Q is the total flow rate in the pipe. This may be solved for θ_2 after a time interval Δt in finite difference form

$$\theta_2 = \theta_1 + \left(q - \frac{\Delta \theta}{\Delta x} \right) \frac{8 \Delta t}{D^2 (1 + \sin^2 \frac{\theta}{2} - \cos^2 \frac{\theta}{2})} \quad (10.33)$$

and in terms of the new θ , using the Strickler approximation for friction losses,

$$Q = \frac{7.7 \sqrt{Sg}}{k^{1/6}} \frac{D^2}{4} \left(\frac{\theta}{2} - \cos \frac{\theta}{2} \sin \frac{\theta}{2} \right) \left\{ \frac{D}{4} \left(1 - \frac{\cos \frac{\theta}{2} \sin \frac{\theta}{2}}{\theta/2} \right) \right\}^{2/3} \quad (10.34)$$

(10.33) and (10.34) are solved successively at different points along the drain at successive time intervals to yield a history of Q versus x and t .

Approximate Method

The following assumptions may often be made in the case of a slug of water released into a drain (Stephenson, 1977).

1. There is no base flow in the drain.
2. A volume of water U , i.e. a 'slug' is injected into the drain over a length L , at uniform depth y . The cross-sectional area of flow is approximately $2/3 yB$ (which is not accurate unless y is small), where B is the surface width.
3. The volume of water travels down the drain at an average velocity v where λ is the Darcy friction factor, R is the hydraulic radius and S is the bedslope.

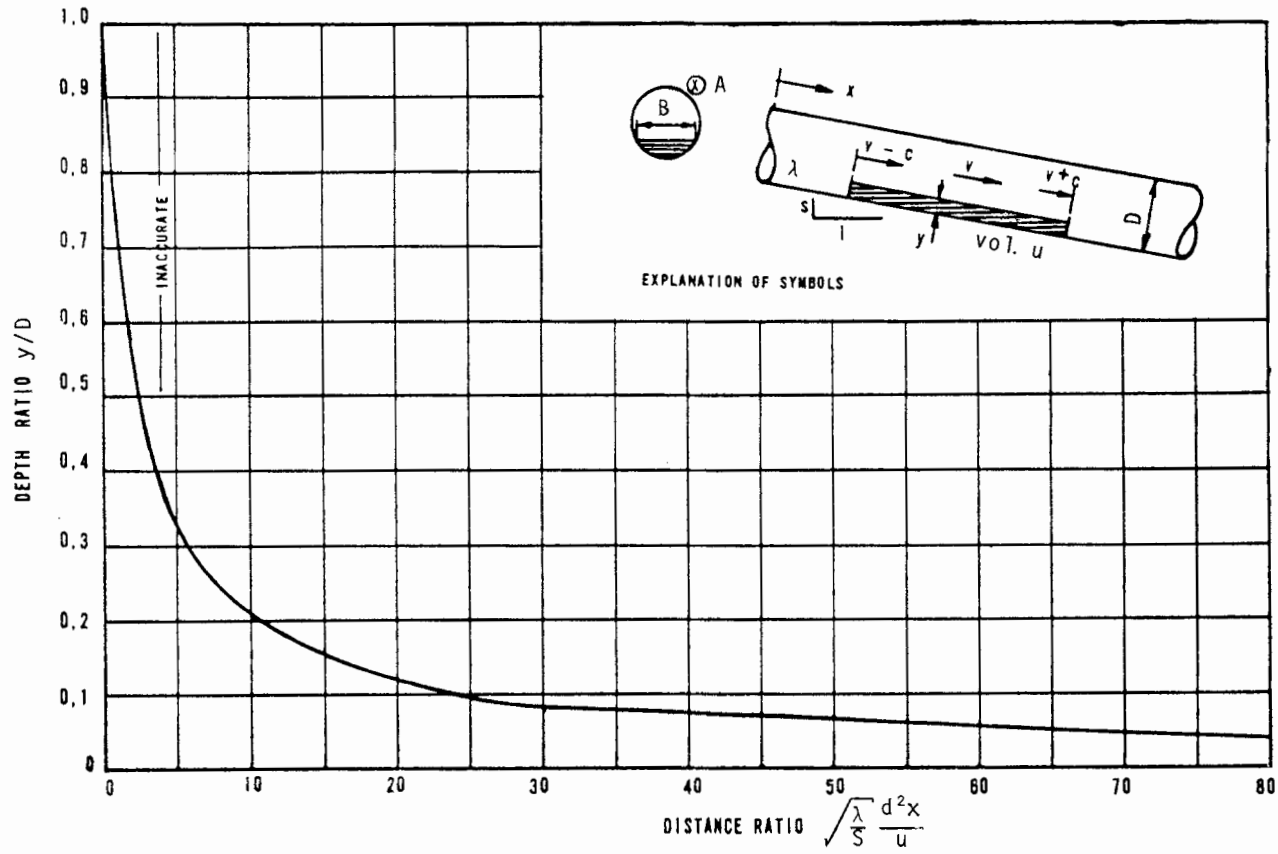


Fig. 10.8 Attenuation of surges in circular drains

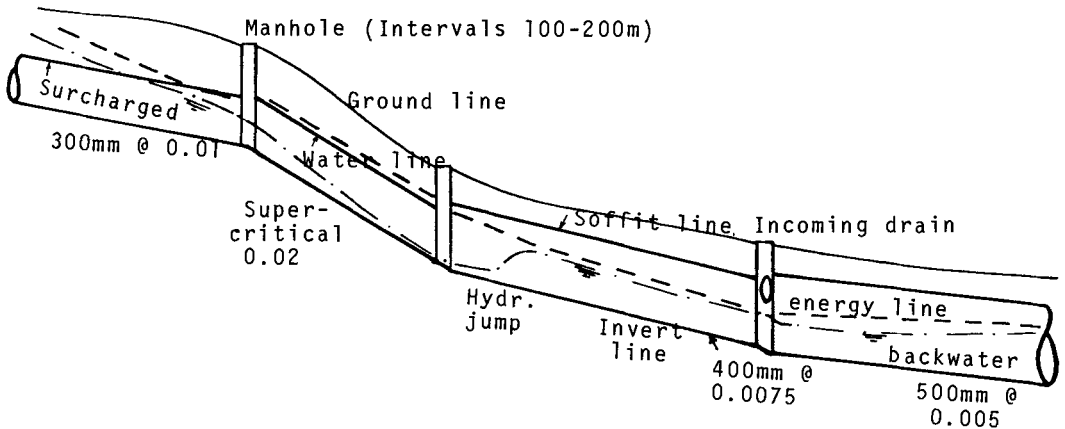


Fig. 10.9 Storm drain profile (vertically exaggerated)

4. The extremities of the volume of water U are travelling outwards relative to the average velocity by the celerity $c = \sqrt{gy}$, i.e. the two ends of the water are travelling at $v-c$ and $v+c$ respectively down the pipe.
5. The depth of water remains uniform over the length.

Then employing the continuity equation and an approximation for area of flow it may be shown

$$\frac{\Delta y}{D} \approx -0.77 \left(\frac{y}{D}\right)^2 \sqrt{\frac{y}{D} - \left(\frac{y}{D}\right)^2} \sqrt{\frac{f}{S} \frac{D^2 \Delta x}{Q}} \quad (10.35)$$

(10.35) was solved in steps to yield a relationship between y and x as shown in Fig. 10.8. This chart represents the attenuation in depth of the surge as it travels down the drain. The chart albeit only an approximation will be satisfactory as a design aid for many problems e.g. the estimation of the attenuation of flow in stormwater drains after high intensity, short duration storms. Thus by routing a storm down a drain it will reduce in intensity, enabling drain sizes to be minimized. It is not suggested that the drain diameter be reduced along the length, as the storm could presumably occur anywhere along its length. However, in summing inputs along the length, the inputs from higher up in the catchment could be suitably routed using the chart so that the total capacity is less than the sum of the inputs. It may also be employed to estimate the amount of water needed to flush a sewer (Watson, 1937).

To estimate the initial flow depth of any input if the duration and total inflow are known one may use the approximation

$$\text{for } y \ll d, y \doteq \left(\frac{\lambda U^2}{10gDSt^2} \right)^{1/4} \quad (10.36)$$

BACKWATERING AND GRADUALLY VARIED FLOW

The computation of backwater surface profiles in circular channels can be done by the standard step method (Henderson, 1966). Nalluri and Tomlinson (1978) presented a direct step method necessitating the use of tables.

Backwatering is easily executed by hand with the assistance of a graph such as Fig. 10.4 depicting proportional area of flow, hydraulic radius and energy gradient.

PROGRAM FOR BACKWATERING IN PART-FULL PIPES

Using the equations for the geometric properties for partly full circular pipes one is able to backwater in a circular pipe. It is a simple matter to program the equations. Such a program is appended.

The friction equation employed in the program is that of Manning, with a constant 'N' value. The Manning friction equation is rendered independent of whether metres or feet are used by expressing it as

$$v = g^{1/3} R^{2/3} S^{1/2} / 2.14N \quad (10.37)$$

Data is read in via device 9 (see lines 3 and 6 in the program).

Free format is used and data is read in the following order:

First line : N, Q, D, C, G, Y(1), E

Second and subsequent lines : (N such lines): Z(M), X(M), T(M)

where N = number of cross sections considered

Q = flow rate

D = pipe diameter

C = Manning's coefficient

G = gravitational acceleration

Y = water depth at section 1.

E = permitted error in depth during computations

Z(M) = invert level of pipe at section M measured above any constant datum

X(M) = distance to next cross section. For the last pipe this may be set at zero

T(M) = turbulent loss coefficient in the pipe immediately before the cross section M ($\Delta H = TV^2/2G$)

The printout on device 5 (see lines 39, 41 and 44) includes input data as well as water levels and velocities at each section. The program can be used to backwater upstream in the case of subcritical flow or downstream in the case of supercritical flow. In the latter case, pipe lengths should be input as negative values.

REFERENCES

- ASCE, 1969. Design and Construction of Sanitary and Storm Sewers, NY. 332pp.
- Camp, T.R., 1946. Design of sewers to facilitate flow. Sewerage Works Journal. 18 (3).
- Diskin, M.H., Sept. 1958. An experimental equation for critical depth in circular channels, Water Power, 10, p350-351.
- Diskin, M.H., Nov. 1960. The limits of applicability of the Hazen-Williams formula. La Houille Blanche, 6.
- Diskin, M.H., July 1962. Specific energy in circular channels, Water Power, 14, p270-271.
- Harris, G.S., June 1970. Real time routing of flood hydrographs in storm sewers. Proc. ASCE, 96,(HY6), 7327, p1247-1260.
- Henderson, F.M., 1966. Open Channel Flow. Macmillan, London, 522pp.
- Jenkner, W.R., January, 1962. Critical depth and minimum total energy in circular channels, Water Power, p14.
- Kalinske, A.A., and Robertson, J.M., 1943. Closed Conduit Flow. Trans, ASCE, 108, 2205, p1435-1516.
- Mussalli, Y.G., July 1978. Size determination of partly full conduits. Proc. ASCE. 104(HY7), 13862, p959-974.
- Nalluri, C and Tomlinson, J.H., July 1978. Varied flow functions for circular channels. Proc. ASCE 104(HY7), 13889, p983-1000.
- Stephenson, D., Nov. 1977. Flow attenuation in sewers. The Public Health Engineer, 5(6).
- Stephenson, D., 1979. Pipeline Design for Water Engineers, Elsevier, Amsterdam, 226pp.
- Watson, J.D., Aug. 1937. Sewer Flushing. Water Works and Sewerage.
- Watson, M.D., July 1979. A simplified method for the solution of pipe flow problems using the Colebrook-White method. Trans, South African Inst. Civil Engineers, 21(7), p169-171.
- Wisner, P., Mohsen, F.N., and Kouwen, N., Feb. 1975. Removal of air from water lines by hydraulic means. Proc. ASCE, 101(HY2), 11142, p243-257.

```

L.0001 C      BACKWATER IN CIRC PIPES
L.0002      DIMENSION Y(90),Z(90),X(90),T(90),U(90),W(90),S(90),H(90)
L.0003      READ(9,10)N,Q,D,C,G,Y(1),E
L.0004 1C     FCRMAT(7Y)
L.0005      DC 100 M=1,N
L.0006      READ(9,11)Z(M),X(M),T(M)
L.0007 11     FCRMAT(3Y)
L.0008      IF(M.LE.1)GO TO 19
L.0009      Y(M)=Y(M-1)
L.0010 19     K=0
L.0011 2C     W(M)=Z(M)+Y(M)
L.0012      TH=2.*ARCCOS(.9999*(1.-2.*Y(M)/D))
L.0013      A=.25*D*D*(TH/2.-COS(TH/2.)*SIN(TH/2.))
L.0014      V=Q/A
L.0015      HE=W(M)+V*V/2./G
L.0016      P=D*.5*TH
L.0017      R=A/P
L.0018      B=2.*D*SGRT(Y(M)/D-Y(M)**2./D/D)
L.0019      S(M)=V*V*C*C/R**1.333*4.53/G**.667
L.0020      IF(M.LE.1)GO TO 65
L.0021      SA=(S(M-1)+S(M))/2.
L.0022      HF=H(M-1)+SA*X(M-1)+T(M)*V*V/2./G
L.0023 60     IF(ABS(HF-HE).LE.E)GO TO 90
L.0024      FS=Q*Q*B/G/A**3.
L.0025      DY=(HF-HE)/(1.-FS+3.*S(M)*X(M-1)/R/2.)
L.0026      Y(M)=Y(M)+DY
L.0027      IF(Y(M).LE.D)GO TO 70
L.0028      Y(M)=D
L.0029      GO TO 90
L.0030 70     K=K+1
L.0031      IF(K.GE.5)GO TO 110
L.0032      GO TO 20
L.0033 65     H(1)=Z(1)+V*V/2./G+Y(1)
L.0034      U(1)=V
L.0035      GO TO 100
L.0036 90     H(M)=HF
L.0037      U(M)=V
L.0038 100    CONTINUE
L.0039      WRITE(S,110)Q,D,C,G,Y(1),E
L.0040 110    FORMAT(' PIPE BACKWATER',6F7.3)
L.0041      WRITE(S,115)
L.0042 115    FORMAT(' SECTION INTVL+ TURB.C BEDLEV WDEPTH WATSURF VELOCITY')
L.0043      DC 150 M=1,N
L.0044 150    WRITE(S,120)M,X(M),T(M),Z(M),Y(M),W(M),U(M)
L.0045 120    FORMAT(7F9.3)
L.0046      STOP
L.0047      END

```

FORTRAN Computer program for backwatering in circular pipes

CHAPTER 11

DRAINAGE NETWORK OPTIMIZATION

INTRODUCTION

One of the engineer's objectives is to produce a satisfactory design such that the overall cost is a minimum. This is referred to as cost optimization.

Economic pressures and the advent of electronic computers have both prompted many researchers to search for cost saving design methods. The conventional design approach is based on a set of design standards and criteria, with no alternatives compared. Optimization is in practice often approximated by investigating a series of designs. The designer selects on the basis of his best professional judgement a system layout and a combination of pipe diameters and grades. He will design and estimate the cost of a number of alternative layout-size-slope combinations. Using conventional design methods it is not feasible to design and evaluate more than a few alternatives. Computers enable a larger number of alternatives to be evaluated, but an optimal solution is not guaranteed.

An ideal optimization model would produce the minimum cost design by simultaneously varying both network layout and pipe design. This has been attempted by a number of researchers. The fact remains, however, that no method is in existence for obtaining such an overall solution. There are, however, design methods which produce the minimum cost design for a system of a given network layout. i.e. if flows are known, the system becomes 'linear' and can be optimized directly.

THE VARIABLES

A drainage network for any area can be anything from a single pipe to an interconnected tree-like network, (Fig.11.1) depending on the size and configuration of the catchment, and the relative economic advantages and cost of the drainage system.

The designer of a drainage network must decide the following:

- Layout plan of the township or catchment
- Location of drains within the permitted zones
- Spacing of inlets
- Location of manholes at bends and changes in grade and diameter.

Capacity of inlets
 Size of surface gulleys
 Diameters of subsurface drains
 Gradient of drains
 Design details of inlets, manholes, drops, branches, etc.

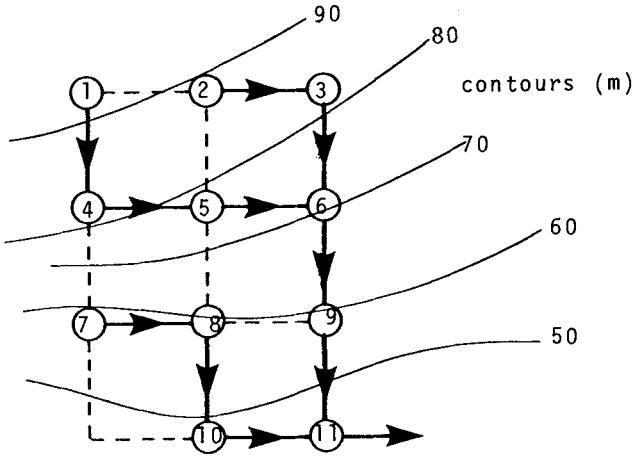


Fig. 11.1 Drainage network with alternative layouts

Many of the design parameters can be selected independently, thus eliminating the number of alternatives. Drain layouts are frequently fixed by the road layout. Drains are located on the downhill side of roads or on both sides. Surface gully sizes depend on the design flows and drain inlet spacing. Assuming each inlet accepts the total gully flow at that point, the problem is to select gully capacity and subsurface drain capacity for least total cost. The problem is analogous to the Highway Drainage System discussed later in the chapter. In the case of systems with fixed layouts and consequently known design flows, the problem is to determine the optimum combination of diameter and grade for each link pipe (Fig. 11.2)

Costs of drainage components depend primarily on the flow in the conduit. This may be a variable if the network layout and inlet spacing are to be determined, or may be fixed if the layout and inlet spacing are pre-selected. Drainage layouts are more often than not of the tree-like layout, with the flow in each successive branch being cumulative. There is often no problem in selecting between alternative routes as

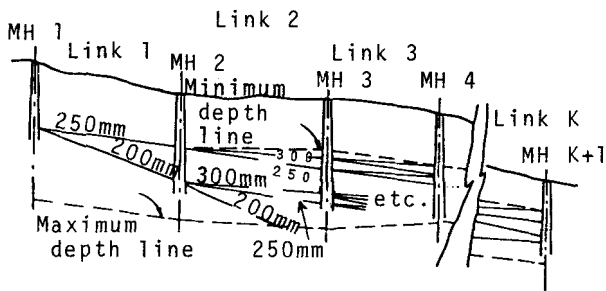


Fig.11.2 Drain profile showing solution procedure for dynamic programming optimization.

the most economic layout is usually with drains flowing downhill. This is unlike water supply networks where the flow in each pipe and the layout have many possibilities (one of which is optimal) (Stephenson, 1979). Cost of drains depend on:

- Diameter
- Depth, which influences excavation and pipe wall thickness
- Manhole spacing
- Locality, such as in built-up or open ground

Dajani and Hasit (1974) and Merritt and Bogan (1973) present some typical cost data, but this is highly dependent on locality and cost escalation, so the engineer is urged to compile cost data to suit the particular project.

There will be a number of practical constraints on the system to be optimized. These include:

- Permissible pipe depth depending on ground conditions
- Available pipe strengths
- Minimum grade or velocity to avoid deposition
- Maximum grade to avoid erosion or noxious gas release
- Minimum diameter for access purposes
- Maximum surcharge
- Pipe diameters must be those commercially available
- Gradient and diameter must be consistent with flow rate and friction factor
- Invert levels of successive pipes at intersections (manholes) must be equal or represent a fall

Head losses at inlets and branches must be allowed for.

Whereas there are many mathematical methods for the selection of a least-cost system, some of the methods cannot accommodate all the constraints rigorously. In particular linear programming and geometric programming require continuous variables. Mixed integer programming can be used to select discrete values, as can dynamic programming.

Implicit in all the following techniques is that the runoff rate into each drain or per unit area of catchment, is known. This means the design storm intensity and consequently the design storm duration, have been estimated beforehand. Flow rates are used as input to the analyses. The computations subsequently produce pipe sizes and grades, and correspondingly, flow velocities. In order to determine the concentration time of the system, the flow should strictly be routed through the system. This may indicate a new concentration time which should equal design storm duration, upon which it would be necessary to revise precipitation rates in the light of the known intensity - duration relationships. In fact the situation is even more complicated as the concentration time and consequently design storm vary down the system. A design approach allowing all possible degrees of freedom would be prohibitively costly though.

It is also assumed the pipes will run full at design flow in the following sections. This could be varied though to suit the design standards.

DYNAMIC PROGRAMMING FOR OPTIMIZING COMPOUND PIPES

One of the simplest optimization techniques, and indeed one which can normally be used without recourse to computers, is dynamic programming, e.g. Meredith, 1971; Walsh and Brown, 1973; Kally, 1980. It is in fact only a systematic way of selecting an optimum program from a series of events and does not involve any mathematics. The technique may be used to select the most economic diameters of a compound pipe which may vary in diameter along the length depending on grades and flows. For instance consider a drain fed by a number of inlets. The diameter of the main is increased as input takes place along the line. The problem is to select the most economic diameter for each section of pipe.

A simple example demonstrates the use of the technique; Consider the line in Fig. 11.3. Two inlets feed stormwater to a drain, and the hydraulic gradient, assuming pipes flow full, should not be above ground level. The elevations of each point and the lengths of each

TABLE 11.1 Dynamic programming optimization of a compound drain

I

HEAD AT B	HYDR. GRAD.	DIA. mm	COST
H_B	h_{A-B}	D_{A-B}	COST \$
13	.009	250	50000
18	.0065	260	52000
23	.004	300	60000

II

$H_C = 7$				12			17		
H_B	h_{B-C}	D_{B-C}	COST \$	h_{B-C}	D_{B-C}	COST \$	h_{B-C}	D_{B-C}	COST \$
13	.006	310	31000 50000 <u>81000</u>	.001	430	43000 50000 <u>93000</u>	-	-	-
18	.011	270	27000 52000 <u>79000*</u>	.006	310	31000 52000 <u>83000*</u>	.001	430	43000 52000 <u>95000</u>
23	.016	250	25000 60000 <u>85000</u>	.011	270	27000 60000 <u>85000</u>	.006	310	31000 60000 <u>91000*</u>

III

H_C	h_{C-D}	D_{C-D}	COST \$
7	.001	430	86000 79000 <u>165000</u>
12	.0035	340	68000 83000 <u>151000*</u>
17	.006	310	62000 91000 <u>153000</u>

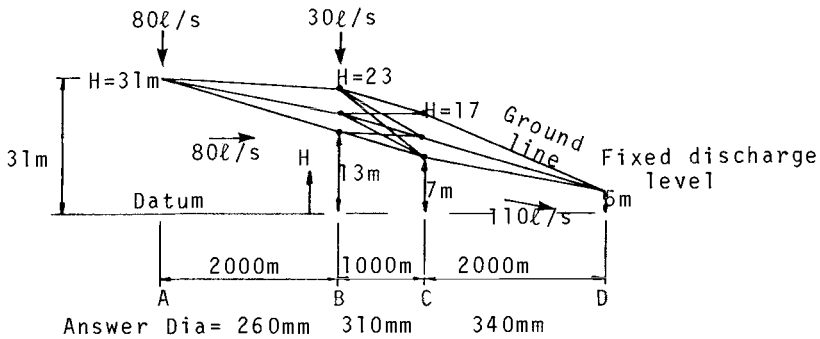


Fig. 11.3 Profile of drainpipe optimized by dynamic programming

section of pipe are indicated. The cost of pipe is 10 cents per millimetre per metre length of pipe. The analysis will be started at the upstream end of the pipe (point A). The most economic arrangement will be with minimum cover (zero say), at point A. The depth at point B may be anything between 13 m and 31 m above the datum, but to simplify the analysis, we will only consider three possible heads with 5 m increments between them at points B and C.

The diameter of the pipe between A and B, corresponding to each of the three allowed heads may be determined from a head loss chart and is indicated in Table 11.1 (I) along with the corresponding cost.

The number of possible hydraulic grade lines between B and C is $3 \times 3 = 9$, but one of these is an adverse gradient so may be disregarded. In Table 11.1 (II) a set of figures is presented for each possible hydraulic grade line between B and C. Thus, if $H_B = 23$ and $H_C = 17$ m then the hydraulic gradient from B to C is 0.006 and the diameter required for a flow of 110 ℓ/s is 310 mm. The cost of this pipeline would be $0.1 \times 310 \times 1\,000 = \$31\,000$. Now to this cost must be added the cost of the pipe between A and B, in this case \$60 000 (from Table 11.1 (I)). For each possible head H_C there is one minimum total cost of pipe between A and C, marked with an asterisk. It is this cost and the corresponding diameters only which need be recalled when proceeding to the next section of pipe. In this example, the next section between C and D is the last and there is only one possible head at D, namely the discharge level.

In Table 11.1 (III) the hydraulic gradients and corresponding diameters and costs for Section C - D are indicated. To the costs of pipe for this section are added the costs of the optimum pipe arrange-

ment up to C. This is done for each possible level at C, and the least total cost selected from Table 11.1 (III). Thus the minimum possible total cost is \$151 000 and the most economic diameters are 260, 310 and 340 mm for Sections A-B, B-C and C-D respectively. It may be desirable to keep pipes to standard diameters in which case the nearest larger standard diameter could be selected for each section as the calculations proceed or each length could be made up of two sections; one with the next larger standard diameter and one with the next smaller standard diameter, but with the same total head loss as the theoretical result. Alternatively one could select head intervals to result in real diameters.

It will be seen that the technique of dynamic programming reduces the number of possibilities to be considered by selecting the least-cost arrangement at each step. Of course many more sections of pipe could be considered and the accuracy would be increased by considering more possible heads at each section. A computer may prove useful if many possibilities are to be considered, and there are standard dynamic programming programs available.

OTHER APPLICATIONS

Dynamic programming has been used to select an optimum layout of a drainage system and the optimum sizes and profiles. It becomes cumbersome to optimize both the layout and profiles especially as the number of legs increases since large computer capacity is required. The required core storage in the computer increases with the square of the number of variables for this type of optimization.

Merrit and Bogan (1973) presented a program for selection of least-cost profile and pipe sizes for a sewer (or drainage system). It was necessary to select a layout and inlet positions on a plan manually. Restraints on pipe minimum and maximum depths and feasible pipe diameters were possible. The program commences analysis at the top of each leg, knowing the flow, and works down each stage between inlets, considering various pipe diameters and grades. Each successive leg depends on the invert level of the end of the previous upstream pipe or pipes. Drops and pumping stations are permitted.

Two computer models were developed - one essentially for sewers where the maximum and minimum velocities could be specified and depths of flow were indicated by the program, and one model which assumed the pipes to flow full but not surcharged. The latter model is the one applicable to storm water drains.

Argaman et al (1973) developed a mathematical model, also using dynamic programming, to optimize the layout of drains or sewers. A number of arbitrary layouts are set out, and flow directions pre-defined. The computer then selects which routes can be omitted, and calculates diameters and grades. In order to reduce the number of variables the pipes were assumed to be parallel to the ground surface, (alternatively the pipe grades could be pre-selected). The depth of flow could be limited, and a range of flows could be considered. This proves useful for sewers where low flow conditions are important. Steady-state flow was assumed and head losses at junctions were neglected. A cost function (a polynomial) is used to estimate pipe costs for different diameters and depths. If the permissible pipe diameters were pre-chosen, the optimized cost of the system as indicated by the program was found to be considerably higher than the cost of a system where any diameter was possible (i.e. a continuous function was used).

Dajani and Hasit (1974) used linear programming to select pipe sizes in a drainage layout. It was necessary to linearize the Manning head-loss equation which somewhat limits the validity of the program. Linear programming produces a least-cost system only if all relationships between variables are linear i.e. of the form $x = ay + b$.

Separable programming methods were employed by Dajani et al (1972) while discrete dynamic programming was used by Mays and Yen (1975) to optimize a fixed layout. Other approaches are illustrated by Barlow (1972) and Davis (1975).

HIGHWAY DRAINAGE SYSTEMS

The layout and spacing of drains along a dual lane carriageway can be difficult to design. The system comprises carriageway drains, cross drains, carrier drains and outfalls such as in Fig. 11.4. Runoff from

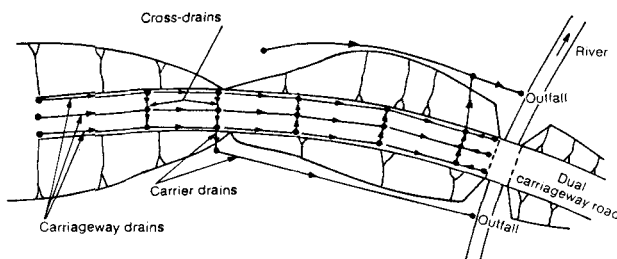


Fig. 11.4 Typical highway storm drainage network.

the pavement enters the carriageway drains in the median strips and centre island via gulleys or through filter media. Cross drains connect the carriageway drains at intervals which in turn lead to the carrier drains. Manholes are placed at maximum intervals, at intersections, changes in pipe diameter, alignment or slope for clearing and maintenance.

In the case of highway drains, the scope of layouts is limited and to some extent repetitive. If the layout is fixed, the only variables are drain size and slope, and previously discussed methods are possible.

The additional variables which were studied by Templeman and Walters (1979) are manhole spacing and cross-drain positions. They proposed a dynamic programming solution. The following section describes their method of solution.

It is assumed that the inflow to each pipe is known. Thus the relationship between concentration time and design storm intensity is not considered. Fig. 11.5 shows the system for which manhole spacing, pipe diameter and grades are to be optimized.

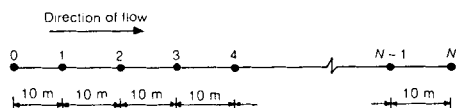


Fig. 11.5 Possible manhole locations along a pipe run.

A drain between fixed manholes 0 and M (flowing towards N) is to have an unknown number of manholes at intervals which are multiples of 10 m for simplicity. Only 3 possible diameters will be considered.

Now if a manhole is positioned at 1 it can be connected to manhole 0 only by the link 0-1. Let there be 10 discrete depths at each manhole and three pipe diameters for each pipe. Although the top pipe depth would normally be fixed at a minimum, let there be 10 possible depths at 0. Then there will be a set of 10 minimum costs for link 0-1 as for the dynamic programming selection of pipe diameters and grades. If a manhole is positioned at 2, it can be connected directly to 0 by link 0-2 or via 1 with link 0-1-2. For each discrete depth at 2, a minimum cost design can be found by selecting the cheaper of 0-2 or 0-1-2. Only the additional cost of link 1-2 need be calculated now as minimum cost designs for link 0-1 have already been calculated and stored.

For a manhole at position 3, possible links are 0-3, 0-1-3, 0-2-3 and 0-1-2-3. For each discrete depth at 3 only one of these four configurations must produce a least cost design. As cheapest designs

for drains up to 2 have already been calculated only the costs of 0-3, 1-3 and 2-3 need be calculated at this stage.

The process is continued to manhole N. At this point 30 cheapest designs will be available (one for each of ten pipe depths and three pipe sizes at N). The lowest cost must be selected. Now it remains to trace back through the system to locate manhole locations and pipe sizes and slopes for the optimal system for any given depth constraint.

The method can readily be extended to include positioning of cross drains (or inlets in the case of a combination of gulleys and drains) (Fig. 11.6). Again it must be assumed that the intensity of runoff is known i.e. is not a function of flow path.

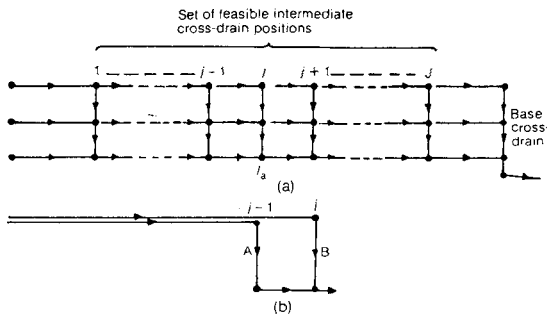


Fig. 11.6 (a) Discrete positions of cross drains
(b) Flow paths with assumed equal travel times

The procedure is similar to that above. One proceeds down the drain making decisions at each possible cross-drain position. The design and cost downstream of any position depend on the depth at that position and decisions downstream. Assuming the costs up to the previous position have been determined, then for each cross-drain position links from all feasible upstream positions must be determined. The cheapest solution resulting in any discrete depth at the manhole in question is stored. When the end manhole is reached, select the cheapest alternative and trace back to determine the least cost system.

REFERENCES

- Argaman, Y., Shamir, U. and Spivak, E., Oct., 1973. Design of optimal sewerage systems. Proc. ASCE, 99 (EE5), 10050, p 703-716.
 Barlow, J.F., June, 1972. Cost optimization of pipe sewerage systems. Proc. ICE, London, Part 2, 7460. p57-64.
 Dajani, J.S., Gemmill, R.S. and Morlok, E.K., Dec. 1972, Optimal design of urban wastewater collection systems. Proc. ASCE, 98 (SA 6), 9414, p853-867.

- Dajani, J.S. and Hasit, Y., April, 1974. Capital cost minimization of drainage networks. Proc. ASCE, 100 (EE2), 10448. p325-337.
- Davis, D.W., Aug. 1975. Optimal sizing of urban flood-control systems. Proc. ASCE, 101 (HY8), p1077-1092.
- Kally, E., Dec. 1980. Automatic computerized computation of an optimal sewerage network by dynamic programming, Water Services, 84 (1018) p723-725.
- Mays, L.W. and Yen, B.C., 1975. Optimal cost design of branched sewer systems. Water Resources Research, 2(1), p37-47.
- Meredith, D.D., 1971, Dynamic programming with case study on the planning and design of urban water facilities. Treatise on Urban Water Systems. Colorado State University, Fort Collins, p599-652.
- Merritt, L.B., and Bogan, R.H., Feb. 1973. Computer based optimal design of sewer systems. Proc. ASCE, 99, EE1, 9578. p35-53.
- Stephenson, D., 1979. Pipeline Design for Water Engineers, Elsevier, Amsterdam, 226pp.
- Templeman, A.B. and Walters, G.A., Sept. 1979. Optimal design of storm-water drainage networks for roads. Proc. ICE, London, Part 2, 67, 8262, p573-587.
- Walsh, S. and Brown, L.C., June, 1973. Least cost method for sewer design. Proc. ASCE, 99 (EE3), 9796, p333-345.

CHAPTER 12

OPEN CHANNELS

STORMWATER CHANNELS

Open stormwater channels provide an economical and sometimes essential alternative to closed drains. It is a fact that open channels offer less frictional resistance due to the smaller wetted perimeter, and consequently require smaller cross sections, than closed conduits. The factor of safety against flooding of a channel is generally greater than that of a pipeline. A small water level rise in a channel increases the discharge capacity disproportionately (discharge is nearly proportional to flow depth to the power of $5/3$) whereas in the case of a pipe, the discharge capacity is only proportional to the square root of the head. Thus rapid overflowing of manholes associated with closed drains and excess surface flow will result with storms more severe than the design storm.

An open channel can be an obstruction or hazard, especially if wide or deep. Open channels may also require regular maintenance due to deposits or vegetation growth. On the other hand, grassed and contoured channels can be attractive. Shallow channels can form natural barriers between traffic and pedestrians without being dangerous.

Above all, channels are more economical than closed drains. Where land is not too valuable and space is allowed at planning stage, channels may be the solution. Away from built up areas, natural water-courses are generally employed, although protective works may be necessary to avoid erosion.

FLOW CLASSIFICATION

The depth of flow in a channel will depend on the flow rate, slope, cross sectional shape and boundary roughness. Even then the water depth and velocity can change in time and space. This may be due to variation in flow rate, non-equilibrium or variations in channel alignment and cross section. Thus the assumption of steady, uniform flow consistent with the discharge rate is often incorrect and depth requirements may be greater than indicated by uniform flow theory.

Methods for the analysis of different types of flow vary with the circumstances. In some cases energy principles are employed and in other

cases momentum principles. Analysis of many conditions, such as rapidly varied flow, transient flow and transitions, are beyond the scope of this text. Many dynamic systems require numerical methods of analysis. Here computer models may be of use or else the engineer may write his own program. There are many good textbooks on basic hydraulics of open channels (Chow, 1959; Henderson, 1966), and equally suitable texts on numerical methods of analysis (Abbott, 1979 ; Connor and Brebbia, 1976). The basic methods of flow analysis sketched here are intended for straightforward conduits. As well as listing some standard classifications of flow profiles, the reader is told of the more complicated problems should he need to consider them in designing a drainage system. Some more common types of flow such as gradually varied flow receive more coverage, and the engineer should be able to select a channel shape and cross sectional area. Although erosion is mentioned, channel linings are generally the construction engineer's problem, and as such are not covered here. The flow classifications following are illustrated in Figure 12.1.

Uniform flow is that which does not vary in space i.e. depth is constant along a regular channel.

Steady flow does not vary in time.

One-dimensional flow means that flow is in one direction (along the axis of the conduit) and lateral and vertical velocity components are neglected. Rapid changes in depth are therefore excluded from the methods of analysis based on this assumption. It is also assumed that the mean velocity across a section is representative and that pressure is represented by the hydrostatic head.

Unsteady flow implies that flow velocity and depth vary significantly in time. This may be in the form of transient surges or waves. If flow is not uniform, it varies (along the conduit). It may be *gradually varied* such as in a backwater caused by a weir, or *rapidly varied* such as at a hydraulic jump.

Uniform flow implies an equilibrium along the channel. Thus if there is a slope to the channel the energy consumed by friction should equal the fall in bed level along any length. The steeper the channel, the greater should be the energy gradient. In order to increase the energy loss for any channel section and discharge rate, velocity must increase and depth must decrease. The equilibrium depth is referred to as the *normal depth*.

If the Froude number $F_r = v/\sqrt{gy}$ (12.1)
for a rectangular channel is greater than unity the flow is said to be *supercritical*. The water velocity is then faster than the speed of

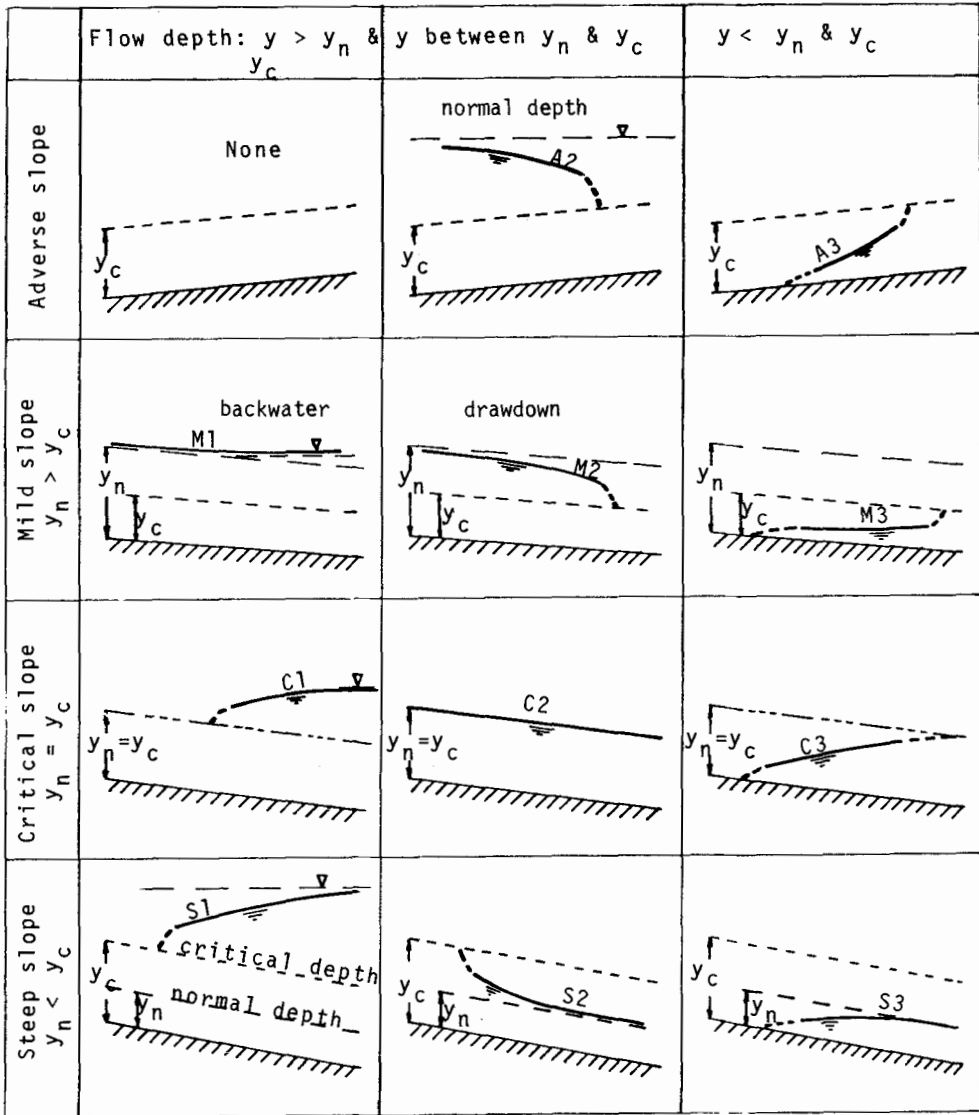


Fig. 12.1 Classification of gradually varied flow profiles.

a wave and violent fluctuations in water level are possible at changes in alignment. *Subcritical flow* occurs if the Froude member is less than unity. The minimum energy per unit weight of water occurs when the depth is *critical*. This depth may be determined by differentiating the equation for energy:

$$E = z + p/w + v^2/2g \tag{12.2}$$

where z is the elevation of the bed above any selected datum
 p is the pressure, equal to $\bar{y}w$ in open channels, \bar{y} is the depth to the centroid, w is the unit weight of water, v is the flow velocity and g is gravitational acceleration.

Specific energy is generally taken as the unit energy without the z term i.e. it is a local property dependent on the depth of flow only, provided discharge and cross section are specified.

Differentiating this expression with respect to velocity v and setting this equal to zero, one can prove that the critical depth y_c is given by the expression

$$y_c = \sqrt[3]{q^2/g} \quad (12.3)$$

The specific momentum of flow in a rectangular channel is

$$M = \frac{q^2}{gy} + \frac{y^2}{2} \quad (12.4)$$

where q is the discharge per unit width.

In situations where there is a rapid change in depth, there may be a considerable energy loss, but there must be momentum balance across the interface for equilibrium. This happens when supercritical flow meets subcritical flow; a discontinuity is formed, termed a hydraulic jump. Employing this concept, one can prove that the relationship between the sequent depths before and after a hydraulic jump is

$$\frac{y_2}{y_1} = \frac{1}{2} (\sqrt{1 + 8 F_{r1}^2} - 1) \quad (12.5)$$

The location of a hydraulic jump can usually only be determined by backwater calculations, proceeding upstream from a known control section for the subcritical flow and downstream for the supercritical flow. The jump will occur where the sequent depth to either assumed depth is equal to the depth computed from the other end. Allowance can be made for the length of the jump.

The energy loss at a jump is determined by comparing the specific energy on each side. In fact although there are two alternate depths (termed conjugate depths) for any energy level, there is only one possible specific energy for any water depth.

The relationship between depth and specific energy is illustrated in general form in Fig. 12.2b and a similar relationship for the momentum function in Fig. 12.2c.

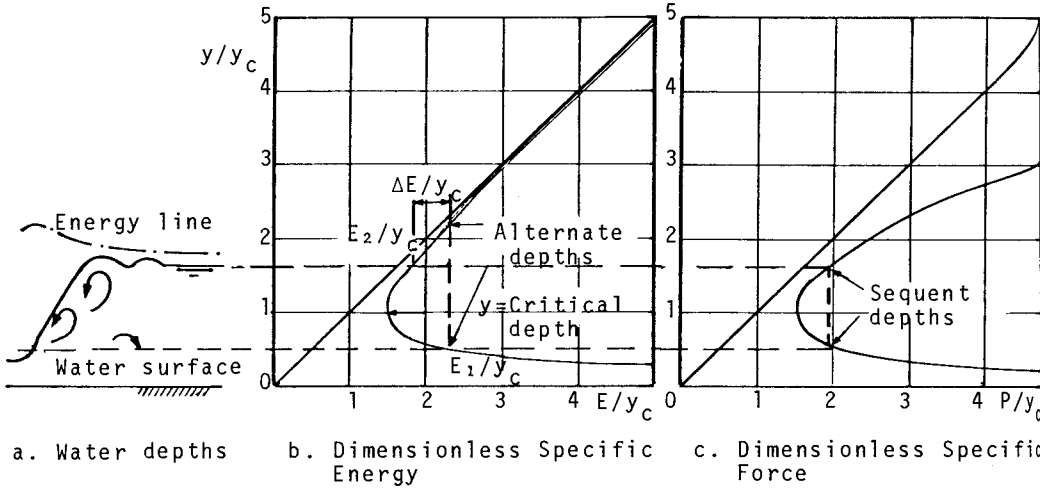


Fig. 12.2 Specific energy and momentum function for rectangular channels.

CHANNEL CROSS SECTION

The cross sectional shape of a channel should be designed for optimum flow. The bigger the wetted perimeter the higher the friction drag. Conversely the smaller the cross-sectional area the more economical the section as a general rule. The maximum discharge is obtained if the wetted perimeter is minimized. Alternatively the minimum cross-sectional area is obtained for any flow if the wetted perimeter is minimized. The geometric properties of various channel shapes are summarized in Fig. 12.3.

The so-called optimum shape or one with minimum area for a given hydraulic radius is a semi-circle. This may be proved by differentiation of the expression for wetted perimeter. Construction procedures are orientated to trapezoidal shapes and the optimum trapezoidal shape is one into which fits a semi-circle, i.e. the base width is $b = 2y/\sqrt{3}$ (Fig. 12.4b). The associated side slopes are 60° to the horizontal which is impractical for construction purposes. The sides are normally cut at slopes as steep as 1/1 for shallow channels in hard clay, reducing for looser non-cohesive materials. 1/1.5 is representative for

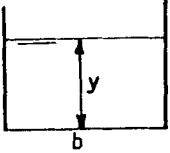
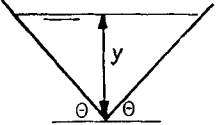
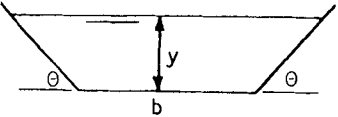
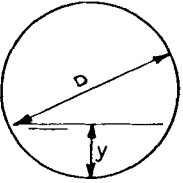
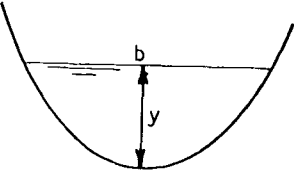
<u>Shape</u>	<u>Area A</u>	<u>Wetted Perimeter P</u>	
	Rectangular	by	$b+2y$
	Triangular	$y^2/\tan\theta$	$2y/\sin\theta$
	Trapezoidal	$by+y^2/\tan\theta$	$b+2y/\sin\theta$
	Circular	$\frac{D^2}{4} \arccos(1-2\frac{y}{D})$ $-(D-2y)\sqrt{yD-y^2}$	$D \arccos(1-2y/D)$
	Parabolic	$\frac{2}{3}by$	$\frac{b}{2} [\sqrt{1+16y^2/b^2} +$ $(b/4y) \ln(4y/b +$ $\sqrt{1+16y^2/b^2})]$ $(\approx b+8y^2/3b \text{ for } y \leq b/4)$

Fig. 12.3 Geometric properties of channel sections

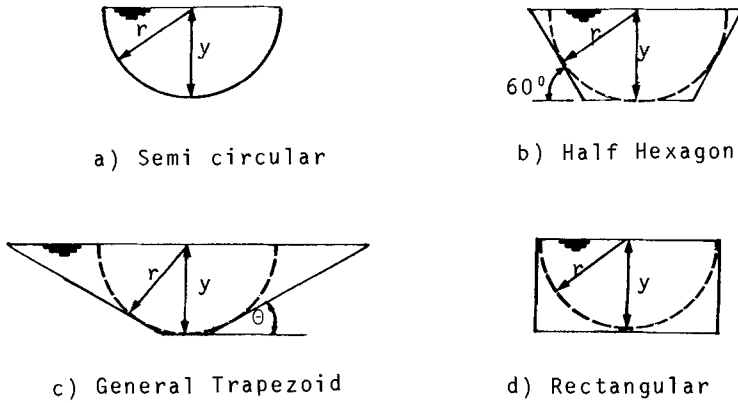


Fig. 12.4 Channel shape for minimum hydraulic radius

firm sandy clay, and for loose fine sand or peaty soils the side slope may be as flat as 1/3 (vertical/horizontal). Flattening of the side slope also facilitates construction and results in a more stable lining.

In built-up zones, the value of land may force the construction of deep rectangular channels. The sides may have to be supported with concrete retaining walls or gabions.

Variable roughness

Where a channel has a variable roughness across the section, the mean velocity may still be computed without actually subdividing the section. For example, if a channel has m sub-sections with wetted perimeters P_j and Manning roughness N_j , then the equivalent average roughness may be calculated as follows:

$$N = \left[\frac{P_1 N_1^{1.5} + P_2 N_2^{1.5} + \dots + P_m N_m^{1.5}}{P} \right]^{2/3} \tag{12.6}$$

The equation is based on the assumption that the same mean velocity exists for each section, and is derived by equating total cross-sectional area to the sum of areas of the individual elements assuming the velocity in each section is similar. The technique is thus only really applicable to a channel with one main section and no flood plains. It is not applicable to composite section channels.

In a similar manner, it is possible to obtain a weighted mean velocity distribution coefficient. Chow (1959) derives formulae for the average velocity distribution coefficients in terms of the coefficients

and flow rates for each section. The analysis does not offer a solution for calculating the total discharge or water level.

Composite section

The velocity distribution across a complex section such as in Fig. 12.5 is far from uniform. The velocity is dependent on the ratio of hydraulic radius to roughness, and is consequently much lower in shallow sections such as over flood plains. The highest velocities and core of the flow will occur in the deepest section.

As an approximation, the hydraulic radius and cross-sectional area could be calculated for the section as a whole provided the side sections were small compared with the main section. It is more accurate to treat the section as comprising a number of separate sections with a common water level.

In the case of a simple cross section, the flow rate is related to the cross section as follows

$$Q = A S^{5/3} / NP^{2/3} \quad (\text{S.I. units}) \quad (12.7)$$

where S is the slope and N is the Manning roughness coefficient. The cross sectional area is A and wetted perimeter is P .

For more complex shapes the area should be subdivided as shown in Fig. 12.5. The cross-sectional area A_j and wetted perimeter P_j of each section should be computed in terms of the depth y_j . If the water surface level is known then the flow velocity and discharge may be computed for each section using Equ. 12.7. The total discharge is then the sum of the individual discharges.

Where the discharge is known and the water surface elevation is to be computed, then the solution is more difficult. An equation expressing depth in terms of discharge for each section is established. The cross-sectional area A_j and wetted perimeter P_j are expressed in terms of water depth y_j for each section. Since the water surface level is the same for each section, all depths may be expressed in terms of that in the deepest section. This depth is preferred as flow is most sensitive to this value. Thus for each section

$$\begin{aligned} Q_j &= A_j^{5/3} S^{1/2} / N_j P_j^{2/3} \\ &= f_j(y_j) S^{1/2} / N_j \end{aligned} \quad (12.8)$$

where the function $f_j(y_j) = A_j^{5/3} / P_j^{2/3}$ depends on the geometry and depth. Thus for a trapezoidal section it is $(by + y^2/\tan \theta)^{5/3} / (b + 2y/\sin \theta)^{2/3}$. Now $Q = \Sigma Q_j$ and $f_j(y_j) = f(y_m)$ where Q is the total flow and y_m the

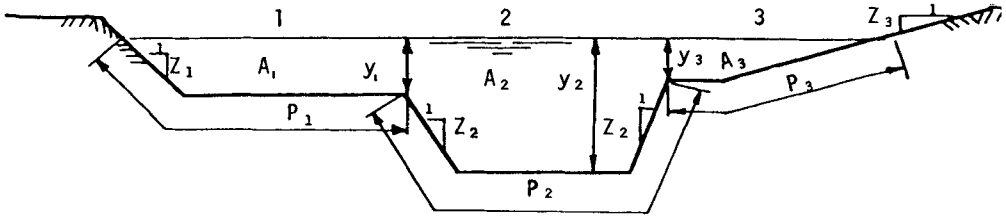


Fig. 12.5 Composite cross section channel

depth at the deepest section.

$$\text{Thus } Q = S^{1/2} \sum_j f(y_m) N_j \quad (12.9)$$

This equation will be a lengthy algebraic expression which may be solved by trial and error for y_m if Q is known, or graphically by plotting Q versus y_m or by successive approximation.

It is unlikely that individual sections will have the same velocity and consequently the same energy line. The total head for the section as a whole may be taken to be $\alpha v_m^2/2g$ above the water surface where v_m is the mean velocity Q/A and the energy coefficient α is defined by the equation

$$\alpha = \frac{\sum v_j^3 A_j}{v_m^3 \sum A_j} \quad (12.10)$$

NON-UNIFORM FLOW COMPUTATION IN IRREGULAR CHANNELS

Calculation of normal depth in a uniformly flowing channel can be performed directly employing a resistance equation such as that of Manning. Where compound sections are involved, the computational procedure may be complicated but a unique solution is still achievable.

In the case of artificial channels, such as may be constructed for storm water collection and discharge, the channel may possess a constant cross-sectional shape and grade. In such cases the assumption of uniform flow is applicable and flow depth determination is simple.

Where the discharge rate, cross-sectional shape and bed gradient vary along the channel, the assumption of uniform flow at any section will lead to errors. Conditions at one section may influence those at an upstream section. For example if there is an obstruction or reservoir, it will back up water for a considerable distance upstream. A free fall or chute may draw down the water surface and this effect would also manifest itself upstream. This is assuming subcritical flow. (Froude

number F less than unity, or water depth greater than critical depth). In the case of supercritical flow (F greater than 1) upstream conditions would control.

The engineer often needs to know the water depths along a channel in order to decide on a channel depth with suitable freeboard, if it is an artificial channel, or for flood plain and catchment management in the case of natural channels. Where overtopping of the banks or even high water levels in the river are likely to occur frequently, the engineer faces a choice of one or both of two solutions. The channel may be improved by widening, deepening, steepening or smoothing. The resulting water levels will subside. Alternatively with appropriate catchment management such as the provision of detention or retention storage, soakaways, indirect runoff routing and avoidance of smooth planes, the discharge can be controlled.

If all else fails the authorities may have to restrict building or other development within the flood plain.

In any case, the engineer has to determine flood limits for various conditions, in order for planning to proceed. The degree of sophistication with which the engineer must compute flood levels will depend on the complexity of the channel.

A variety of methods is available and described in many text books on open channel flow (e.g. Henderson, 1966, Chow, 1959). The following list describes the limits of applicability of techniques of increasing sophistication. The problem is assumed to be the determination of water surface elevation, all other variables such as channel geometry and discharge rate being known. Other situations may arise where flow depth or channel properties have to be determined, in which case a trial and error approach may be employed.

In practical problems involving river channels, cross sections are surveyed at pre-defined positions. The computations should thus proceed from one section to the next, proceeding upstream in the case of subcritical flow in order to determine water levels at each section. The method of computation most favoured in practice is the standard step method (e.g. Henderson, 1966). It is a numerical method, suited to digital computer programming, (e.g. Weiss and Midgley, 1978).

The method is based on the calculation of energy level at successive cross sections by two means. The water surface elevation is initially estimated and refined after comparing the two energy levels so resulting. One energy head is simply the assumed water level plus velocity head which we will refer to as H_e . The other is derived by adding to the energy level at the downstream section, the friction head loss

TABLE 12.1 Summary of methods of computation of water levels in open channel

METHOD	EQUATIONS	LIMITATIONS
1. Direct solution of resistance equation for flow depth	$Q = \frac{S^{1/2}}{N} \frac{A^{5/3}}{P^{2/3}}$ $A, P = f(y)$	Uniform flow in regular channel
2. Direct step method. Computation of distance at which flow depth reaches a pre-selected figure.	$\Delta x = \frac{\Delta E}{S_o - S_f}$ $S_f = (NQ)^2 P^{4/3} A^{10/3}$ $E = y + Q^2/2gA^2$ $= \Delta y(1-F^2)$ $F^2 = Q^2 B/gA^3$	Uniform channels, i.e. constant cross section and slope.
3. Direct integration	$\frac{dy}{dx} = S_o \frac{1-(y_o/y)^n}{1-(y_c/y)^m}$	Uniform channels
Bresse (m=n=3) :	$S_o x = y - y_o [1 - (y_c/y_o)^3] \phi$	Require tabulations of Bresse's function ϕ
Bakhmeteff :	$S_o \frac{dx}{dy} = 1 - (1-\beta) / [1 - (y/y_o)^n]$ $\beta = F^2 S_o / S_f$	
Chow :	$x = \frac{y_o}{S_o} [u - F(u, n) + \frac{(y_c)^m}{y_o} \frac{J}{n} F(v, J)] + A_1$	Require Tabulations

TABLE 12.1 continued

METHOD	EQUATIONS	LIMITATIONS
4. Graphical Methods: Depth from distance	Plot E, U against y, where $U = E - \frac{1}{2}S_f \Delta x$	
Ezra	$h_2 + F(h_2) = h_1 + F(h_1)$ $F(h) = \frac{\alpha v^2}{2g} + S_f \frac{\Delta x}{2}$	
Grimm	$Q = K S_w^{1/2}$	Requires only stage-discharge relationships, but inaccurate.
Escoffier	$\Delta h = \frac{S_{f1} + S_{f2}}{2} \Delta x$	
5. Standard Step Methods	$H_{2e} = y_2 + z_2 + \frac{v_2^2}{2g}$	Trial and error method speeded by
Single channels	$H_{2f} = H_1 + (S_{f1} + S_{f2}) \Delta x / 2$	$\Delta y_2 = \frac{H_{2f} - H_{2e}}{1 - \alpha F_2^2 + \frac{3S_{f2} \Delta x}{2R_2}}$
Compound sections	$H_2 = y_2 + z_2 + \frac{\alpha v_2^2}{2g}$ $\alpha = \frac{(\sum A_i)^2 (K_i^3)}{(\sum K_i^3) \sum (A_i^2)}, \quad K = \frac{AR^{2/3}}{N}$	At bridges $\frac{\Delta y}{y_3} = K F_3^2 (K + 5F_3^2 - .6)(r + 15r^4)$ K = 0.9 to 1.25, r = pier width/ span ratio

determined from the mean friction gradient at the two sections, and any eddy losses which may occur. We thus obtain H_f . Successive estimates of water surface level, or stage, may be determined from the following approximation: We require to eliminate the difference between H_e and H_f where

$$H_{2e} = z_2 + y_2 + \frac{\alpha v_2^2}{2g} \quad (12.11)$$

$$\text{and } H_{2f} = H_1 + \Delta x (S_{f1} + S_{f2})/2 \quad (12.12)$$

where subscript 1 refers to the previous (downstream) section and 2 to the present section. α is the velocity coefficient

$$\alpha = \Sigma(v_i^3 A_i) / v_m^3 \Sigma A_i \quad (12.13)$$

which may be nearly unity for simple sections.

$$\text{Thus if } \Delta H = H_e - H_f \quad (12.14)$$

$$\text{then } \frac{dH}{dy} = \frac{d}{dy} \left(y_2 + \frac{\alpha v_2^2}{2g} - \Delta x S_{f2} / 2 \right) \quad (12.15)$$

$$= 1 - \frac{Q^2 B}{g A^3} - \frac{\Delta x}{2} \frac{dS_f}{dy_2} \quad (12.16)$$

$$\doteq 1 - \alpha F_2^2 + \frac{3 S_{f2} \Delta x}{2 R_2} \quad (12.17)$$

$$\therefore \Delta y_2 = \frac{H_{2f} - H_{2e}}{1 - \alpha F_2^2 + \frac{3 S_{f2} \Delta x}{2 R_2}} \quad (12.18)$$

Thus the second approximation to y is obtained by adding Δy_2 to the original estimate. It is seldom necessary to make more than one such correction unless the water surface slopes steeply.

Where there are eddy losses in addition to friction losses, e.g. due to a bend or expansion in section, there will be an additional head loss $K_t \frac{\alpha v^2}{2g}$ (12.19)

This should be added to the friction loss in computing H_f . Similarly losses at bridges and culverts should be added as explained later. Thus, the loss due to bridge pier contractions may be estimated from Yarnell's equation

$$\frac{\Delta y}{y_3} = K_C F_3^2 (K_C + 5F_3^2 - 0.6) (r + 15r^4) \quad (12.20)$$

where y_3 is the downstream depth, Δy is the increase in depth through the bridge, F is the Froude number, $F^2 = Q^2 B / g A^3$, and r is the total pier width to span ratio. K_C is a contraction coefficient which varies

from 0.9 for rounded pier fronts to 1.25 for square fronted piers.

With compound sections the assumption of a uniform velocity across the section may not be satisfactory. In such cases the cross section must be divided and treated as follows.

$$\text{Define } K = \frac{A}{N} R^{2/3} \quad (\text{S.I. units}) \quad (12.21)$$

$$\text{Then } Q = K S_f^{1/2} \quad (12.22)$$

Equating friction slope S_f for each subsection of the river,

$$\frac{v_1 A_1}{K_1} = \frac{Q_1}{K_1} = \frac{Q_2}{K_2} = \dots = \frac{\Sigma Q_i}{\Sigma K_i} = \frac{v_m \Sigma A_i}{\Sigma K_i} \quad (12.23)$$

where subscript m refers to the mean and i to the subsections.

$$\text{Now } \alpha = \frac{\Sigma (v_i^3 A_i)}{v_m^3 \Sigma A_i} \quad (12.24)$$

$$= \Sigma \left(\frac{K_i^3}{A_i^2} \right) \frac{(\Sigma A_i)^2}{(\Sigma K_i)^3} \quad (12.25)$$

An example (Table 12.2) demonstrates the application of the techniques to determine the water surface profile along the channel configuration illustrated in Fig. 12.6. The columns are almost self explanatory. The computations for each successive section start with an initial assumption for water surface level (except for the first, downstream, section which must have water surface level defined). If the energy levels H_e and H_f do not correspond after performing the computations for any column, the assumed water surface level is revised by the amount in the last column, and the computations are repeated. If there is reasonable agreement, the mean H is inserted in the last column and this is the value to use for subsequent sections.

UNSTEADY FLOW

If discharge rate or flow depth vary at any point in time, the flow is said to be unsteady. In many cases of slowly changing flow the steady state equations of motion are still applicable. The steady-state friction equation and discharge-depth relationships are assumed to apply. Thus accelerations in time and space are neglected. Many flood routing techniques are based on this premise. In particular the kinematic equations were so derived. The only allowance for the dynamic condition was in the continuity equation. It is rarely the drainage engineer needs to adopt more sophisticated methods of analysis.

Situations where the dynamic forces are important are in the case of

TABLE 12.2 Example - backwater analysis of river by standard step method. See Fig. 12.6

(1)	(2)	(3)	(4)	(5)	(6)	(7)	(8)	(9)	(10)	(11)	(12)	(13)	(14)	(15)	(16)
River chain. m	River stage m	River area A m ²	P m	R m	$K = \frac{AR^{2/3}}{N}$	$K^3/A^2 \times 10^6$	$\alpha = \frac{(\sum A)^2}{(\sum K)^3}$	$v_m = \left(\frac{K^3}{A^2}\right) m/s$	$\frac{\alpha v_m^2}{2g}$	H_e m	$S_f = \left(\frac{Q}{\sum K}\right)^2 \times 10^{-3}$	$S_{f, mean} \times 10^{-3}$	$h_f = S_f \Delta x$	H_f	$\pm \Delta y$ or H_m
0	8.50	264	49	5.39	27060	284	1.00	2.765	0.390	8.890	0.728				
180	9.10	196	33	5.94	21430	256									
		38	20	1.90	1940	5									
		<u>234</u>	<u>53</u>	<u>7.84</u>	<u>23370</u>	<u>261</u>	1.12	3.12	0.556	9.656	0.976	0.852	0.153	9.043	-0.7
	8.40	178	31	5.74	19030	217									
		26	17	1.53	1150	2									
		<u>204</u>	<u>48</u>	<u>7.27</u>	<u>20180</u>	<u>219</u>	1.11	3.58	0.725	9.125	1.31	1.018	0.183	9.073	9.10
340	8.4	77	19	4.05	6530	47									
		31	21	1.48	1340	3									
		<u>108</u>	<u>40</u>	<u>5.53</u>	<u>7870</u>	<u>50</u>	1.20	6.76	2.800	11.20	8.60	4.96	0.793	11.29	11.25
570	10.7	345	53	6.51	40117	542	1.00	2.12	0.228	10.93	0.33	4.47	1.028	12.27	+1.13
	11.8	437	60	7.28	54610	853	1.00	1.67	0.142	11.94	0.18	4.39	1.010	12.26	12.10
	11.95														
	Through bridge				$\Delta y = 10.9 \times 1.0 \times 0.057(1.0 + 5 \times 0.057 - 0.6)(.34 + 15 \times .34^4) = 0.23$										
					: $H_e = 11.95 + .23 + .14 = 12.32$										
760	12.1	402	60	6.71	47690	671	1.00	1.82	0.168	12.17	0.23	0.20	0.038	12.36	12.26

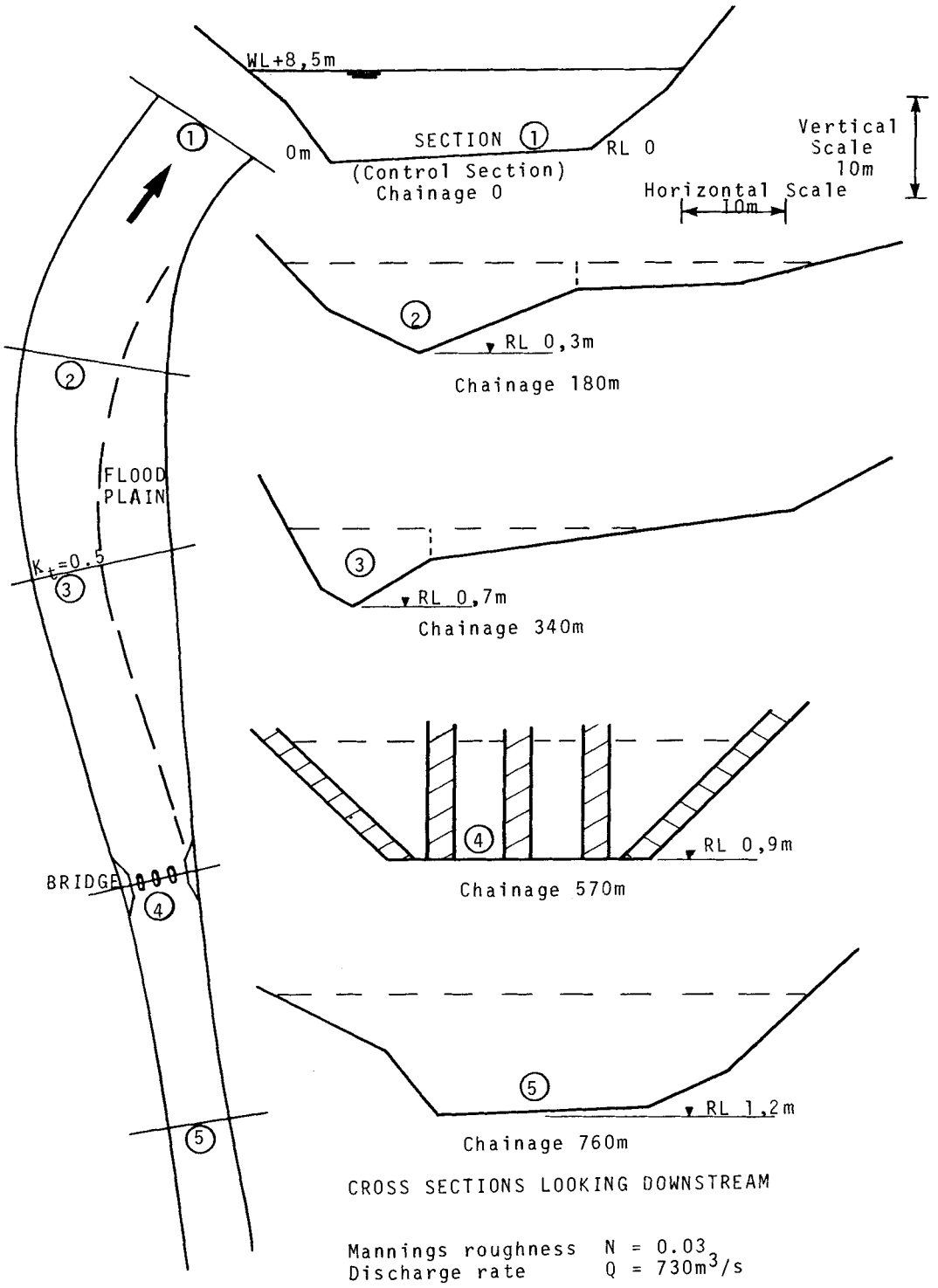


Fig. 12.6 River sections for backwater computation example

surges and waves. A surge can be caused by a rapid variation in discharge rate, such as by closing a sluice gate in a canal. A positive surge will travel upstream at a speed of approximately $c = \sqrt{gy} - v$ (12.26) where y is the water depth, g is gravitational acceleration and v is the initial water velocity. Methods of analysing systems subject to changes in flow are presented by Pickford (1969) and others.

Waves are more complicated to predict and analyse than surges. This is because water particle motion in the vertical direction can no longer be neglected. Waves may be caused by the same disturbance that creates a surge. The rapid vertical acceleration at the surge front may cause the water surface to oscillate.

More common, or of greater concern, are waves created by wind action on the surface of the water. Wave height is dependent on the wind speed, the fetch or distance over which the waves build up, and wind speed (e.g. Hasselman, 1976). Freeboards varying from 0.1 to 0.5 metres are often allowed on canals for wave action.

Cross-waves or diagonal standing waves may be caused by sharp bends in the canal, especially if the flow is supercritical. Under supercritical flow conditions transitions should be very carefully designed or even modelled to account for the high velocity head and centrifugal forces.

CHANNEL STABILIZATION

In nature channels and rivers erode or deposit until they reach stable regimes. Bed slope, meanders, cross sectional area, shape and bed form adjust until they are consistent with the discharge, specific energy and sediment load of the stream. The natural shape of channels is altered by constructing bridges, banks and other works.

Urbanization will affect the regime. Flooding will become more severe unless on-site storage is provided. Streams will be confined to improved channels due to the increased cost of flooding. These actions will aggravate the erosion problem.

Replacement of natural streams by lined channels can make the flood problem more severe downstream. The increased hydraulic radius and the smoother perimeter result in higher velocities and faster concentration times. The construction of impermeable concrete or asphalt linings could thus magnify the flow problem.

Rockfill provides an economical alternative lining and can be adequately designed to prevent scour of underlying soils. The roughness of a natural channel may be maintained so that concentration times are

not affected.

The cost of loose rockfill is considerably less than that of concrete or even asphalt. Although a thicker layer may be required for rockfill, especially where graded filters are required, there is a number of added advantages in the use of rockfill:

- (i) Rockfill is more economical per unit volume of lining than most other linings.
- (ii) It is easier to repair if the lining is damaged.
- (iii) It is flexible and consequently does not undergo as much damage as concrete or asphalt due to ground settlement or excessive loads.
- (iv) It is permeable, so that there is no danger of soil backpressure causing spalling of the lining.
- (v) Rockfill is usually readily available, as it is a natural material, and in fact in many cases it is a waste product from excavations.
- (vi) It is aesthetically pleasing, especially gabion walls and reno mattresses. Rockfill blends in with the environment and in fact mellows with age.
- (vii) It is environmentally acceptable since it does not prohibit growth of natural vegetation or exclude fish life.
- (viii) The weight and roughness of rockfill help maintain the stability of banks and the lining itself.
- (x) Well-selected rock will be durable and weather-resistant.

The disadvantages of rockfill can usually be compensated for. It provides a rougher surface than concrete for instance, for the passage of water. Thus channel cross-sectional areas are larger for any discharge rate. In many cases, however, there is excess energy which has to be dissipated and channel friction losses reduce the cost of stilling basins or other artificial energy dissipation devices. Where the channel drops steeply, drops or steps may be constructed of gabions, (Essey and Horner, 1978; Stephenson, 1979).

The rock size and grading should be selected to satisfy the design criteria. Factors which need to be borne in mind are:

- (i) Friction factor or channel roughness
- (ii) Resistance of the channel lining to erosion - on the bed and on the banks
- (iii) Prevention of erosion of the underlying bed material by the use of suitably graded filters.

There is a relationship between the channel roughness and erodibility of the lining. Both criteria depend on rock size. In fact the larger the stone size, the greater the friction factor and the lower the water velocity. The cross sectional area for any specified discharge thus

depends on the lining characteristics and is larger the rougher the lining. Large stones are less liable to erosion though. In fact simultaneous solution of the two criteria is feasible and produces an optimum stone size.

FRICITION LOSSES

The most popular equation for determining the energy gradient due to friction in channels is the Manning equation. This equation applies to the uniform flow of water at normal temperatures, and the relationship is dependent on the roughness of the lining. Manning's equation is

$$v = \frac{K}{N} \left(\frac{A}{P}\right)^{2/3} S^{1/2} \quad (12.27)$$

where $K = 1.0$ in S.I. units and 1.486 in f.p.s. units. (12.28)

v is the mean flow velocity, N is the Manning roughness coefficient, A is the cross sectional area, P is the wetted perimeter and S is the energy gradient.

Manning's equation has two drawbacks: the form of the equation is dependent on the units used, and empirical data is needed to evaluate the roughness, N . The advantage of the equation over the alternative equations of Darcy-Weisbach and Chezy, is that the roughness N is a unique value for any channel and is not dependent on the flow depth.

Strickler took Manning's equation a step towards rationalization by expressing the friction factor in terms of the boundary roughness, which is analogous to the Nikuradse roughness, an absolute measure of protrusion of particles such as stones on the perimeter of the conduit. The Strickler equation is

$$v = 7.7 (R/k)^{1/6} (RSg)^{1/2} \quad (12.29)$$

where R is the hydraulic radius, A/P , and k is a measure of roughness. k may be approximated by median stone size d in channels with loose rocks lying on the bed. In the case of hand-packed rockfill linings, the roughness is less and it may be approximated by nd where n is the porosity (ratio of voids to total volume) of the rockfill. Fortunately the resulting discharge is not particularly sensitive to the value of k , since k is to the power of $1/6$. Acceptable values of roughness k in millimetres and the corresponding Manning roughness N are tabulated in Table 12.3 for straight channels with steady uniform flow.

In the case of stones which vary in size the weighted mean stone size applies.

Near the bed of the channel the velocity will be lower than the mean cross sectional velocity. In the interstices between rocks the energy

TABLE 12.3 : Roughness of channel linings

Surface	Manning's N	Roughness, k (mm)
Reno mattress, grouted	0.016	4
Reno mattress with selected stone hand packed	0.022	40
Reno mattress with quarry stone mechanically placed	0.025	90
Gabions, mechanically filled with quarry stone	0.027	125
Boulder lined	0.03	180

loss gradient will be as in the channel and the corresponding velocity may be calculated from the equation

$$S = \frac{K_f v_v^2}{gd} \quad (12.30)$$

where v_v is the velocity in the rock voids. K_f is a friction factor which is given by the equation

$$K_f = \frac{800\nu}{v_v d} + K_t \quad (12.31)$$

where ν is the kinematic viscosity of the water (about $1.1 \times 10^{-6} \text{m}^2/\text{s}$) and K_t is the turbulent friction factor which depends on stone shape and roughness. K_t varies from 1 for smooth marbles to 4 for sharp angular stone with a mean value of 3 for crushed stone.

A relationship between flow velocity in the channel and in the interstices of the rock may be established for the turbulent flow case. Eliminating S and putting $k = d$ and $R = y$ for a wide channel with one stone layer,

$$v_v/v \doteq 0.075 (d/y)^{2/3} \quad (12.32)$$

Thus if one knows the scour velocity of the underlying bed material (e.g. Table 12.4), the rockfill size d on the bed may be selected to ensure v_v is maintained below the scour figure. Unfortunately the flow depth y is affected by the overlying rock size.

STABILITY OF ROCKFILL LININGS

The lining must be stable under the action of flowing water. The erosive velocity of particles on the perimeter of a channel depends on the bed slope, bank slope, and stone characteristics. An isolated stone will wash away at a lower velocity than rockfill packed into a layer

TABLE 12.4 Scour Velocities according to USBR

Material	Particle Size (mm)	Scour Velocity (m/s)	ft/s
Fine silt	0.01	0.17	0.5
Fine sand	0.1	0.24	0.75
Medium sand	1.0	0.55	1.5
Gravel	10	1.0	3
Pebbles	100	3.0	10

with an even finish. Ravelling of rockfill packed in Reno mattresses will occur at even higher velocities owing to the wire mesh holding down stones against uplift and thus increasing friction. An expression for the stable size of stones on a bed or bank exposed to flowing water may be derived by equating overturning to stabilizing forces (see fig. 12.7).

When the flow is horizontal, parallel to the bank i.e. such as along the banks of a trapezoidal channel, the minimum stable rock size is approximately

$$d = \frac{0.25 v^2}{g(G-1) \cos\theta (\tan^2\phi - \tan^2\theta)^{1/2}} \quad (12.33)$$

ϕ is the angle of friction of the rockfill and G is the relative density or specific gravity. θ is the slope angle from the horizontal.

The values of the constants were evaluated experimentally (Izbash and Khaldre, 1970).

REFERENCES

- Abbott, M.B., 1979. Computational Hydraulics, Pitman, London 324pp
 Chow, V.T., 1959. Open Channel Hydraulics, McGraw Hill, N.Y. 680pp
 Connor, J.J. and Brebbia, C.A., 1976. Finite Element Techniques for Fluid Flow, Newnes-Butterworths, London 310pp
 Essery, I.T.S. and Horner, M.W., 1978. The Hydraulic Design of Stepped Spillways. Report 33, CIRIA, London, 45pp.
 Hasselman, K., 1976. A parametric wave prediction model, J. Phys. Oceanography, 6(2).
 Henderson, F.M., 1966. Open Channel Flow. Macmillan, N.Y. 522pp.
 Izbash, S.V. and Khaldre, Kh.Yu. 1970. Hydraulics of River Channel Closure. Transl. Cairns, G.L., Butterworths, London, 174pp.
 Pickford, J., 1969. Analysis of Surge, Macmillan, London, 203pp
 Stephenson, D., 1979. Rockfill in Hydraulic Engineering, Elsevier, Amsterdam, 215pp.
 Stephenson, D., 1980. Rockfill linings for channels. Proc. Symposium on Watershed Management. ASCE. Div. of Irrig. and Drainage, Boise.

Vanoni, V.A. (Editor), 1975. Sedimentation Engineering, ASCE, N.Y., 745pp.
 Weiss, H.W., and Midgley, D.C., 1978. Suite of mathematical flood plain models. Proc. ASCE, 104, HY3, 13604, p361-376.

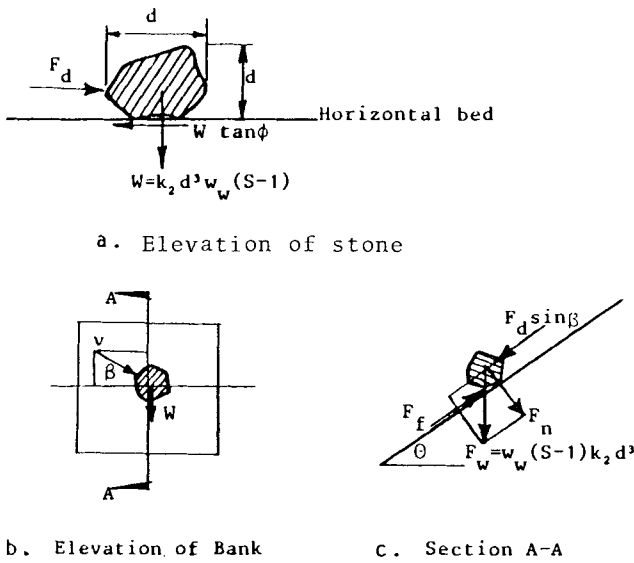


Fig. 12.7 Stability of stone in flowing water

CHAPTER 13

HYDRAULICS OF BRIDGES

INTRODUCTION

Bridges, culverts, causeways and fords are constructed by engineers to get traffic across waterways. A single span over a full channel width would not interfere with the flow in the channel. Economics and structural limitations usually require the bridge length to be less than the water surface width at maximum flow. The restriction on width and opening height often has the effect of backing up the water upstream of the bridge. The backwater thus created floods additional land upstream. A compromise between bridge opening and flooded area can often be achieved on an economic basis.

The problem of flooding over the top of the bridge and the consequent hazard to traffic is difficult to assess, and for this reason engineers correctly tend to be more cautious than pure economic grounds would indicate necessary. Like with the design of culverts, good hydraulic design of the approach to the bridge can minimize the backwater effect. The bridge embankments and piers can be shaped to streamline the flow.

In the case of bridges, the control is usually at the entrance to the channel constriction, so streamlining the approach flow can increase the hydraulic capacity of the opening.

The local reduction in width will cause higher water velocities than average, with the result that the scour regime is affected and local scour in the vicinity of the bridge is likely unless some form of bed and bank protection is employed. (Laursen, 1962; Kindsvater, 1957).

Beyond the constriction, the flow expands again to the full cross section of the channel. The flow expands after the constriction at a rate of 5° to 6° from the centre line on each side. There is dead water on the downstream side of the embankments, and even some circulation which dissipates energy. The energy loss through the constriction is a function of the velocity head difference in the constriction and downstream. The downstream water level, in the case of subcritical flow, is controlled further downstream. It may be normal level if there is a long uniform channel downstream. Fig. 13.1 shows the flow pattern between two encroaching embankments.

The U.S. Department of Transport (1978) has conducted considerable research into the hydraulics of flow through bridges. The research took place in the form of model tests and examination of field data. The

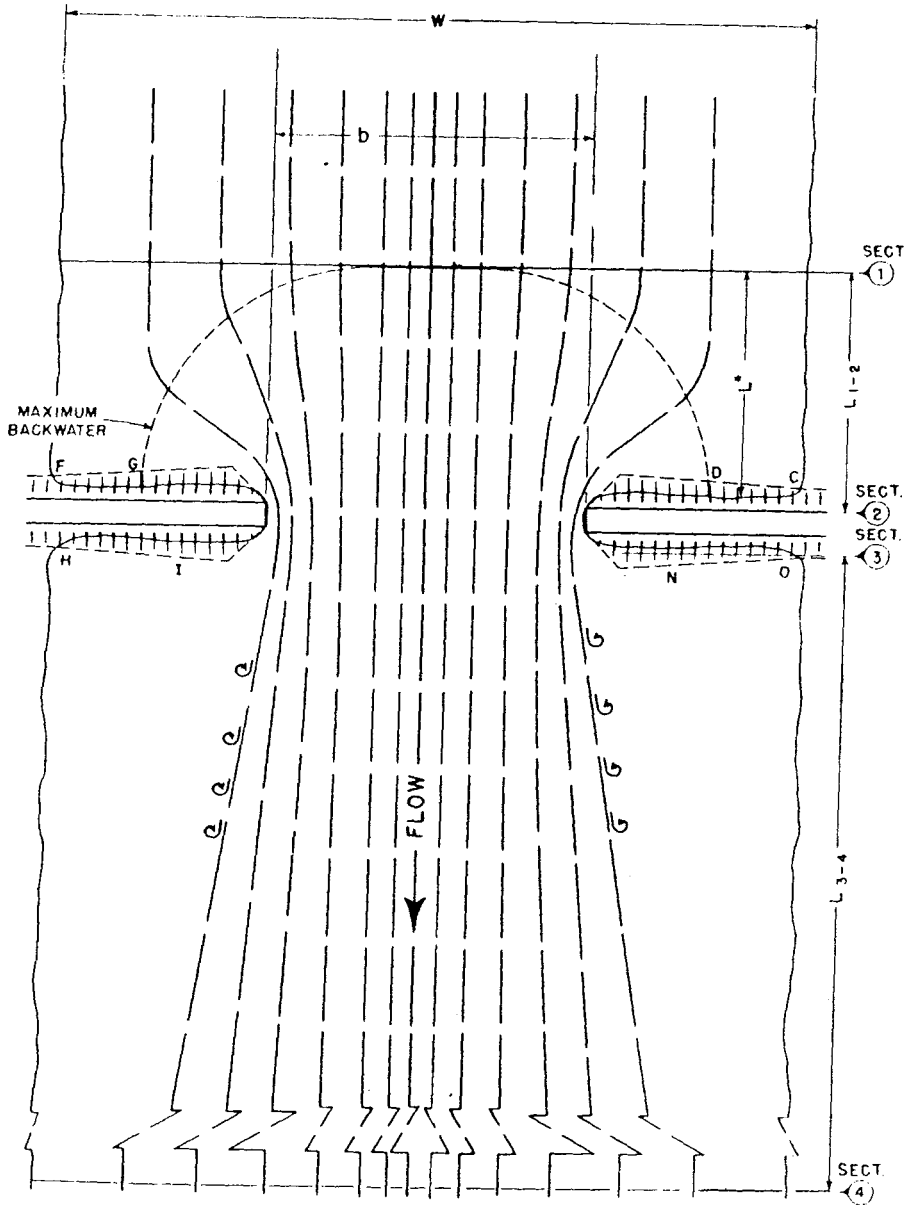


Fig. 13.1 Flow lines for normal bridge crossing

results of the research culminated in the way of design curves for estimation of head losses and water surfaces through bridges. Much of the following is based on their work.

FLOW THROUGH GAP

The velocity through the trapezoidal shape formed by two facing embankments across a river gap obeys a relationship of the form

$$v = C\sqrt{2g(y_1 - y_2)} \tag{13.1}$$

$$\text{and flow } Q = C A_2 \sqrt{2g(y_1 - y_2)} \tag{13.2}$$

where the depth y_1 is upstream of the gap and y_2 is in the gap as indicated in Fig. 13.2. In the case of drowned flow y_2 is taken as the depth downstream or y_3 above bed level in the gap. The value of the coefficient C was found by Naylor (1976) to vary from 0.75 to 1.09 with a mean of 0.9. In the case of supercritical flow through the gap y_2 should be replaced by the critical depth y_c .

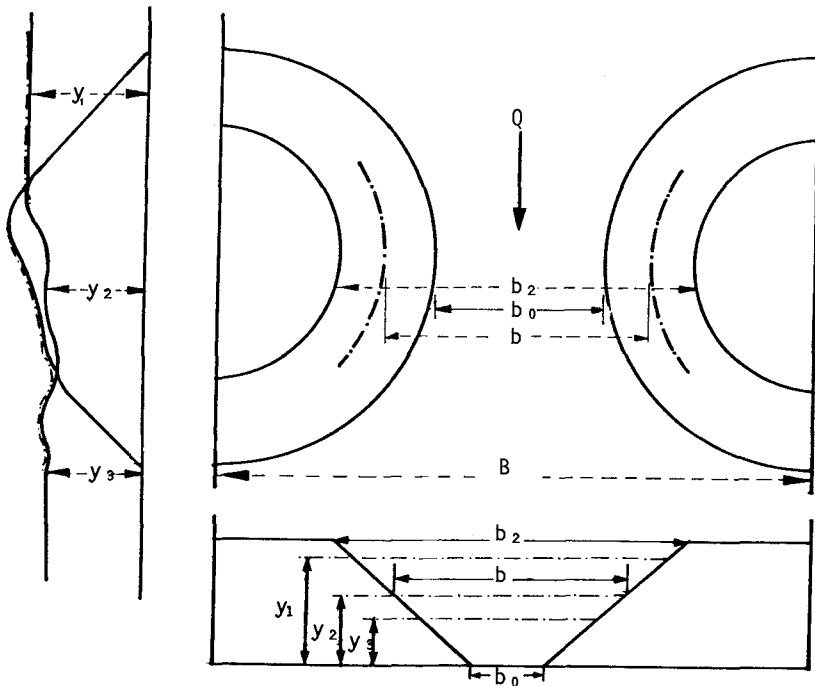


Fig. 13.2 End-tipped embankment

The critical depth in a trapezoidal section is given by

$$y_c/y_1 = 0.4 [1 - 1.5p + \sqrt{1 + 2p + 2.25p^2}] \quad (13.3)$$

where $p = b_0 \tan \theta / 2y_1$ and b_0 is the bottom width at the control section in the gap. The value of y_c/y_1 varies between 0.67 for wide gaps and 0.80 for triangular gaps. Thus for a triangular gap with free flow,

$$Q = 0.26\sqrt{2g} y_1^{5/2} / \tan \theta \quad (13.4)$$

For the triangular shaped gap it is possible to solve for the inside slope for stability of a granular or rockfill surfacing. Eliminating v and y_1 from Eqs. 13.1 and 13.4 and combining with an expression for stable stone size d , we get an expression for θ in terms of d and Q (Stephenson, 1979),

$$\frac{(\tan \theta)^{2/5}}{\cos \theta \sqrt{\tan^2 \phi - \tan^2 \theta}} = \frac{8.25 dg^{1/5} (S-1)}{Q^{2/5}} \quad (13.5)$$

The equation may be solved by trial and error or iterative techniques.

SURFACE PROFILE

There may be three types of flow through a bridge waterway. The corresponding water surface profiles are depicted in Fig. 13.3 and described below:

(I) If the water surface is above critical depth at every section the flow is subcritical (type I flow). This is the condition normally encountered in practice and the calculation procedures following generally refer to this type of flow.

(II) The flow depth may pass through critical in the constriction. Under these conditions the water depth upstream becomes independent of downstream conditions. If the depth passes through critical in the constriction, but not below critical depth downstream, it is referred to as type IIA flow. If the flow depth drops below downstream critical depth, it is referred to as type IIB flow. In this case a hydraulic jump will occur below the constriction if downstream depth is above critical depth.

(III) If normal flow in the channel is supercritical, the water level in the constriction will rise as illustrated in Fig. 13.3. Undulations of the water surface will probably occur and waves may occur upstream and downstream. No backwater in the normal sense will occur.

The backwater effect due to a constriction in a channel may be evaluated from energy considerations. The analysis hereunder is for the case of a straight channel sloping uniformly with the bridge perpendicular

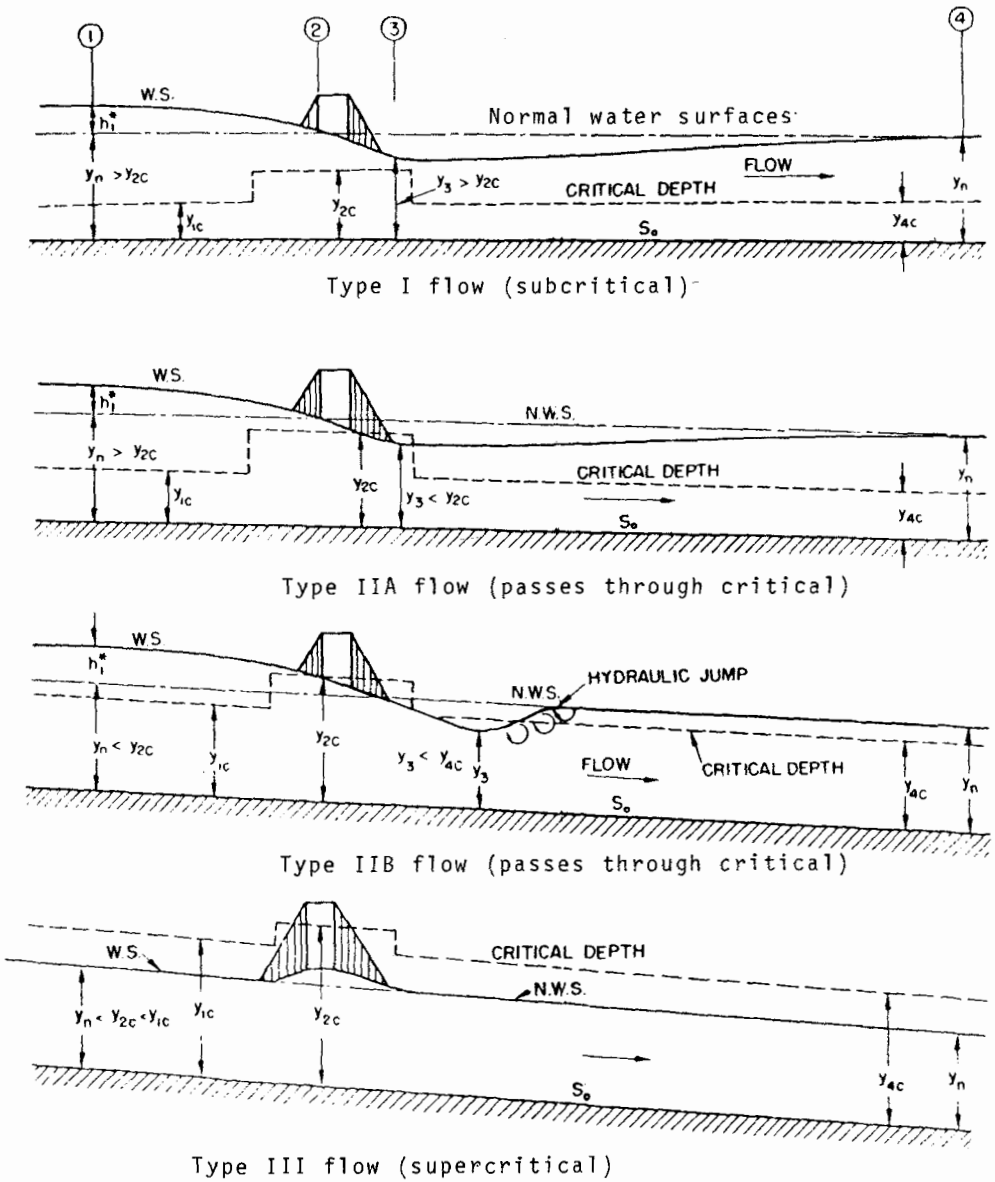


Fig. 13.3 Flow profiles past embankments

to the flow direction. Flow is assumed to be steady and subcritical. Without the bridge constriction energy loss in friction would just balance the drop in bed level between sections 1 and 4 in Fig. 13.3. The additional head loss due to the constriction will be designated h_b and this is assumed to be given by an expression of the form

$$h_b = K \alpha_2 v_2^2 / 2g \quad (13.6)$$

where v_2 is the average velocity at cross section 2 (the constriction) for water level at normal depth for the river section and α is a velocity energy coefficient, yielded by an integration across the section of qv :

$$\alpha = \frac{\sum_i q_i v_i^2}{Q V^2} \quad (13.7)$$

Q is the total discharge and V is the mean velocity across the section

$$\text{Thus } h_b = y_1 - y_4 = \frac{\alpha_4 v_4^2}{2g} - \frac{\alpha_1 v_1^2}{2g} + \frac{K \alpha_2 v_2^2}{2g} \quad (13.8)$$

Now since sections 1 and 4 are essentially the same,

$\alpha_1 = \alpha_4$ and by continuity $A_1 v = A_2 v_2 = A_4 v_4$. Therefore

$$h_b = \frac{K \alpha_2 v_2^2}{2g} + \alpha_1 \left\{ \left(\frac{A_2}{A_4} \right)^2 - \left(\frac{A_2}{A_1} \right)^2 \right\} \frac{V^2}{2g} \quad (13.9)$$

It should be noted that $y_1 - y_4$ is not the difference in water levels; it represents the buildup in water level (or backwater) upstream of the bridge. In addition there will be friction head losses due to normal flow.

The backwater head loss coefficient K_b for flow normal to a symmetrical restriction may be read from Fig. 13.4. Here M is the bridge opening ratio,

$$Q_b / (Q_a + Q_b + Q_c) \quad (13.10)$$

where Q_b is flow which would pass through the same section as the bridge opening without the bridge there (See Fig. 13.1).

Since A_1 is not known until h_b has been determined, it is necessary to estimate h_b initially from

$$h_b = K \alpha_2 v_2^2 / 2g \quad (13.11)$$

The value of A in (13.9) can then be determined.

The backwater head loss is also affected by:

- (i) The number, size, shape and orientation of piers in the constriction.
- (ii) The eccentricity of the bridge in the river section
- (iii) Skewness of the bridge relative to the direction of the river.

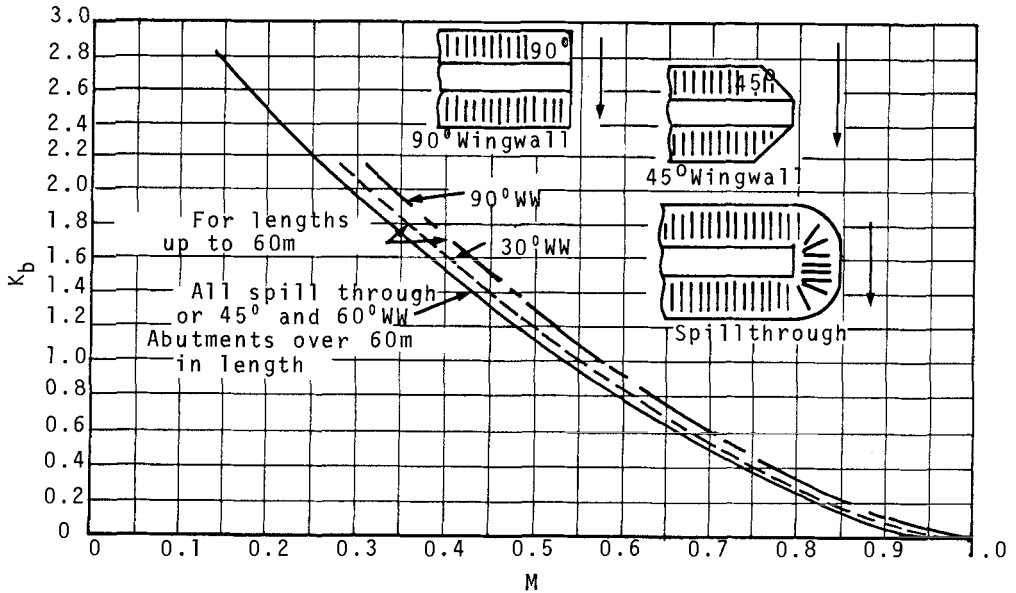


Fig.13.4 Backwater coefficient base curves (subcritical flow)

The influence of these effects on K is given in Figs. 13.5 to 13.7. Thus the K to use should be $K = K_b + \Delta K_p + \Delta K_e + \Delta K_s$ (13.12)

In the case of skew openings, the projected width of opening and not the total width of opening should be employed to determine M .

It should be noted that the results here are based on the assumption of one-dimensional flow. Laursen (1970) indicates that lateral flow can significantly increase the backwater effect.

DROP IN WATER LEVEL

The difference between the water level upstream and downstream of the bridge embankment is not the same as the backwater. The water level in the restriction is difficult to evaluate theoretically and it was investigated by model testing. Fig. 13.8 presents the resulting data. To use the curve, compute the contraction ratio M and read off D_b the differential level ratio where $D_b = h_b / (h_b + h_s)$. Now with the previously computed backwater for a normal crossing, h_b , compute h_s , the drop in level.

$$h_s = h_b \left(\frac{1}{D_b} - 1 \right) \tag{13.13}$$

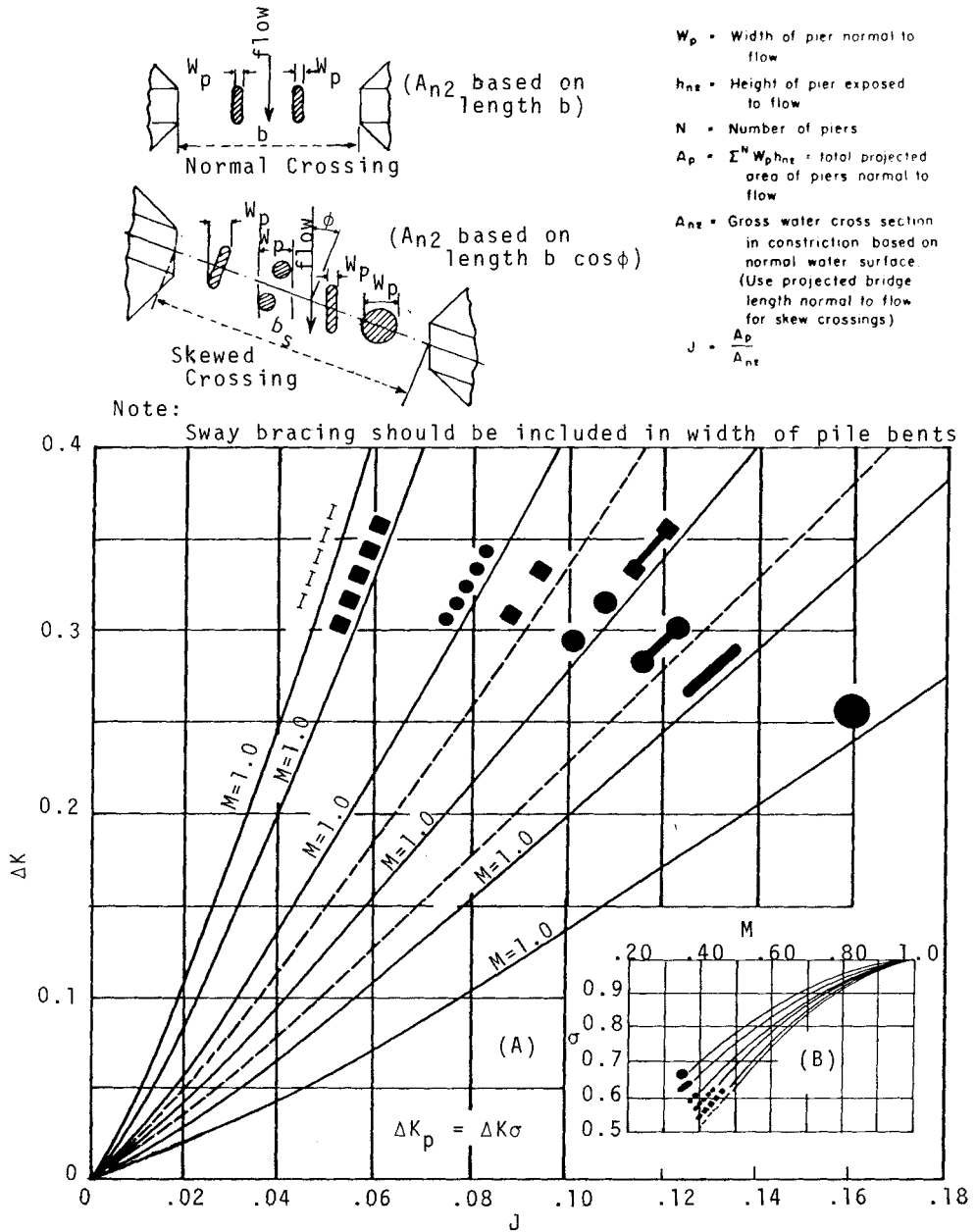


Fig. 13.5 Increment on backwater coefficient for piers

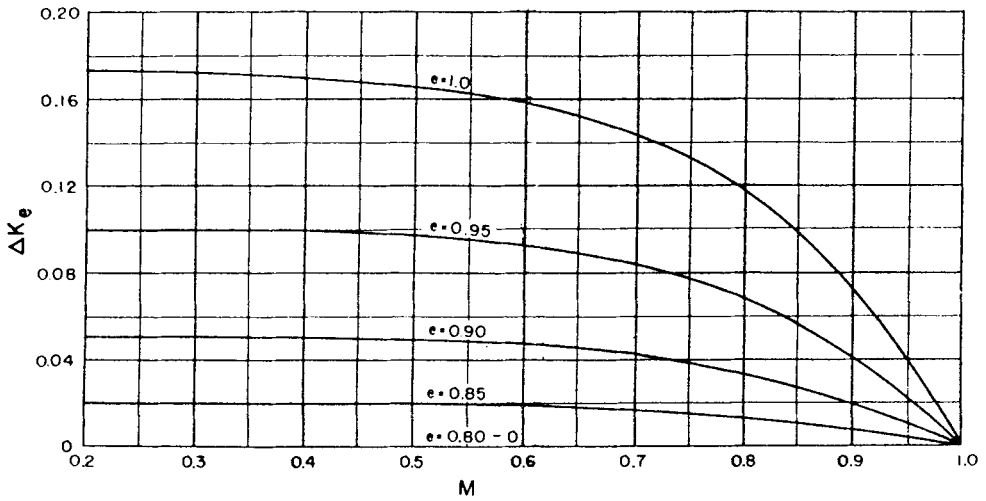
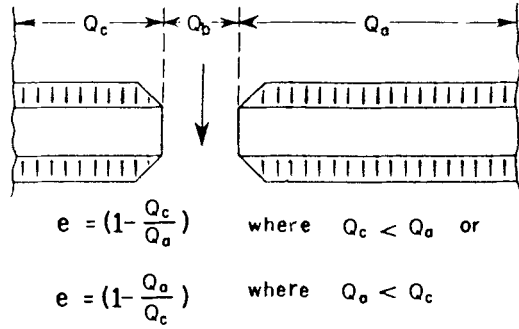


Fig. 13.6 Increment on backwater coefficient for eccentricity

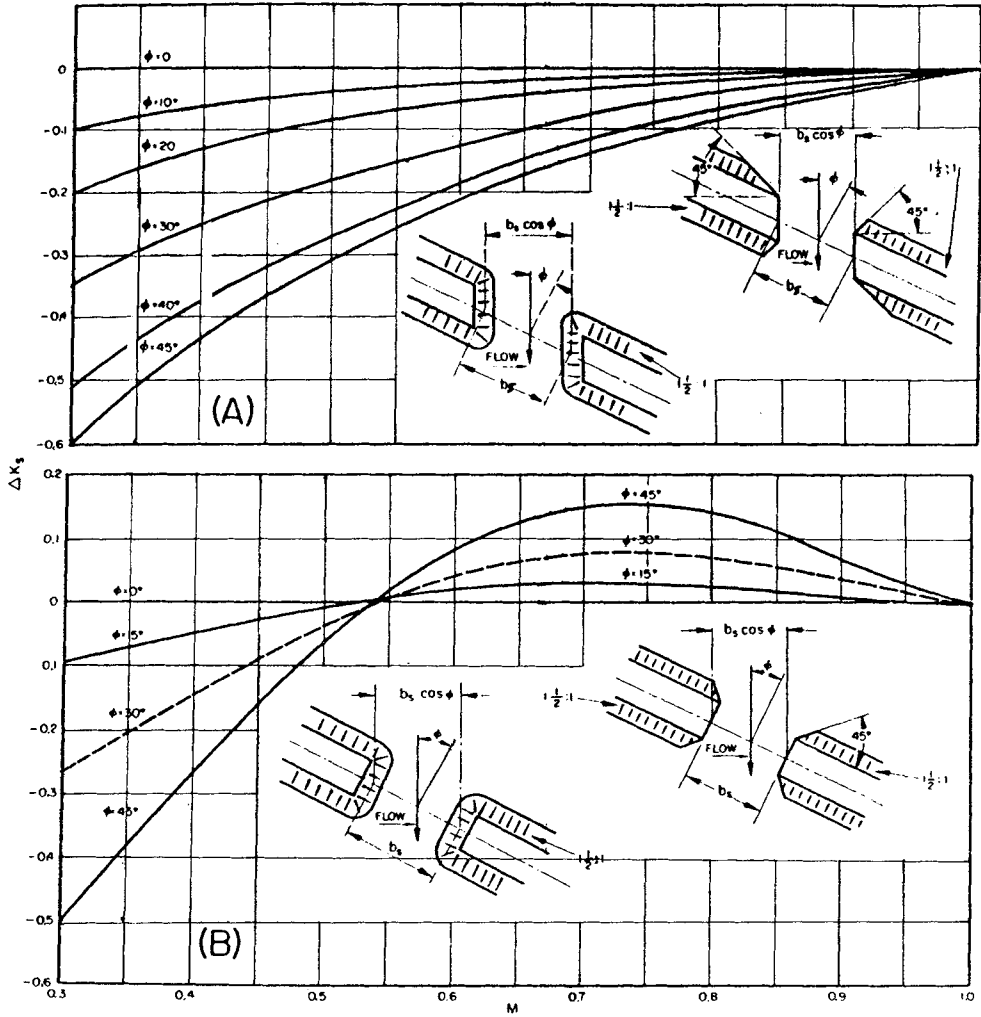


Fig. 13.7 Increment on backwater coefficient for skew

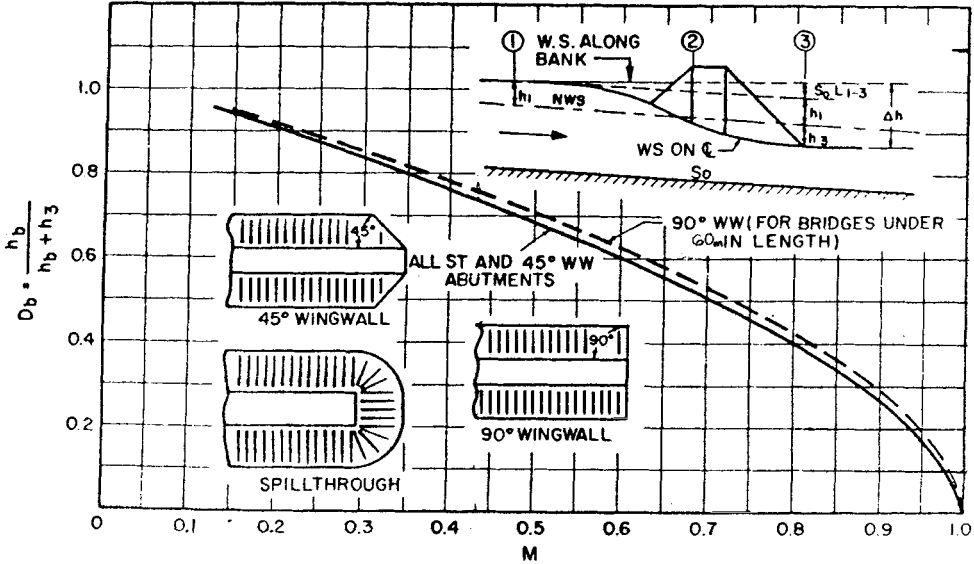


Fig. 13.8 Differential water level ratio base curves

The water level downstream of the constriction is h_3 below normal level. With piers, it was found that although backwater h_b increased, h_3 remained as for a constriction with no piers.

In the case of eccentric or skew crossing one adds the additional backwater Δh_c or h_s to h_b and determines h_3 from

$$h_3 = (h_b + \Delta h_c \text{ or } \Delta h_s) \left(\frac{1}{D_b} - 1 \right) \tag{13.14}$$

where D_b is obtained as before.

Now the total difference in water level across the embankment is

$$\Delta h = h_3 + h_1 + S_0 L_{1-3} \tag{13.15}$$

where h_1 is the total backwater allowing for piers or eccentricity, S is the bed slope and L is the distance from section 1 to 3.

DISTANCE TO MAXIMUM BACKWATER

The distance from the waterline on the upstream face of the embankment to the point of maximum backwater was evaluated and is presented in a tentative chart by the U.S. Department of Transportation (1978).

The distance is of the order of

$$L = 5b \Delta h / \bar{y} \quad (13.16)$$

where b is the width of opening at the waterline, Δh is the drop in water level across the opening and $\bar{y} = A_2/b$ (13.17)

Since Δh is a function of L it is necessary to estimate L first, and then calculate Δh and then revise L .

COMPLEX STRUCTURES

In the case of two bridges in close proximity the backwater effect is not necessarily the sum of the individual effects. The closer the two bridges, the nearer the resulting effect approaches that of one bridge. The backwater was found to increase by 30 to 50% for a distance between two identical bridges varying from three to ten times the embankment width at waterline level in the direction of flow. It would be wise to model the system in a hydraulics laboratory in order to confirm the water levels where complex bridge structures are contemplated.

Where scour of the bed is possible under the bridge (Laursen, 1962) the backwater effect may be reduced due to the reduced velocity through the constriction. Spur dykes (Fig. 13.9) have been found to assist greatly in reducing scour where it is likely to be a problem. Diving currents beside steep banks and around piers have been known to cause extensive damage to foundations.

OBSTRUCTION BY BRIDGE PIERS

Although the approach embankments are generally the major contraction effect on the channel width, piers across the section can also add to the backwater. The obstruction is aggravated by the contraction of flow between the piers.

The backwater effect of piers perpendicular to the flow was investigated in detail by Yarnell (1934) and Lin et al (1957). The parameters employed were the Froude number $F = v/\sqrt{g\bar{y}}$ at the downstream section and the pier width to span ratio R . The research applies to subcritical flow although the depth could also pass through critical beyond the piers. The results may be summarized by the equation

$$\Delta y/y_3 = KF_3^2 (K + 5F_3^2 - 0.6) (R + 15 R^4) \quad (13.18)$$

where K is characterized by the pier shape in accordance with Table 13.1. The figures are for pier length to width ratio of four, and K reduces slightly for longer piers.

especially if air is trapped between girders. In this case the lateral force required to dislodge the bridge deck is reduced since frictional resistance is reduced.

Flow conditions under a submerged bridge are similar to those through a culvert with inlet control. Flow may also occur over the top of the embankment and bridge. This is a case of a broad crested weir.

The depth/discharge relationship over a broad crested weir such as an embankment is more difficult to analyze than for a sharp crest on account of the unknown position at which critical depth occurs, and the problem of evaluating energy losses. The hydraulics of flow over a broad crested weir may be studied using momentum principles and neglecting friction. Equating the net force on the water body between sections 1 and 2 in Fig. 13.10 to change in momentum,

$$wy_1^2/2 - wy_2^2/2 - wh(y_1 - h/2) = (wq/g)(q/y_2 - q/y_1) \quad (13.19)$$

Solving for q , the flow per unit width of crest,

$$q = \sqrt{[y_1^2 - y_2^2 - h(2y_1 - h)] gy_1 y_2 / 2(y_1 - y_2)} \quad (13.20)$$

Chow (1959) indicates that experiments have proved that

$$y_2 \doteq (y_1 - h)/2 \quad (13.21)$$

$$\text{and that } q = 0.612\sqrt{g} \left[\frac{y_1}{y_1 + h} \right]^{\frac{1}{2}} (y_1 - h)^{\frac{3}{2}} \quad (13.22)$$

$$\text{or } q = C\sqrt{g} H^{\frac{3}{2}} \quad (13.23)$$

where $H = y_1 - h$. Over the maximum range of h from zero to y_1 , C could vary from 0.612 to 0.432. From observations it is found to vary from 0.54 for low sill height to 0.47 for a high sill or weir.

The previous theory applied to a weir or sill with the tailwater level above or below the critical depth over the weir. If the tailwater is lowered below the critical depth level, the depth over the sill will fall until it reaches critical depth. At this stage the specific energy of the flowing water, $y + v^2/2g$, is a minimum, and the critical depth is given by

$$y_c = \sqrt[3]{q^2/g} \quad (13.24)$$

When the tailwater drops below the critical depth over the sill it no longer affects the flow conditions over the sill. Actually the critical depth for a free overflow occurs a little way upstream (about $3y_c$) from the crest. The depth at the crest is less than y_c on account of the non-parallel flow. Depth is found for a free drop crest to be $y_c/1.4$, so that the flow in terms of the depth over the crest y_o is

$$q = 1.65\sqrt{g}y_o^{3/2} \quad (13.25)$$

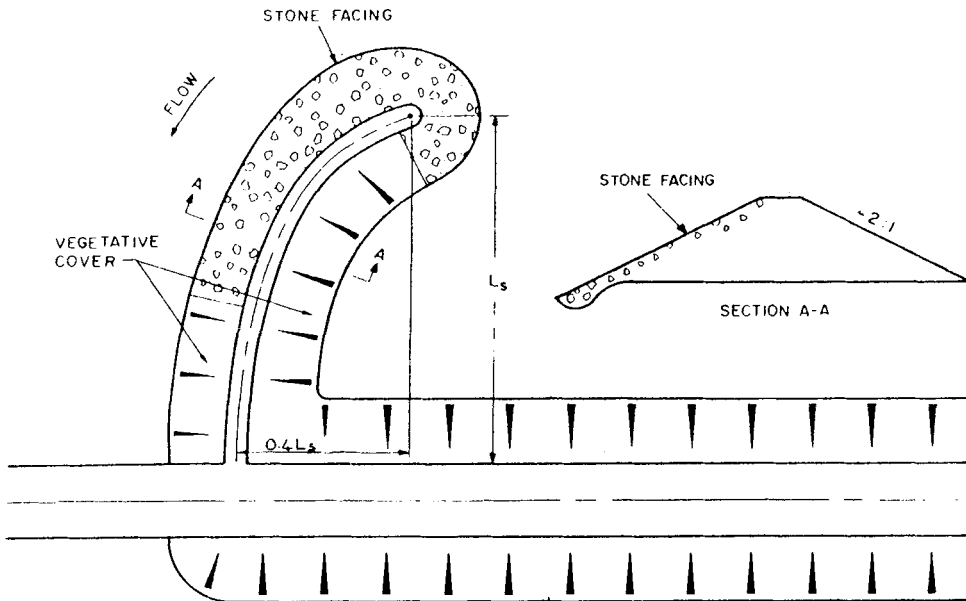


Fig. 13.9 Plan and cross section of spur dyke

TABLE 13.1 Pier Shape Factor K

	K
Semi-circular nose and tail	0.90
Lens-shaped nose and tail	0.90
Twin cylinder pier with connecting diaphragm	0.95
Twin cylinder pier without diaphragm	1.05
90° triangular nose and tail	1.05
Square nose and tail	1.25

INUNDATION OF BRIDGE

If upstream water level rises to above the soffit of the bridge, flow conditions may alter. If the water touches the upstream face, orifice flow may result instead of free flow. Discharge is then proportional to the square root of the head and not the head to the power of $3/2$. In this case the upstream water level rises considerably in order to achieve an increase in discharge when compared with free surface discharge. Inundation of the roadway is highly likely. Other problems also arise if this type of flow occurs. Damage to the superstructure by floating objects is possible. The opening may become blocked more easily by floating debris. There may occur uplift under the superstructure.

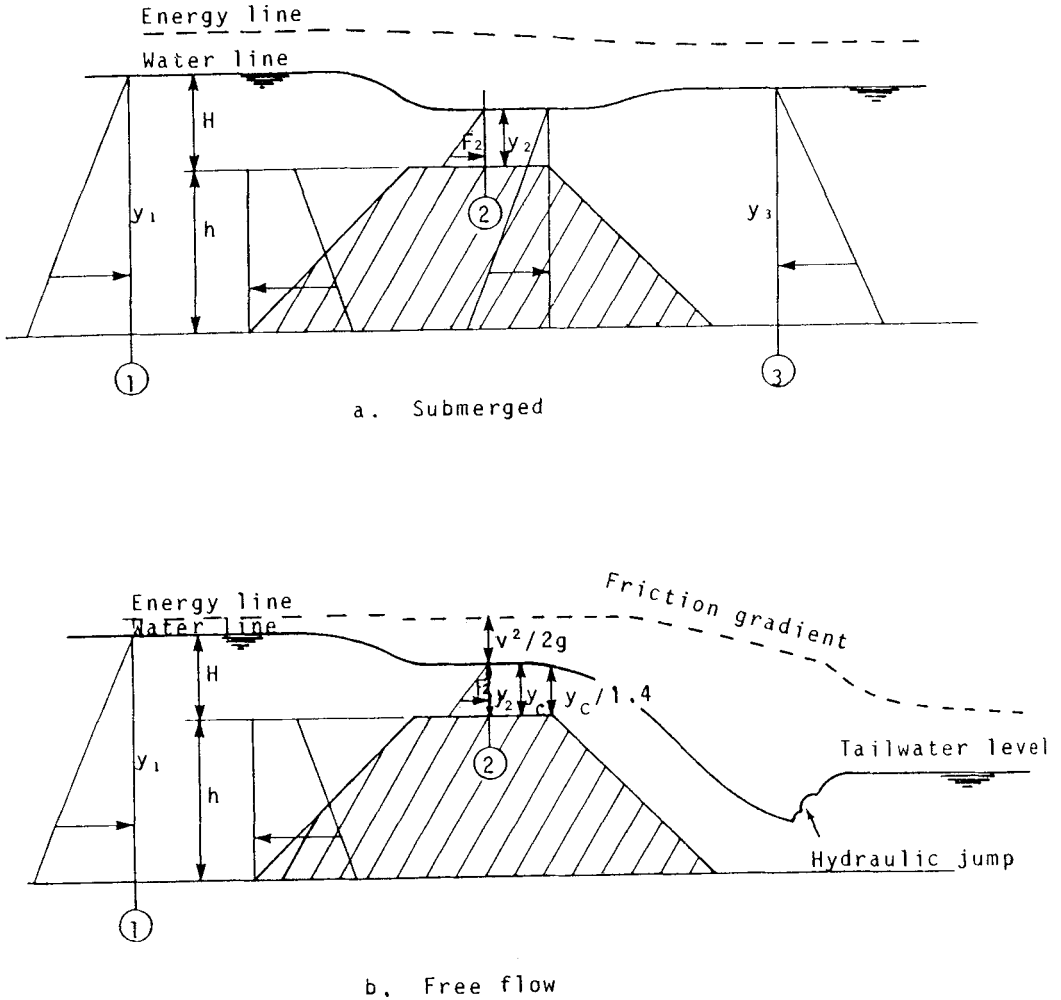


Fig. 13.10 Broad crested weir flow

EROSION DUE TO OVERFLOW

It is now possible to estimate the maximum height of embankment to avoid erosion by flow over the crest. The scour velocity over the crest may be estimated from the equation

$$d = \frac{0.25 v^2}{g(S-1) \cos \theta (\tan \phi - \tan \theta)} \tag{13.26}$$

where d is the erosive particle size.

For a flat horizontal crest, with ϕ equal to 35° , this gives the

permissible velocity over the crest as

$$v_2 = 1.6\sqrt{dg(S-1)} \quad (13.27)$$

REFERENCES

- Chow, V.T., 1959. Open Channel Hydraulics. McGraw Hill, N.Y. 680pp.
- Henderson, F.M., 1966. Open Channel Flow, MacMillan N.Y. 522pp.
- Kindsvater, C.E., 1957. Discussion on flood erosion protection for highway fills. Trans. ASCE, 122, p548.
- Laursen E.M., 1962. Scour at bridge crossings. Trans. ASCE. 127(1) p.166.
- Laursen, E.M., April, 1970. Bridge backwater in wide valleys, Proc. ASCE. HY4, p1019-1038.
- Lin, H.K., Bradley, J.N., and Plate, E.J., October 1957. Backwater effects of piers and abutments, Colorado State University, Civil Engineering Section, Report CER57HKL10, 364pp.
- Naylor, A.H. 1976. A method for Calculating the Size of Stone Needed for Closing end tipped Rubble Banks in Rivers, CIRIA, Report 60, London, 56pp
- Stephenson, D., 1979. Rockfill in Hydraulic Engineering, Elsevier, Amsterdam, 216pp.
- U.S. Department of Transport. 1978. Hydraulics of Bridge Waterways, Washington, 111pp.
- Yarnell, D.L., 1934. Bridge Piers as Channel Obstructions. U.S. Department Agriculture, Tech. Bull. No. 442.

CHAPTER 14

CULVERT HYDRAULICS

DESIGN APPROACH

A culvert is defined here as a structure for conveying stormwater under an embankment. A culvert or a bridge would be constructed over a natural river or man-made channel to assist traffic to pass over the waterway.

The design of culverts to convey stormwater under roads or embankments has been the subject of considerable research and considerable misunderstanding. The difficulty invariably arises in connection with the point of control - either inlet or outlet control is usually the case. However in order to appreciate the problem it is necessary to start a step earlier in the design process. That is to understand why a culvert is a control structure at all. For this we need to consider the aspects of economics and risk.

Economic design

The cost of a culvert is much greater than the cost of the equivalent length of channel. The culvert will have to be designed and built to resist high earth and superimposed loads, both vertical and lateral. The structure will also have to protect the embankment against scour, and provide a passageway for water. The cost of the culvert per unit length is highly dependent on the cross sectional area and shape. The cross sectional area of a culvert is invariably smaller than that of the water in the channel at flood flow in order to reduce the cost of the culvert.

A culvert also has a larger wetted perimeter than a channel as it is closed on top. The head loss and average energy gradient through the culvert is therefore steeper than in the channel without the culvert. If the channel bed is prefixed at a subcritical gradient, the only way this steepening of the hydraulic gradient through the culvert can occur is by raising the headwater level above the normal depth. This causes a backwater in the channel upstream of the embankment. Head is gained by reducing the friction loss in the upstream channel. Inlet conditions into the culvert then control the discharge through the culvert.

If the channel is at a supercritical bed gradient, the culvert will probably be installed at a flatter grade, with the result that the

water level will fall towards the discharge end and may reach critical depth. This condition gives rise to outlet control conditions.

Outlet control is more likely to occur for culverts in defined streams or channels. Inlet control is more likely in the case of an embankment across a catchment which collects water towards the culvert crossing. Flow is thereby concentrated at the inlet whereas the outlet will be free.

Risk

The headwater level at the entrance to a culvert cannot be increased indefinitely without consequences. Associated with a depth increase in a river a channel is a backwater effect. Water may rise above the banks of the channel and cause flooding of the surrounding land. The social and economic consequences could be severe.

Of more relevance to the road engineer may be flooding of the embankment through which the culvert passes. A water level rise on the upstream side of the embankment may affect any of the following:

- i) The stability of the bank as a whole or either face,
- ii) The structural loads on the culvert (lateral and vertical),
- iii) Scour of earth embankment and possibly washaway if there is severe overtopping,
- iv) Interruption of traffic,
- v) Danger to life and vehicles,
- vi) Flooding of upstream land,
- vii) Erosion of downstream channel.

The culvert cross-sectional area and hydraulic properties are therefore important. Where the consequences of a headwater rise can be evaluated economically they can be balanced against the cost of the culvert and embankment height. The structure with least total cost i.e. of structure and due to flooding, should be selected. Construction and engineering costs could be discounted to a time basis common with the economic losses and a least cost system selected. The resulting culvert will discharge a certain design flood without overtopping the embankment but there may still be some risk of a greater flood occurring.

The probability of the design flood being exceeded could be established or estimated from a hydrological analysis. The cost of a flooding should be multiplied by the probability of a flood occurring in any year in evaluating the average economic cost of flooding. The probable cost of one, two or more floods in any year should be summated in the comparison.

Principle of Controls

An hydraulic device is said to control flow if it limits the flow of water which would otherwise exceed that flow with the prevailing upstream and downstream conditions. If the river flow is specified then neglecting backwater storage the head will adjust across the control section until the inflow equals the discharge.

Flow can be controlled from either the upstream side or the downstream side depending on whether flow is supercritical or subcritical respectively. The velocities of water relative to that of an hydraulic reaction dictate whether flow is supercritical or subcritical. Thus if the flow is supercritical, the water velocity is faster than the velocity of a wave, so that waves cannot pass upstream, and control cannot be effected from downstream. A downstream control or constriction would create a standing wave which may be in the form of an hydraulic jump.

A control from upstream will uniformly affect the downstream flow depth.

On the other hand if the velocity is subcritical waves can travel upstream at a speed faster than the water is flowing, so any control on the flow downstream will back up water until it reaches an equilibrium profile upstream of the control. Flow downstream will be at normal depth.

Supercritical depth occurs when the Froude number, $F = v/\sqrt{gy}$ is greater than unity, i.e. $v > \sqrt{gy}$ where \sqrt{gy} is the celerity of a shallow water wave. If F is less than 1, the flow is subcritical.

The relative gradient of the culvert and channel and the geometry will dictate where the control section is in a culvert section. It can be altered by careful design, and in fact if control can be transferred from the inlet to the outlet, or else if a balanced design is achieved, the possibility of upstream flooding is minimized for any outlet size.

HYDRAULIC PROFILES

Some of the different water surface profiles with the corresponding control sections, are indicated in Figs. 14.1 and 14.2. In the case of inlet control, the tailwater level will be relatively low so that the culvert runs part full for some or all of its length. The slope of the bed may be supercritical in which case depth will pass through critical at the entrance (case A). It may even occur that the headwater is higher than the barrel soffit without the water touching it if there were an inlet taper. H/D should exceed approximately 1.2 for submergence,

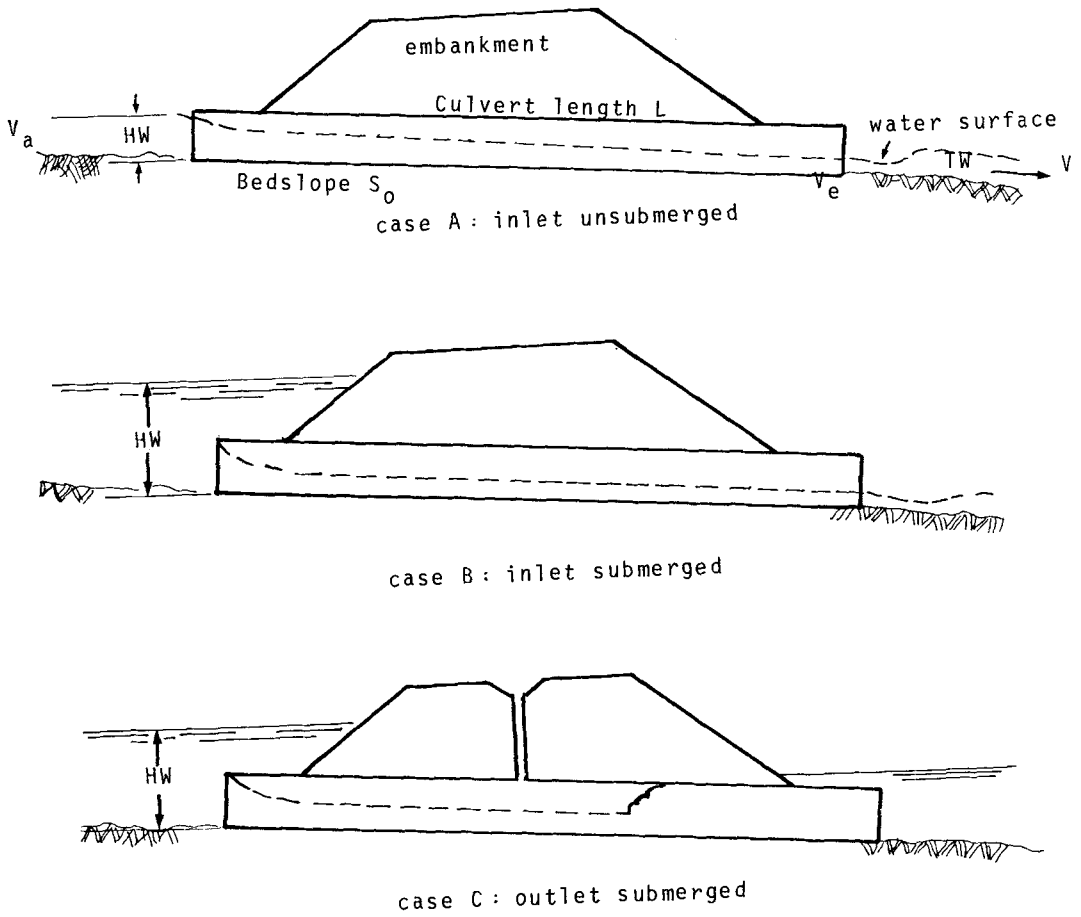
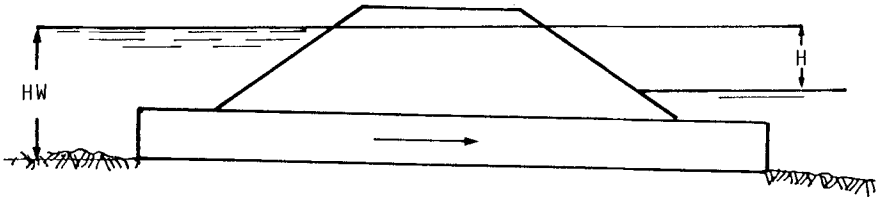
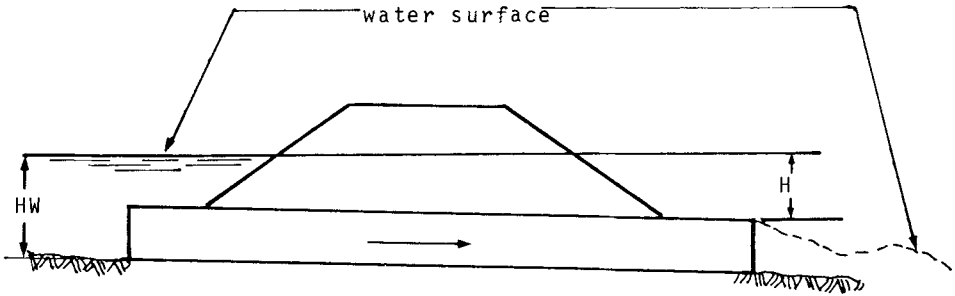


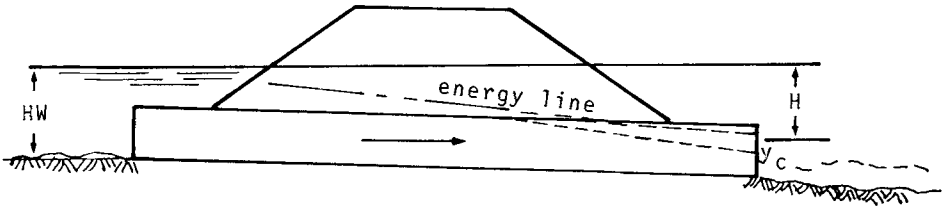
Fig. 14.1 Culvert longitudinal sections illustrating inlet control conditions



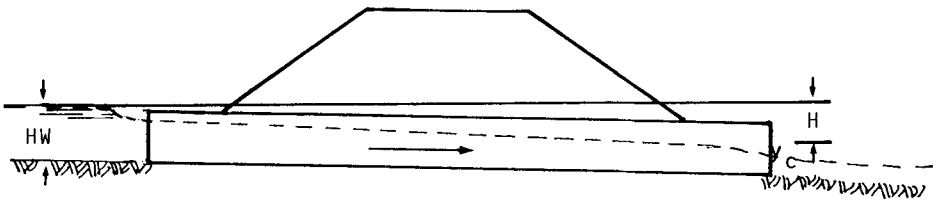
case D : submerged



case E : outlet free, barrel full



case F : outlet surface free



case G : free surface flow

Fig. 14.2 Culvert longitudinal sections illustrating outlet control conditions

(USBR, 1960). If discharge were higher, the headwater may cover the entrance in which case the situation would be case B for a low tailwater. Critical depth could be induced at this inlet either by a steep downstream slope, or a high headwater H , creating a high velocity and large contraction. Case C where a hydraulic jump occurs is possible for a high tailwater. Observe that for case C to be stable the culvert barrel upstream of the jump would have to be vented. Kalinske and Bliss (1943) indicate a jump would evacuate air at a rate $0.006 Q(F_1-1)^{1.4}$ where Q is the water discharge and F_1 the upstream Froude number $v_1/\sqrt{gy_1}$. With no ventilation the jump would move upstream creating sub-atmospheric pressures and possible instability at the entrance.

In each of the inlet control cases the barrel size beyond the inlet could be reduced without affecting the discharge. Conversely if the inlet conditions were improved the capacity of the culvert for any limiting headwater could be increased.

For a tailwater level so high that it drowned the culvert completely, the discharge would be controlled by the difference between entrance and exit water levels. This is a form of outlet control (case D).

Assuming the barrel was reduced in capacity until it limited the flow or increased the headwater, control would transfer to the barrel (but this is classified as one form of outlet control, Case E).

The latter two cases are equivalent to pipe flow, with the head drop being consumed primarily in conduit friction. The slope could be subcritical or supercritical. For relatively long culverts the inlet end only may be surcharged and the discharge end may run with a free surface. This case (F) will only occur with a low tailwater level and subcritical slope. In some extremes with a flat culvert bed gradient and large cross-section the flow may be free-surface and subcritical the entire length, which is illustrated as case G.

INLET DESIGN

If the culvert cross sectional area is to be fully utilized or conversely is to be minimized the culvert should run full or nearly full. In the case of low tailwater levels or steep gradients this may be a problem. It was indicated that for these cases the control is often at the inlet. Careful attention is therefore necessary in the design of the inlet to ensure minimum contraction of the flow (French, 1969). The objective is to ensure that flow rounds the edges of the inlet with minimum of separation, thereby filling the barrel cross section as much as possible. The discharge coefficient is there maximized. Full design

details and nomographs for the design of improved inlets were given by the U.S. Department of Transport (1972) from which much of the following is abstracted.

The improvement may be obtained with a steep throat, a drop inlet, wing walls, a hood, or just bevelled edges. The shape of the top entrance appears to be the most important, and the bottom or invert the least important since flow there is horizontal. Thus an inlet meeting the battered embankment is highly conducive to flow contraction and results in a low discharge coefficient.

A taper should be in straight sections for ease of construction and rounded edges are found to have little improvement over plane bevels. Nevertheless there are shaped precast concrete inlets available for circular culverts in the smaller sizes. It is always good policy to lay pipes with the barrel end facing upstream as this provides something of a transition.

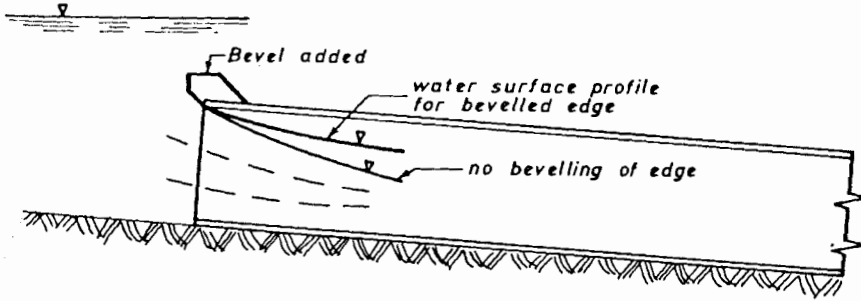
Fig. 14.3 illustrates some possible inlet arrangements. The simplest type of improvement is a vertical head-wall on top of the entrance to the culvert in the case of a battered embankment. This eliminates the re-entrant angle. The next step would be to bevel the top of the inlet. The bevel should be at least 10% of the culvert height at 33° to 45° to the axis of the culvert. In the case of skew culverts, the acute approach edge should also be bevelled. This will increase flow by up to 20%.

The second degree of improvement would be to taper the sides of the inlet. A taper angle of 45° (angle measure from the culvert axis) is perhaps the best compromise between hydraulic efficiency and length of approach. This will increase flow 25 to 40% over a square-edged inlet. Associated with side taper is usually a bevelled soffit, or a drop inlet to ensure the soffit height is not the control.

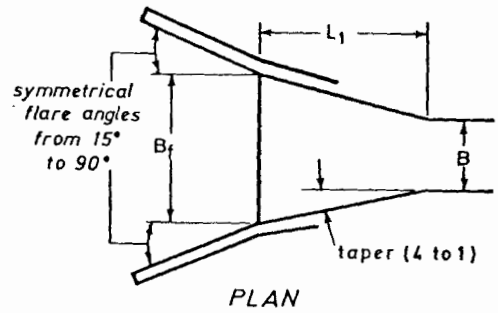
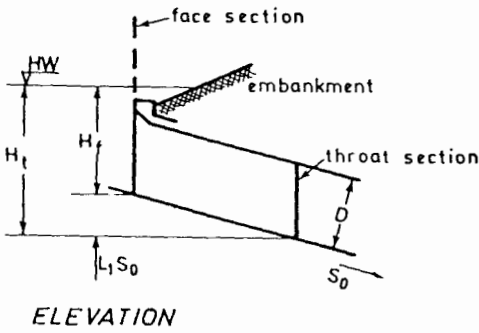
A slope-tapered section (see Fig. 14.3c) is the third degree of improvement (Southwood, 1978). This form of design increases the head on the barrel as well as tapering the inlet and 100 percent improvement in flow is possible. There are many different possible combinations of side-taper and throat taper, and the position of the control section within the inlet will have to be determined by trial.

Inlet control equations for box culverts

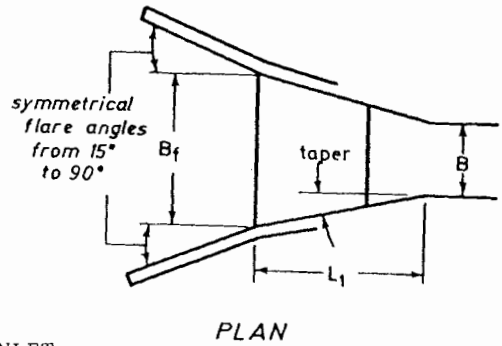
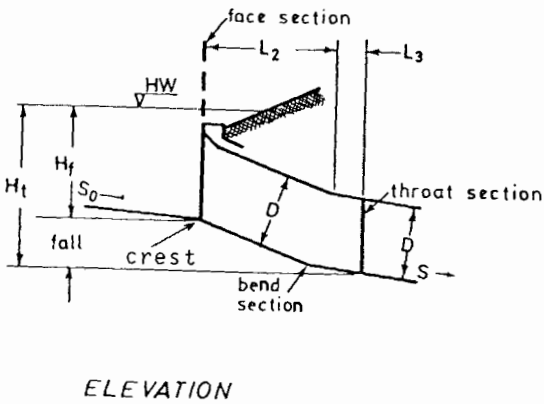
The position of the control section in a box culvert will depend on the type of inlet. In the case of composite designs, e.g. with wing walls, a slope taper or a drop inlet, the necessary headwater at each



a. BEVELED TOP



b. SIDE-TAPERED INLET



c. SLOPE-TAPERED INLET

Fig. 14.3 Inlet Details.

change in section should be determined. The type of flow at the relevant section will depend on whether the soffit (top of barrel) is submerged or there is a free surface.

If the inlet control is due to a drop or a narrow entrance and flow is free, then the depth at the entrance is critical depth and weir flow occurs. This occurs for H/D less than about 1.2. Thus

$$Q = C_B B g^{1/2} (2/3 H)^{3/2} \quad (14.1)$$

where B is the width at that point and H is the headwater level above the invert or effective weir crest. Strictly H is the energy level of the headwater, not the water level, but in most cases the approach velocity is negligible. Values of the discharge coefficient C_B are tabulated in Table (14.1).

Where the water touches the soffit, the culvert acts as an orifice. Discharge is related to head according to an equation of the form:

$$Q = C_C B D \{2g(H - C_h D)\}^{1/2} \quad (14.2)$$

It is implied that the remaining head loss between the control section and headwater is negligible. This is the case for crest control or face control. By assuming throat or head control it is implied the crest and face are sufficiently wide to avoid separation and near to the control section to eliminate friction. It may be necessary in some situations to add the head loss for each section.

Multiple-barrel rectangular culverts

A set of rectangular culverts in parallel can be treated as a single culvert ignoring the dividing walls, for the purpose of selecting wing-walls. The noses of the dividing walls should, however, have a bevel. Practical considerations may limit the side taper on very wide culvert sets.

Circular pipe culverts

A circular cross section has better hydraulic characteristics than a rectangular one. Head losses are lower. The structural resistance is good as arching is induced. A higher headwater may however be needed for any cross sectional area owing to the shape if it is to run full at the entrance. For this reason the inlets are often rectangular with a subsequent transition to a circular section (see Fig. 14.4).

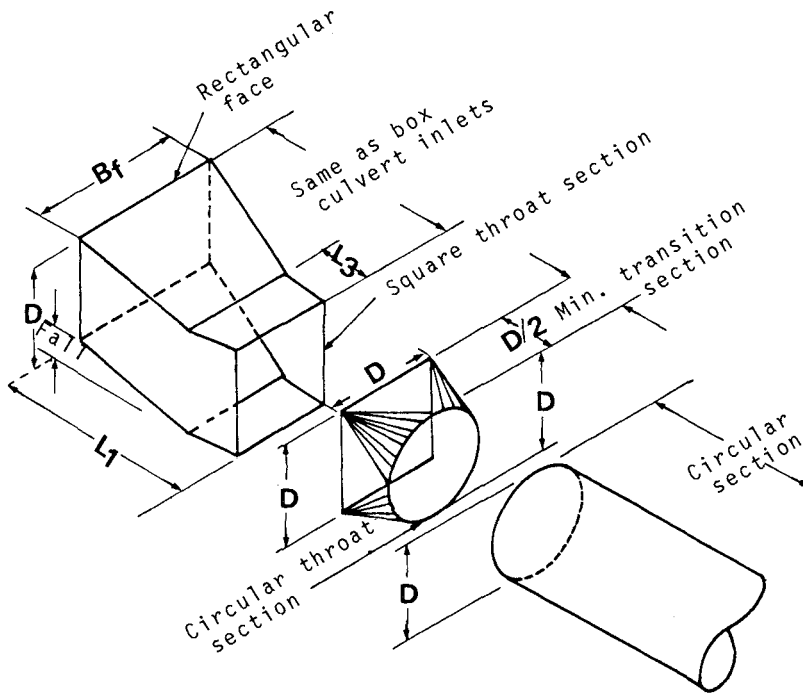


Fig. 14.4 Slope-tapered inlet transition for circular pipe

Where rectangular section inlets are provided, the discharge control equations are similar to those for box culverts. In circular sections, the type of control is generally similar to that for rectangular sections and similar equations apply in the case of submerged flow. The inlet is normally submerged if H/D is greater than 1.25.

For free surface discharge a control section will occur where the depth is critical depth. Direct derivation of an expression for critical depth is difficult for circular conduits (see chapter 10), but the principle of minimum specific energy is used to derive the relationship as for rectangular sections. The resulting expression for all shapes is

$$A_c^3/B = \frac{Q^2}{g} \quad (14.3)$$

where A_c is the cross sectional area of flow at critical depth, B is the width of surface and Q is the discharge rate. This expression cannot be solved directly for critical depth y_c as a function of diameter D , and the relationship must be derived numerically (see chapter 10). The relationship between discharge and critical specific energy,

E_c , can be approximated over the range E_c/D less than 0.8 by the expression

$$Q = 0.48C_B g^{1/2} D^{5/2} (E_c/D)^{1.9} \quad (14.4)$$

As a guide the discharge coefficients C_B in Table 14.1 for box culverts could be used, although Henderson (1966) indicates they are sensitive to slope. There are difficulties in evaluating specific energy or discharge at any particular depth in non-rectangular conduits. Diskin (1962) produced dimensionless charts of use for circular conduits running part full.

For submerged inlets, the discharge equation is the orifice equation

$$Q = C_c A \{2g (H - C_h D)\}^{1/2} \quad (14.5)$$

Blaisdell (1960) indicated that a considerable improvement in inlet capacity of circular culverts was possible with a hood and vortex suppressor over the entrance.

TABLE 14.1 Discharge coefficients for culverts.

Control position	Flow condition	Coefficient	Box culverts		Circular Culverts
			Side taper	Slope taper	
Crest	Unsubmerged	C_B	0.92	0.92	
Face	Unsubmerged	C_B	0.77	0.92	
15-26° wingwalls + top bevel		C_c	0.59	0.59	Square edge 0.57
or 26-90° wingwalls, no bevel		C_h	0.84	0.64	Square edge 0.79
26-45° wingwalls with top bevel		C_c	0.64	0.64	Bevel edge 0.65
or 45-90° with top and side bevel		C_h	0.86	0.70	Bevel edge 0.83
Bend	Unsubmerged	C_B	-	-	
	Submerged	C_c	0.80	0.8	
	Submerged	C_h	0.87	0.87	
Throat	Unsubmerged	C_B	1.00	1.00	
	Submerged	C_c	0.94	0.93	0.89
	Submerged	C_h	0.95	0.96	0.89

OUTLET CONTROL

The outlet may be free-discharging in which case the depth in the culvert at the outlet will be critical, or submerged in which case the culvert will flow full. Alternatively the tailwater depth may be above critical depth in the culvert but below the soffit of the culvert. In either case of free surface discharge the downstream water level is known in which case one can backwater (using the direct step method) to determine the point beyond which the culvert will run full.

In all cases where the culvert runs full the head loss along the culvert can be determined from a friction formula, eg. Darcy-Weisbach

$$S_f = \frac{\lambda}{4R} \frac{v^2}{2g} \quad (14.6)$$

where R is the hydraulic radius A/P , and λ is a friction factor which for most culvert cases is the fully developed turbulent factor and is obtainable from a Moody diagram. Alternatively the Manning resistance equation can be employed. The head losses at the entrance may be evaluated from an equation of the form

$$h_L = K_e \frac{v^2}{2g} \quad (14.7)$$

where the coefficient K_e may be determined from Table 14.2.

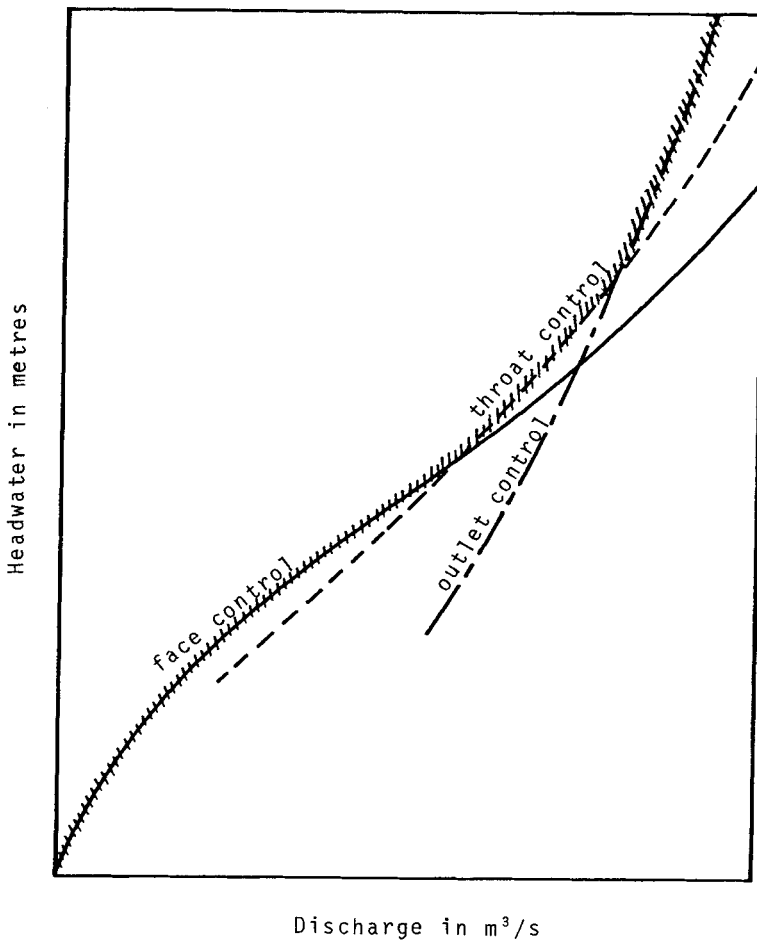


Fig. 14.5 Culvert performance curves for locating control section

BALANCED DESIGN

The discharge characteristics as a function of headwater for each section of a culvert will differ with the type of flow. Thus flow into the inlet is usually orifice-type flow (Q proportional to $H^{1/2}$). Barrel control may be similar (Q proportional to $H^{1/2}$) while outlet conditions may be weir flow (Q proportional to $H^{3/2}$). Under different headwaters different sections may control the flow. It is therefore useful to plot the discharge characteristics of each section on a common chart, such as Fig. 14.5. It will be seen that at lower headwater levels, the inlet conditions limit the flow, while at higher heads, the outlet conditions may limit the flow.

The optimum design will be that for which inlet and outlet conditions give a similar discharge (the design flow) for the required maximum headwater permitted. Inlet control curves should be plotted for different inlet configurations (Fig. 14.6). The required inlet configuration for any headwater and barrel size can then be read off the plot.

TABLE 14.2 Entrance Loss Coefficients

Outlet Control, Full or Partly Full	
Entrance head loss $H_e = K_e \frac{v^2}{2g}$	
Type to Structure and Entrance Design	Coefficient K_e
<i>Pipe</i>	
Projecting from fill, socket end	0.2
Projecting from fill, square cut end	0.5
Headwall or headwall and wingwalls	
Socket end of pipe or rounded	0.2
Square-edge	0.5
Mitered to conform to fill slope	0.7
End-Section conforming to fill slope	0.5
Beveled edges, 33.7° or 45° bevels	0.2
Side-or slope-tapered inlet	0.2
Metal pipe projecting from fill, no headwall	0.9
<i>Reinforced Concrete Box Section</i>	
Headwall parallel to embankment, no wingwalls	
Square on 3 edges	0.5
Round 3 edges to radius 1/12 barrel or beveled 3 sides	0.2
Wingwalls 30° to 75° to barrel. Square edged at crown	0.4
Crown edge rounded to radius 1/12 barrel or beveled top	0.2
Wingwall 10° to 25° to barrel. Square-edged at crown	0.5
Wingwalls parallel (extension of sides). Square at crown	0.7
Side-or slope-tapered inlet	0.2

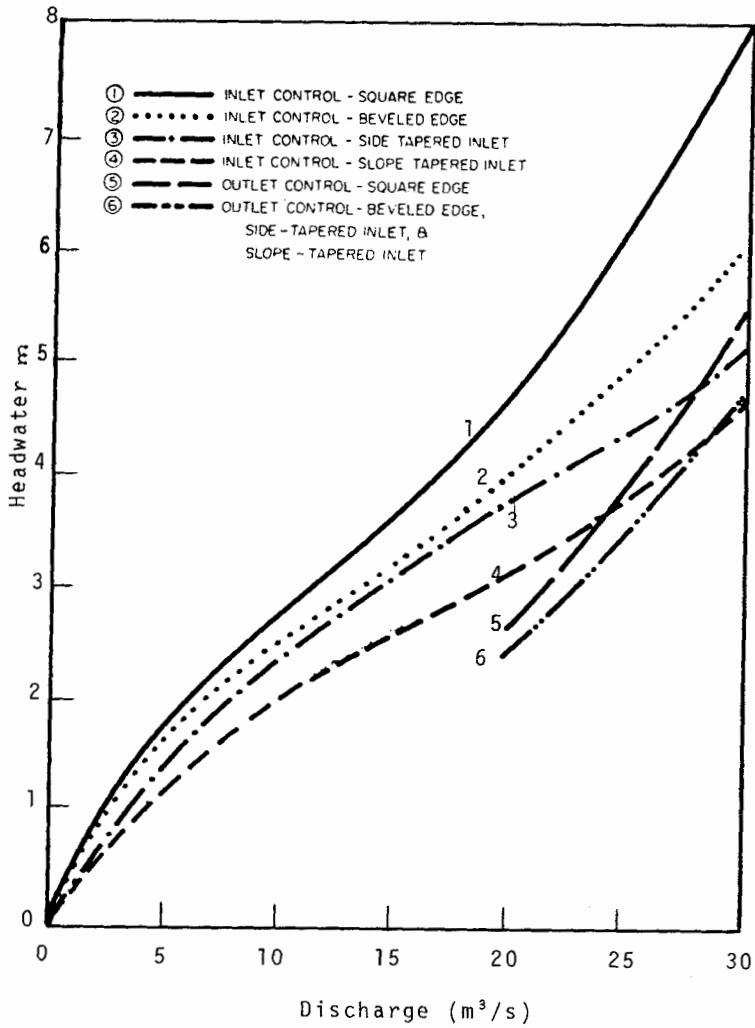


Fig. 14.6 Performance curves for single 2m box culvert with alternative inlets

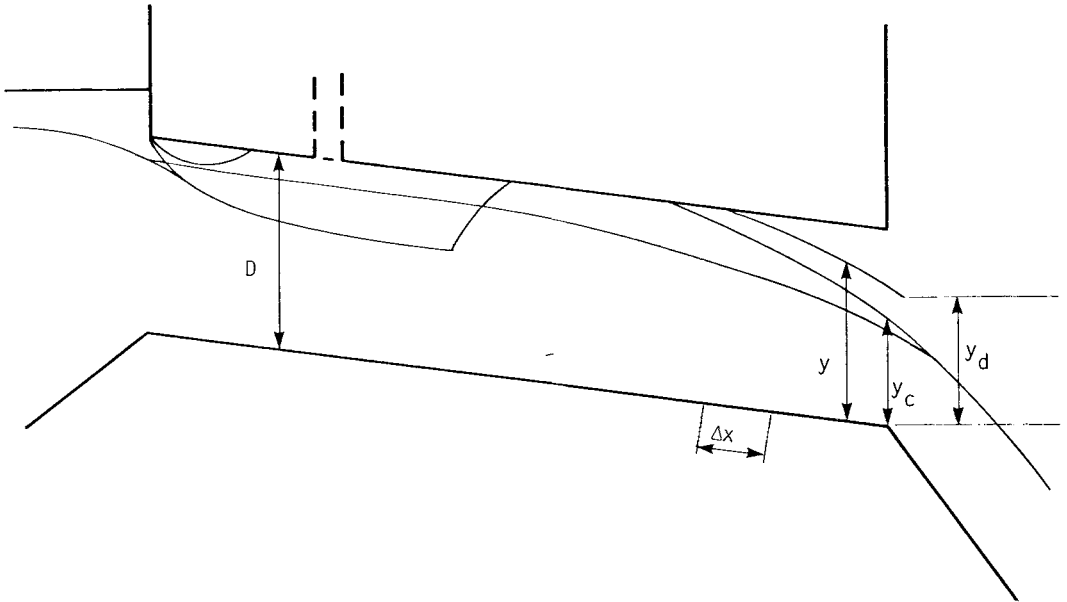


Fig. 14.7 Alternative water profiles

COMPUTER PROGRAM FOR CALCULATION OF FLOW PROFILES IN RECTANGULAR CULVERTS

The number of possible flow profiles in a culvert is obviously vast. Careful analytical procedures can however isolate the possibilities and enable the flow profile to be established for any condition. The analytical procedure can be programmed for a computer.

The engineer should, however, establish his objectives in order to minimize the trial and error approach. There are three problems the engineer is likely to encounter:

- 1) Design of a culvert to discharge a given flow with a specified headwater and tailwater level: The most economical solution is to select a practical inlet and barrel such that they are both equal in capacity i.e. equal to the design flow. As the barrel is usually the most expensive component this should be designed to run full, so that the inlet should be carefully designed to prevent control there.
- 2) For any given culvert design and headwater conditions to determine the discharge capacity: If the control section cannot be readily identified, it will be necessary to consider a number of alternative flow rates. The rating curve can be plotted as in Fig. 14.6 in order to

establish which condition controls the flow at the prescribed head-water level.

3) For a given culvert and discharge rate, determine the water surface profile: This is a confirmatory measure but a recommended step in the design process.

The latter analytical procedure can most readily be programmed for a computer. The procedure is summarized below for a box culvert with a simple inlet.

- 1) Start at the downstream end, knowing the water level in the channel or pool downstream of the culvert. If the water surface downstream is below critical depth in the culvert the depth then will be critical depth. Otherwise the energy level is set equal to that in the channel plus exit losses.
- 2) Calculate the water surface and energy levels at suitable intervals proceeding upstream. A backwater procedure is used for free surface flow and a friction gradient equation for full flow.
- 3) If the depth at any section works out to be less than critical depth ($y_c = \sqrt[3]{q^2/g}$) proceed to the inlet and set $y = y_c$ at the control section there.
- 4) Backwater downstream from the control at the inlet to determine the supercritical water surface profile.
- 5) Establish the position of the hydraulic jump if any at the point where the depth computed from the downstream end is equal to the sequent depth to the supercritical depth calculated from the upstream end.
- 6) If the hydraulic jump is not ventilated negative pressures (down to vapour pressure) may be assumed in the barrel in which case the effective water level is higher.
- 7) The headwater energy level is calculated by adding entrance losses to the energy level in the inlet.

REFERENCES

- Blaisdell, F.W., May 1960. Hood inlet for closed conduit spillways. Proc, ASCE, 86 (HY5), p7.
- Diskin, M.H., July 1962. Specific energy in circular channels, Water Power, 14, p270.
- French, J.L., Nov. 1969. Nonenlarged box culvert inlets. Proc. ASCE 95(HY6), 6928, p2115-2137.
- Henderson, F.M., 1966. Open Channel Flow, Macmillan, N.Y., 522pp.
- Kalinske, A.A., and Bliss, P.H., Oct. 1943. Removal of air from pipelines by flowing water. Civil Engineering, ASCE, 13(10) p480.
- Southwood, S.R., 1978. Culvert Hydraulics. Course on Urban Hydrology and Drainage, SAICE, Durban.
- U.S. Bureau of Reclamation, 1960. Design of Small Dams. 611pp.

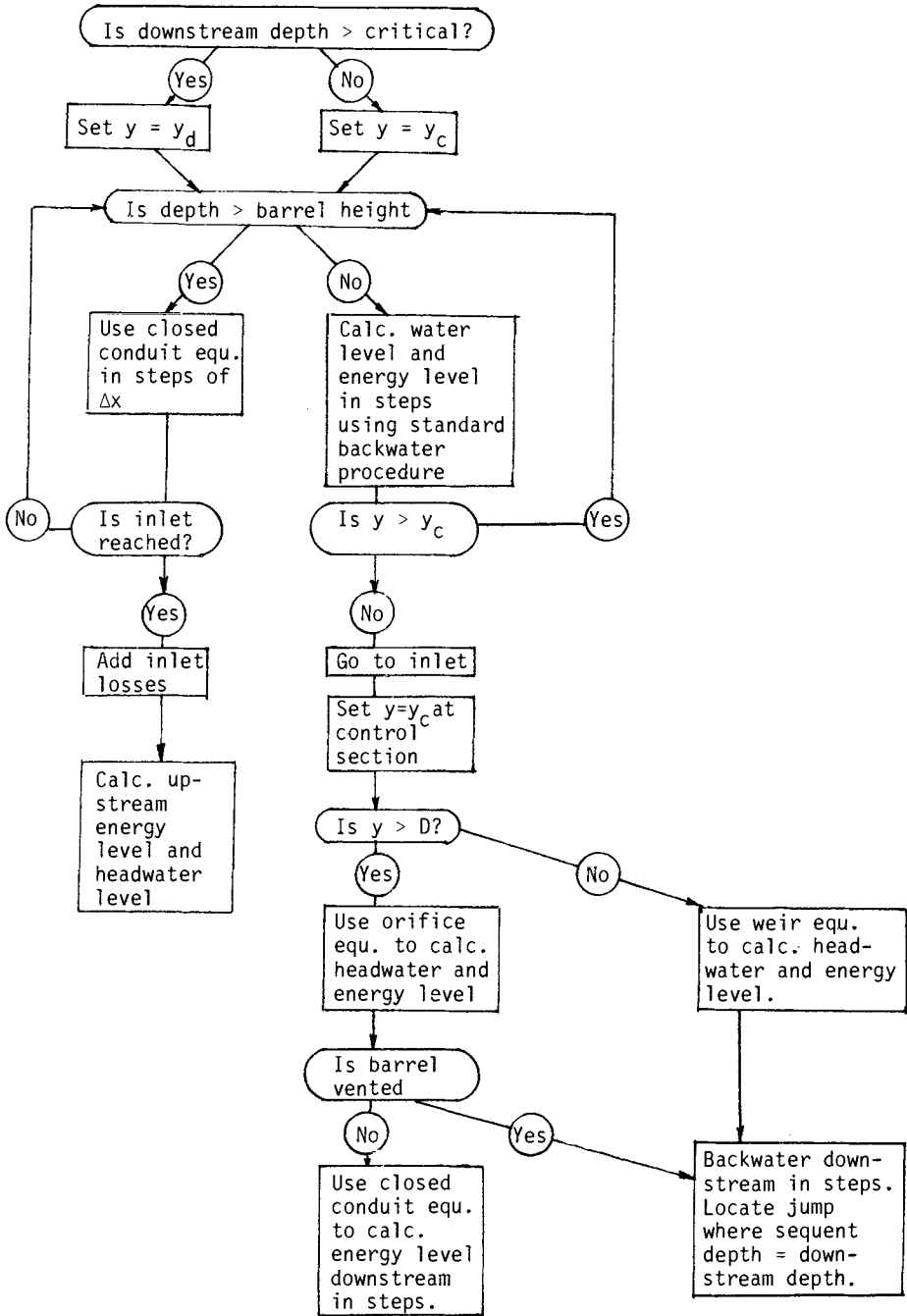


Fig. 14.8 Computation of flow profile in simple rectangular culvert

U.S. Department of Transport, Aug. 1972. Federal Highway Commission,
Hydraulic Design of Improved Inlets for Culverts, Hydraulic Eng.
Circular 13, 172pp.

CHAPTER 15

WATER QUALITY

POLLUTION PARAMETERS

Stormwater runoff from urban catchments in particular contains a surprisingly high pollutant concentration even if no sewage or waste water is discharged into the system. Setting aside combined sewage-stormwater systems, the source of contaminants ranges from material precipitated from the atmosphere (dust or in rain) to seepage from waste tips or industrial zones. There may be discharge of wastes from factories and commercial concerns which, intentionally or not, finds its way to stormwater drains. This type of pollution is referred to as point-source, whereas natural spread inflow is referred to as non point-source pollution. Animal faeces, garden fertilizer, soil erosion, motor vehicles (oils and rubber from tyres) and decaying vegetable matter are some of the known sources. The concentration of sulphates, nitrates and suspended solids in rain is not inconsiderable. Increasing attention is being focussed on the acidity of rain - caused by fumes from traffic and industry. Runoff from rural catchments is also frequently contaminated. Fertilizers and decaying vegetable matter are frequently the source in agricultural areas, and salts leached from the ground may contaminate water in mineral-rich areas,

The rate and amount of pollution of streams due to incoming stormwater can vary widely. The intensity of rain will affect the rate of transport. The 'first flush' is known to bring down most of the pollutants. In fact many pollution models assume an exponential decay rate in the pollution washoff through a storm. The Environmental Protection Agency (EPA)(1971) in the USA indicated a storm depth of 12.5 mm would remove 90% of road surface particles.

Table 15.1 indicates a reasonable range of measured parameters as obtained from various sources. The values cannot be taken as representative for any particular catchment. They merely indicate that pollution does occur and the degree of pollution can vary widely.

The parameter by which pollution is measured is in terms of concentration. Thus dissolved salts e.g. chlorides and sulphates are measured per litre (mg/l) as are suspended solids such as silt. A specific nutrient such as nitrate is measured in terms of the mg/l of nitrogen. The total nitrogen content may comprise organic nitrogen, ammonia nitrogen, nitrite and nitrate. The oxidation of ammonia to nitrite,

TABLE 15.1 Urban runoff quality characteristics

Characteristics		Low	Average	High
BOD	(mg/ℓ)	10	30	500
Suspended Solids	(mg/ℓ)	20	200	10 000
Coliform	(No./100mℓ)	50	10 000	100 x 10 ⁶
Total chlorides	(mg/ℓ)	10	200	10 000
Total dissolved solids	(mg/ℓ)	300	1 000	10 000
pH	(mg/ℓ)	5.3	7	8.7
Nitrogen	(mg/ℓ)	1	3	100
Phosphate	(mg/ℓ)	0.1	1	50
Phenols	(mg/ℓ)	0		0.2
Oils	(mg/ℓ)	0		110
Lead	(mg/ℓ)	0		2

TABLE 15.2 Accepted limits for selected water quality parameters in streams

Parameter	Designation	Limit	Units	Reason
Dissolved oxygen	DO	5 minimum	mg/ℓ	Aquatic life
Temperature	T	30 max	°C	Life
Free hydrogen	pH	6-9		Acid-Alkali
Coliform	MPN	10000max	No/100mℓ	Disease
Total dissolved solids	TDS	1000max	mg/ℓ	Agriculture
Chloride	Cl	250 max	mg/ℓ	Agriculture
Pesticide	DDT	0.04 max	mg/ℓ	Health
Phenols		0.001 max	mg/ℓ	Taste
Suspended solids	SS	100		Colour
Nitrate as N	N	0.9		Eutrophication

then nitrate, and subsequent biological reduction to free nitrogen is termed the denitrification process and occurs in nature but is also forced at wastewater treatment works. Phosphate is also a nutrient, and in the correct proportions in the presence of nitrate can support life such as aquatic weeds and algae. Formation of algae in warm climates in particular is objectionable, and is termed eutrophication.

Biological matter in waters requires oxidation in order to render it innocuous. This includes decaying vegetable matter, faeces, and some industrial wastes, e.g. from paper factories or abattoirs. The oxygen required is measured in mg/ℓ and termed the biochemical oxygen demand (BOD). It is a slow test to determine BOD and frequently the 5-day or 20-day values are taken as indicators of the ultimate BOD. Due to the difficulty in measuring BOD many researchers prefer to use chemical oxygen demand (COD) or total organic carbon (TOC) as an indicator of oxygen demand.

Free oxygen is measured as dissolved oxygen (DO). Other parameters of interest are the conductivity which is often related to the dissolved salts content, turbidity, (related to suspended solids), colour and temperature. pH is a measure of acidity, with 7.0 being neutral and lower values indicating acidity. Bacteria are measured in terms of the most probably number (MPN) per 100ml sample. Faecal coliform and faecal streptococci are the significant bacteria.

The water quality has an effect on many uses of water. Thus agriculture can accommodate nutrients but not high salt contents. For domestic water supplies, coliform count, colour and taste are important as well as most other parameters. For recreational purposes, similar criteria are often applied. The standards required vary from country to country and Table 15.2 indicates some of the acceptable limits.

OXYGEN BALANCE IN STREAMS

Polluted water, especially if it contains organic pollutants, may require oxygenation to aid purification. The pollution may be measured in terms of the oxygen shortage. The BOD (biochemical oxygen demand) is a commonly used indicator of the oxygen deficit. Oxygen may be absorbed at the water surface or in some cases produced by plant photosynthesis. Dissolved oxygen (DO) in the water will reduce the BOD at a rate dependent on the relative concentration.

A first attempt to describe the relationships between DO, atmospheric reaeration and bacterial respiration was by Streeter and Phelps (1925). They postulated a linear decay rate for BOD as follows:

$$\frac{dB}{dt} = -K_1 B \quad (15.1)$$

similarly for DO deficit

$$\frac{dD}{dt} = K_1 B - K_2 D \quad (15.2)$$

where D is the oxygen deficit, $C_s - C$, C is the saturation DO which is dependent on temperature and other parameters, t is time, B is the BOD, K_1 is a decay constant and K_2 a reaeration coefficient.

The equations maybe refined by introducing terms for diffusion, convection, sources and sinks, (Cheverreau, 1973)

$$\frac{\partial B}{\partial t} = E \frac{\partial^2 B}{\partial x^2} - U \frac{\partial B}{\partial x} - K_1 B + S \quad \text{and} \quad (15.3)$$

$$\frac{\partial D}{\partial t} = E \frac{\partial^2 D}{\partial x^2} - U \frac{\partial D}{\partial x} + K_1 B - K_2 D - P \quad (15.4)$$

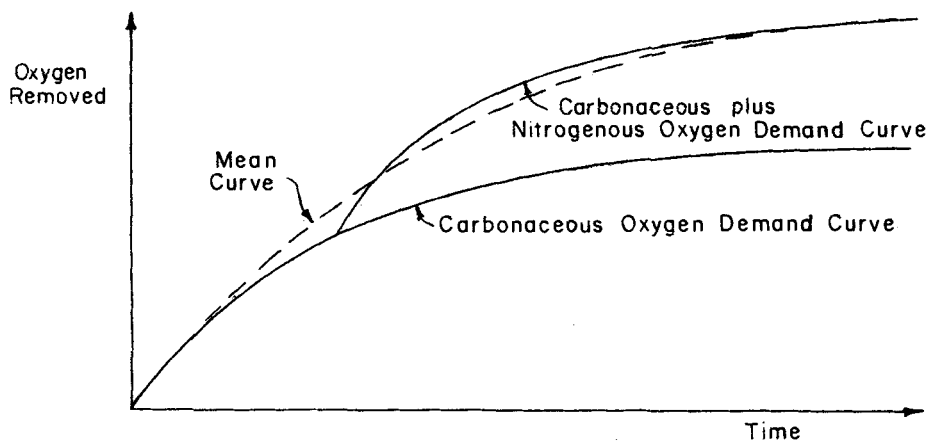


Fig. 15.1 Carbonaceous and nitrogenous oxygen demand curves

where E is the longitudinal dispersion coefficient, U is the flow velocity in the x direction, S is a net source of BOD and P is a net source of oxygen, both per unit volume and time.

The dispersion or diffusion term is primarily due to turbulence and the molecular diffusion is negligible. In real systems the longitudinal term is usually negligible, implying plug flow. The latter two equations are termed the coupled BOD-DO equations. If the river is depleted of oxygen the first equation (15.3) is no longer valid and must be replaced by

$$K_1 B = K_2 D - P \quad (15.5)$$

which states that the rate of oxygen consumption equals the rate of oxygen introduction.

The reaeration coefficient K_2 is a function of temperature and may be approximated by the formula

$$K_2(T) = K_2(20^\circ\text{C}) 1.024^{(T-20)} \quad (15.6)$$

$$\text{where } K_2(20^\circ\text{C}) = 3.9U^{0.5}/H^{1.5} \text{ per day} \quad (15.7)$$

and T is in degrees Celsius, U is the water velocity in metres per second and H is the water depth in metres.

The saturation concentration of dissolved oxygen, C_s , may be obtained from the following empirical relationship for water at 760 mm Hg:

$$C_s = 14.652 - 0.41022T + 0.007991T^2 - 0.00077774T^3 \quad (15.8)$$

The variation in the decay coefficient K_1 with temperature may be obtained from the following relationship (Thomann, 1972).

$$K_1(T) = K_1(20^\circ\text{C}) 1.047^{(T-20)} \quad (15.9)$$

where $K_1(20^\circ\text{C})$ must be determined on site. Laboratory values of 0.1 per day are typical whereas values obtained from stream tests have been as high as 20 per day although 1.0 is more representative.

The linear decay assumption is a gross simplification of the process which occurs in a river. There are many reactions, but laboratory BOD tests indicate two predominant oxygen depletion reactions. Initially oxygen is taken up by carbonaceous matter, and oxygen removed increases asymptotically as indicated in Fig. 15.1. At a later stage nitrogenous matter takes a more important part in absorbing oxygen.

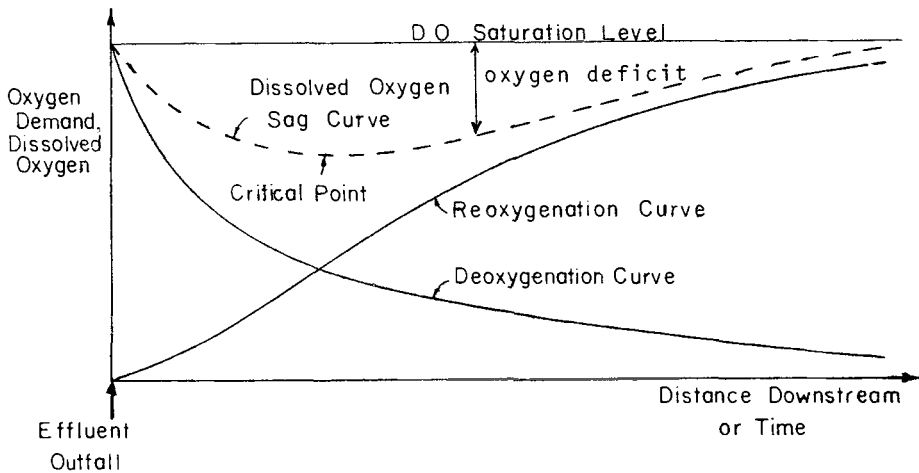


Fig. 15.2 Dissolved oxygen sag curve

The inter-relationships between the oxygen demand and dissolved oxygen in a stream may be indicated graphically as in Fig. 15.2. Assume a BOD is introduced into a stream initially saturated with oxygen. Immediately beyond (downstream of) the point of injection, the dissolved oxygen diminishes. This will cause reoxygenation due to the deficit, so further downstream the DO again increases as the BOD is depleted and the input rate of oxygen again exceeds the depletion rate.

EUTROPHICATION OF RECEIVING WATERS

Algal growth in water bodies is a nuisance from the health and appearance points of view. Algae may be present as a result of high nutrient

loading, i.e. nitrogen and phosphorus. Problems are likely to be experienced if the phosphorus concentration is somewhere above about 0.1 mg/l and nitrogen level above 10 mg/l. Residence time, temperature, carbonaceous matter and cell availability also appear to have a bearing on the formation of algae.

Chlorophyll is frequently used as an indicator of eutrophic level. Thus a chlorophyll level of about 100 mg/l is usually eutrophic while a level less than 10 mg/l indicates an oligotrophic level (underenriched). The intermediate stage is referred to as mesotrophic.

Reservoirs are often stratified as indicated in Fig. 15.3. Thermal strata form the epilimnion overlying a hypolimnion. Following a cooling of the upper layers, one may get temperature inversion of the water body resulting in mixing. Wind action can also contribute to the mixing. One would expect oxygen concentration decreasing from the surface to the bed but this may be upset by mixing. In fact Henderson-Sellers (1979) indicates ways of causing mixing in order to improve water quality. The balance between life and inputs to a water system is delicate and complicated as depicted by Roesner (1979) (Fig. 15.4).

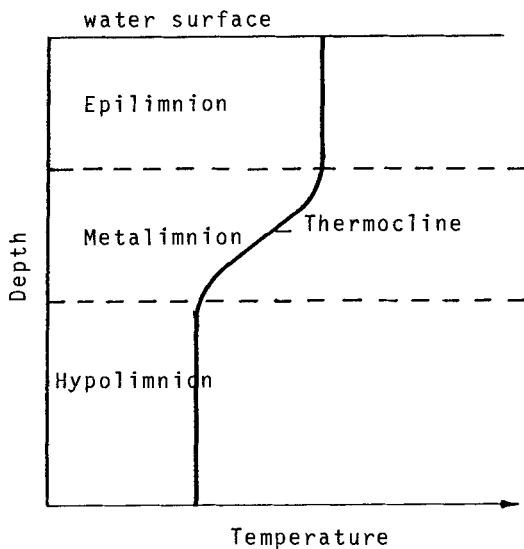


Fig. 15.3 Temperature profile in a reservoir

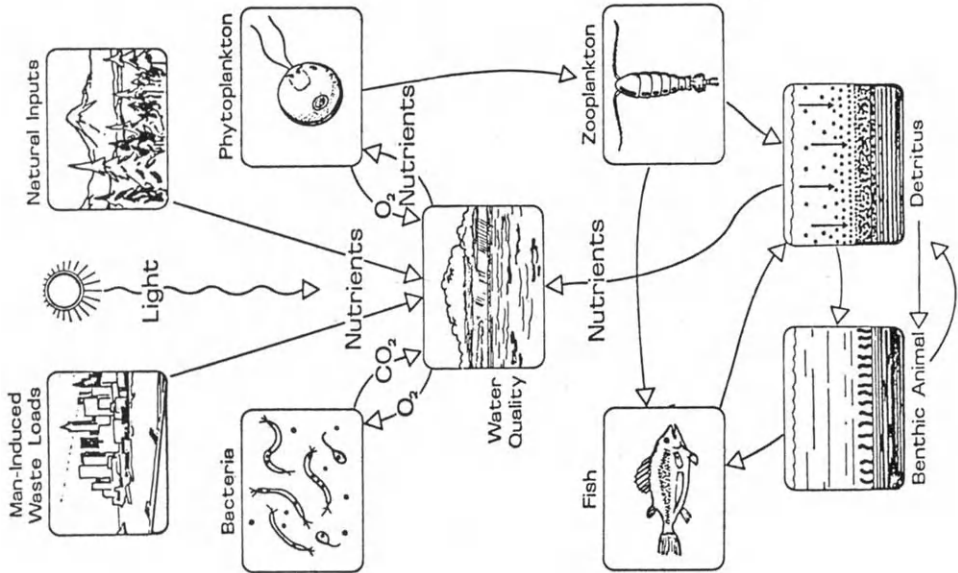


Fig. 15.4 Depiction of a healthy ecosystem (Roesner, 1979)

SEDIMENT EROSION

The erosion of soil in catchments, in the form of sheet erosion or rill and gully erosion is a complex phenomenon. Research into the process is manifesting itself in the form of mathematical models. Some of the relationships thus produced are outlined below.

The amount of sediment detached by rainfall is based on kinetic energy of the rain and may be approximated by an equation of the form

$$D_r = S_{dr} A_s I^2 \tag{15.10}$$

where A_s is the land surface area, I is the rainfall intensity and S_{dr} is a constant dependent on soil type and land surface conditions.

Sediment detachment by overland flow is assumed proportional to the square of the flow velocity which in turn is proportional to the cube root of the slope and flow rate:

$$D_f = S_{df} A_s S^{2/3} Q^{2/3} \tag{15.11}$$

where S is the land surface slope, Q is the flow rate and S_{df} is a constant. To account for imperviousness (or ground cover) the above equations may be multiplied by $(1-IMP)$ where IMP is the proportion of impervious area.

The sediment transport capacity due to rainfall is

$$T_r = S_{tr} S I \quad (15.12)$$

The sediment transport capacity due to overland flow is

$$T_f = S_{tf} S^{5/3} Q^{5/3} \quad (15.13)$$

Thus provided all the constants could be evaluated, the computational procedure is to estimate the erosion rate due to rainfall and overland flow. The transport rate will increase as indicated by (15.10) plus (15.11) until the limit indicated by either (15.12) or (15.13) is reached. (Meyer and Wischmeir, 1969).

The Universal Soil Loss Equation

An empirical equation for the prediction of soil erosion rates was developed at Purdue University in the 1950's (Wischmeir and Smith, 1965) Although it was originally developed for croplands it has been adapted to other erosion loss problems. The equation, termed the Universal Soil Loss Equation (USLE) is

$$A = RKLSCP \quad (15.14)$$

where A = soil loss in tons per acre per time period

R = rainfall factor per unit time period

K = soil erodibility factor

L = slope length factor

S = slope gradient factor

C = cropping management factor

P = erosion control practice factor

The rainfall factor R is a function of the kinetic energy of a storm times its maximum 30-minute intensity, summed over the time period which is usually a year. Values of R were given by Wischmeir and Smith (1965) for the United States. These values range from 20 per year on the west coast and in the arid north west, to 350 in the wetter south east.

The soil erodibility factor K depends on soil size distribution, structure and organic content. It varies from 0.02 for sands to 0.2 for clay and it may be as high as 0.6 for silt. It decreases slightly for high organic content.

The slope length factor L and slope gradient factor S are usually combined to give a topographic factor, which may be estimated from the formula

$$LS = \left(\frac{X}{72.6}\right)^m \frac{(430Z^2 + 30Z + 0.43)}{6.57} \quad (15.15)$$

where X = field slope length in feet

Z = slope in feet per feet

m = 0.5 for slope equal to or greater than 5%

0.4 for slope of 4%

0.3 for slope less than or equal to 3%

It may be necessary to break the catchment into a number of planes to account for varying topographic factors.

The cropping management factor C is also called the cover factor. It varies widely, from 0.01 for urban land or pasture to 0.1 for cropland. It may be as high as 1.0 for fallow land.

The erosion control practice factor P allows for reduction in erosion due to practices such as contouring, terracing and strip cropping.

For land slopes less than 2% it may be as low as 0.3, increasing to 0.5 for slopes over 20%. The factor is halved by terracing but increases for contour strip cropping.

Considerable experience is obviously necessary in applying the USLE. It does, however, hold promise for urban systems subject to further research into the various factors.

SEDIMENT TRANSPORT IN DRAINS

Stormwater drains and sewers are usually designed hydraulically on the basis of clear water flowing through them. The depth of flow, friction gradients and other head losses are estimated without allowance for suspended matter in the water.

It frequently occurs that silt, sand and organic matter is picked up by overland flow and transported into and down drains. Although suspended matter is seldom more than one percent by weight in stormwater drains from built up areas, in rural areas silt concentrations can be as high as 5 percent or more if severe erosion is possible. Particle sizes are typically less than 0.1 mm but in the case of runoff from gravel roads, sand and grit may be considerably larger. A unique problem occurs in some developing countries such as parts of Africa where folk use sand for washing pots.

Fine particles (less than 0.04 mm nominal diameter) normally mix completely with the water and the mixture is effectively homogeneous with a relative density equal to $1+c(S-1)$ where c is the volumetric concentration of suspended matter and S is the relative density (or specific gravity) of the sediment.

In the case of larger particles, there is a tendency to settle out, and the mixture is a heterogeneous one. Energy is expended in maintaining the particles in suspension and friction gradients are larger than for clear water. Conversely in any pipe flowing part-full at a pre-selected grade, the mixture will flow slower and hence deeper. The capacity of the pipe is thereby reduced. The reduction in velocity may also result in excessive deposition and even blockage.

Transport Mechanics

There are many theories in use for predicting silt loads in channels (see eg. Vanoni, 1975). Most theories for the transport of silt in open channels are based on uniform flow where the silt in suspension is in equilibrium with the bed. The rate of settling out is equal to the rate of re-suspension from the bed due to turbulence. There has been little effort to establish the effect of the suspended load on the energy gradient. In many channels this effect is low on account of the low silt concentrations.

On the other hand, research into the transport of sediment in pipes has been concerned primarily with the effect of the sediment on the energy gradient. Sediment concentrations up to 60 percent by weight are used in pumping systems and at these concentrations there is a considerable energy requirement to maintain the sediment in suspension or drag it along the conduit.

The effect of bed load on the sediment transport process is difficult to assess. Many of the pipe transport formulae are said to apply whether or not there is bed load. It is accepted that coarse particles especially at low velocity will tend to settle, or roll or slide or hop along the bed, rather than remain in suspension. Open channel theories tend to consider the bed load separately from the suspended load.

There is in fact a complicated interaction between channel shape, sediment transport rate, flow velocity, depth and energy gradient. One of the degrees of freedom, namely, channel shape, is absent in pipe flow but there remains still the possibility of settlement which could reduce the cross sectional bore.

If the sediment characteristics are incompatible with the normal flow velocity i.e. the water velocity in the pipe without sediment would be insufficient to maintain the sediment in suspension then the following may occur; coarse particles would settle out initially thereby changing the cross-sectional shape. This has the effect of reducing the hydraulic radius and increasing friction drag so that the flow velocity could reduce even further. The final result may be a blocking of the bore. It is more likely to reduce the cross-sectional area until the velocity increases again for some flow conditions, provided a head buildup at the entrance was possible.

If the suspended sediment added significantly to the energy gradient, the dropping of sediment may permit an increase in velocity so that an equilibrium is reached in time. Shedding of sediment, however, implies a non-equilibrium or a gradual buildup in sediment within the pipe, initially at the top end and subsequently lower down the length of the pipe. Ultimately the entire pipe length will have the same bed load and the system will tend to adjust to a regime with minimum specific energy. That is, the flow depth and consequently the flow velocity adjust until the energy gradient is a minimum consistent with the sediment load.

Alternatively, for a given conduit gradient (which in turn must equal the energy gradient for uniform flow) the flow depth and consequently velocity adjust to cause the friction gradient to equal the bed gradient

Head Loss in Sediment-Laden Pipes

The relationships between the head loss and flow in a pipe conveying sediment have been investigated by many researchers. For particles less than 0.04 mm, the mixture is generally homogeneous and the Darcy equation would apply. Generally large particles (0.04 mm to 0.15 mm) form a heterogeneous mixture and particles larger than 0.15 mm proceed by saltation and in suspension. The equation for heterogeneous flow most accepted is that of Durand and Condolios, which may be written in the form

$$i_{mw}/i_w = 1 + 81c \left\{ \frac{gD(S-1)}{V^2 C_D^{1/2}} \right\}^{1.5} \quad (15.16)$$

where i_{mw} is head loss gradient of the mixture, in metres of water per metre of pipe. i_w is the head loss gradient of water at the same velocity V , c is the volume concentration of sediment in the pipe as a fraction, g is gravitational acceleration, D is the pipe internal

diameter, S the sediment relative density or specific gravity and C_D is the effective drag coefficient of the suspended particles. The term on the right hand side is the excess energy gradient relative to water, in metres of water per metre of pipe, due to the particles.

For particles of varying size, the expression may be replaced by

$$i_{mw}/i_w = 1 + 81c \frac{\{gD(S-1)\}^{1.5}}{V^2} \sum \frac{P_i}{C_{Di}^{0.75}} \quad (15.17)$$

The equation is really only applicable to particles of limited size such that they travel at about the same velocity as the water. Very coarse particles (greater than about 25 mm) obey a relationship of a different form.

Although the equation was not originally intended for use in other than full circular pipes, according to Bain and Bonnington (1970) it may be rewritten in a form applicable to part-full pipes by replacing D by $4R$ where R is the hydraulic radius, Q is the discharge rate and A is the cross sectional area of the flow. If one substitutes the term C_f for $81c\{gD(S-1)A_f^2/Q^2C_D^{1/2}\}^{1.5}$ the equation may be written in dimensionless form as follows:

$$i_{mw}/i_w = 1 + C_f Y^{1.5} \quad (15.18)$$

where Y is $RA^2/R_f A_f^2$ and is a function of the relative depth of flow y/D only, and R_f and A_f are the hydraulic radius and area of the full pipe i.e. $D/4$ and $\pi D^2/4$ respectively.

One thus has an expression relating the hydraulic gradient of the solids/water mixture to that in water. The equation applies for any given depth of flow. In view of the difficulty in solving for Y as a function of y/D , the relationship is plotted in Fig. 15.5. Thus for any specified depth of flow and sediment function C_f one may establish the energy gradient relative to that of clear water. Thus for a sediment concentration of one percent, a C_D of 1.0 and a pipe diameter of 500 mm it will be found that at 50% full flow the head loss increases 60 percent.

Invariably the pipe gradient cannot be altered to suit the sediment load, unless at design stage. What would happen in practice is that the depth would adjust to accommodate the additional energy requirement to transport the sediment. Thus if one writes the energy equation as

$$i_{mw}/i_{wf} = i_w/i_{wf} (1 + C_f Y^{1.5}) \quad (15.19)$$

where i_{wf} is the head loss gradient at flow Q of water in the pipe running full, then Fig. 15.6 may be plotted. Now if the Darcy equation

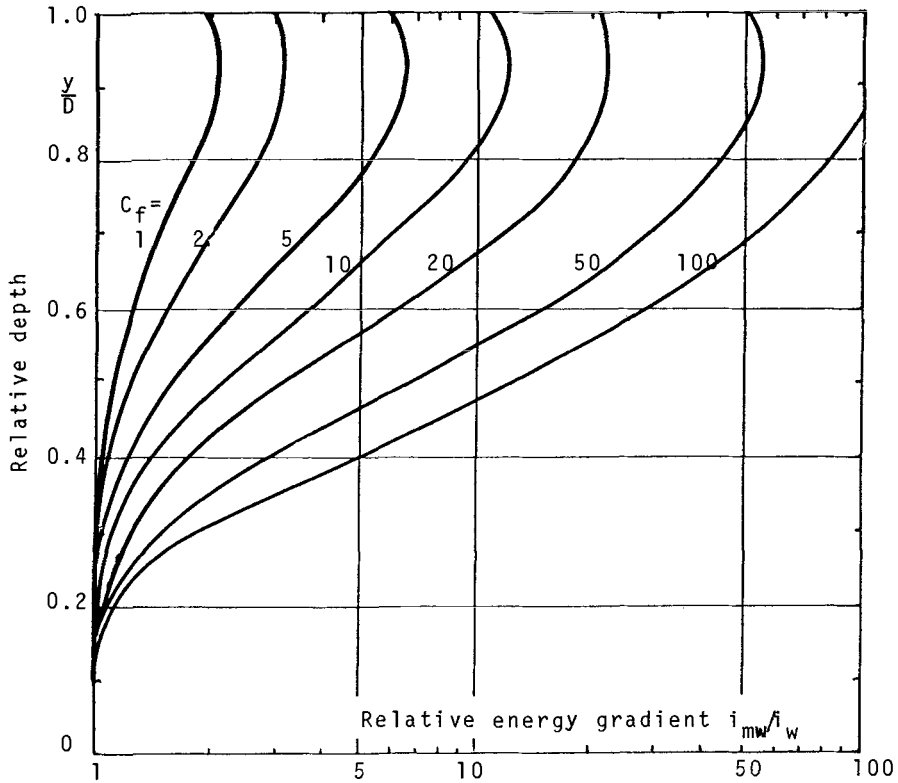


Fig. 15.5 Energy gradient for part full pipes transporting sediment

is used for friction losses

$$\text{then } i_w/i_{wf} = A_f^2 R_f / A^2 R = 1/Y \tag{15.20}$$

$$\text{since } i_{wf} = \lambda Q^2 / 2gDA_f^2 \tag{15.21}$$

Fig. 15.6 may thus be plotted to yield the depth of flow at different concentration functions for any given gradient. It should be noted that i_w and i_{mw} are the gradients in metres of water per metre length. For high concentrations the gradient should be corrected for the relative density of the silt laden mixture. Thus the relative density of mixture is $1 + c(S - 1)$

Hence the true gradient in metres of mixture per metre of pipe is $i_m = i_{mw} / \{1 + c(S - 1)\}$ (15.22)

For a gradient of $i = 0.0185$, $i_{mw} = 1 + 0.05(2.6 - 1) = 0.02$, $Q = 0.3 \text{ m}^3/\text{s}$, $\lambda = 0.012$, $D = 0.5\text{m}$, then $i_{wf} = 0.00286$ and $i_{mw}/i_{wf} = 7.0$. From Fig. 15.6 the depth of flow for clear water ($C_f = 0$) is $0.42 \times 0.5 = 0.21\text{m}$ and

for $c=0.05$, $S=2.6$ and $C_D=10.0$ then $C_f=4.43$ and $y=0.48 \times 0.5=0.24\text{m}$, i.e. the depth of flow increases. If C was much higher however, it may be found that at no depth would the pipe transport the load, so that blockage is possible.

Self Cleansing Velocities

It is commonly accepted that the minimum velocity in sanitary sewers to avoid settling is 0.6 metres per second (Yao, 1974). This criterion applies to the full-flow condition. It takes no account of sediment characteristics and is probably applicable to biological matter. During some periods the sewers may not run at capacity and the flow velocity will be less than that at full capacity. Under these conditions in the case of sanitary sewers it was recommended that the minimum velocity be attained at least once a day.

The criteria for storm sewers are different. There is normally little problem of putrefaction of deposits which is fortunate, as self cleansing velocities may not occur for months on end. The sediment transported by storm sewers is likely to be silt, sand, and even refuse such as bottles or cans.

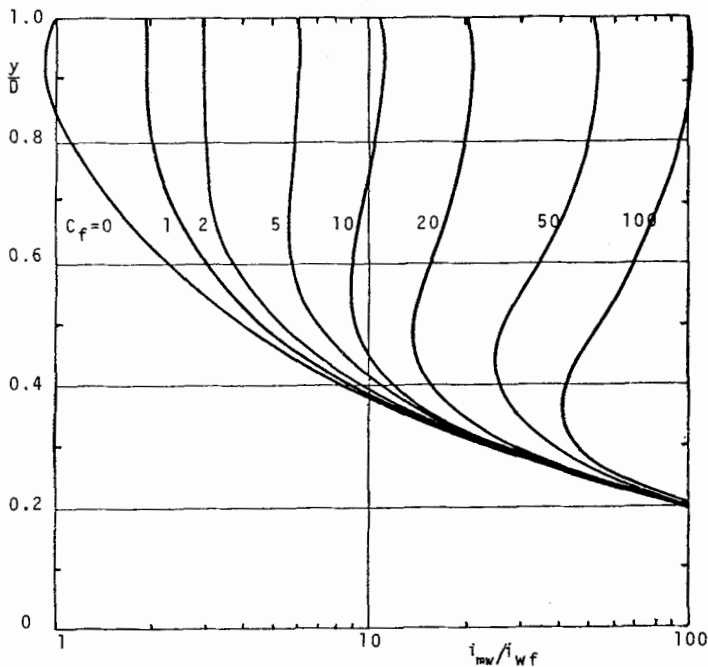


Fig. 15.6 Depth of flow in part-full pipes transporting sediment

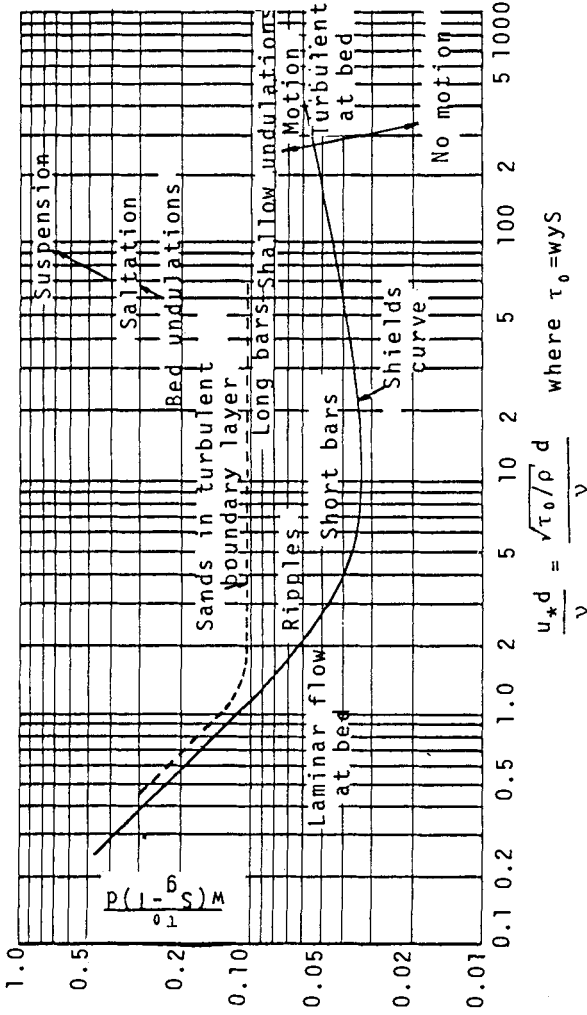


Fig. 15.7 Shields' diagram for scour of sediment

A more rational theory than the minimum velocity concept is the tractive shear stress approach. The theory was developed by Shields who obtained his results from tests in a horizontal flume. He showed that the limiting bed shear stress for incipient motion of non-cohesive particles was given by an equation of the form

$$\frac{\tau}{w(S-1)d} = F(R_d) \quad (15.23)$$

where τ is the bed shear stress, w is the unit weight of water, S is the relative density of silt and d is the particle size. R_d is a Reynolds number in terms of particle size

$$R_d = U_* d / \nu \quad (15.24)$$

$$\text{and } U_* \text{ is the shear velocity } \sqrt{(\tau/\rho)} \quad (15.25)$$

The numerical value of F is 0.06 for coarse particles increasing for smaller particles (Fig. 15.7).

Employing the Darcy friction equation and solving for water velocity V , for a full pipe

$$v = \sqrt{8g d (S-1)F/\lambda} \quad (15.26)$$

For part-full pipes the relationship between τ and friction factor λ is more complicated. The fact that the roughness of the deposits is different to that of the rest of the wetted perimeter further complicates the solution for self cleansing velocity V . Camp (1946) indicated self-cleansing velocities assuming the equation for permissible velocity as above and varying friction factor λ with relative flow depth.

The Equ. 15.26 is similar in form to the critical deposit velocity found in pipeline transport. For full pipes this is

$$V = F_c \sqrt{2gD(S-1)} \quad (15.27)$$

where F_c lies between 0.8 and 1.0 for concentrations between 2% and 15% by volume and particle size d greater than about 0.2 mm.

PLANNING AND MANAGEMENT

Our water resources of the future may be limited more by pollution than by drought. Integrated water resource management such as initiated in the United Kingdom will become necessary. This means the control of surface water and ground water, wastewater treatment and possibly stormwater treatment. Methods of treating stormwater will be similar in principle to those for concentrated sewage and industrial wastes but will vary greatly in scale and effort. Nevertheless, locations of collection works, treatment facilities and discharge points will require integrated planning (e.g. Stephenson, 1978; Rinaldi et al 1978).

Management of catchments and drainage systems will require the attention of sanitary engineers as well as hydrologists. Preservation of resources is closely related to optimal management and research on these lines in the USA is now bearing fruit (e.g. Wanielista, 1978).

REFERENCES

- Bain, A.G. and Bonnington, S.T., 1970. The Hydraulic Transport of Solids by Pipeline. Pergamon Press, Oxford, 249pp.
- Camp, T.R. 1946. Design of sewers to facilitate flow. Sewage Works Journal, 18, p3-16.
- Cheverreau, G., 1973. Mathematical model for oxygen balance in rivers. In 'Models for Environmental Pollution Control'. Deininger, R.A. (Ed.) Ann Arbor Science, Ann Arbor, P107-136.
- EPA (Environmental Protection Agency), 1971. Storm Water Management Model, Vol. 1.
- Henderson-Sellers, B., 1979. Reservoirs, Macmillan, London, 128pp.
- Meyer, L.D., and Wischmeir W.H., Dec. 1969. Mathematical simulation process of soil erosion by water. Trans American Society of agricultural engineers, 12(6)
- Rinaldi, S., Soncini-Sessa, R., Stehfest, H. and Tamura, H., 1978. Modelling and Control of River Quality. McGraw Hill, N.Y. 380pp.
- Roesner, L.A. (1979), Response, Water Problems of Urbanizing Areas. Proc. Res. Conf. ASCE.
- Stephenson, D., 1978. Optimal planning of regional wastewater treatment. Proc. Int. Conf. Modelling the Water Quality of the Hydrological Cycle, IIASA, Baden, p351-360.
- Streeter, H.W. and Phelps, E.B., 1925. A study of the pollution and natural purification of the Ohio river, U.S. Public Health Bulletin, 146.
- Thomann, R.V., 1972. Systems Analysis and Water Quality Management, McGraw Hill, N.Y. 286pp.
- Vanoni, V.A., (Ed.) 1975. Sedimentation Engineering. Amer. Soc. Civil Engrs. 745pp.
- Wanielista, M.P. 1978. Stormwater Management, Quantity and Quality. Ann Arbor Science, Ann Arbor, 383pp.
- Wischmeir, W.H. and Smith, D.D., 1965. Predicting rainfall erosion losses from cropland east of the Rocky Mountains. Agricultural Handbook 282, ARS-USDA.
- Yao, K.M., April, 1974. Sewer line design based on critical shear stress. Proc. ASCE, 100, EE2, 10480, p507-520.

AUTHOR INDEX

- Abbot, M.B. 199, 218
 Ackers, P. 151, 164
 Adrian, D.D. 115
 Ardis, C.V. 38, 54
 Argaman, Y. 96, 100, 194, 196
 Arnold, H. 31, 37

 Bain, A.G. 265, 270
 Barlow, J. F. 194, 196
 Beard, L.R. 118, 126, 132
 Bell, F.C. 18, 19, 37
 Blaisdell, F.W. 246, 251
 Bliss, P.H. 241, 251
 Bonnington, S.T. 265, 270
 Bogan, R.H. 96, 100, 189, 193
 197
 Bradley, J.N. 231, 235
 Brebbia, C.A. 199, 218
 Brown, L.C. 190, 197
 Burton, G.S. 152, 154, 164
 Bury, K.V. 120, 132

 Camp, T.R. 175, 185, 269, 270
 Carcich, I.G. 5, 15
 Chen, C.W. 112, 115
 Chevereau, G. 256, 270
 Childrey, M.R. 126, 132
 Chow, V.T. 199, 204, 207, 218,
 235
 Chu, H.H. 25, 37
 Clarke, W.G. 112, 115
 Connor, J.J. 199, 218
 Constantinides, C.A. 58, 76, 92,
 100
 Crump, E.S. 164
 Culligan, P.T. 133, 144

 Dajani, J.S. 96, 100, 189, 194,
 196, 197
 Davis, D.W. 194, 197
 Dawson, F.M. 140, 143
 Deininger, R.A. 114, 115
 Dick, T.M. 112, 115
 Diskin, M.H. 170, 185, 246, 251
 Ducker, K. J. 38, 54

 Eagleson, P.S. 59, 76
 Escritt, L.B. 53, 54
 Essery, I.T.S. 215, 218

 Farell, R.P. 5, 15
 Fiering, M.B. 123, 132
 Fisher, R.A. 122, 132
 Forbes, H.J.C. 157, 164
 French, J.L. 241, 251
 Fried, J.J. 115

 Gemmell, R.S. 194, 196
 Geyer, J.C. 54, 152, 154, 164
 Grigg, N.S. 2, 15
 Gringorten, I.I. 125, 132
 Gumbel, E.J. 122, 132

 Haan, C.T. 120, 125, 132
 Hall, M.J. 7, 15
 Harbaugh, T.E. 21, 30, 37, 126,
 132
 Harris, G.S. 181, 185
 Hasit, Y. 96, 100, 189, 194, 197
 Hasselman, K. 214, 218
 Hawkins, R.H. 32, 37
 Heeps, D.P. 112, 115
 Henderson, F.M. 59, 76, 149, 164,
 184, 185, 199, 207, 218, 246, 251
 Henderson-Sellers, B. 259, 270
 Hetling, L.J. 5, 15
 Hicks, W.I. 29, 37
 Hiemstra, L.A.V. 30, 37
 Hinds, J. 136, 143
 Hockin, D.L. 7, 15
 Holton, H.N. 72, 76
 Horner, D.W. 115
 Horner, M.W. 215, 218
 Horton, R.E. 29, 37, 72, 76
 Huff, F.A. 25, 37

 Izbash, S.V. 218

 Jackson, T.J. 146, 164
 Jenker, W.R. 177, 185
 Jewell, T.K. 115
 Jones, D.E. 38, 54

 Kalinske, A.A. 140, 143, 180, 185
 Kally, E. 190, 197, 241, 251
 Kamedulski, G.E. 5, 15
 Keifer, C.J. 25, 37
 Khaldre, Kh.Yu. 218
 Kindsvater, C.E. 220, 235
 Knapp, J.W. 21, 30, 37, 54, 126,
 132
 Kohler, M.A. 129, 132
 Kouwen, N. 180, 185

 Labadie, J.W. 2, 15
 Lardieri, A.C. 133, 143
 Laursen, E.M. 220, 226, 231, 235
 Lenz, A.T. 38, 54
 Lewis, G.L. 21, 30, 37, 126, 132
 Li, W.H. 152, 154, 164
 Liggett, J.A. 59, 77, 76
 Lin, H.K. 231, 235
 Linsley, R.K. 129, 132
 Lloyd-Davies, D.E. 38, 44, 45, 54

- Marsalek, I. 112, 115
 Martin, K.G. 135, 137, 139, 143
 Mays, L.W. 126, 132, 194, 197
 McCuen, R.H. 5, 15
 Meadows, M.E. 58, 61, 69, 76, 78, 100, 114, 115
 Mein, R.G. 112, 115
 Meredith, D.D. 190, 197
 Merritt, L.B. 96, 100, 189, 193, 197
 Meyer, L.D. 261, 270
 Midgley, D.C. 207, 219
 Miles, L.C. 6, 15
 Mohsen, F.N. 180, 185
 Morlok, E.K. 194, 196
 Mussalli, Y.G. 177, 185

 Nalluri, C. 184, 185
 Naylor, A.H. 222, 235

 Orlob, G.T. 112, 115
 Overton, D.E. 58, 61, 69, 76, 78, 100, 114, 115

 Pagan, A.G. 133, 144
 Papadakis, C.N. 108, 115
 Paulus, J.L.H. 129, 132
 Pearson, K. 122, 132
 Pegram, G.C.S. 30, 37
 Phelps, E.B. 256, 270
 Pickford, J. 214, 218
 Plate, E.J. 231, 235
 Poertner, H.G. 7, 15, 133, 144
 Preul, H.C. 115
 Prins, J.R. 164, 165

 Rinaldi, S. 114, 115, 269, 270
 Robertson, J.M. 180, 185
 Roesner, L.A. 259, 270
 Rogan, R.M. 146, 164
 Rossmiller, R.L. 42, 54

 Saint-Venant, A.J.C. 57, 76
 Sarginson, E.J. 9, 15
 Schaaake, J.C. 38, 54
 Schneider, W.J. 1, 15
 Schulze, R.E. 31, 37
 Schwartz, H.I. 133, 144
 Sevuk, A.S. 96, 100
 Shamir, U. 96, 100, 194, 196
 Smith, D.D. 261, 270
 Soncini-Sessa, R. 114, 115, 269, 270
 Southwood, S.R. 242, 251
 Spivak, E. 96, 100, 194, 196
 Stall, J.B. 106, 115
 Stehfest, H. 114, 115, 269, 270
 Stephenson, D. 58, 69, 76, 77, 97, 100, 167, 181, 185, 189, 197, 215, 218, 223, 235, 269, 270
 Streeter, H.W. 256, 270

 Tamura, H. 114, 115, 269, 270
 Templeman, A.B. 195, 197
 Terstriep, M.L. 106, 115
 Thiessen, A.H. 21, 37
 Thomann, R.V. 114, 116, 257, 270
 Tippett, L.H.C. 122, 132
 Tomlinson, J.H. 184, 185
 Townsend, R.D. 164, 165
 Trent, R.E. 126, 132
 Trotta, P.D. 2, 15

 Vanoni, V.A. 215, 219, 263, 270
 Velz, C.J. 114, 116
 Videkovich, R.M. 5, 15
 Viessman, W. 21, 30, 37, 112, 116, 126, 132
 Visser, A.T. 146, 165

 Walesh, S.G. 5, 15
 Walsh, S. 190, 197
 Walters, -G.A. 195, 197
 Wanielista, M.P. 2, 15, 33, 37, 112, 270
 Watkins, L.H. 50, 54, 100, 106, 116
 Watson, J.D. 183, 185
 Watson, M.D. 9, 15, 170, 185
 Weiss, H.W. 207, 219
 White, J.B. 46, 50, 54
 Wilson, E.M. 9, 15, 30, 37
 Wipple, W. 11, 15
 Wischmeir, W.H. 261, 270
 Wisner, P.E. 112, 115, 180, 185
 Wooding, R.A. 58, 59, 62, 65, 77, 78, 100
 Woolhiser, D.A. 59, 77
 Wright-McLaughlin, 9, 15

 Yao, K.M. 267, 270
 Yarnall, D.L. 19, 37, 231, 235
 Yen, B.C. 2, 15, 37, 96, 100, 126, 130, 132, 194, 197
 Yevjevich, V. 120, 123, 132
 Young, G.K. 126, 132

 Zucchini, W.S. 30, 37
 Zwamborn, J.A. 154, 165

SUBJECT INDEX

- Abstraction 28
 Adverse slope 199
 Aeration 11
 Agriculture 254
 Air 167, 177
 Algae 258
 Alternatives 188
 Analytical 78
 Annual 123
 Antecedant moisture 26, 32, 67
 Aquifer 29
 Areal distribution 78
 Asphalt 254
 Attenuation 4

 Backwater 184, 201, 226, 230, 251
 Bacteria 265
 Balanced design 248
 Barrel 238, 241
 Base flow 34
 Bend 137
 Bernoulli 154, 166
 Bevel 244
 Bicycle 157
 Biological 254
 Biochemical oxygen demand 256
 Birmingham formula 38
 Blockage 264
 Box culvert 242
 Box receivers 136
 Bottom opening 157
 Bridge 127, 220
 Buildings 135

 Calibration 97
 Canal 198
 Catchment 40, 65, 67, 86
 -stream model 65
 Channel 14, 85, 198
 Chemical oxygen demand 256
 Chicago storm 25
 Chute 164
 Circular drain 166, 245
 Circulation 258
 Coefficient 246
 Combined sewers 254
 Compound pipes 190
 Composite section 205
 Computer program 97, 102, 184, 193, 250
 Concentration 14, 55, 60, 93
 Condensation 16
 Confidence band 122, 125
 Contraction 241
 Contributing area 46
 Control 238
 Contour 46
 Convection 16

 Correlation 117
 Cost 128, 187, 138
 Crest 232, 242
 Critical depth 138, 175, 199, 232, 236, 245
 Cross section 148, 198, 202
 Culvert 236
 Current 231
 Curve number 33, 42
 Cyclone 16

 Dam 4
 Damage 128, 133
 Darcy 168, 269
 Data 117
 Debris 254
 Decay 29, 88, 115, 254
 Deck 220
 Deicing 3
 Deposit 264
 Depression 155
 -storage 29
 Depth 78, 145, 195, 201, 257, 267
 Design 1, 38, 95, 126
 -storm 25
 Detention storage 6
 Dew point 16
 Diameter 166
 Discharge 126, 146, 246
 Discretize 104
 Dissolved oxygen 256
 Diversion 129, 241
 Downpipe 12, 139
 Drain 166
 Drop 161, 167
 Duration 18, 61
 Dust 254
 Dyke 231
 Dynamic 55, 78
 -programming 190

 Ecology 254
 Economics 6, 127, 236
 Embankment 236, 242
 Energy 151, 164, 166, 225, 267
 Engineer 1, 2
 Environmental Protection Agency, 116, 254
 Equations of motion 55, 79
 Equilibrium 41, 45, 60
 Erosion 1, 4, 164, 217, 234, 260
 Eutrophication 258
 Evaporation 28
 Evapotranspiration 28
 Excess flow 85
 Exponential 120
 Extreme value 118

- Factor of safety 5
 Faeces 254
 Fertilizer 5
 Field 254
 Finite difference 81
 Flood 4, 237
 -routing 181
 Flow classification 198
 Flush 183, 254, 267
 Foundation 231
 Freeboard 6
 Free surface 198, 241
 Frequency 117
 Friction 145, 167
 Froude number 206, 238

 Gabion 204
 Gamma 120
 Gap 222
 Geometry 202
 Grade 46, 167, 238, 267
 Gradually varied flow 184, 199, 206
 Graphical 206
 Grass 3
 Grate 160
 Grill 142
 Groundwater 29
 Gutter 136, 157, 167

 Hazard 145
 Hazen Williams 168, 170
 Head 166
 Head loss 166, 242, 264
 Headwater 237
 Highways 164, 194
 Holding pond 10
 Hood 241
 Hydraulic jump 175, 177, 201, 251
 -radius 216
 Hydraulics 113, 220, 236
 Hydrodynamic 45
 Hyetograph 18, 26
 Hydrological cycle 16
 Hydrograph 34, 59, 86
 Hydrology 17

 Ice 3
 Initial loss 72
 ILLUDAS 106
 Impact 104
 Impervious 32, 44
 Infiltration 29, 62
 -factor 70
 Inlet 139, 149, 188, 241
 Intensity 18, 42, 53, 183
 -duration 67
 Interception 18
 Inundation 237
 Invert 92, 264

 Isochrone 48, 53, 104, 106
 Isohyet 19

 Kerb 147, 151
 Kinematic flow 55
 Laboratory 231
 Lag 36, 61
 Lake 258
 Laminar 58
 Land use 38
 Lateral inflow 85, 149, 152
 Layout 187
 Legislation 6
 Linear programming 194
 Lloyd-Davies 38, 44
 Log 120
 Loss 28, 69, 74

 Management 2, 104, 269
 Manhole 180, 195
 Manning 58, 92, 145, 172, 216
 Mass curve 4, 36
 Mathematical distribution 118
 Mean 119
 Median 119
 Mild slope 199
 Mixed integers 190
 Mode 119
 Model 92, 260
 Moment 120
 Momentum 57, 147, 151, 164, 167, 177
 Moody 169
 Mulching 3
 Multiple regression 120
 Muskingum 36

 Network 187
 Nikuradse 168
 Non-circular 172
 Non-conservative 112
 Non-point source 254
 Non-uniform flow 206
 Normal 120, 199
 Numerical 78
 Nutrient 254

 Oil 254
 One-dimensional 199
 On-site detention 6
 Optimization 114
 Organic 254
 Orifice 160
 Orographic precipitation 17
 Outlet 246
 Overland flow 14, 58, 92
 Overtop 129, 237
 Oxygen 112, 256

 Pan evaporation 28
 Park 6

- Parking lot 11
- Part full 92, 173, 263
- Partial series 123
- Pavement 1, 145
- Peak 80
- Pearson distribution 120
- Percolation basin 9
- Permeability 29
- Pervious 28
- Photosynthesis 260
- Pier 231
- Pipe 48, 92, 166, 173, 244, 264
- Planning 269
- Plotting position 125
- Plug flow 257
- Point rain 18
 - source 254
- Policy 2
- Pollution 4, 115
- Pollutograph 112
- Population 1
- Precipitation 16
- Prediction 117
- Pressure 251
- Probability 117
- Profile 184, 206, 223, 238, 250
- Public 1, 254
- Purification 11

- Quality 10, 112, 254

- Radiation 17
- Rainfall 16
- Random 117
- Rank 123
- Rating 250
- Rational method 38
- Record 123
- Receiving water 258
- Recession 40
- Recreation 256
- Rectangular culverts 250
- Recurrence interval 19, 118, 125
- Refuse 264
- Regression 112
- Research 104
- Retardation 14, 70, 175
- Retention 6
- Return period 118
- Reynolds number 58, 170
- Risk 117, 127, 129, 236
- River 198
- Road 145, 254
- Road Research Laboratory 106
- Rockfill 217
- Roof 12, 133
- Roughness 75, 168, 204, 216
- Routing 8, 36
- Runoff 16, 74, 108, 117
- Rural 147

- S-curve 36
- Safety 5, 145, 198
- Saint-Venant 57
- Salt 254
- Saturation 30
- Scour 217, 260
- Screen 149, 157
- Sediment 260
- Seepage 10, 254
- Self cleansing 267
- Semi-full 92, 173, 263
- Sensitivity 102
- Separation 241
- Sequent depth 201
- Series 123
- Settlement 264
- Sewer 254
- Shape 172
- Shields 268
- Sideweir 151
 - taper 242
- Silt 11, 254
- Simulation 97
- Skewness 120
- Slope 242, 262
- Snow 3
- Soffit 242
- Soil 30
- Soil Conservation Service 30
- Solids 264
- Spatially varying storm 84
- Specific energy 201
 - force 202
- Spillway 6
- Stabilization 214, 217, 237
- Standard deviation 120
- Statistics 117
- Steady flow 199
- Step method 44, 208
- Stochastic 117
- Storage 4
- Storm distribution 78
- Stream 65, 237
- Streamline 154
- Street sweeping 3
- Streeter-Phelps 260
- Strickler 58, 216
- Structure 2, 231
- Submerge 238
- Supercritical flow 137, 149, 199
- Surcharge 93, 241
- Surface 145
- Surge 200
- Suspended matter 260
- Swales 3
- SWM 108
- SWMM 106
- Synthetic storm 25

- Tailwater 246
- Tangent method 50

Taper 242
Temperature 259
Thiessen polygon 20
Thunderstorm 16
Time - area 48, 106
 - of concentration 60, 68
 - of entry 46, 51
 - varying storm 81
Topography 262
Transient 200
Traffic 145, 151, 237
Transition 245
Transpiration 28
Transport 108
Trapezoid 222
Travel time 48, 60
Treatment 108, 269
Trophic state 260
Turbulent 58
Two-dimension model 90
Tyre 145

Uncertainty 117
Uniform 80
 Flow 199
 loss 69
Universal Soil Loss Equation 2, 61
UCURM 108
Unsteady flow 83, 104, 211
Urbanization 1

Vapour 17
Variables 102
Variability 117
Vegetation 3, 254
Velocity 139
Vena-contracta 142, 167
Ventilate 251
Verge 3
Viscosity 58, 170
Void ratio 10
Vortex 242

Water cycle 1
 -level 226
Watershed 20
Waterproof 133
Wave 238
Weibull 123
Weir 138, 155
Wetted perimeter 202
Wind 20
Wing wall 242